Phenotypic and gene expression analysis of potato (*Solanum tuberosum*) subjected to intermittent abiotic stress

Analysen des Phänotyps und der Genexpression der Kartoffel (*Solanum tuberosum*) unter intermittierendem abiotischem Stress

Der Naturwissenschaftlichen Fakultät der
Friedrich-Alexander-Universität Erlangen-Nürnberg zur
Erlangung des Doktorgrades Dr. rer. nat.

vorgelegt von
Jessica Van Harsselaar
aus Gießen

Als Dissertation genehmigt von der Naturwissenschaftlichen Fakultät der Friedrich-Alexander-Universität Erlangen-Nürnberg

Parts of this thesis have been published in the following papers:

Van Harsselaar, J.K., Lorenz, J., Senning, M., Sonnewald, U., Sonnewald, S., 2017. Genome-wide analysis of starch metabolism genes in potato (Solanum tuberosum L.). BMC Genomics 18, 1–18. doi:10.1186/s12864-016-3381-z

Van Harsselaar, J.K., Claußen, J., Lübeck, J., Wörlein, N., Uhlmann, N., Sonnewald, U., Gerth, S., 2021. X-Ray CT Phenotyping Reveals Bi-Phasic Growth Phases of Potato Tubers Exposed to Combined Abiotic Stress. Front. Plant Sci. 12, 1–15. https://doi.org/10.3389/fpls.2021.613108

Author's contributions to publications:

Van Harsselaar et al. 2017:

JVH, JL and MS performed the experimental and molecular biological work related to RNA-isolation and preparation for microarray hybridization for the experiments that had not been published before. JVH analyzed the pooled microarray data. Identification of potato genes encoding enzymes involved in starch metabolism was done by JVH. JVH performed the *in-silico* analysis of starch genes and co-expression analyses with support of SS. JVH did the molecular biological work to confirm the transcriptome data (qPCR). All figures, graphs and tables were prepared by JVH. The writing of the manuscript was done by JVH with input from US and SS.

All co-authors have approved the use of the manuscript as part of this thesis.

Van Harsselaar et al. 2021:

JC, SG, and JVH performed the experiments and drafted the manuscript. Chapters concerning stress biomarkers and starch metabolism were written by JVH. JVH contributed to the introduction and discussion parts of the paper and wrote the sections about the impact of abiotic stress on potato. Plants were grown and cared for at the Fraunhofer Institute for integrated circuits. JVH did the sampling, sample preparation and molecular biological work (qPCRs) for analysis of gene expression and wrote all parts of the manuscript in this regard. SG supervised and together with JC performed the CT work. NW and JC performed the image and data analysis. US and NU provided the project funding, conceived and led the study, and contributed to writing the manuscript.

All co-authors have approved the use of the manuscript as part of this thesis.

Table of contents

Table of contents

1 Summary / Zusammenfassung

1.1 Summary

The potato (*Solanum tuberosum* L.) is one of the most important food plants worldwide. In addition to essential ingredients such as vitamins and minerals, the tubers of the potato plant contain starch in particular. This serves as a source of carbohydrates for human nutrition and thus as an important energy supplier. In addition, potato starch is also used as a raw material in a wide variety of industries, such as bioethanol production, paper manufacturing and for adhesives. Due to its versatility and its role in human and animal nutrition, increasing the starch content in potato tubers is a goal of plant breeding. To achieve this goal, a comprehensive knowledge of starch metabolism is of great importance. This knowledge includes both the enzymes and metabolites involved in starch breakdown and degradation and the regulation of these pathways at the transcriptional as well as translational and post-translational levels. A major factor influencing the quality of potato tubers in terms of starch content is climate. The changes caused by climate change - increased temperatures and drought - have devastating effects on potato yields, which are mainly determined by their starch content. Detailed insights into the mechanisms triggered by abiotic stress in potato and how these are related to tuber development can be important to breed resistant varieties.

In this work, the enzymes involved in starch metabolism in potato were described at the genome level and their expression was investigated using microarray experiments. Leaf- and tuber-specifically expressed isoforms as well as new, previously undescribed isoforms could be identified. Co-expression analysis with key enzymes of starch synthesis and degradation in potato tubers identified transcription factors potentially involved in the regulation of starch metabolism.

To identify the factors involved in the regulation of starch metabolism as well as in the determination of sink- and source-specific metabolic pathways, potato plants were exposed to a period of abiotic stress (heat) during the tuber growth phase. Heat stress impairs tuber formation and growth and can lead to secondary tuber growth ("second-growth"). This morphological response to stress suggests that the sink-source identity is disturbed and that an inhibition of starch metabolism is associated with it. To investigate this, potato plants of different varieties were subjected to a period of heat stress at different times in their development. Heat stress during the filling phase of the tubers led to increased second-growth in some potato varieties. This phenomenon was observed most strongly in the variety Agria. The transcriptional analysis of primary and secondary tubers of the variety Agria showed that they differed strongly in their gene expression patterns. Overall, anabolic processes, such as

starch synthesis, were down-regulated in primary tubers, while they tended to be up-regulated in secondary tubers. These gene expression patterns were mirrored by the expression of the tuber-inducing SP6A. Furthermore, its expression in leaves was confirmed as a biomarker for tuber induction. Thereby, heat stress, depending on the time of application, led to a strong decrease of SP6A expression as well as to the inhibition of tuber formation and growth.

The formation of second-growth suggests the premature breaking of dormancy, leading to the assumption that a connection between the tendency to second-growth and the length of dormancy exists. To investigate the phenomenon of second-growth in more detail and to shed light on the relationship between second-growth and dormancy, three cross-breeding populations of the potato varieties characterized in previous experiments were cultivated and characterized. Adjustments in growing conditions, i.e. smaller pots and short days, allowed the simultaneous cultivation of a large number of plants in phytochambers for phenotypic characterization. Screening of the three populations focused on the appearance of tubers and aboveground plant organs as well as the duration of dormancy after harvest. In each population, lines were identified that germinated relatively early or late. These were grown again in larger numbers and subjected to a period of heat stress during the tuber filling phase or left under ambient temperatures (control). The duration of dormancy could thus be confirmed for all lines selected due to their particularly early or late germination behavior. After harvest, but before the first potatoes germinated, samples were taken from the tissue below the apical eyes of particularly early or late germinating lines. These were used to determine by gene expression analysis which signaling and metabolic pathways are activated or deactivated before the visible breaking of dormancy. One of the early germinating lines, SA69/12-HotPot #57 appeared to be particularly suitable for this purpose, as its gene expression pattern in a cluster analysis was very close to samples of germinating eyes, while the other lines clustered more with dormant eyes.

The gene expression profile of line #57 showed unique changes in the expression of genes encoding enzymes of hormone biosynthesis. Here, the plant hormone ethylene was particularly conspicuous, with its biosynthetic pathway represented in the significantly upregulated genes. Furthermore, the functional category "signaling" was overrepresented in the significantly upregulated genes. Here, some genes that can be assigned to phototropism were particularly conspicuous. In line with this observation, genes that can be associated with phototropism were also identified among the down-regulated genes indicating that this mechanism, which had earlier been implicated in stress response, might be of importance in the regulation of dormancy.

In order to gain deeper insight into tuber development under stress conditions, a series of experiments were conducted with different potato cultivars under combined abiotic stress (heat

and drought). The two-week stress period was applied during the filling phase of the tubers. Tuber development was observed *in vivo* using an optimized X-ray computed tomography technique without exposing the tubers to disturbing factors such as light. In this series of experiments, it was observed that tuber growth dropped sharply within the first week of stress application and was in parts completely inhibited. After termination of the stress, the tubers resumed their growth and partly showed strongly increased daily growth rates. Thus, the effects of the stress on the final tuber volume were more or less compensated compared to tubers from plants under control conditions. The expression of potential stress markers confirmed that the changed environmental conditions were perceived in the tubers. Parallel gene expression studies of enzymes involved in starch metabolism showed that starch synthesis was inhibited during the stress period, but appeared to return to normal after the stress ended.

This work provides insights into the gene expression of potatoes under stress conditions, in particular heat and combined heat and drought - stresses that are becoming more frequent due to climate change and are therefore of utmost relevance. The gene expression studies are considered in the context of phenotypic adaptations of tubers in response to stress. The knowledge gained in this work can serve as a basis for further studies on the effects of climate change on potato production and help in breeding stress-resistant varieties.

1.2 Zusammenfassung

Die Kartoffel (*Solanum tuberosum* L.) ist eine der bedeutendsten Nahrungspflanzen weltweit. Neben essentiellen Inhaltsstoffen wie Vitaminen und Mineralstoffen enthalten die Knollen der Kartoffelpflanze vor allem Stärke. Diese dient in der menschlichen Ernährung als Kohlenhydratquelle und somit als wichtiger Energielieferant. Darüber hinaus wird Kartoffelstärke auch als Rohstoff in verschiedensten Industriezweigen verwendet wie beispielsweise in der Bioethanolproduktion, der Papierherstellung sowie für Klebstoffe. Durch die vielseitige Anwendbarkeit sowie seine Rolle in der menschlichen und tierischen Ernährung, ist die Erhöhung des Stärkegehaltes in Kartoffelknollen ein Ziel der Pflanzenzucht. Um dieses Ziel zu erreichen ist ein umfassendes Wissen über den Stärkestoffwechsel von großer Bedeutung. Dieses Wissen umfasst sowohl die beteiligten Enzyme und Metabolite des Stärkeauf- und –abbaus als auch die Regulation derselben auf transkriptioneller sowie translationaler und post-translationaler Ebene. Ein wesentlicher Faktor, der die Qualität der Kartoffelknollen im Sinne des Stärkegehaltes beeinflusst, ist das Klima. Die durch den Klimawandel bedingten Veränderungen – erhöhte Temperaturen und vermehrte Trockenheit – haben verheerende Auswirkungen auf die Erträge der Kartoffel die vor allem durch deren Stärkegehalt bestimmt werden. Detaillierte Einblicke in die Mechanismen, die durch abiotischen Stress in der Kartoffel ausgelöst werden und wie diese mit der Entwicklung der Knollen in Zusammenhang stehen, können bei der Züchtung resistenter Sorten von Bedeutung sein.

Im Rahmen dieser Arbeit wurden die am Stärkestoffwechsel beteiligten Enzyme in der Kartoffel auf Genomebene beschrieben und deren Expression anhand von Microarray-Experimenten untersucht. Es konnten Blatt- und Knollenspezifisch exprimierte Isoformen sowie neue, bisher unbeschriebene Isoformen identifiziert werden. Durch Ko-Expressionsanalyse mit Schlüsselenzymen der Stärkesynthese und des Stärkeabbaus in Kartoffelknollen wurden Transkriptionsfaktoren identifiziert, die potentiell an der Regulation des Stärkestoffwechsels beteiligt sein könnten.

Um die Faktoren, die an der Regulation des Stärkestoffwechsels sowie an der Determinierung von sink- und source-spezifischen Stoffwechselwegen beteiligt sind zu identifizieren, wurden Kartoffelpflanzen während der Knollenwachstumsphase einer Periode abiotischen Stresses (Hitze) ausgesetzt. Hitzestress beeinträchtigt die Knollenbildung sowie deren Wachstum und kann zu sekundärem Knollenwachstum („second-growth", „Zwiewuchs") führen. Diese morphologische Reaktion auf Stress lässt vermuten, dass die „sink-source" Identität gestört wird und eine Hemmung des Stärkestoffwechsels damit einhergeht. Um dies zu untersuchen wurden Kartoffelpflanzen unterschiedlicher Sorten zu unterschiedlichen Zeitpunkten ihrer Entwicklung einer Periode von Hitzestress ausgesetzt. Hitzestress während der Füllphase der

Knollen führte bei einigen Kartoffelsorten zum vermehrten Auftreten von Zwiewuchs. Am stärksten konnte dieses Phänomen bei der Sorte Agria beobachtet werden. Die transkriptionelle Untersuchung von primären und sekundären Knollen der Sorte Agria zeigte, dass diese sich stark in ihren Genexpressionsmustern unterschieden. Insgesamt waren anabole Prozesse, wie beispielsweise die Stärkesynthese, in primären Knollen herunterreguliert, während sie bei sekundären Knollen tendenziell hochreguliert waren. Diese Genexpressionsmuster wurden von der Expression des knolleninduzierenden SP6A widergespiegelt. Darüber hinaus konnte dessen Expression in Blättern als Biomarker für die Knolleninduktion bestätigt werden. Dabei führte Hitzestress, je nach Zeitpunkt der Applikation, zu einer starken Absenkung der SP6A-Expression sowie zur Hemmung der Knollenbildung und des Knollenwachstums.

Die Ausbildung von Zwiewuchs weist auf das vorzeitige Brechen der Keimruhe hin, sodass ein Zusammenhang zwischen der Neigung zum Zwiewuchs und der Länge der Dormanz angenommen wurde. Um das Phänomen des Zwiewuchses genauer zu untersuchen, sowie den Zusammenhang von Zwiewuchs und Dormanz zu beleuchten, wurden drei Kreuzungspopulationen der Kartoffelsorten angebaut, die in vorherigen Experimenten charakterisiert wurden. Anpassungen der Wachstumsbedingungen, d.h. kleinere Töpfe und Kurztag, ermöglichten den gleichzeitigen Anbau einer großen Anzahl von Pflanzen in Phytokammern, um diese phänotypisch zu charakterisieren. Das Screening der drei Populationen fokussierte auf das Aussehen der Knollen und der oberirdischen Pflanzenorgane sowie die Dauer der Keimruhe nach der Ernte. Es konnten in jeder Population Linien identifiziert werden, die verhältnismäßig früh oder spät keimten. Diese wurden erneut in größerer Anzahl angebaut und während der Knollenfüllphase einer Periode von Hitzestress ausgesetzt oder unter ambienten Temperaturen belassen (Kontrolle). Die Dauer der Keimruhe konnte dadurch für alle, aufgrund ihres besonders frühen oder späten Keimverhaltens, ausgewählten Linien bestätigt werden. Nach der Ernte, jedoch vor dem Keimen der ersten Kartoffeln, wurden Proben aus dem Gewebe unterhalb der apikalen Augen einiger besonders früh oder spät keimender Linien genommen. Diese wurden verwendet um durch Genexpressionsanalyse festzustellen, welche Signal- und Stoffwechselwege bereits vor dem sichtbaren Brechen der Keimruhe aktiviert oder deaktiviert werden. Eine der besonders früh keimenden Linien, SA69/12-HotPot #57 erschien dabei besonders geeignet, da ihr Genexpressionsmuster in einer Clusteranalyse sehr nah an Proben keimender Augen angeordnet war, während die anderen Linien mehr mit dormanten Augen clusterten.

Das Genexpressionsprofil der Linie #57 zeigte einzigartige Veränderungen in der Expression von Genen, die für Enzyme der Hormon-Biosynthese kodieren. Hier fiel besonders das Pflanzenhormon Ethylen auf, dessen Biosyntheseweg bei den signifikant hochregulierten Genen repräsentiert war. Des Weiteren war die funktionelle Kategorie „Signaling"

überrepräsentiert bei den signifikant hochregulierten Genen. Hier fielen besonders einige Gene auf, die dem Phototropismus zugeordnet werden können. In Übereinstimmung mit dieser Beobachtung, konnten auch unter den herunterregulierten Genen solche identifiziert werden, die mit Phototropismus in Verbindung gebracht werden können. Dies deutet darauf hin, dass diesem Mechanismus, der bereits mit der Stressregulation in Verbindung gebracht wurde, eine Rolle bei der Regulation der Keimruhe zukommen könnte.

Um einen tieferen Einblick in die Knollenentwicklung unter Stressbedingungen zu erhalten, wurden Versuchsreihen mit unterschiedlichen Kartoffelsorten unter kombiniertem abiotischem Stress (Hitze und Trockenheit) durchgeführt. Die zweiwöchige Stressapplikation erfolgte dabei während der Füllphase der Knollen. Die Knollenentwicklung wurde durch ein optimiertes Röntgen-Computertomographie-Verfahren *in vivo* beobachtet, ohne die Knollen dabei störenden Faktoren wie Licht auszusetzen. Bei diesen Versuchsreihen wurde beobachtet, dass das Knollenwachstum innerhalb der ersten Woche der Stressapplikation stark absank und teilweise komplett gehemmt wurde. Nach Beendigung des Stresses nahmen die Knollen ihr Wachstum wieder auf und zeigten teils stark erhöhte tägliche Wachstumsraten. Dadurch konnten die Auswirkungen des Stresses bezogen auf das finale Knollenvolumen im Vergleich zu Knollen von Pflanzen unter Kontrollbedingungen quasi ausgeglichen werden. Die Expression von potenziellen Stressmarkern bestätigte, dass die veränderten Umweltbedingungen in den Knollen wahrgenommen wurden. Parallele Untersuchungen der Genexpression von Enzymen, die am Stärkestoffwechsel beteiligt sind, zeigten, dass während der Stressperiode die Stärkesynthese gehemmt wurde, sich aber nach Beendigung des Stresses wieder zu normalisieren schien.

Diese Arbeit gibt Einblicke in die Genexpression von Kartoffeln unter Stressbedingungen, insbesondere Hitze und kombinierter Hitze und Trockenheit – Stressbedingungen, die durch den Klimawandel gehäuft auftreten und daher von höchster Relevanz sind. Die Untersuchungen der Genexpression werden im Zusammenhang mit phänotypischen Anpassungen der Knollen als Reaktion auf den Stress betrachtet. Die in dieser Arbeit gewonnen Erkenntnisse können als Grundlage weiterer Untersuchungen zu den Auswirkungen des Klimawandels auf die Kartoffelproduktion dienen und bei der Züchtung stressresistenter Sorten helfen.

2   Introduction

2.1   Relevance of the potato for food, feed and feedstock

The potato plant originated from the Andes in Peru (Spooner et al., 2005) where it had been cultivated long before its discovery by Spanish conquistadors who introduced the potato to Europe in the 16th century. While it spread across the continent, it didn't gain much importance in Europe until the late 18th century, when it was strongly promoted to combat food shortages (De Jong, 2016).

Nowadays Potato (*Solanum tuberosum*) is one of the world's most important crop plants. The total world potato production is estimated at 370 million tons in 2019 (FAO, 2021). It is cultivated for its underground tubers which serve as food for humans. Potato tubers are rich in starch and contain minerals like potassium and magnesium and vitamins like vitamin C and vitamins of the B-complex as well as essential amino acids. Due to its nutrient composition, it serves as staple food and animal feed and gains importance as staple food especially in the developing world, thereby playing a significant role for global food security (Birch et al., 2012). Potato plants need less land and water per ton produced compared to other important staple foods like rice and wheat, thus offering sustainable food supply (Robertson et al., 2018). Furthermore, the starch from potato tubers serves as feedstock for many industrial purposes including bioethanol production and as a food thickener. Moreover, potato starch is used in the paper and textile industry.

2.2   Sink-source transition during potato life cycle

Potato plants are able to propagate via seeds (true potato seeds) but mainly propagate vegetatively via tubers. Seed potatoes planted in the soil develop sprouts which emerge to the surface. Those sprouts are nurtured by the potato tuber which acts as the source tissue to deliver metabolites like carbohydrates and protein to the developing sprout. Once the sprout has reached the surface, leaves are formed and become photosynthetically active. Thereby the above-ground plant becomes autotrophic and can sustain its' growth through metabolites from the leaves which become the main source tissue. The fully grown plant develops flowers and approximately at the same time tuber formation is initiated under favorable environmental conditions. Tubers develop from underground stems called stolons (Fernie and Willmitzer, 2001). The developing potato tuber becomes the major sink organ, importing nutrients which are delivered by source tissues like leaves. The imported nutrients are mainly converted into starch and proteins, which serve as storage compounds in the tubers while the above-ground

plant senesces and dies. The tubers enter a stage of dormancy, where visible growth is ceased, until environmental and genetically determined signals lead to dormancy break and the development of sprouts, completing the life cycle of the potato plant (Claassens and Vreugdenhil, 2000).

2.3   Development of potato tubers as starch storage organs

Potato tubers are specialized storage organs that originate through differentiation of underground stems called stolons in a process called tuberization (Appeldoorn et al., 1999). Depending on the developmental stage, tubers represent either the major sink tissue of potato plants or the major source tissue. During tuber induction, longitudinal growth of the stolon is inhibited and radial growth of the subapical region of the stolon tip is initiated (Appeldoorn et al., 1997; Xu et al., 1998b). The tuber is subsequently formed by cell expansion, cell division and the deposition of starch and tuber-specific glycoproteins in the perimedullary region. The latter changes in carbohydrate and protein metabolism are indicative for the transition from stolon to tuber (Struik et al., 1999).

The changes in carbohydrate metabolism during tuberization are drastic. Carbohydrates are transported mainly in the form of sucrose to the stolon or tuber via the phloem. Sucrose unloading from the phloem switches from apoplastic to symplastic during tuberization (Viola et al., 2001). Apoplastic phloem unloading involves the action of cell wall bound invertase (cw-Inv, E.C. 3.2.1.26) for sucrose cleavage which has been shown to play only a minor role during tuber development. Symplastically imported sucrose is cleaved by sucrose synthase (SuSy, E.C. 2.4.1.13) into UDP-glucose and fructose (Appeldoorn et al., 1997). Before the onset of tuberization, elongating stolons exhibit high activities of invertases, both soluble and cell-wall bound types, whereas sucrose synthase is absent (Struik et al., 1999). This changes with the onset of tuberization where the activity of invertases decreases while SuSy activity drastically increases (Appeldoorn et al., 1997; Ross et al., 1994). Thus, SuSy can be regarded as the major driver of sink strength and a marker for tuberization (Zrenner et al., 1995).

2.3.1   Photoperiodic regulation of tuberization in *S. tuberosum*

The regulation of tuberization involves hormonal control and signals originating from distant parts of the plant (Struik et al., 1999). Important influence on tuberization is exerted by external factors like day length and temperature (Jackson, 1999). Under conditions favoring tuber formation i.e. long nights, low nitrogen supply and moderate temperatures, a signal (termed "tuberigen") is produced in the leaves and transported to the stolons (Kumar and Wareing, 1973). In recent years, many advances have been made to identify this "tuberigen".

Most of the current knowledge about the signaling axis between the circadian clock and flowering comes from research in *Arabidopsis thaliana*. However, research on this signaling pathway for tuberization in potato has enabled the establishment of models for this pathway (Abelenda et al., 2014, 2011; Hannapel et al., 2017; Kloosterman et al., 2013).

One key-regulator of tuber induction is the phloem-mobile signal SELF-PRUNING6A (SP6A), a homolog of *Arabidopsis thaliana* FLOWERING-LOCUS T (FT) (Navarro et al., 2011). Regulation of SP6A takes place in potato leaves from where the protein is supposedly transported via the phloem to the stolon. Other homologs of FT like SP3D are components of the flowering pathway, indicating that related mechanisms control flowering and tuberization (Abelenda et al., 2014). Both, tuberization and flowering, are regulated by the circadian clock. Photoperiod is perceived in the leaves by photoreceptors such as phytochrome B (PHYB), a starting point for the photoperiodic control of tuberization (Jackson et al., 1998, 1996). Under long-day conditions, PHYB has a stabilizing effect on CONSTANS (CO) via components of the circadian clock, leading to repression of SP6A and inhibition of tuber formation (Abelenda et al., 2016; Kloosterman et al., 2013; Rodríguez-Falcón et al., 2006). Silencing of CO leads to tuberization even under non-inductive conditions (González-Schain et al., 2012). The SP6A inhibiting effect of CO is mediated by another FT homolog, SP5G, which is activated by CO and acts as a repressor of SP6A (Abelenda et al., 2016). CO is regulated by Cycling Dof factor1 (CDF1) which suppresses *CO* transcription thereby releasing its inhibitory effect on *SP6A* (Kloosterman et al., 2013). *CDF1* allelic variation has been proposed as a key factor in potato domestication for growth in northern latitudes under long-day conditions. In photoperiod dependent potato varieties, CDF1 is controlled by circadian clock components GIGANTEA (GI) and FLAVIN-BINDING KELCH REPEAT F-BOX PROTEIN 1 (FKF1) and regulates CO (Kloosterman et al., 2013). In modern cultivars, this mechanism seems to be impaired, enabling CDF1 to suppress CO under long-day conditions, thus allowing for tuberization even under these non-inducing conditions (Kloosterman et al., 2013; Morris et al., 2014). There is evidence that the CO/SP6A axis may not be the only route of *SP6A* regulation but that there might be an additional layer of regulation between CO, SP5G and SP6A (Plantenga et al., 2019). One possible way of post-transcriptional regulation of SP6A has been described recently by Lehretz et al., (2019). They identified a putative miRNA termed suppressing expression of SP6A (SES) which might decrease *SP6A* transcript accumulation and has been implicated in the heat-dependent suppression of *SP6A* transcript abundance (Lehretz et al., 2019).

SP6A is hypothesized to form a "tuberigen activating complex" (TAC) with a basic leucine zipper (bZIP) TF called FLOWERING LOCUS D-Like (FDL1), their interaction being mediated by 14-3-3 proteins (Teo et al., 2017). In *Arabidopsis*, the flowering activating complex can activate and interact with APETALA1 (AP1) and LEAFY (LFY) thus inducing the floral pathway

(Hannapel et al., 2017; Wigge et al., 2005). The targets of the TAC in potato are yet to be discovered.

SP6A has also been proposed to interact with the clade III sucrose efflux carrier SWEET11 (sucrose will eventually be exported transporter 11; SWEET11), thereby reducing sucrose leakage into the apoplast and likely promoting symplastic sucrose transport (Abelenda et al., 2019).

In addition to negatively regulating levels of SP6A, potato CO was shown to negatively affect the transcript levels of *StBEL5*, another promoter of tuberization (González-Schain et al., 2012). BEL-like TFs are members of the three-amino acid-loop-extension (TALE) superfamily. The *StBEL5* transcript is phloem-mobile and has been shown to be induced under conditions favorable for tuberization and to enhance tuber formation (Banerjee et al., 2006). In the stolon, the StBEL5 protein is expressed and together with potato homeobox 1 (POTH1), a KNOX-type TF, as an interacting partner, has been suggested to target genes involved in growth processes and regulate gibberellic acid content in stolons (Chen et al., 2004; Lin et al., 2013; Sharma et al., 2016). Furthermore, StBEL5 is suggested to regulate *SP6A* in the leaves and in the stolons (Sharma et al., 2016) as well as *CDF1* (Kondhare et al., 2019), and could therefore be one of the alternative routes for SP6A regulation (Plantenga et al., 2019). While StBEL5/POTH may pose an additional stimulus for tuber formation and may regulate processes required for tuberization, they cannot alone induce tuberization (Abelenda et al., 2011).

Another potential regulator of tuberization is the micro-RNA 172 (*miR172*). It has been demonstrated that tuberization is induced when *miR172* overexpressing scions were grafted onto wild-type stocks of potato, but not the other way around, suggesting that *miR172* has a role in modulating the tuberization signal but isn't the signal itself (Martin et al., 2009). In *Arabidopsis*, *miR172* is regulated in a PHYB- and photoperiod-dependent way by GI, but not by CO (Jung et al., 2007). Interestingly, in potato plants overexpressing *miR172*, StBEL5 is also upregulated (Banerjee et al., 2006).

miR156 is another micro-RNA which has been proposed to be phloem-mobile and implicated in the regulation of tuberization (Bhogale et al., 2014; Kondhare et al., 2020). Overexpression of *miR156* was associated with decreased levels of SP6A and *miR172* and decreased below-ground tuber yield (Bhogale et al., 2014). However, the exact role of miR156 in the regulation of tuberization has yet to be elucidated.

Models for the regulation of tuberization by SP6A, StBEL5 and the micro-RNAs *miR172* and *miR156* have been proposed, yet, more components will likely be discovered in the future to complete the network (Abelenda et al., 2011; Hannapel et al., 2017; Sarkar, 2008; Kondhare et al., 2020).

2.3.2 Hormonal regulation of tuberization

Tuberization is also controlled by hormonal regulation. However, the exact roles of phytohormones in tuberization and how they are regulated are mostly still obscure. Gibberellic acid (GA), when applied to potato plants, has been shown to promote stolon elongation but to inhibit tuber formation (Cheng et al., 2018; Jackson and Prat, 1996; Kumar and Wareing, 1974). At the onset of tuberization, GA levels decline sharply via down-regulation of GA synthesis and up-regulation of GA oxidation (Bou-Torrent et al., 2011; Kloosterman et al., 2007). Furthermore, overexpression of the GA-degrading enzyme GA 2-oxidase (StGA2ox1) led to earlier *in vitro* tuberization while plants with reduced expression of StGA2ox1 showed delayed *in vitro* tuberization (Kloosterman et al., 2007), indicating the inhibiting role of GA on tuber initiation.

The role of Abscisic acid (ABA) has been proposed as a stimulant of tuberization. It is often regarded as a regulator that counteracts GA-stimulated processes (Xu et al., 1998a). Promotive effects of exogenously applied ABA on tuber initiation and formation have been described in potato (Menzel, 1980). Correlative data confirm that ABA levels increase relative to GA under tuber inducing conditions, like e.g. low nitrogen supply (Krauss and Marschner, 1982; Machackova et al., 1998).

Further roles of plant hormones like auxin (Roumeliotis et al., 2013, 2012; Xu et al., 1998a), cytokinin (Tao et al., 2010) and jasmonic acid (Begum et al., 2022; Sohn et al., 2011) in the process of tuberization have been proposed. However, a clear picture is still elusive (Fernie and Willmitzer, 2001).

2.4 Starch metabolism in potato plants

In the potato plant, long-term storage of energy in the form of starch is located in the potato tuber. On the other side, in the leaves of the potato plant, transitory starch is synthesized during the day and degraded during the night and thus serves as short-term energy storage.

Potato starch is composed of two fractions, branched amylopectin and linear amylose and is synthesized inside plastids, where both polymers are associated in semi-crystalline, water-insoluble granules through the orchestrated action of various enzymes (Lloyd and Kossmann, 2015; Sonnewald and Kossmann, 2013). As depicted in Figure 1 and described in Van Harsselaar et al. 2017, the starting point for starch biosynthesis in the plant is the generation of photoassimilates in the Calvin-Benson-Cycle in source leaves. In form of Fructose-6-phosphate (F6P), these can be converted to starch in the chloroplasts of the leaves or as triose-phosphates (TP) transported to the cytosol via the triose-phosphate/phosphate translocator (TPT) in exchange for inorganic phosphate (Pi) where they can be metabolized to

the plant's major transport carbohydrate sucrose. In both compartments, F6P is synthesized and subsequently converted by phosphoglucoisomerase (PGI, E.C. 5.3.1.9) into glucose 6-phosphate (G6P) and into glucose 1-phosphate (G1P) by phosphoglucomutase (PGM, E.C. 5.4.2.2). Plastidial G1P can directly be used for starch biosynthesis in the chloroplast (Bahaji et al., 2014). In the cytosol, G1P is metabolized to sucrose via UDP-glucose and sucrose 6-phosphate and as such can be transported through the phloem to sink tissues like the growing tubers of the potato plant. After cleavage by sucrose synthase (SuSy, E.C. 2.4.1.13) into UDP-glucose and fructose, UDP-glucose is converted to G1P by UDP-glucose pyrophosphorylase (UGPase). G1P subsequently is transferred to G6P by cytosolic PGM which can be imported into the amyloplast by the G6P translocator (GPT). In the amyloplast G6P is then reconverted into G1P by plastidial PGM and as such can serve as a substrate for starch biosynthesis (Nakamura, 2015).

Figure 1: Proposed pathway of starch metabolism in leaves and tubers of potato.

a) In source leaves, photoassimilates are generated in the Calvin-Benson-Cycle. In form of F6P, these can be converted to G1P in two subsequent steps catalyzed by PGI and PGM. G1P serves as substrate for AGPase for starch biosynthesis. TPs from the Calvin-Benson-Cycle can also be transported to the cytosol via the TPT in exchange for Pi where they can be metabolized e.g. to sucrose. b) In the tuber, sucrose is cleaved by SuSy into UDP-glucose and fructose. UDP-glucose is converted to G1P by UGPase. G1P subsequently is transferred to G6P by cytosolic PGM which can be imported into the amyloplast by GPT. In the amyloplast G6P is then reconverted into G1P by plastidial PGM and as such can serve as a substrate for starch biosynthesis (figure taken from Van Harsselaar et al. 2017).

The first committed step of starch biosynthesis is the formation of ADP-glucose from G1P and ATP releasing inorganic pyrophosphate (PPi) by ADP-glucose pyrophosphorylase (AGPase, EC 2.7.7.27), a heterotetrameric enzyme consisting of two large (APL) and two small (APS) subunits in the plastid. This step is rendered irreversible upon hydrolysis of PPi to Pi by a high activity of inorganic pyrophosphatase (IP, E.C. 3.6.1.1) (Nakamura, 2015; Stitt and Zeeman, 2012). Glucan chain elongation is catalyzed by starch synthases (SS, EC 2.4.1.21) belonging to the family of glycosyltransferases which use ADP-glucose as substrate for the transfer of the glucosyl moiety to the reducing end of α-(1→4)-linked glucan chains. Amylose chain elongation is mainly catalyzed by a granule-bound form of SS (GBSS), while amylopectin is synthesized by the action of soluble SS as well as branching and debranching enzymes. Starch branching enzymes (SBE, EC 2.4.1.18) cleave internal α-(1→4)-bonds and transfer the reducing ends to C6 hydroxyl groups to produce α-(1→6)-linked branch points (Tetlow et al., 2004). The action of debranching enzymes like isoamylase (ISA, EC 3.2.1.68) and limit dextrinase (LDE, EC 3.2.1.41) as well as degradative enzymes like α-amylases (AMY, EC 3.2.1.1) and β-amylases (BAM, EC 3.2.1.2) is needed to establish the complex structure of starch (D'Hulst and Mérida, 2010).

One prerequisite for starch breakdown is glucan phosphorylation by glucan, water dikinase (GWD, E.C. 2.7.9.4) and phosphoglucan, water dikinase (PWD, E.C. 2.7.9.5). Both enzymes introduce phosphate esters in the amylopectin, but while GWD phosphorylates glucose units at the C-6 position, PWD transfers phosphate esters to the C-3 position. Amylopectin phosphorylation is thought to increase the accessibility to the starch granule for glucan hydrolytic enzymes (Edner et al., 2007; Hejazi et al., 2008). However, phosphate hydrolyzing activity of phosphoglucan phosphatases like starch excess 4 (SEX4, E.C. 3.1.3.48) and Like starch-excess Four2 (LSF2) is required for complete starch degradation possibly due to the interference of phosphate in the exo-amylolytic activity of BAM (Edner et al., 2007; Kotting et al., 2009; Santelia et al., 2011). Additionally, debranching enzymes hydrolyzing the α-1,6-branch points of the glucans as well as disproportionating enzyme (DPE, E.C. 2.4.1.25) play an important role in starch degradation. Alpha-glucan phosphorylase (PHO, E.C. 2.4.1.1) releases G1P from glucan chains but may also play a role in starch biosynthesis. The exact role of Pho is not yet clear (Zeeman et al., 2010). The products of starch breakdown, mainly maltose and glucose (Weise et al., 2004), can be exported from the plastid into the cytosol via the maltose transporter (MEX1) (Niittylä et al., 2004) or the glucose transporter (GLT) (Cho et al., 2011), where they can be metabolized by cytosolic glucan-processing enzymes (Lu and Sharkey, 2004).

Starch breakdown can thus be described as the highly concerted action of various enzyme activities acting interdependently to release soluble glucans from the starch granule into the stroma.

2.5 Regulation of starch metabolism

As described in Van Harsselaar et al., 2017, the pathways of starch biosynthesis and degradation are thought to be basically similar in leaves and tubers, involving the same set of enzymes (Ferreira et al., 2010; Tetlow et al., 2004), differing mainly in substrate origin. It is clear though, that the regulation of these pathways has to be different in both tissues explaining the different rates of starch turnover.

In leaves, starch is synthesized and degraded diurnally, serving as a nocturnal energy resource to maintain energy supply for biological processes. Starch in potato tubers is accumulated and stored over a long period of time and serves as energy supply for the outgrowth of developing buds and shoots. Unlike in leaves, where ATP is generated during photosynthesis, in tubers, ATP which is needed for starch biosynthesis has to be imported into the plastid via the plastidic nucleotide transporter (NTT). Moreover, the origin of glucosyl donors for starch biosynthesis differs between phototrophic and heterotrophic tissue plastids. In leaf chloroplasts, the generation of ADP-glucose is directly linked to the generation of photoassimilates in the Calvin-Benson-Cycle via two enzymatic steps. Phosphoglucoisomerase (PGI, E.C. 5.3.1.9) isomerizes fructose-6-phosphate (F6P) into glucose-6-phosphate (G6P) which is converted into G1P by phosphoglucomutase (PGM, E.C. 5.4.2.2) (Bahaji et al., 2014). The glucosyl donor for tuber starch biosynthesis is derived from sucrose which is transported from photosynthetically active leaf tissues to the developing tuber. Sucrose is the main carbohydrate transport form in the phloem of plants. In leaves, sucrose is synthesized in the cytosol starting from triose-phosphates (TP) originating from the Calvin-Benson-Cycle in chloroplasts. TP are transported to the cytosol via TPT in exchange for Pi. In the cytosol, TP is converted to F6P via the action of cytosolic Aldolase (E.C. 4.1.2.13) and fructose-bisphosphatase (FBPase, E.C. 3.1.3.11). Subsequently, F6P is metabolized to G1P by the cytosolic forms of PGI and PGM. G1P is converted to UDP-glucose by the enzyme UDP-glucose pyrophosphorylase (UGPase, E.C. 2.7.7.9). Together with F6P, UPD-glucose is converted to sucrose-6-phosphate by the enzyme sucrose-6-phosphate synthase (SPS, E.C. 2.4.1.14). A final dephosphorylation step, catalyzed by sucrose phosphatase (SPP, E.C. 3.1.3.24) yields the final product sucrose which is loaded into the phloem and transported to sink tissues (Ruan, 2014).

"Many genes coding for enzymes involved in starch metabolism are organized in gene families. Members of these families may play distinct roles in starch biosynthesis and breakdown in source and sink tissues, respectively (Zeeman et al., 2010). In rice, this has been shown for isoforms of ADP-glucose pyrophosphorylase (AGPase), starch branching enzyme (SBE), starch phosphorylase (PHO), disproportionating enzyme (DPE), starch synthase (SS) and debranching enzyme (DBE) by qRT-PCR analysis of leaf and endosperm tissues (Nakamura, 2015; Ohdan et al., 2005).

Regulatory mechanisms have been described concerning post-translational modifications like protein-protein interactions, phosphorylation and redox regulation (Bahaji et al., 2014; Kotting et al., 2009; Sparla et al., 2006; Tiessen et al., 2002). In addition, accumulation of starch metabolic enzymes is controlled at the transcriptional level. Transcript abundance of many starch genes is regulated by the circadian clock and by sugar availability (Kötting et al., 2010; Lu et al., 2005; Smith et al., 2004). In *Arabidopsis* leaves, expression of the *GBSS1* gene was shown to be controlled by two clock transcription factors (TFs), namely the Myb-related CIRCADIAN CLOCK ASSOCIATED 1 (CCA1) and LATE ELONGATED HYPOCOTYL (LHY) (Tenorio et al., 2003), while in rice endosperm, *GBSS* was reported to be regulated by two interacting proteins belonging to the MYC and EREBP families (Zhu et al., 2003). Further evidence for transcriptional regulation of starch metabolism comes from barley, where a sugar-inducible TF, SUSIBA2, belonging to the WRKY class TFs, was shown to bind to the promoter of the ISA1 gene and exhibited an expression pattern similar to ISA1 (Sun et al., 2003). In a co-expression analysis in rice, putative regulators of starch biosynthesis were identified and functional studies showed that an APETALA2 (AP2)/EREBP-type TF negatively regulates genes involved in starch biosynthesis and is important for starch content and structure (Fu and Xue, 2010). In sweet potato, SRF1, a Dof protein, was found to have an indirect positive effect on starch biosynthesis (Tanaka et al., 2009). An effect on starch gene expression was also described in relation with FLO2 (FLOURY ENDOSPERM2) in rice seeds (She et al., 2010). These examples emphasize the significance of transcriptional regulation of starch metabolism which still remains largely elusive." (Van Harsselaar et al. 2017).

2.6   Potato physiology under abiotic stress

The Potato plant is grown worldwide and thus, is subjected to a wide variety of climatic conditions. It originated in the Andes of South America, where potatoes were cultivated at high altitudes in regions characterized by short day length, moderate temperatures, high humidity and high light intensity (Levy and Veilleux, 2007). Selection for variants, where tuber induction was not inhibited by long photoperiods, enabled the cultivation of potatoes as crop plant also in European countries. Moderate temperatures in combination with elongated photoperiods allow for high yields in European countries but also parts of the northern USA. At the same time, potatoes are susceptible to high temperatures which inhibit tuber formation in both, short and long days but the inhibitory effect of heat is much greater in long photoperiods (Jackson, 1999). Similarly, drought negatively affects tuberization.

"Independent climate change models predict that global temperatures will increase, and patterns of rainfall will change entailing periods of drought on the one hand and floods on the other hand (Cook et al., 2007). As a result, plants will be - and are already - exposed to

changing environmental conditions which cause substantial yield losses (Ciais et al., 2005; Hijmans, 2003). […] In potato, both, heat and drought, have been shown to inhibit tuberization causing decreased tuber number, size and quality (Deblonde and Ledent, 2001; Levy, 1985). These adverse effects are caused by an interference of heat and drought with the formation of the tuberization signal SP6A (Hastilestari et al., 2018; Navarro et al., 2011), carbon allocation to developing tubers (Gawronska et al., 1992; Wolf et al., 1990), and tuber filling (Krauss and Marschner, 1984). In addition, starch mobilization has been described during both, heat and drought stress, leading to increased reducing sugar content of the tubers (Dahal et al., 2019)." (Van Harsselaar et al., 2021). In the leaves, heat stress leads to a reduction of photosynthesis (Hammes and De Jager, 1990) and an increase of photorespiration (Salvucci and Crafts-Brandner, 2004), thus decreasing the leaves' source capacity and reducing the export of metabolites to sink-tissues like the tuber (Wolf et al., 1991).

Abiotic stress like heat and drought can also lead to second-growth of potato tubers. Several forms of second-growth have been described like elongated tubers, bottlenecks, knobby tubers, secondary tuber formation and sprouted tubers (Bodlaender et al., 1964). Second-growth has been suggested to be the result of a reversal of tuber induction which can be elicited by a change in the conditions that led to the induction of tuberization (Van Den Berg et al., 1990). It has further been hypothesized that tuber dormancy is broken by high temperatures and/or severe drought leading to heat sprouting of the tuber and eventually the formation of a secondary tuber either directly connected to the primary tuber or connected via a stolon (see Bodlaender et al., 1964 and references therein). In primary tubers, glassiness, a symptom of decreased starch content, has often been reported, leading to quality loss and inedibility (Lugt, 1960). While it is hypothesized that the secondary tuber is dominant over the primary tuber with respect to growth and substrate allocation (Lugt et al., 1964), the role of the primary as a source of nutrients has not been elucidated until now.

Overall, the effects of heat and drought, especially when present over longer periods of time are detrimental to potato yield and quality. More knowledge about underlying processes and their regulation as well as factors leading to higher resistance against these stresses is required to enable the breeding of resistant potato plants.

2.7 Aims of this thesis

Abiotic stress factors like heat and drought have a detrimental impact on potato tuber development and yield. These environmental cues influence sink-source signaling and partitioning and negatively affect tuber formation. The signaling network leading to the induction of tuberization has recently become clearer and interference of stress has been observed. Metabolic processes which are linked to tuber formation, like starch biosynthesis

are also impaired under abiotic stress conditions. However, how metabolic processes like starch biosynthesis are regulated in the potato tuber is an unanswered question yet. In order to shed light on the regulation of starch biosynthesis, the roles of enzymes involved in this process in the potato tuber need to be established. Currently, it is unclear whether there are specific isoforms which are predominantly involved in transient starch turnover in leaves or in storage starch metabolism in tubers. Yet, this knowledge would facilitate the identification of regulatory mechanisms involved in storage starch formation.

Therefore, one aim of this thesis was to identify enzymes involved in transient starch metabolism in potato leaves and those involved in storage starch metabolism in tubers. Detailed genomic analysis and annotation of genes encoding enzymes involved in starch metabolism was conducted in this thesis to reach this aim. Expression patterns were observed and compared between leaves and tubers to identify tissue-specific isoforms. Furthermore, correlation analysis was used to find co-expressed entities which might have a role in regulating these genes as identifying potential regulators of starch metabolism was another goal of this work. In this regard, the formation of second-growth of potato tubers is a remarkable example of impaired sink-source signaling. As heat stress has been shown to inhibit tuberization and to lead to impaired tuber formation and induction of second-growth, heat was applied to potato plants to switch off tuber formation. Subsequent recovery under ambient temperatures was used to switch tuber formation back on. The formation of second-growth is supposedly linked to premature dormancy break of the primary tuber. Furthermore, a transition from source to sink may happen in primary tubers in response to environmental changes which might leave them as the nutrient source for the secondary tuber. The patterns of gene expression in primary and secondary tubers were analyzed to gain insight into metabolic changes and identify possible regulatory mechanisms in these tubers.

To investigate the link between heat stress and the regulation of dormancy further, cross-breeding populations segregating in their response toward abiotic stress were characterized. Transcriptomic differences between lines exhibiting early and late sprouting of tubers were analyzed to find out about the processes potentially underlying the timing of dormancy break and the role that heat stress plays in shifting dormancy break toward an earlier time point.

For the analysis of potatoes during the growth period it is important to know in which stage of their development they are. Since they grow belowground, a visual assessment is impossible under normal conditions. To gain more insight into the phenotypic response of potato tubers to periods of abiotic stress, an x-ray CT work-flow was implemented enabling the observation of potato tubers before, during and after a period of combined heat and drought stress. Furthermore, the implications of the stress period on selected marker genes of starch metabolism and stress response were analyzed.

3 Results

3.1 *In silico*-analysis of starch metabolism genes and their expression

Sequencing and publication of the potato genome in 2011 (The Potato Sequencing Consortium (PGSC), 2011) enables the identification of unknown or incompletely known genes and their products as well as the examination of their genomic structure and organization. Enzymes involved in starch biosynthesis have been subject to numerous studies and their function and sequences have been described (Schwarte et al., 2015; Sonnewald and Kossmann, 2013), but their tissue specificity remains elusive. Many functional studies made use of the model organism *Arabidopsis thaliana* to characterize the role of selected enzymes in starch biosynthesis and degradation (e.g. Edner et al., 2007, Roldán et al., 2007) but this solely allows drawing conclusions about their function in transitory starch turnover in leaves. The identification of enzymes involved in storage starch metabolism in potato tubers will enable targeted manipulation of this pathway and the elucidation of its underlying regulatory mechanisms.

In this chapter, the confirmation of available annotations of genes encoding starch metabolism associated enzymes and the identification so far unknown potential isoforms *in silico* is described. Furthermore, leaf and tuber specific isoforms of enzymes involved in starch metabolism are determined by comparative gene expression analysis. The data presented in this chapter has been published in Van Harsselaar et al., 2017 and has been updated according to recent developments.

3.1.1 Annotation of genes encoding enzymes of potato starch metabolism

The basis for the identification of genes encoding enzymes of starch metabolism was a review published in 2013 by Sonnewald and Kossmann describing starch-related genes in *Arabidopsis.* Additionally, genes encoding proteins which have been shown to participate in starch metabolism more recently and therefore had not been considered in the review article were accounted for, e.g. Early Starvation (ESV) and Protein Targeting to Starch (PTST) (Feike et al., 2016; Helle et al., 2018; Seung et al., 2015). Coding sequences of *Arabidopsis* genes were downloaded and imported into the Geneious 5.5.6 software (http://www.geneious.com, Kearse *et al.*, 2012) where they were blasted against the scaffold sequences of the potato genome. For accurate annotation, sequences from *Arabidopsis* were also blasted in NCBI (http://www.ncbi.nlm.nih.gov/) against solanaceous species to obtain sequences with higher similarity to potato or even potato sequences. After alignment of the obtained sequences to

the potato genomic sequence, exons and introns were annotated as described previously (PhD thesis Anja Hartmann, 2011) and introns were removed to receive an open reading frame (ORF). If an ORF was identified, it was compared to the transcript sequences available online on the PGSC homepage (http://potato.plantbiology.msu.edu/) to verify the annotation.

"Based on sequence similarity 44 out of 46 *Arabidopsis* open reading frames (ORF) were assigned to homologous potato transcripts (Table 1). No homologous sequences were found for At4g24450 (GWD2), At2g21590 (APL4) and At5g17523 (similar to MEX1) in the Spud DB (Hirsch et al., 2014) or the NCBI databases. For all other *Arabidopsis* query sequences, a homologous sequence was found in the potato genome (Table 1).

Table 1: ***Arabidopsis thaliana*** **homologous genes of** ***Solanum tuberosum*** **(modified after Van Harsselaar et al. 2017)**

Results

Enzyme	PGSC Gene ID	PGSC Transcript ID	iTAG Transcript ID	NCBI Reference Sequence / GenBank	Locus At
ADP-glucose pyrophosphorylase large subunit 1 (AGPL1)	PGSC0003DMG400009026	PGSC0003DMT400023304	Sotub01g024100.1.1	NM_001288466.1	At5g19220
ADP-glucose pyrophosphorylase large subunit 2 (AGPL2)	PGSC0003DMG400015952	PGSC0003DMT400041215	Sotub07g011850.1.1	NM_001318669.1	At1g27680
ADP-glucose pyrophosphorylase large subunit 3 (AGPL3)	PGSC0003DMG400000735	PGSC0003DMT400001935	Sotub01g047210.1.1	X61187.1	At4g39210
ADP-glucose pyrophosphorylase small subunit 1.1 (AGPS1.1)	PGSC0003DMG400031084	PGSC0003DMT400079823	Sotub07g023520.1.1	NM_001288195.1	At5g48300
ADP-glucose pyrophosphorylase small subunit 1.2 (AGPS1.2)	PGSC0003DMG400046891	PGSC0003DMT400097320	Sotub12g006530.1.1		At5g48300
ADP-glucose pyrophosphorylase small subunit 2 (AGPS2)	PGSC0003DMG400025218	PGSC0003DMT400064936	Sotub08g010520.1.1		At1g05610
Alpha-amylase 1.1 (AMY1.1)	PGSC0003DMG400007974	PGSC0003DMT400020591	Sotub04g031900.1.1	M81682.1	At4g25000
Alpha-amylase 1.2 (AMY1.2)	PGSC0003DMG400020603	PGSC0003DMT400053110	Sotub03g021150.1.1	A21347.1	At4g25000
Alpha-amylase 2 (AMY23)	PGSC0003DMG400009891	PGSC0003DMT400025601	Sotub04g035480.1.1	M79328.1	At1g76130
Alpha-amylase 3 (AMY3)	PGSC0003DMG401017626	PGSC0003DMT400045435	Sotub05g011310.1.1		At1g69830
Alpha-amylase 3-like (AMY3-like)			Sotub02g012780.1.1		At1g69830
Alpha-glucan phosphorylase 1a (PHO1a)	PGSC0003DMG400007782 PGSC0003DMG400003495 PGSC0003DMG400002479	PGSC0003DMT400020094 PGSC0003DMT400008970 PGSC0003DMT400006337		D00520.1	At3g29320
Alpha-glucan phosphorylase 1b (PHO1b)	PGSC0003DMG400028382	PGSC0003DMT400072963	Sotub05g005530.1.1	NM_001288199.1	At3g29320
Alpha-glucan phosphorylase 2a (PHO2a)	chr00:18163346..18176781			M69038.1	At3g46970
Alpha-glucan phosphorylase 2b (PHO2b)	PGSC0003DMG400031765	PGSC0003DMT400081273	Sotub02g020370.1.1		At3g46970
ATP-ADP antiporter 1 (NTT1)	PGSC0003DMG400005612	PGSC0003DMT400014304	Sotub03g033540.1.1		At1g80300
ATP-ADP antiporter 2 (NTT2)	PGSC0003DMG400028641	PGSC0003DMT400073724	Sotub12g021790.1.1	NM_001287865.1	At1g15500
Beta-amylase 1 (BAM1)	PGSC0003DMG400001549	PGSC0003DMT400003933	Sotub09g026990.1.1		At3g23920
Beta-amylase 2 (BAM2)	PGSC0003DMG400024145	PGSC0003DMT400062050	Sotub08g006590.1.1		At5g45300
Beta-amylase 3.1 (BAM3.1)	PGSC0003DMG400005612	PGSC0003DMT400004686	Sotub08g032340.1.1	NM_001288243.1	At4g17090
Beta-amylase 3.2 (BAM3.2)	PGSC0003DMG402020509	PGSC0003DMT400052839	Sotub08g006070.1.1		At4g17090
Beta-amylase 4 (BAM4)	PGSC0003DMG400012129	PGSC0003DMT400031627	Sotub08g027460.1.1		
Beta-amylase 6.1 (BAM6.1)	PGSC0003DMG400026199	PGSC0003DMT400067403	Sotub07g021140.1.1		At2g32290
Beta-amylase 6.2 (BAM6.2)	PGSC0003DMG400026166	PGSC0003DMT400067289	Sotub07g021110.1.1		At2g32290
Beta-amylase 6.3 (BAM6.3)	PGSC0003DMG400026198	PGSC0003DMT400067400	Sotub07g021090.1.1		At2g32290
Beta-amylase 7 (BAM7)	PGSC0003DMG400000169	PGSC0003DMT400000485	Sotub01g031940.1.1		At2g45880
Beta-amylase 9 (BAM9)	PGSC0003DMG400010664	PGSC0003DMT400027659	Sotub01g021680.1.1		At5g18670
Branching enzyme I.1 (SBE1.1)	PGSC0003DMG400022307	PGSC0003DMT400057446	Sotub07g029010.1.1		At3g20440
Branching enzyme I.2 (SBE1.2)			Sotub07g025820.1.1		At3g20440
Branching enzyme II (SBE2)			Sotub09g011090.1.1	NM_001288538.1	At2g36390
Branching enzyme III (SBE3)	PGSC0003DMG400009981	PGSC0003DMT400025846	Sotub04g035850.1.1	NM_001288254.1	At5g03650
Disproportionating enzyme 1 (DPE1)	PGSC0003DMG400016589	PGSC0003DMT400042739	Sotub04g021520.1.1	NM_001287852.1	At5g64860
Disproportionating enzyme 2 (DPE2)			Sotub02g006950.1.1	NM_001288247.1	At2g40840
Early Starvation 1 (ESV1)	PGSC0003DMG400029318	PGSC0003DMT400075384	Sotub12g027850.1.1	XM_006342482.2	At1g42430
Early Starvation 2 (ESV2)	PGSC0003DMG400009975	PGSC0003DMT400025823	Sotub04g035730.1.1	XM_006342053.2	At1g42430
Like Early Starvation (LESV)	PGSC0003DMG400016314	PGSC0003DMT400042064	Sotub06g016860.1.1	XM_006350593.2	At3g55760
Glucan water dikinase (GWD)	PGSC0003DMG400007677	PGSC0003DMT400019845	Sotub05g014130.1.1	NM_001288123.1	At1g10760
Glucose transporter (GLT1)	PGSC0003DMG400026402	PGSC0003DMT400067884	Sotub02g029320.1.1	AF215853.1	At5g16150
Glucose-6-phosphate translocator 1.1 (GPT1.1)	PGSC0003DMG400001041 PGSC0003DMG400005602	PGSC0003DMT400002701 PGSC0003DMT400014284	Sotub07g025910.1.1		At5g54800
Glucose-6-phosphate translocator 1.2 (GPT1.2)			Sotub03g008220.1.1		At1g61800
Glucose-6-phosphate translocator 2.1 (GPT2.1)	PGSC0003DMG400005269	PGSC0003DMT400013500	Sotub05g021450.1.1	AF020816.1	At1g61800
Glucose-6-phosphate translocator 2.2 (GPT2.2)	PGSC0003DMG400025495	PGSC0003DMT400065527			At1g61800
Granule bound starch synthase 1 (GBSS1)	PGSC0003DMG400012111	PGSC0003DMT400031568	Sotub08g026990.1.1	NM_001287989.1	At1g32900
Inorganic pyrophosphatase (PPase)	PGSC0003DMG400003103	PGSC0003DMT400006028	Sotub01g043620.1.1		At5g09650
Inorganic pyrophosphatase-like (PPase-like)	PGSC0003DMG400026784	PGSC0003DMT400068875	Sotub10g017670.1.1		At5g09650
Isoamylase 1.1 (ISA1.1)	PGSC0003DMG400020699	PGSC0003DMT400053345		NM_001288008.1	At2g39930
Isoamylase 1.2 (ISA 1.2)	PGSC0003DMG400030253	PGSC0003DMT400077770	Sotub10g015570.1.1	NM_001288008.1	At2g39930
Isoamylase 2 (ISA2)	PGSC0003DMG400000954	PGSC0003DMT400002502	Sotub09g015190.1.1	NM_001287875.1	At1g03310
Isoamylase 3 (ISA3)	PGSC0003DMG402007274 PGSC0003DMG401007274	PGSC0003DMT400018766 PGSC0003DMT400018765	Sotub06g007640.1.1	NM_001288291.1	At4g09020
Limit dextrinase (LDE)			Sotub11g012510.1.1 Sotub11g012520.1.1 Sotub11g012530.1.1 Sotub11g012540.1.1		At5g04360
Maltose excess 1 (MEX1)	PGSC0003DMG400024812	PGSC0003DMT400063824	Sotub04g024480.1.1		At5g17520
Phosphoglucan phosphatase (like SEX four 1, LSF1)	PGSC0003DMG400030092	PGSC0003DMT400077364	Sotub12g017200.1.1		At3g01510
Phosphoglucan phosphatase (like SEX four 2, LSF2)	PGSC0003DMG400029073	PGSC0003DMT400074765	Sotub06g009920.1.1		At3g10940
Phosphoglucan phosphatase (SEX4)	PGSC0003DMG400015246	PGSC0003DMT400039423	Sotub03g023920.1.1	NM_001318586.1	At3g52180
Phosphoglucan phosphatase (SEX4-like)	PGSC0003DMG400027327	PGSC0003DMT400070294	Sotub11g010680.1.1	NM_001318586.1	At3g52180
Phosphoglucan water dikinase (PWD)	PGSC0003DMG400016613	PGSC0003DMT400042818	Sotub09g030460.1.1	NM_001287941.1	At5g26570
Phosphoglucoisomerase (PGI)	PGSC0003DMG400012910	PGSC0003DMT400033620	Sotub04g029550.1.1	NM_001247654.3	At4g24620
Phosphoglucoisomerase-like 1 (PGI-like1)	PGSC0003DMG400015341	PGSC0003DMT400039665	Sotub12g005010.1.1	NM_001288294.1	At5g42740
Phosphoglucoisomerase-like 2 (PGI-like2)	PGSC0003DMG400030128	PGSC0003DMT400077470			
Phosphoglucomutase 1 (PGM1)			Sotub03g007170.1.1	NM_001288352.1	At5g51820
Phosphoglucomutase 2.1 (PGM2.1)			Sotub07g017160.1.1	NM_001288404.1	At1g23190
Phosphoglucomutase 2.2 (PGM2.2)	chr04:35711900..35685400				At1g23190
Protein Targeting to Starch (PTST)	PGSC0003DMG400030609	PGSC0003DMT400078656	Sotub02g030070.1.1		At5g39790
Putative Phosphoglucomutase (pPGM)			Sotub05g017780.1.1		At1g70820
Starch Synthase I (SS1)	PGSC0003DMG402018552	PGSC0003DMT400047731	Sotub03g013130.1.1	NM_001288145.1	At5g24300
Starch Synthase II (SS2)	PGSC0003DMG400001328	PGSC0003DMT400003356	Sotub02g034860.1.1	NM_001288048.1	At3g01180
Starch Synthase III (SS3)	PGSC0003DMG400016481	PGSC0003DMT400042496	Sotub02g037340.1.1	X94400.1	At1g11720
Starch Synthase IV (SS4)	PGSC0003DMG400008322	PGSC0003DMT400021444	Sotub02g017380.1.1		At4g18240
Starch Synthase V (SS5)	PGSC0003DMG400030619	PGSC0003DMT400078688	Sotub02g030260.1.1	NM_001288111.1	At5g65685
Starch Synthase VI (SS6)	PGSC0003DMG402013540	PGSC0003DMT400035218	Sotub07g015820.1.1	NM_001247458.1	
Sucrose Synthase 1 (SuSy1)	PGSC0003DMG400015547	PGSC0003DMT400035264	Sotub07g016120.1.1		At5g20830
Sucrose Synthase 2 (SuSy2)	PGSC0003DMG400013546	PGSC0003DMT400035262	Sotub07g016110.1.1	NM_001287982.1	At5g49190
Sucrose Synthase 3 (SuSy3)	PGSC0003DMG400006672	PGSC0003DMT400017087		NM_001288308.1	At4g02280
Sucrose Synthase 4 (SuSy4)	PGSC0003DMG400002895	PGSC0003DMT400007506	Sotub12g008670.1.1	M18745.1	At3g43190
Sucrose Synthase 6 (SuSy6)	PGSC0003DMG400031046	PGSC0003DMT400079728	Sotub03g023000.1.1		At1g73370
Sucrose Synthase 7 (SuSy7)	PGSC0003DMG400016730	PGSC0003DMT400043117	Sotub02g024410.1.1		At5g37180
Triose-phosphate/phosphate translocator (TPT)	PGSC0003DMG400022832	PGSC0003DMT400058772	Sotub10g009470.1.1	NM_001287896.1	At5g46110
Triose-phosphate/phosphate translocator-like (TPT-like)			Sotub01g020040.1.1		At5g46110
UDP-glucose pyrophosphorylase 1 (UGPase1)			Sotub05g026990.1.1		At3g03250
UDP-glucose pyrophosphorylase 2 (UGPase2)	PGSC0003DMG401013333	PGSC0003DMT400034699	Sotub11g007290.1.1	NM_001288019.1	At5g17310
Vacuolar Glucose Transporter 3-like (VGT3-like)	PGSC0003DMG401010374	PGSC0003DMT400026885	Sotub03g022010.1.1		At5g59250

For the identification of isoforms of starch metabolic enzymes, a keyword search in the Spud DB database was undertaken using the enzyme names as queries. Additionally, manually corrected potato transcript sequences resulting from the homology and keyword searches were re-BLASTed against the potato genome and the sequence of the respective second-best hit was analyzed to identify putative isoforms. Therefore, the scaffold sequence of the second-best hit was extracted to enable an alignment of the transcript against this scaffold. If a sequence similar to the transcript was found within the scaffold (Figure 2), the sequence was extracted and blasted against the PGSC and NCBI databases to find the annotated transcript sequence matching the scaffold as well as already described sequences. This led to the discovery of two genes which had not been annotated, namely *PGM2.2* and *PHO2a*. *PGM2.2* could be assigned to chromosome 4 while *PHO2a* was located on an unanchored scaffold.
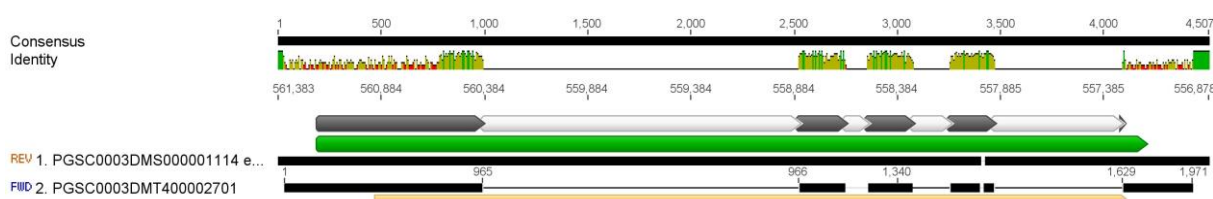
Figure 2: Alignment of the transcript sequence of GPT1.1 against the second-best BLAST hit in the potato genome scaffold database.

Eventually, predicted transcript sequences of all identified genes were compared to published mRNA sequences available on the NCBI data base via a BLAST search. Sequence alignments were conducted to check for completeness of the ORFs and the predicted protein sequences. The exon-intron structure of the genes was manually re-annotated and/or corrected, if required. Correct assignment of potato transcripts compared to the corresponding *Arabidopsis* ortholog was verified by protein sequence comparison. Phylogenetic trees were constructed using the translated ORF sequences of all putative members of a gene family. If ambiguities were encountered, a motif search was conducted using the online tool MEME (Bailey and Elkan, 1994). The presence and order of motifs was compared between sequences assuming a high degree of similarity between members of the same gene family (Jupe et al., 2012). If this was the case the identified gene was considered as an isoform." (Van Harsselaar et al. 2017).

Application of the above-mentioned strategies resulted in the identification of 81 loci coding for enzymes of starch metabolism in potato (Table 1). "In comparison to *Arabidopsis*, additional putative isoforms of AGPS1, PHO1 and PHO2, TPT, BAM3, BAM6, SBE1, GPT1 and GPT2, PPase, ISA1, SEX4, PGM2, PGI, AMY1 and AMY3 were found. The deduced transcripts of

BAM6.2, BAM6.3, SBE1.2 and ISA1.2 were highly identical to their respective paralogs but did not seem to comprise full-length transcripts. This might be either a result of an incorrect genome assembly or incomplete gene duplication events.
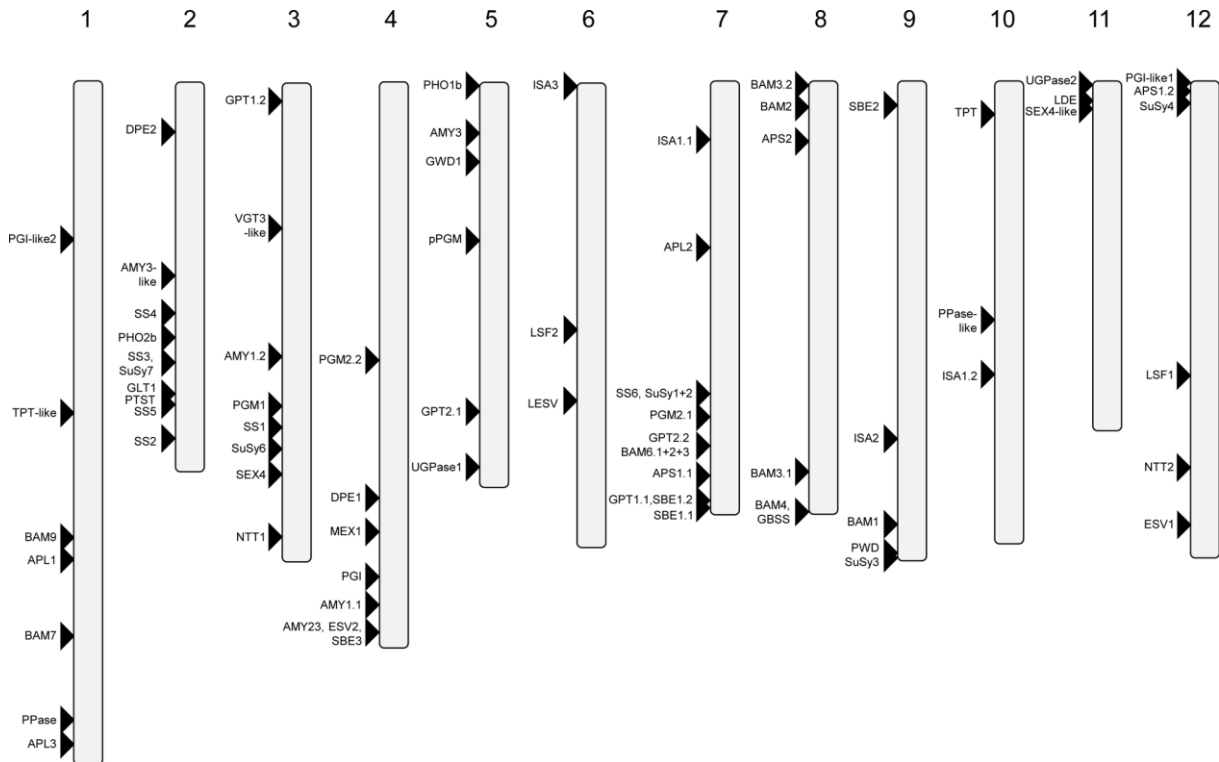
Figure 3: Ideogram of physical positions of starch metabolism enzymes in the potato genome. The relative map positions of 79 genes encoding starch metabolism genes are shown on the individual pseudomolecules depicting the chromosomes 1-12 (modified after Van Harsselaar et al. 2017).

Chromosomal positions of putative starch genes were retrieved from the Spud DB genome browser v4.03 (http://solanaceae.plantbiology.msu.edu/cgi-bin/gbrowse/potato/) and visualized using the location-based display tool on the Ensembl plants website (http://plants.ensembl.org/Solanum_tuberosum/Location/Genome, Kersey *et al.*, 2015). Manual editing allowed the visualization of genes as an ideogram (Figure 3). For two genes, *PHO1a* and *PHO2a*, no physical position could be defined since their genes are located on unanchored scaffolds, but orthologous sequences from tomato are located on chromosomes 3 and 9, respectively. This is in accordance with results from quantitative trait loci (QTL) analyses in potato that mapped two glucan-phosphorylases to those chromosomes (Chen et al., 2001; Werij et al., 2012).

Figure 3 shows that genes coding for starch metabolism enzymes are distributed over all twelve potato chromosomes. There is a concentration of *SS* (*SS2*, *SS3*, *SS4*, *SS5*) on

chromosome 2 and many genes encoding BAMs are located on chromosome 8. SuSy and ISA encoding genes are distributed across different chromosomes. An interesting finding was the discovery of two *PGM2* isoforms *PGM2.1* and *PGM2.2* which are located on chromosome 7 and 4, respectively. The sequence identity between both transcripts is 99.5%, but the corresponding genes differ significantly in their non-coding regions showing only 59% sequence similarity. However, the structure of both genes appears to be conserved. The *PGM2.2* isoform has not been predicted by the PGSC or iTAG and was identified by BLASTing the transcript sequence Sotub07g017160.1.1 against the scaffold sequences. Investigating the tomato genome available on the Sol Genomics website (https://solgenomics.net, Fernandez-Pozo et al. 2015) for *PGM2* genes revealed that only one locus is present which is localized on chromosome 4. Therefore, it is conceivable that the *PGM2.1* gene on chromosome 7 is the result of a recent gene duplication event, however this needs to be further investigated by bioinformatics analysis." (Van Harsselaar et al. 2017).

3.1.2 Identification of suitable microarray identifiers to investigate gene expression

"Two oligonucleotide-based microarray platforms (Agilent Technologies) are available for global gene expression analysis in potato. The POCI array was designed in 4x44k format based on a collection of expressed sequence tags (EST) (Kloosterman et al., 2008) while the 8x60k microarray is based on predicted transcript sequences of the DM potato genome by the PGSC (Hancock et al., 2014). In this study, experimental data of both microarray designs were used. The prerequisite for the comparative expression analysis was the identification of suitable microarray oligonucleotides (identifiers) matching the transcript of interest, particularly in case of the POCI platform. Therefore, prior to expression analysis, oligonucleotide binding accuracy to the target genes was assessed. To this end, transcript and genomic sequences of starch genes were BLASTed against the POCI database (http://apex.ipk-gatersleben.de/apex/f?p=194:1) and resulting EST sequences were aligned to the genomic sequence to allow for assessment of their corresponding oligonucleotide binding capacities to the transcript. Oligonucleotides matching the reference sequence with 85% or more identity were considered for the analysis of expression profiles. Due to the lack of matching EST-sequences or to binding of the corresponding oligonucleotides within predicted introns, no suitable oligonucleotides were found for *AMY3-like*, *AGPS1.2*, *AGPS2*, *TPT*, *TPT-like*, *GPT1.2*, all *BAM6* isoforms, *BAM7*, *BAM9*, *PGI-like2* and *pPGM* in the POCI platform.

Since oligonucleotide sequences of the 8x60k microarray were deduced from predicted transcript sequences of the DM genome, they perfectly match the corresponding transcript available at the Spud DB website. In these cases, the position of the oligonucleotide within the gene was assessed to rule out that the binding site is within a putative intron. Oligonucleotide specificity was investigated by multiple sequence alignments. The high sequence similarity

between the transcripts of some isoenzymes prevented the assignment of specific oligonucleotides discriminating the isoforms of *ISA1*, *SEX4-like*, *SBE1* and *BAM6.2* and *BAM6.3*. Table 2 lists all identifiers from both platforms that met our criteria and that were considered for further analyses." (Van Harsselaar et al. 2017).

Table 2: Valid Microarray-Identifiers used for expression analyses in this study (taken from Van Harsselaar et al. 2017)

Name	PrimaryAccession	8x60k Identifier	Systematic POCI
alpha amylase 1.1 (AMY1.1)	PGSC0003DMT400020591	CUST_29091_PI426222305	BPLI18M23TH_724
alpha amylase 1.2 (AMY1.2)	PGSC0003DMT400053110	CUST_31840_PI426222305 CUST_31863_PI426222305	MICRO.12059.C1_688 cSTS23K12TH_696
Alpha-amylase 2 (AMY23)	PGSC0003DMT400025601	CUST_7397_PI426222305 CUST_7533_PI426222305	MICRO.4817.C1_1119 MICRO.4817.C2_704
Alpha-amylase 3 (AMY3)	PGSC0003DMT400045435	CUST_33499_PI426222305	MICRO.10844.C1_1047 MICRO.10844.C2_1026 STMHI11TH_723 MICRO.4576.C1_839
Alpha-glucan phosphorylase 1a (PHO1a)	PGSC0003DMT400006337 PGSC0003DMT400020094 PGSC0003DMT400008970	CUST_52715_PI426222305	MICRO.984.C1_1323 MICRO.984.C2_3132 MICRO.984.C4_138 ACDA03110D02.T3m.scf_427
Alpha-glucan phosphorylase 1b (PHO1b)	PGSC0003DMT400072963	CUST_19133_PI426222305 CUST_19428_PI426222305 CUST_19365_PI426222305 CUST_19289_PI426222305	MICRO.5784.C1_417 MICRO.5784.C2_937 MICRO.4388.C1_905 cSTB6G20TH_366
Alpha-glucan phosphorylase 2a (PHO2a)	PGSC0003DMS000000588		MICRO.845.C1_132 MICRO.845.C2_2423
Alpha-glucan phosphorylase 2b (PHO2b)	PGSC0003DMT400081273	CUST_45149_PI426222305 CUST_45158_PI426222305	MICRO.7362.C1_869 MICRO.14642.C1_854
ATP-ADP antiporter 1 (NTT1)	PGSC0003DMT400014304	CUST_6775_PI426222305	POACX37TV_325 cSTA24O19TH_29 MICRO.1831.C1_2060
ATP-ADP antiporter 2 (NTT2)	PGSC0003DMT400073724	CUST_15514_PI426222305	bf_acdaxxxx_0055c01.t3m.scf_574 TBSK02104FH04.t3m.scf_236 MICRO.1831.C2_2451
Beta-amylase 1 (BAM1)	PGSC0003DMT400003933	CUST_5141_PI426222305	MICRO.189.C3_1092 cSTS23M18TH_384 MICRO.189.C19_907
Beta-amylase 2 (BAM2)	PGSC0003DMT400062050		MICRO.1426.C1_1953
Beta-amylase 3.1 (BAM3.1)	PGSC0003DMT400004686	CUST_35620_PI426222305	MICRO.13823.C1_1872 POACG68TP_872
Beta-amylase 3.2 (BAM3.2)	PGSC0003DMT400052839	CUST_42396_PI426222305	MICRO.13368.C1_1225
Beta-amylase 4 (BAM4)	PGSC0003DMT400031626 PGSC0003DMT400031627	CUST_10788_PI426222305 CUST_10750_PI426222305	MICRO.15855.C1_538 bf_suspxxxx_0009h07.t3m.scf_136 MICRO.2492.C1_702 bf_ivrootxx_0060e03.t3m.scf_583
Beta-amylase 6.1 (BAM6.1)	PGSC0003DMT400067403	CUST_38257_PI426222305	
Beta-amylase 7 (BAM7)	PGSC0003DMT400000485	CUST_3218_PI426222305 CUST_3148_PI426222305	
Beta-amylase 9 (BAM9)	PGSC0003DMT400027659	CUST_8549_PI426222305 CUST_8536_PI426222305	
Branching enzyme II (SBE2)	Sotub09g011090.1.1		MICRO.16220.C1_158
branching enzyme III (SBE3)	PGSC0003DMT400025846	CUST_7752_PI426222305 CUST_7612_PI426222305 CUST_7418_PI426222305 CUST_7544_PI426222305	MICRO.1689.C3_1473 MICRO.1689.C4_21
Disproportionating enzyme 1 (DPE1)	PGSC0003DMT400042739	CUST_43198_PI426222305 CUST_43195_PI426222305 CUST_43191_PI426222305	MICRO.1834.C1_1863
Disproportionating enzyme 2 (DPE2)	Sotub02g006950.1.1		bf_mxlfxxxx_0002e03.t3m.scf_310 MICRO.6841.C1_2057 MICRO.6841.C3_328
Glucan water dikinase (GWD)	PGSC0003DMT400019845	CUST_34051_PI426222305	MICRO.3453.C1_1094 MICRO.3453.C3_795 MICRO.3453.C4_1606
Glucose transporter (GLT1)	PGSC0003DMT400067882 PGSC0003DMT400067884	CUST_33731_PI426222305 CUST_33608_PI426222305	STMDP74TH_751 cSTA28H16TH_144 MICRO.1289.C2_2016
Glucose-1-phosphate adenylyltransferase, large subunit 1 (APL1)	PGSC0003DMT400023304	CUST_19529_PI426222305	MICRO.4772.C1_335 MICRO.10340.C1_351
Glucose-1-phosphate adenylyltransferase, large subunit 2 (APL2)	PGSC0003DMT400041215	CUST_16077_PI426222305	MICRO.7806.C1_974 MICRO.7806.C2_1772
Glucose-1-phosphate adenylyltransferase, large subunit 3 (APL3)	PGSC0003DMT400001935	CUST_46835_PI426222305 CUST_46813_PI426222305	MICRO.2198.C1_1938
Glucose-1-phosphate adenylyltransferase, small subunit 1.1 (APS1.1)	PGSC0003DMT400079823	CUST_49639_PI426222305	MICRO.367.C1_1738

Results

Glucose-1-phosphate adenylyltransferase, small subunit 1.2 (APS1.2)	PGSC0003DMT400097320	CUST_21291_PI426222305	
Glucose-1-phosphate adenylyltransferase, small subunit 2 (APS2)	PGSC0003DMT400064936	CUST_23457_PI426222305	
Glucose-6-phosphate translocator 1.1 (GPT1.1)	PGSC0003DMT400014284 PGSC0003DMT400002701	CUST_52676_PI426222305 CUST_48268_PI426222305	BF_CSCHXXXX_0014E05.T3M.SCF_603 MICRO.4029.C1_965 MICRO.4029.C2_1110 MICRO.4029.C4_100
Glucose-6-phosphate translocator 2.1 (GPT2.1)	PGSC0003DMT400013500	CUST_32932_PI426222305	174G02AF.esd_341 MICRO.1076.C1_1353
Glucose-6-phosphate translocator 2.2 (GPT2.2)	PGSC0003DMT400065527	CUST_50631_PI426222305 CUST_50617_PI426222305 CUST_50625_PI426222305	BPLI8C14TH_659
Granule-bound starch synthase 1 (GBSS1)	PGSC0003DMT400031568	CUST_10538_PI426222305 CUST_10857_PI426222305	MICRO.920.C2_1499 MICRO.920.C5_1
Inorganic Pyrophosphatase (PPase)	PGSC0003DMT400008028	CUST_41325_PI426222305	MICRO.1068.C1_98
Inorganic Pyrophosphatase-like (PPase-like)	PGSC0003DMT400068875	CUST_44987_PI426222305	MICRO.1068.C2_1019
Isoamylase I (ISA1)	PGSC0003DMT400053345		MICRO.7513.C1_357 MICRO.7513.C2_974
Isoamylase II (ISA2)	PGSC0003DMT400002502	CUST_30734_PI426222305	MICRO.17391.C1_799 MICRO.13258.C1_792 MICRO.12035.C1_53
Isoamylase III (ISA3)	PGSC0003DMT400018766	CUST_30862_PI426222305	MICRO.10651.C1_2421
Limit dextrinase (LDE)	Sotub11g012510.1.1 Sotub11g012520.1.1 Sotub11g012530.1.1 Sotub11g012540.1.1		MICRO.7780.C1_734 MICRO.7780.C2_1012
Maltose excess 1 (MEX1)	PGSC0003DMT400063824	CUST_31220_PI426222305	MICRO.10450.C1_752 MICRO.7618.C1_930
Phosphoglucan phosphatase (like SEX4 1, LSF1)	PGSC0003DMT400077364	CUST_6121_PI426222305	MICRO.4510.C1_1136 MICRO.4355.C1_1130
Phosphoglucan phosphatase (like SEX4 2, LSF2)	PGSC0003DMT400074765	CUST_40278_PI426222305	MICRO.1486.C1_1676
Phosphoglucan phosphatase (SEX4)	PGSC0003DMT400039423	CUST_22394_PI426222305	MICRO.1811.C1_1152 MICRO.1811.C6_939
Phosphoglucan water dikinase (PWD)	PGSC0003DMT400042818	CUST_36027_PI426222305 CUST_36019_PI426222305	MICRO.14475.C1_510 MICRO.14475.C2_1330 cSTB40I22TH_371
Phosphoglucoisomerase 1 (PGI)	PGSC0003DMT400033620	CUST_499_PI426222305 CUST_366_PI426222305	MICRO.1497.C1_1715 MICRO.1497.C2_391
Phosphoglucoisomerase-like 1 (PGI-like1)	Sotub12g005010.1.1		MICRO.299.C1_2024
Phosphoglucoisomerase-like 2 (PGI-like 2)	PGSC0003DMT400077470	CUST_37079_PI426222305	
Phosphoglucomutase 1 (PGM1)	PGSC0003DMS000001397		bf_swstxxxx_0059a07.t3m.scf_523 MICRO.1743.C1_547 MICRO.1743.C2_1865
Starch Synthase 2 (SS2)	PGSC0003DMT400003355	CUST_1543_PI426222305 CUST_1080_PI426222305	MICRO.1850.C1_2877 MICRO.1850.C2_999 bf_arrayxxx_0090e03.t7m.scf_21 bf_arrayxxx_0002h07.t7m.scf_270
Starch Synthase I (SS1)	PGSC0003DMT400047729	CUST_22194_PI426222305 CUST_22275_PI426222305	cSTA36J3TH_509 cPRO10K18TH_711
Starch Synthase III (SS3)	PGSC0003DMT400042496	CUST_18637_PI426222305	MICRO.15381.C1_1426 MICRO.4682.C1_1259 MICRO.1658.C1_1149
Starch Synthase IV (SS4)	PGSC0003DMT400021444	CUST_47388_PI426222305	MICRO.16059.C1_614 STMEK83TV_214 MICRO.594.C1_528
Starch Synthase V (SS5)	PGSC0003DMT400078688	CUST_33739_PI426222305	MICRO.7847.C1_749 MICRO.7847.C2_16 MICRO.7989.C1_747
Starch Synthase VI (SS6)	PGSC0003DMT400035218		bf_arrayxxx_0102g09.t7m.scf_372 MICRO.13669.C1_824 MICRO.9415.C1_595 MICRO.9415.C3_1041
Sucrose Synthase 1 (SUSY1)	PGSC0003DMT400035264	CUST_26861_PI426222305	MICRO.15082.C1_1400
Sucrose Synthase 2 (SUSY2)	PGSC0003DMT400035262	CUST_26822_PI426222305 CUST_26827_PI426222305	MICRO.196.C1_1191 MICRO.196.C2_1792 MICRO.196.C5_699 STMHE19TV_557

Sucrose Synthase 3 (SUSY3)	PGSC0003DMT400017087	CUST_51694_PI426222305	MICRO.16466.C1_909 bf_suspxxxx_0008E08.t3m.scf MICRO.1765.C1_1320
Sucrose Synthase 4 (SUSY4)	PGSC0003DMT400007506	CUST_13211_PI426222305	bf_cswcxxxx_0003h03.t3m.scf_323 MICRO.196.C8_1 027D03AF.esd_415
Sucrose Synthase 6 (SUSY6)	PGSC0003DMT400079728	CUST_45543_PI426222305	MICRO.2837.C1_518 cSTB36H8TH_497
Sucrose Synthase 7 (SUSY7)	PGSC0003DMT400043117	CUST_18531_PI426222305	MICRO.9800.C1_469
Triose-phosphate/phosphate translocator 1 (TPT1)	PGSC0003DMT400058772	CUST_39634_PI426222305	
UDP-glucose pyrophosphorylase 2 (UGPase2)	PGSC0003DMT400034699	CUST_25411_PI426222305	bf_stolxxxx_0025b04.t3m.scf_134 MICRO.108.C5_235
Vacuolar Glucose Transporter 3-like (VGT3-like)	PGSC0003DMT400026885	CUST_8667_PI426222305 CUST_8641_PI426222305	MICRO.1246.C3_1111 MICRO.13130.C1_755

3.2 Co-expression analysis with tuber-specifically expressed starch genes

The approach to determine putative regulators of starch biosynthesis in potato tubers was to identify starch gene isoforms that are specifically expressed in tuber tissue when compared to leaves. Therefore, tissue specificity of starch genes was analyzed. This was done based on a meta-analysis of results obtained by joint-experiment analyses on three different gene expression platforms (see Chapter 3.2.1).

Selection of starch genes for co-expression analysis was further based on their expected gene expression pattern in samples associated with starch biosynthesis, starch breakdown or homeostasis. Through co-expression analysis with these starch genes, a group of co-regulated genes could be identified. These co-regulated genes were analyzed further to identify regulatory genes like transcription factors which might play a role in controlling the expression of starch metabolic genes. Their possible roles in starch gene regulation are discussed (see chapter 4.1.3). The data presented in this chapter have been published in Van Harsselaar et al. 2017.

3.2.1 Identification of genes that are highly expressed in leaves or tubers

"For the gene expression analysis, samples taken from leaf and tuber tissues were selected from different microarray experiments (Table 3). Raw data files of the different samples were uploaded into the GeneSpring 12.6.1. GX software and were normalized together. Direct comparisons of gene expression were made within the individual platforms first. Afterwards derived results were compared between the different platforms.

Results

Table 3: Description of samples used to identify starch genes specifically expressed in tubers or leaves (modified after Van Harsselaar et al. 2017).

Experiment no.	Experiment Name	Platform	Description	Reference
1	Diurnal leaf	POCI 4x44K	cv. Solara plants were grown under 14h light / 10h dark cycle	Ferreira et al. 2010
2	Tuber induction	POCI 4x44K	cv. Solara plants were grown under LD	Ferreira et al. 2010
3	Growth velocity	POCI 4x44K	cv. Solara plants were grown under LD	Ferreira et al. 2010
4	Dormant buds	POCI 4x44K	cv. Solara plants were grown under LD for 3 months. Tubers were stored at RT for 1 week.	This study (MS)
5	Tuber sprouts	POCI 4x44K	cv. Solara plants were grown under LD for 3 months. Tubers were stored at RT for 12 weeks.	This study (MS)
6	Time course of leaves and tubers	8x60K	cv. Desirée plants were grown under LD for 8 weeks. Samples were taken thereafter every 4 hours.	Hancock et al. 2013
7	Primary and secondary tubers, normal tubers and leaves under elevated and normal temperature	8x60K	cv. Agria plants were grown under LD for 6.5 weeks, then one group was subjected to mild heat treatment for 1 week prior to a 2 week regeneration period and subsequent harvest. Leaf samples were taken before the treatment, at the end of the treatment and at the end of the growth phase	This study (JVH)
8	Tubers and leaves under normal temperaure	8x60K	Plants (cv. Agria) were grown under tuber inducing SD for 30 days, then shifted to LD for 10 days until harvest	This study (JL)
9	Tubers and leaves	RNA-seq	doubled monoploid *S. tuberosum* Group Phureja DM1-3 (DM) and *S. tuberosum* Group Tuberosum RH89-039-16 (RH)	Spud DB

To identify starch genes that are preferentially expressed in leaves or tubers, the fold-change between the mean relative expression value detected in leaf and tuber samples was calculated using the GeneSpring 12.6.1. GX software and displayed in Figure 5. For genes, whose expression was ascertainable in both microarray platforms, the log2 fold-change was calculated and depicted in Figure 4. We considered genes that were on average more than 10-fold overexpressed in one tissue to be tissue-specific. The comparison between the two array platforms revealed that several genes are specifically expressed in leaves or tubers, respectively (Figure 4). Hence, a strong tuber-specific expression was detected for *GPT2.1* and *SuSy4* followed by *SEX4* and *SS5*, whereas *BAM3.1*, *APL1* and *AMY1.1* were found to be highly expressed in leaves. Fold-change differences between leaf and tuber samples were often greater in the 8x60k array than in the POCI array but the tendency was similar (Figure 5). The only exception was *GPT2.2* whose expression was unchanged between leaf and tuber samples hybridized onto the POCI array but showed a 17.5-fold higher expression in leaves than in tubers in samples analyzed on the 8x60k array (Figure 4, Figure 5).
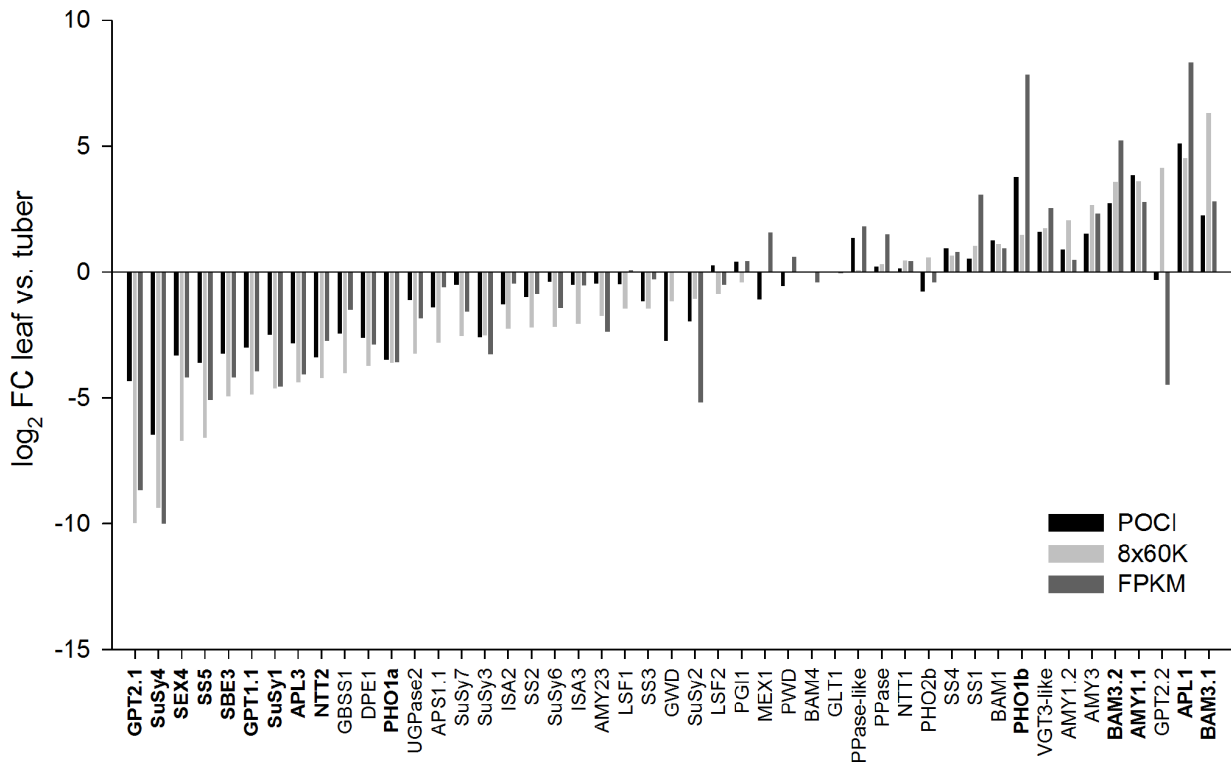
Figure 4: Relative expression of starch genes in leaf vs. tuber tissue.

Fold-change values for individual genes between leaf and tuber samples were exported from GeneSpring or calculated from FPKM values from the PGSC database. Genes whose expression cannot be detected in either platform were excluded. Tissue-specific genes are highlighted with bold letters. Light grey bars: values from 8x60 microarray, black bars: values from 4x44k POCI array, dark grey bars: FPKM values (taken from Van Harsselaar et al. 2017).

To confirm our results, FPKM (Fragments Per Kilobase Of Exon Per Million Fragments Mapped) values of corresponding genes were downloaded from RNA-sequencing data available on the Spud DB website and leaf and tuber samples were selected. Ratios between leaf and tuber values were calculated and compared to the results from the microarray analyses. Fold-change values of the RNA-Seq data compared well to the microarray data (Figure 4, Figure 5). Thus, *GPT2.1* and *SuSy4* are highly tuber-specifically expressed genes. Their expression was 20- to 1000-fold higher in tubers compared to leaves. Leaf-specific expression of *AMY1.1*, *APL1* and *BAM3.1* could also be confirmed by the RNA-Seq data. They were found to be 7-fold to 320-fold higher expressed in leaves than in tubers (Figure 5).

Results

Name	FC leaf vs tuber		
	POCI	8x60k	FPKM
AMY1.1	14.48	12.01	6.89
AMY1.2	1.85	4.17	1.39
AMY23	-1.37	-3.33	-5.12
AMY3	2.86	6.31	5.02
APL1	34.45	22.80	321.89
APL2	-1.12	n.d.	-1.95
APL3	-7.17	-20.78	-16.73
APS1.1	-2.64	-7.05	-1.52
APS1.2	n.d.	-8.48	-4.06
APS2	n.d.	-1.66	n.d.
BAM1	2.40	2.18	1.94
BAM2	1.08	n.d.	-1.57
BAM3.1	4.73	79.36	7.00
BAM3.2	6.65	11.92	37.56
BAM4	0.97	0.00	-1.33
BAM6.1	n.d.	3.03	212.92
BAM6.2	n.d.	n.d.	63.77
BAM6.3	n.d.	n.d.	2.13
BAM7	n.d.	1.91	-1.19
BAM9	n.d.	-2.54	-5.96
DPE1	-6.07	-13.30	-7.42
DPE2	-1.87	n.d.	n.d.
GBSS1	-5.37	-16.07	-2.80
GLT1	0.00	0.24	-1.04
GPT1.1	-8.07	-29.05	-15.43
GPT2.1	-19.95	-1014.59	-405.99
GPT2.2	-1.25	17.53	-22.21
GWD	-6.65	-2.26	-1.00
PPase	1.16	1.26	2.84
PPase-like	2.55	1.05	3.52
ISA1.1	-5.82	n.d.	1.33
ISA1.2	n.d.	n.d.	1.87
ISA2	-2.43	-4.80	-1.38
ISA3	-1.43	-4.21	-1.44
LDE	-7.29	n.d.	n.d.
LSF1	-1.40	-2.72	1.07
LSF2	1.21	-1.86	-1.41
MEX1	-2.14	-1.02	2.97
NTT1	1.12	1.38	1.35
NTT2	-10.45	-18.53	-6.74
PGI	1.34	-1.33	1.36
PGI-like1	1.21	n.d.	n.d.
PGI-like2	n.d.	-1.29	1.97
PGM1	-5.45	n.d.	n.d.
PHO1a	-11.16	-12.33	-11.92
PHO1b	13.64	2.76	227.11
PHO2a	-3.28	n.d.	n.d.
PHO2b	0.59	1.49	-1.33
PWD	-0.69	-0.33	1.52
SBE1.1	n.d.	n.d.	1.92
SBE2	1.39	n.d.	n.d.
SBE3	-9.48	-30.56	-18.01
SEX4	-9.95	-103.78	-18.12
SEX4-like	n.d.	n.d.	1.02
SS1	1.45	2.06	8.49
SS2	-2.01	-4.61	-1.80
SS3	-2.26	-2.71	-1.22
SS4	1.93	1.58	1.72
SS5	-12.21	-96.00	-33.73
SS6	1.70	n.d.	-3.23
SuSy1	-5.63	-24.82	-23.59
SuSy2	-3.92	-2.09	-36.17
SuSy3	-5.96	-5.69	-9.53
SuSy4	-88.80	-662.28	-1024.66
SuSy6	-1.32	-4.55	-2.70
SuSy7	-1.42	-5.77	-2.98
TPT	n.d.	12.68	33.41
VGT3-like		3.33	

-20   20

Figure 5: Heat Map representing fold-changes in gene expression levels of starch genes in leaf vs. tuber samples (taken from Van Harsselaar et al. 2017).

Verification of differential expression of selected genes was carried out by quantitative real-time PCR (qRT-PCR). As shown in Figure 6, tuber-specific expression was confirmed for *SuSy4*, *GPT2.1* and *SS5* as well as the leaf-specific expression of *AMY1.1*, *APL1* and *BAM3.1* (Figure 6 a-f). In addition, we selected two genes, *APL2* and *LSF2*, showing a similar expression in leaves and tubers in all three transcriptome platforms. Again, qRT-PCR analysis confirmed the transcriptome data (Figure 6 g, h)." (Van Harsselaar et al. 2017).
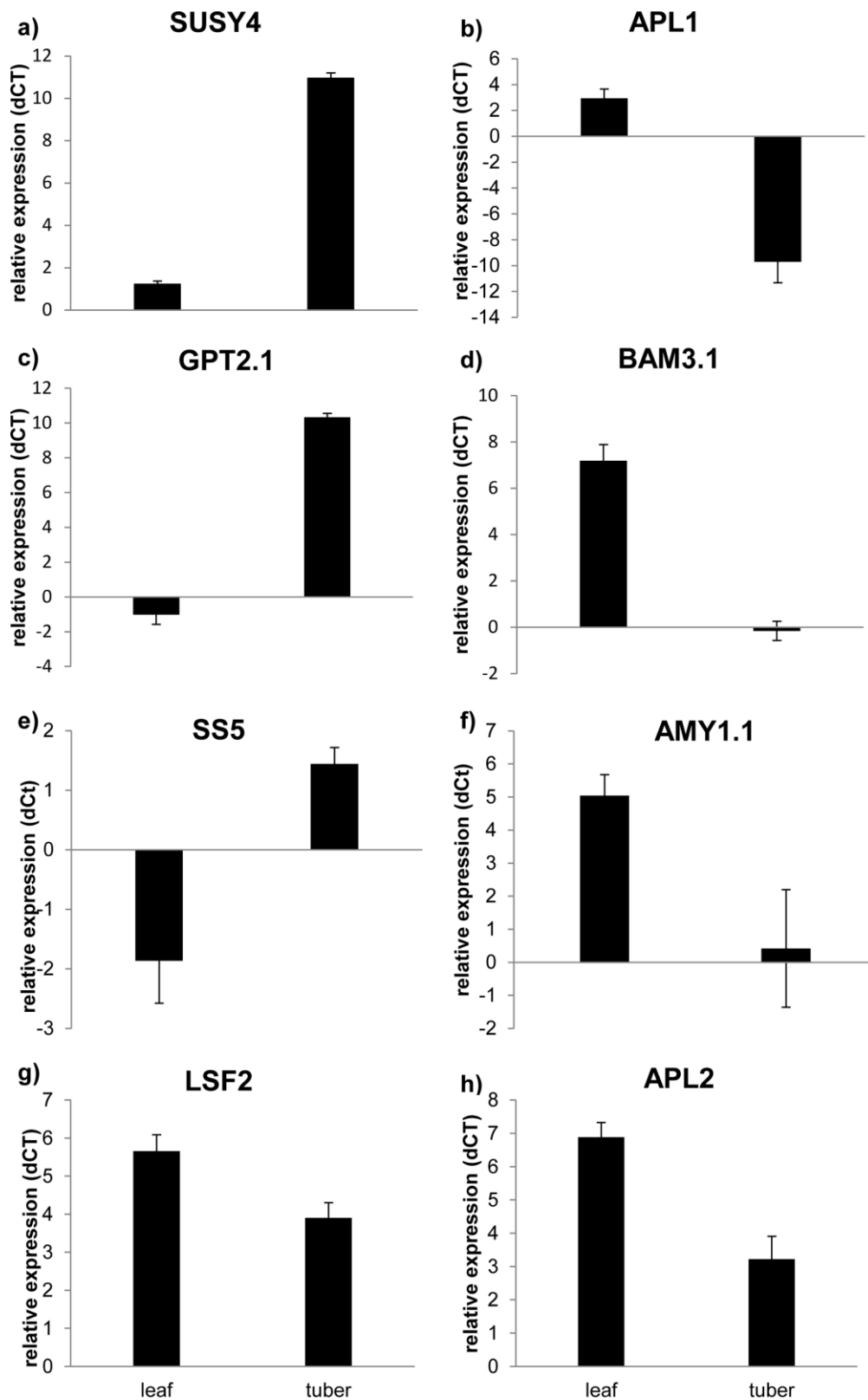
Figure 6: qRT-PCR analysis of selected starch metabolism genes in potato leaves and tubers.
Plants were grown in a greenhouse for 11 weeks until harvest and sampling. Mean relative expression of four biological replicates normalized to EF1alpha is illustrated as dCT-value of a) SuSy4, b) APL1, c) GPT2.1, d) BAM3.1, e) SS5, f) AMY1.1, g) LSF2, h) APL2. Error bars represent standard deviation (taken from Van Harsselaar et al. 2017).

3.2.2 Selection of query genes for co-expression analysis

"The main goal of the co-expression analysis (chapter 3.2.3) was to identify possible regulators of starch biosynthesis in potato tubers. Therefore, the genes used as queries for the analysis were selected by two criteria; first, they had to be specifically expressed in the tuber and second, their expression pattern had to follow starch accumulation. The first criterion was fulfilled most strongly by *GPT2.1*, *SuSy4*, *SEX4*, *SS5* and *SBE3* (Figure 4). For the evaluation of the second criterion, increasing gene expression during tuber development was chosen. It is known that during tuberization the rate of starch biosynthesis increases significantly (Kloosterman et al., 2005). Therefore, genes involved in starch biosynthesis should be up-regulated during this process. To identify these genes, microarray data from the tuber induction experiment described by Ferreira *et al.* (2010) were inspected and the ratio of transcripts detected in small tubers (stage 5) vs. those measured in unswollen stolons (stage 1) were calculated and illustrated as log2 values (Figure 7). The highest up-regulation from stage 1 to stage 5 was seen for *SuSy4*, *SBE3*, *GPT2.1* and *LDE*. *SEX4*, which was identified as specifically expressed in tubers, showed a pronounced down-regulation in the course of tuber development (Figure 7). Therefore, *SuSy4*, *SBE3* and *GPT2.1* were chosen as query genes for the co-expression analysis." (Van Harsselaar et al. 2017).
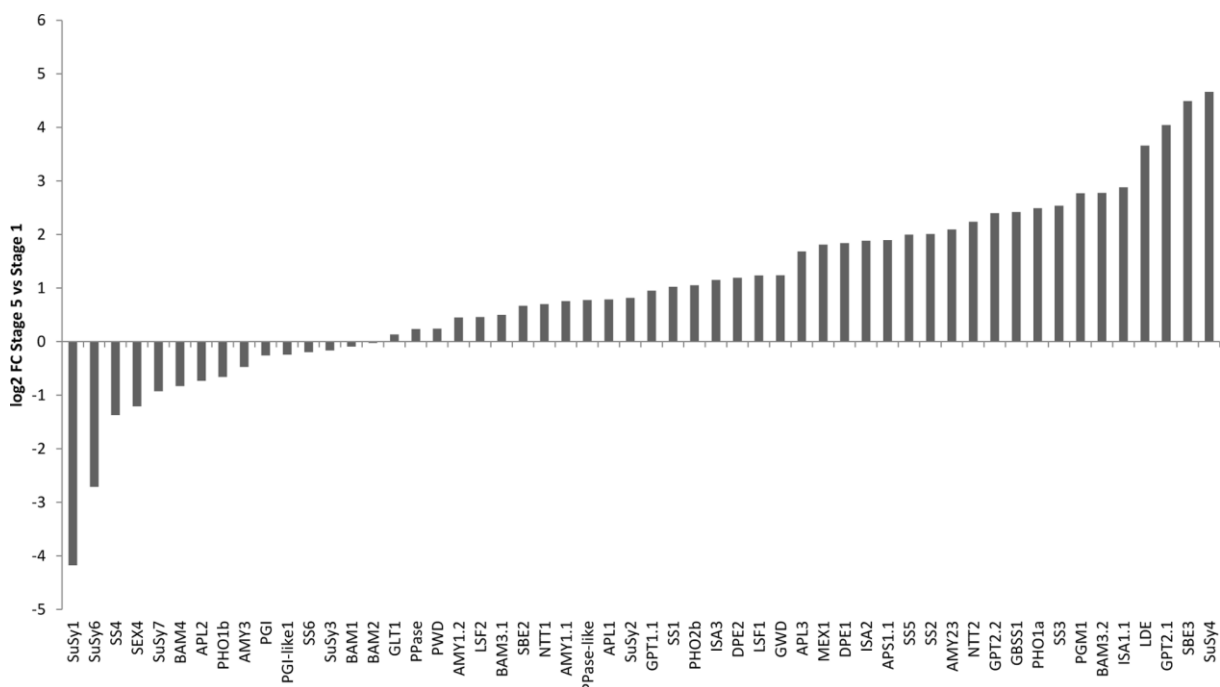
Figure 7: Relative changes in expression of starch genes during tuber development (stage 5 vs. stage 1). Given are log2 transformed fold-changes. Data were taken from Ferreira *et al.* 2010. Figure taken from Van Harsselaar et al. 2017.

3.2.3 Co-regulation analysis to identify putative regulators of starch metabolism in potato tubers

"To identify possible regulators of starch biosynthesis in potato tubers, all valid microarray identifiers for each of the selected genes (see Table 2) were used as queries in a Pearson correlation search on all detected entities in both microarray platforms including all data sets. In addition, RNA-Seq data were also analyzed. A Pearson correlation coefficient (PCC) of 0.8 was used as cut-off. Within each platform, the overlap of entities co-expressed with all three query genes was determined using VENN diagrams (Figure 8). The numbers of genes co-regulated with *GPT2.1*, *SuSy4* and *SBE3* differed greatly between platforms ranging between 283 entities in the POCI array, 868 for the RNA-Seq data set and 2998 in the 8x60k array (Figure 8 a-c). To compare the results from the different platforms, found entities were assigned to their corresponding PGSC gene identification number. This resulted in a list of 40 different genes that were consistently co-expressed with *GPT2.1*, *SuSy4* and *SBE3*. Besides the three query genes, five other starch genes, namely *APL3*, *PHO1a*, *SS5*, *NTT2* and *GPT1.1* were among the co-expressed genes. Twenty percent of the co-expressed genes encode known storage proteins like patatin and protease inhibitors (Jørgensen et al., 2011).
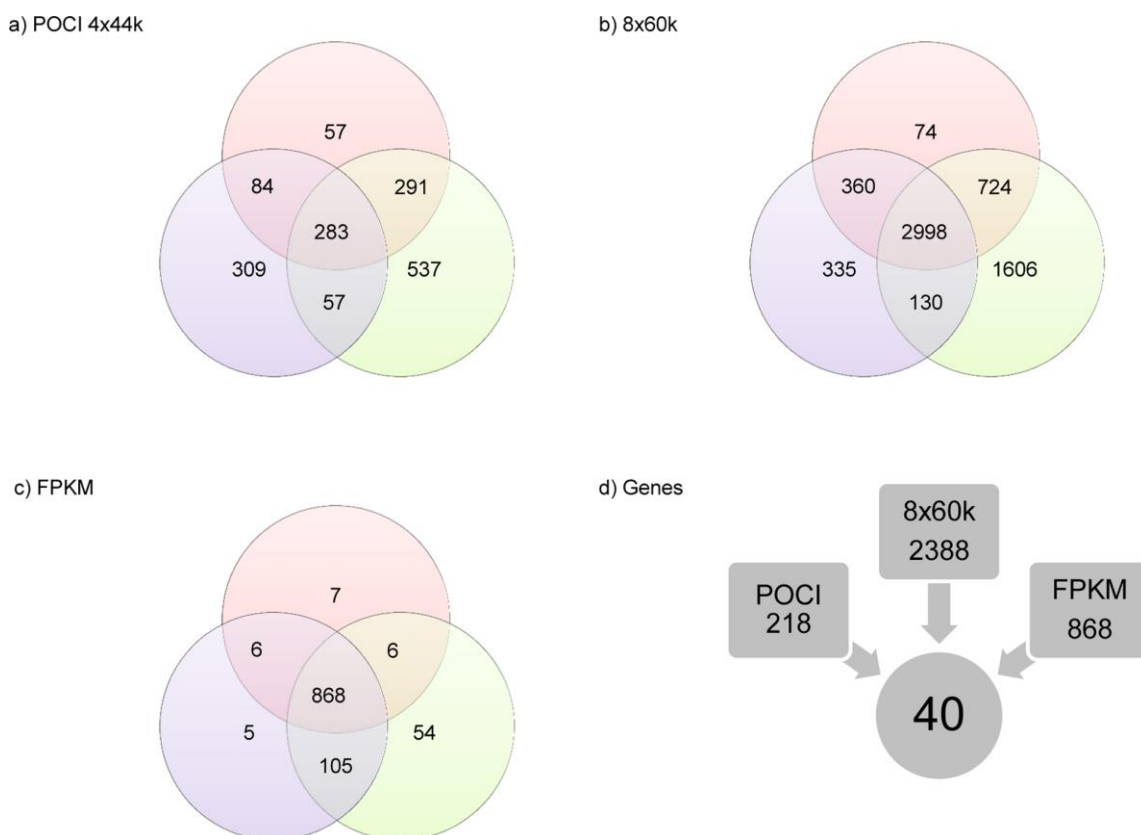
Figure 8: Overview of co-expression analysis.
a-c) Venn-analysis of co-expressed entities with SuSy4 (red circles), SBE3 (blue circles) and GPT2.1 (green circles). Co-expression analysis was conducted using a PCC cut-off of 0.8<=r<=1.0. a) Co-expressed

entities in the POCI microarray platform, b) co-expressed entities in the 8x60k microarray platform, c) co-expressed entities in the RNA-sequencing data. d) After conversion of the co-expressed entity lists to gene lists, the lists were compared and the common genes in all three lists were retrieved. Figure taken from Van Harsselaar et al. 2017.

To identify possible transcriptional regulators of starch biosynthesis in potato tubers, we paid special attention to putative TFs. Among those, TFs with homology to regulators of organogenesis from *Arabidopsis* like Petal Loss (PTL), Lateral Organ Boundaries (LOB), Blade On Petiole2 (BOP2) and Lateral Root Primordium protein (LRP) were found. Furthermore, a WRKY-type TF (WRKY4) and a member of the plant-specific TIFY (or ZIM) motif containing protein family TIFY5a, were co-expressed with the starch biosynthesis genes.

To confirm the expression profiles, four putative TF (PTL, TIFY5a, LOB and WRKY4) as well as SuSy4 and GPT2.1 were selected for qRT-PCR analysis. The relative amount of the corresponding mRNA was quantified in an independent set of samples representing four different stages of tuber development, namely unswollen stolons (stage 1), swollen stolons (stage 3-5), growing tubers and dormant tubers. The results were compared to microarray data derived from similar stages of tuber development (stage 1, stage 5, growing tubers and non-growing tubers (Ferreira et al., 2010)). As shown in Figure 9, the results from qRT-PCR were generally comparable to the results from microarray analysis when considering similar stages of tuber development. One exception was the expression profile of *PTL*. While its expression was lower in growing and non-growing tubers as compared to stage 5 in the microarray experiments, the mRNA level increased steadily across all developmental stages in the qRT-PCR reaching its maximum in dormant tubers (Figure 9)." (Van Harsselaar et al. 2017). Furthermore, expression of the TIFY TF showed an initial increase during tuber induction and remained at the same level in growing and non-growing tubers in the microarray samples, while the qRT-PCR revealed a decreased expression in dormant tubers which matches the expression pattern of *SuSy4* and *GPT2.1*. The expression profile of *WRKY4* in the samples used for qRT-PCR analysis was in accordance with the microarray, while for LOB there were slight differences (Figure 9). In the microarray, *LOB* expression was highest in stolons at stage 5 of tuber development and decreased to a stable level in growing tubers and non-growing tubers (Figure 9 a). In the qRT-PCR, *LOB* expression in swollen stolons was high but also showed high variability. The highest *LOB* expression was seen in growing tubers, while expression was strongly decreased in dormant tubers (Figure 9 b).
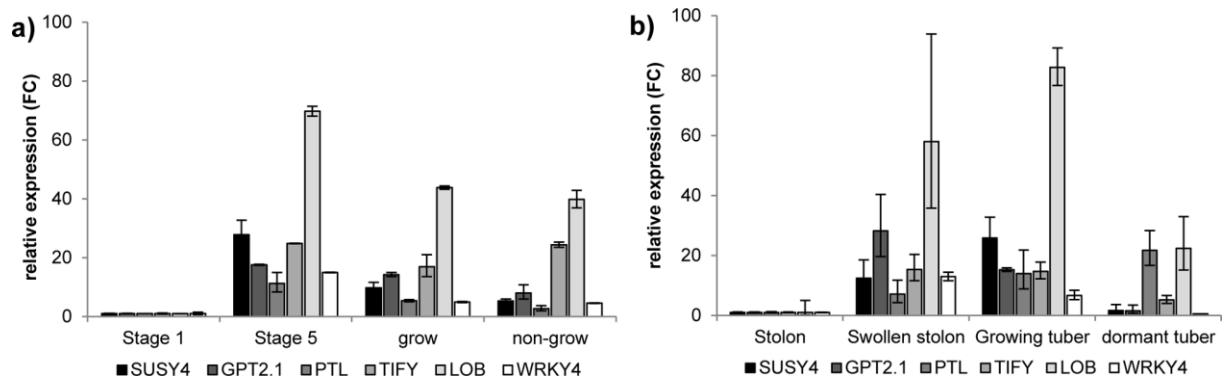
Figure 9: Expression profiles of tuber-specific starch genes and co-expressed transcription factors.
a) Gene expression calculated as fold-change relative to the value at stage 1 in the microarray experiments.
b) qRT-PCR analysis of the same genes in independent samples. Each value represents the mean of 3-4
biological replicates. Black bars: SuSy4, dark grey bars: GPT2.1, grey bars:PTL, medium grey bars: TIFY5a,
light grey bars: LOB domain containing protein, white bars: WRKY4 (taken from Van Harsselaar et al. 2017).

A Pearson correlation matrix was constructed evaluating similarity of the expression profiles determined by qRT-PCR (Table 4). Most Pearson Correlation Coefficients (PCC) values were greater than 0.6 indicating that most genes were co-regulated in the samples analyzed by qRT-PCR. However, the PCC values were lower than in the global co-expression analysis due to the decreased sample number. Thus, the qRT-PCR analysis corroborated that expression profiles of *TIFY5a*, *LOB* and *WRKY4* are similar to those of *SuSy4* and *GPT2.1* during tuber development. The PCCs for *PTL* were generally low supporting the observation that the expression pattern of this gene in the samples used for qRT-PCR deviated from the microarray." (Van Harsselaar et al. 2017).

Table 4: Pearson correlation coefficients between starch genes and TFs based on qRT-PCR analysis (taken from Van Harsselaar et al. 2017)

	GPT2.1	SuSy4	PTL	TIFY5a	LOB	WRKY4
GPT2.1	1.00	0.61	-0.16	**0.90**	0.74	**1.00**
SuSy4		1.00	0.12	**0.84**	**0.96**	0.58
PTL			1.00	0.16	0.26	-0.22
TIFY5a				1.00	**0.95**	0.88
LOB					1.00	**0.71**
WRKY4						1.00

Results from the qRT-PCR analysis of starch genes and transcription factors were subjected to a Pearson correlation analysis using Microsoft Excel. Correlation coefficients with p ≤ 0.1 are indicated in bold letters.

3.3 Analysis of heat-induced second-growth of potato tubers

Potato plants are considered susceptible with regard to heat stress (Jackson, 1999). Heat stress leads to decreases in carbon allocation toward developing tubers thereby decreasing tuber yield (Gawronska et al., 1992; Krauss and Marschner, 1984; Wolf et al., 1990). Tuberization can be completely inhibited by elevated temperatures coinciding with substantial decreases of the putative tuberization signal SP6A (Hastilestari et al., 2018; Navarro et al., 2011; Singh et al., 2015). Furthermore, heat stress has been described to lead to heat-sprouting and second-growth of potato tubers (Lugt, 1960) indicating disruptions in potato dormancy. The metabolic changes and possible signaling mechanisms that are associated with these responses are poorly described. In order to gain more insight, heat stress was applied to potato plants and morphological, biochemical and transcriptomic changes are described in this chapter.

3.3.1 Description of cultivars

The agronomical traits of the cultivars were taken from the European Cultivated Potato Database (European cultivated potato database, 2017), proplanta® Das Informationszentrum für die Landwirtschaft (proplanta® Das Informationszentrum für die Landwirtschaft, 2017), PGRDEU Pflanzengenetische Ressourcen in Deutschland ("PGRDEU" 2017) and Solana (Solana GmbH, 2017) and are summarized in Table 5.

Table 5: Traits of cultivars used to study second-growth under mild heat stress

	Agria	Princess	Ramses	Saturna	Tomensa
Tubers per plant	Few to medium	Many to very many	Many	Many to very many	Many to very many
Yield potential	Very low to very high	High to very high	Medium to high	Low to high	Medium
Starch content	Low to medium		High	Medium to very high	High to very high
Maturity	Intermediate to late	Very early to early	Medium early	Intermediate to late	Early
Dormancy period	Long to very long	Medium		Medium to very long	Long to very long
Secondary growth	Low	Medium	Low to medium	Very low to high	Low to medium

Potato cultivars selected for the study have been described to differ in their predisposition to develop second-growth. Since available data on the phenotypic characteristics of the cultivars was in some cases inconsistent and may vary under the conditions used in this study, they were grown in the greenhouse and the phyto-chamber to gather information about their properties under the experimental conditions used here.

3.3.2 Phenotypic response to mild heat treatment in various potato cultivars

For the phenotypic characterization of the different potato cultivars, a mild heat stress experiment was conducted. Therefore, cultivars were grown under five different temperature regimes as depicted in Figure 10. The cultivar Princess was not included in this experiment because it was only available at a later time-point. The control treatment was designated Treatment 1. Treatment 2 consisted of an initial acclimatization phase of one week before the heat application started which lasted until the end of the experimental period. Plants in Treatment 3 were treated analogously to Treatment 2 but transferred to control conditions for the last two weeks of the experimental period. In Treatment 4, plants were grown under control conditions until the emergence of tubers after approximately 6.5 weeks and then transferred to heat conditions for the rest of the experimental period. The fifth treatment was similar to Treatment 4, with the exception that plants were transferred back to control conditions after one week of heat stress. In Treatments 2 and 3, plants were subjected to the heat treatment before tuber induction had occurred while in Treatments 4 and 5 heat, application started after the onset of tuberization. All temperature regimes were applied under long-day conditions (16h light / 8h dark). All plants were harvested after the 10-week experimental period.
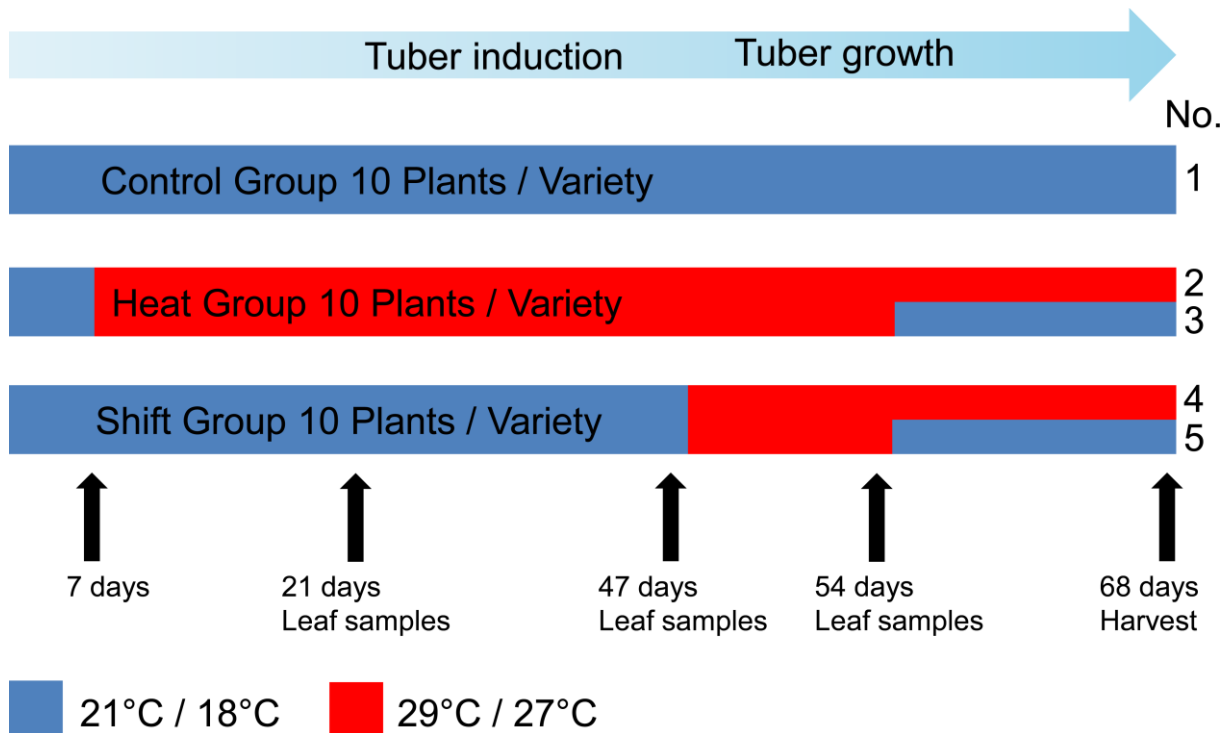
Figure 10: Overview of temperature conditions for the heat stress experiment. The light blue arrow represents the developmental stage of the potato plant. Treatment numbers are given next to their respective graphical representation. Black arrows indicate time-points on which plants were transferred or where samples were taken.

At the end of the experimental period, tubers were harvested and phenotypically characterized. The trait "tubers per plant" showed a strong response to the different treatments (Figure 11). A strong relationship between the duration of the heat treatment and the number of tubers per plant was observed. When plants had been grown under heat conditions throughout the entire experimental period (Treatment 2), tubers hardly developed. In Treatment 3, where stress was released for the last two weeks of the experiment, cultivars responded differently regarding their tuber number. In the cultivar Ramses, tuber number was the same as under control conditions, whereas in Tomensa tuber number remained very low. In Saturna and Agria tubers had developed but their number was lower than under control conditions. These results indicate that tuber formation was inhibited under heat treatment but started after the heat was released. When heat stress was applied during the tuber bulking phase (Treatment 4), it led to decreased numbers of tubers in the cultivars Saturna and Agria, but showed no effect in Ramses and Tomensa. A short period of elevated temperature for one week (Treatment 5) had no effect on the number of tubers in any of the cultivars studied (Figure 11).
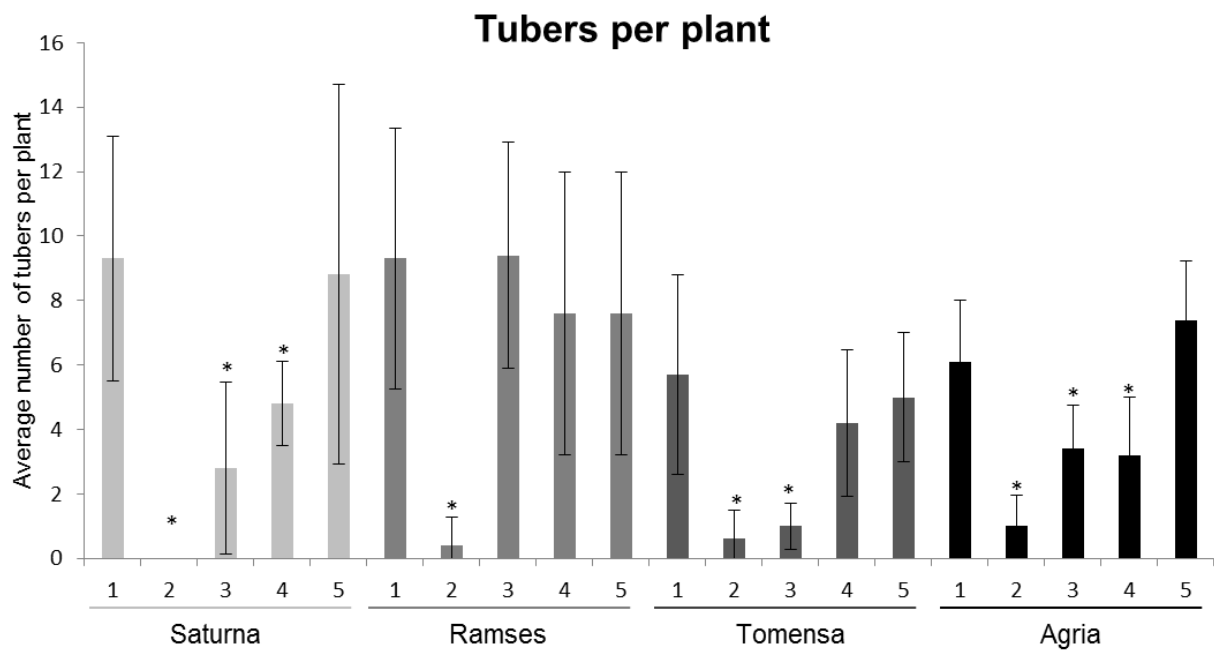
Figure 11: Average tuber number per plant of four different cultivars in five experimental conditions. Error bars represent standard deviations of five (Treatments 2-5) or ten (Treatment 1) biological replicates. Statistically significant differences from the respective control were determined using two-tailed t-tests assuming unequal variance and are indicated by asterisks (P≤ 0.05).

Regarding the trait "tuber yield per plant", the picture looked similar to the trait "tubers per plant" (compare Figure 11 and Figure 12). Extended heat treatment especially during the tuber induction phase significantly decreased tuber yields of all cultivars (Figure 12, Treatments 2 and 3). In the cultivar Tomensa, heat application during the tuber bulking stage did not lead to a significant loss of tuber biomass (Treatment 4), although the tendency was clearly visible. In all other cultivars, final tuber yield was diminished by extended heat at the end of the growth period. A one-week heat period led to decreased tuber yields in Saturna and Ramses but not in Tomensa and Agria, indicating that the latter are more resistant to the influence of heat on tuber yield (Figure 12, Treatment 5). In the cultivar Agria, the duration of the heat treatment correlated well with final tuber yield.
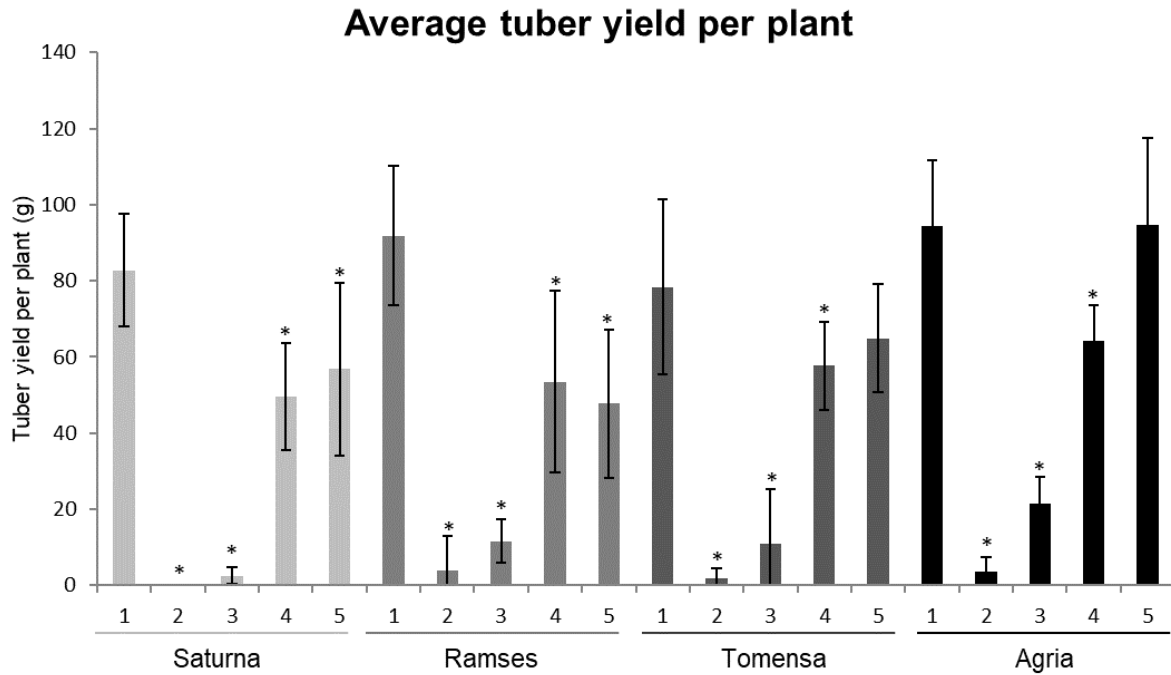
Figure 12: Average tuber yield per plant of four different cultivars in five experimental conditions. Error bars represent standard deviations of five (Treatments 2-5) or ten (Treatment 1) biological replicates. Statistically significant differences from the respective control were determined using two-tailed t-tests assuming unequal variance and are indicated by asterisks (P≤ 0.05).

Combining the results of the two traits "tuber number" and "tuber yield" revealed that heat influences the induction as well as the growth of tubers and that there are cultivar-specific differences in the response towards the treatments.

Results
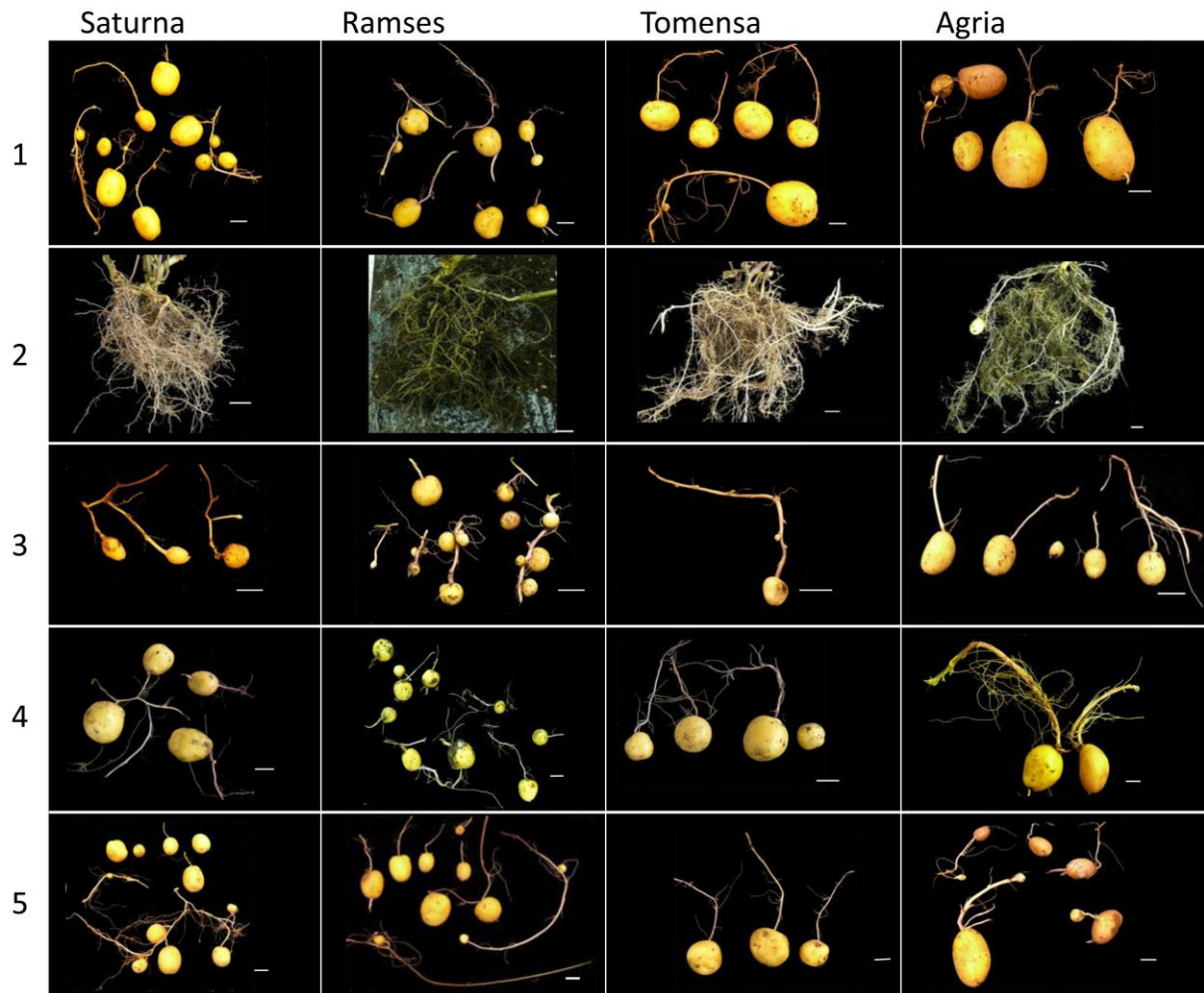
Figure 13: Tuber phenotypes of four different potato cultivars under five different treatments. Treatments 1-5 are described in the text and Figure 10. Scale bars represent approximately 1.5 cm.

Another trait which was considered was the formation of "second-growth". At harvest, plants were evaluated for the formation of chain tubers, elongated tubers, knobby tubers, bottleneck tubers and heat sprouting. The results are depicted in Figure 14. The cultivar Ramses showed a high rate of second-growth without the influence of heat (Treatment 1). These were mainly sprouted tubers and a few chain tubers. Under permanent heat treatment the relative number of second-growth tubers went up to 50% in Ramses and 66% in Tomensa but this represents one sprouted tuber of two and three tubers in total as can be derived from the average number of tubers per plant (Figure 11). In Treatment 3 no second-growth was detected supporting the hypothesis that tuber initiation occurred after the heat stress had been released and thus, developing tubers were not subjected to the elevated temperature. In Treatment 4, three of the four cultivars exhibited second-growth tubers (Figure 14). This was mainly caused by heat sprouting rather than other second-growth phenomena. A short period of heat stress (Treatment 5) caused the strongest reactions in terms of second-growth in the cultivars

Ramses and Agria. Increased heat sprouting and chain tubers were detected under these conditions.

Formation of second-growth (%)
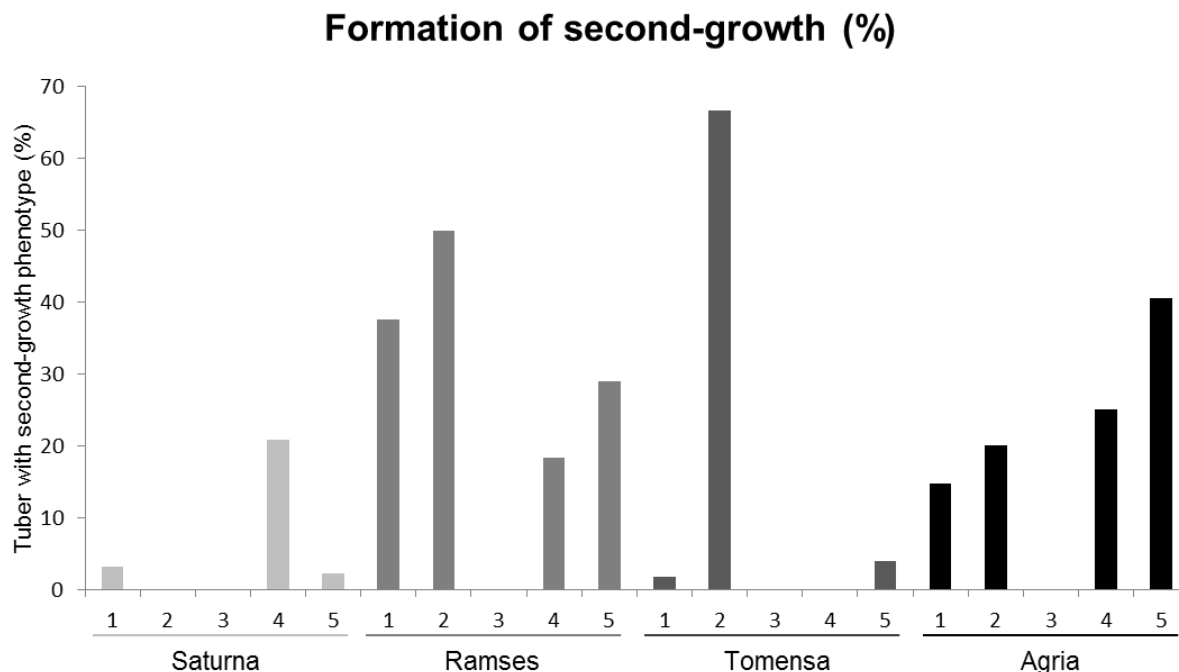
Figure 14: Formation of second-growth phenomena in tubers of the cultivars Saturna, Ramses, Tomensa and Agria under five different treatments.
Description of treatments is given in the text above. Percent second-growth was calculated by dividing the number of tubers showing second-growth by the total number of tubers.

Due to its predisposition to develop second-growth, and its responsiveness to the heat treatment in terms of tuber yield, the cultivar Agria was chosen for further analyses.

3.3.3 SP6A gene expression decreases under mild heat stress

In order to gain insight into possible regulatory circuits influencing tuberization and / or tuber growth, gene expression of the potential "tuberigen" SP6A was analyzed in leaf samples of the cultivar Agria. In plants grown under control conditions, *SP6A* expression increased over time from day 21 to day 54 and then reached a plateau (Figure 15). The initial increase in expression coincided with tuber induction while the maximum expression was measured during the tuber bulking stage. This is in accordance to SP6As proposed role as a tuber-inducing signal which is transported from the leaves to stolons and tubers (Navarro et al., 2011). Moreover, the expression profile suggests a possible role in the maintenance of tuber growth.

The heat treatment suppressed *SP6A* expression in leaves at all time-points analyzed which is in agreement with the lack of tubers in heat-treated plants. Transferring the plants, which had been grown under control conditions until tuber induction, to heat (Treatment 4) decreased the expression of *SP6A*. This effect could be reversed by transferring the plants back to control temperature (Figure 15, Treatment 5). The data support the suggested role of SP6A as tuber-inducing compound or "tuberigen".
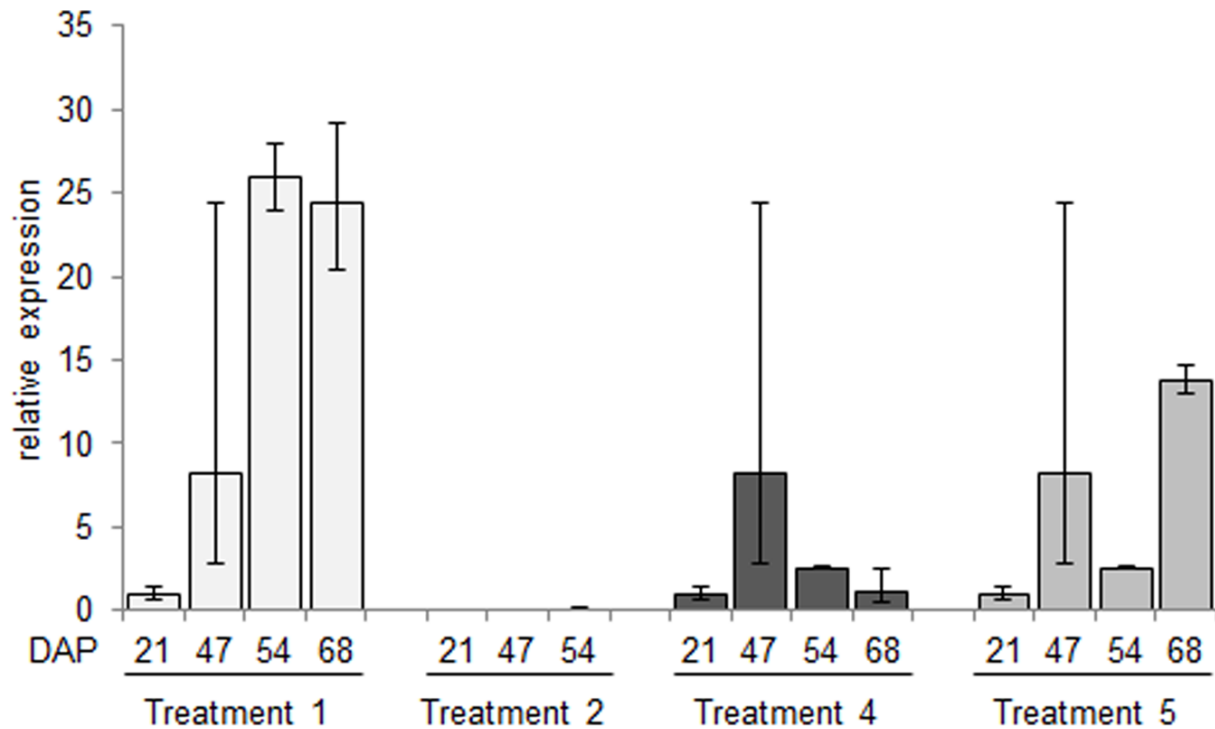
Figure 15: Relative expression of *SP6A* in leaves under different temperature regimes and time-points in the cultivar Agria. Days after planting (DAP) are depicted on the x-axis. Error bars represent standard deviation of two biological replicates.

3.3.4   Sucrose Synthase 4 expression in tubers showing a second-growth phenotype

To evaluate if the heat treatment had an inhibitory effect on starch biosynthesis, expression of *SuSy4*, the major SuSy isoform in potato tubers and a marker for sink strength, was analyzed by qRT-PCR. Therefore, normally growing tubers which had developed under Treatments 1, 4 and 5 as well as chain tubers which had developed under Treatments 1 and 5 were selected. Chain tubers were categorized as either primary tubers or secondary tubers. Primary tubers were attached to a stolon on the plant while secondary tubers were connected to a primary tuber through a stolon formed by this respective primary tuber. The results of the qRT-PCR show that average transcript levels of *SuSy4* are higher in secondary tubers than in primary tubers or normal growing tubers. The expression in primary tubers is similar to tubers with a normal phenotype (Figure 16a). These results indicate that secondary tubers are still actively

growing while starch biosynthesis in primary tubers and normal growing tubers is decreased. This result is partly unexpected, since it was assumed that in primary tubers starch could be degraded for the benefit of the secondary tubers and thus, *SuSy4* expression should be even lower than in normal growing tubers. But due to the plants' age it could be possible that the growth phase of the tubers was already at the end.
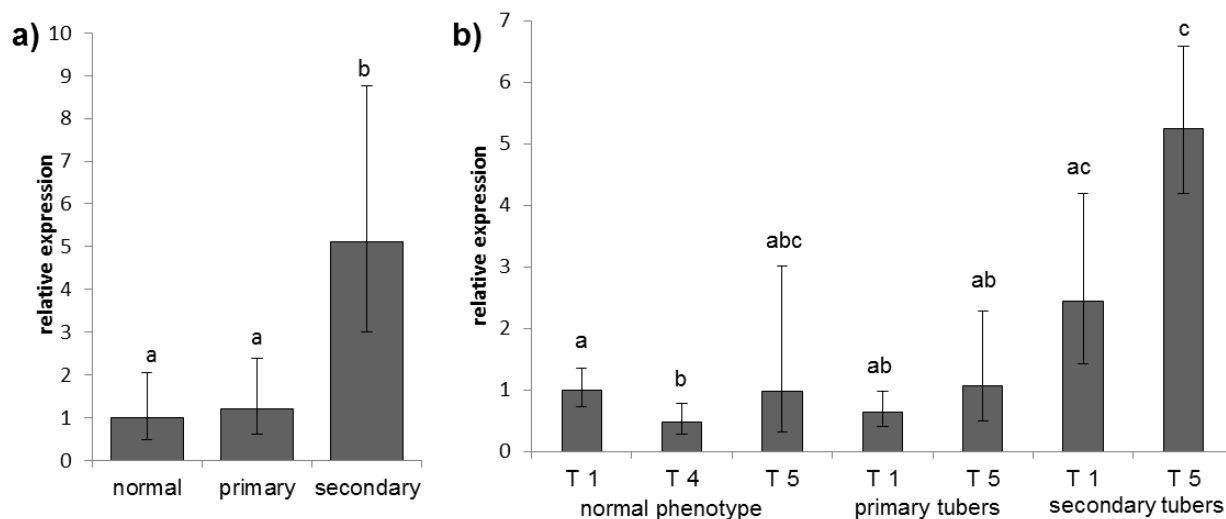
Figure 16: Relative expression of *SuSy4* in normal growing tubers, primary tubers and the corresponding secondary tubers under different temperature regimes (T1, T4, T5).
Statistically significant differences are marked with different letters. a) mean *SuSy4* expression values of all tubers with respective growth characteristics, b) mean *SuSy4* expression values of tubers with particular phenotype under defined treatment regime.

Separating the samples used for qRT-PCR for Treatment revealed that tubers with a normal growth phenotype which were grown in Treatment 4 exhibited a significantly decreased *SuSy4* expression when compared to normal growing tubers from Treatment 1 suggesting an inhibitory effect of the heat treatment (Figure 16b). Another interesting finding was that secondary tubers from plants grown under Treatment 5 showed a significantly increased *SuSy4* expression while secondary tubers from control-treated plants showed only a slightly enhanced *SuSy4* expression. This seems like an over-compensation of the previous repression of expression due to the heat treatment.

3.3.5 Transcriptome analysis of cv. Agria leaf and tuber samples

In order to gain a more detailed picture of the transcriptomic changes triggered by heat stress in leaves and to identify changes in metabolism of tubers exhibiting heat-induced second-growth, microarray analysis was applied. Leaf samples were taken from potato plants of the

cultivar Agria grown under ambient conditions (Treatment 1) and from plants subjected to a heat period of seven days (Treatment 5) at days 47, 54 and 68 after planting. Two pools of leaf samples from five (Treatment 1) and two to three (Treatment 5) different plants each per condition and time-point were used for the experiment. Tuber samples were taken at the end of the growth period, at day 68 after planting, from two normal-growing tubers from Treatment 1 and two heat-induced second-growth primary tubers and the corresponding secondary tubers from Treatment 5.

For microarray analysis, the 8x60k microarray introduced by Hancock et al. (2014) was utilized. It was designed according to the predicted transcripts from assembly v.3.4 of the DM potato genome (Xu et al., 2011) representing 52848 transcripts (including alternative isoforms). Normalization of microarray data was performed as described in chapter 5.12.2 but baseline subtraction was performed for leaf and tuber samples separately. For tuber samples, the baseline was set to normal growing tubers from control conditions. For leaf samples, leaf samples from control conditions at 47 days were used for baseline subtraction since they represented the initial time-point.

3.3.5.1 Analysis of leaf stress response

To gain detailed insight into the acute and long-term responses to a heat period in potato leaves, leaf samples from Agria plants in Treatment 1 and 5 were taken at 47, 54 and 68 days after planting corresponding to time-points before the treatment, at the end of the one-week heat period and two weeks after the cessation of the heat treatment and the respective control treated leaves.

First, the response of the leaf transcriptome to the one-week heat treatment was analyzed by comparing control treated leaves at day 54 to heat-treated leaves at day 54 after planting. A moderated t-test ($p \leq 0.05$, fold-change ≥ 2) revealed 1554 differentially regulated entities between the two treatments. Of the 1554 differentially regulated entities, 924 entities were up-regulated and 630 were down-regulated in heat-treated leaves. A list of all significantly regulated entities can be found in the appendix (Table A 1). Functional category analysis of these entities showed that the categories "Biodegradation of Xenobiotics", "minor CHO metabolism" and "TCA" were enriched amongst the up- and the down-regulated features. The category "Photosynthesis" was the most overrepresented category amongst the down-regulated entities. Furthermore, the categories "Cell Wall", "Gluconeogenesis" and "nucleotide metabolism" were overrepresented. Among the up-regulated features, the categories "C1-metabolism", "OPP", "misc", "Glycolysis" and "stress" were enriched more than two-fold (Figure 17).
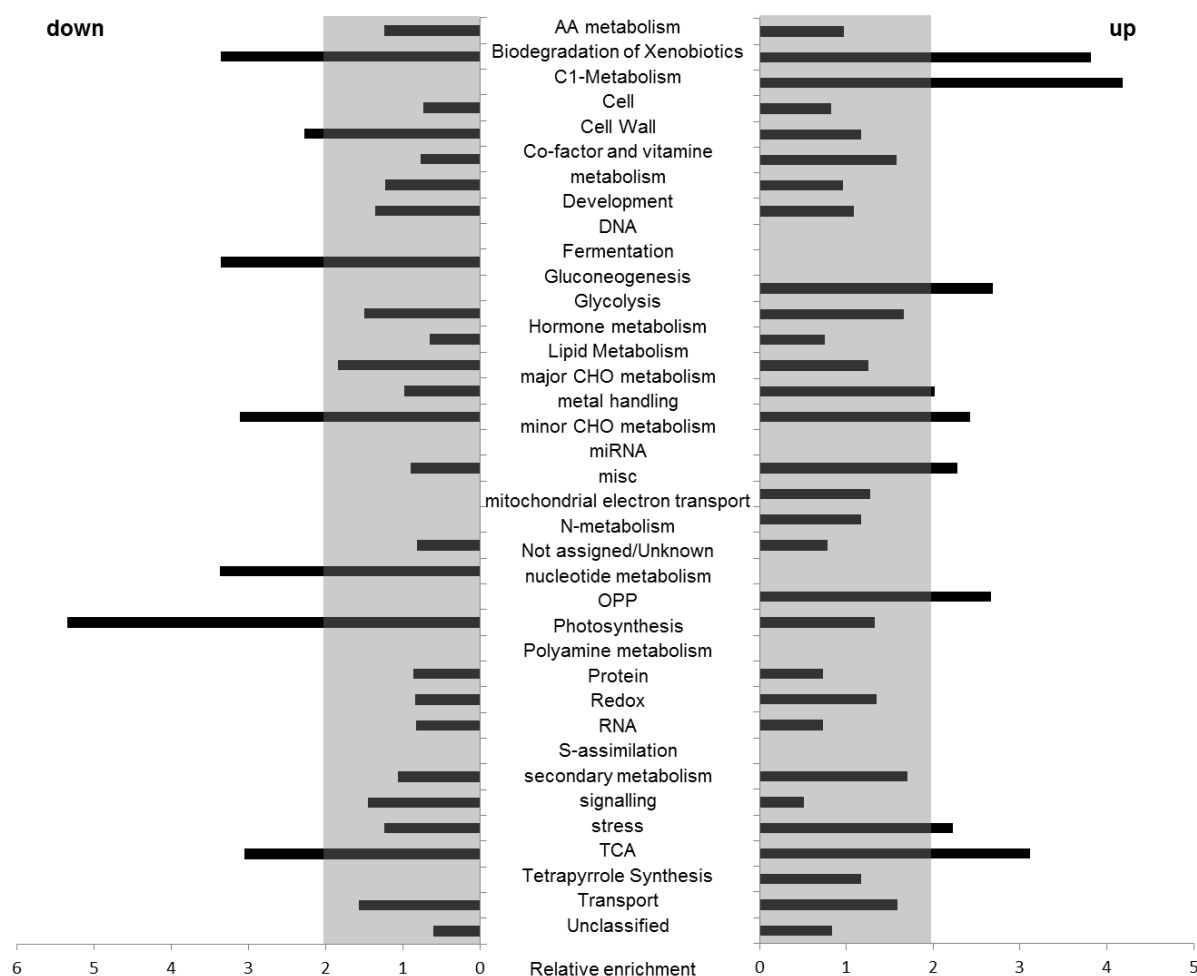
Figure 17: Relative enrichment of functional groups in differentially expressed transcripts of heat-treated leaves compared to leaves under control temperature at 54 days after planting.
Categorization was based on MapMan categories. Relative enrichment was calculated by dividing the percentage of co-regulated entities within a particular functional group by the percentage of all entities within the respective category relative to the entire array.

A down-regulation of components of the photosynthesis (PS) machinery is in concordance with previous reports about decreased photosynthesis during heat stress in potato (Hastilestari et al., 2018). A more detailed analysis of genes included in the category "photosynthesis" showed that the majority of significantly down-regulated genes belonged to the subcategory "light reaction", specifically to the nuclear-encoded chlorophyll a, b binding proteins. These proteins are part of the light harvesting complex II and play an important role in Chlorophyll assembly to the core complexes of the photosystems (Wang and Grimm, 2015). To get a more complete picture about the regulation of photosynthesis genes under elevated temperatures, gene expression of known components of PS was analyzed and it became clear that most of them were down-regulated (Table 6).

Results

Table 6: Transcriptional changes of components of the photosynthetic light reaction machinery in potato leaves in response to elevated temperatures when compared to control treated leaves at day 54 after planting. Entities representing the components of the light reaction were chosen according to KEGG (http://www.genome.jp/kegg/kegg2.html), MapMan (http://mapman.gabipd.org/) and Metacyc (http://www.plantcyc.org). Red color indicates up-regulated features while blue color indicates down-regulated features. Fold-change values are log2 transformed. Colors saturate at +/-1.3 log2 FC.

Light reaction			
Component	description	log2 FC	Transcript
Photosystem II	P680 reaction center D2 protein	-0.28	PGSC0003DMT400044462
	Q(B) protein	0.06	PGSC0003DMT400010772
	Q(B) protein	-0.65	PGSC0003DMT400041003
	Q(B) protein	1.95	PGSC0003DMT400004989
	Q(B) protein	-0.73	PGSC0003DMT400094795
	Thylakoid lumenal 21.5 kDa protein	0.11	PGSC0003DMT40002772
	Ultraviolet-B-repressible protein	0.05	PGSC0003DMT400000865
	Ultraviolet-B-repressible protein	-0.36	PGSC0003DMT400000864
	Ultraviolet-B-repressible protein	-0.56	PGSC0003DMT400000866
	D2 protein	-0.10	PGSC0003DMT400074870
	D2 protein	-0.51	PGSC0003DMT400020261
	D2 protein	-0.47	PGSC0003DMT400016094
	D2 protein	-0.53	PGSC0003DMT400004386
	Lhcb7	-0.79	PGSC0003DMT400025715
	Reaction center W protein	-0.34	PGSC0003DMT400051899
	PsbP domain-containing protein 3	0.16	PGSC0003DMT400075598
	Thylakoid lumenal 29.8 kDa protein	0.92	PGSC0003DMT400063835
	Thylakoid lumenal 29.8 kDa protein	-0.17	PGSC0003DMT400067194
	Subunit X	-0.65	PGSC0003DMT400092522
	CP47 chlorophyll apoprotein	-0.68	PGSC0003DMT400038938
	CP47 chlorophyll apoprotein	-0.62	PGSC0003DMT400096732
	CP47 chlorophyll apoprotein	-0.48	PGSC0003DMT400016568
	PsbP domain-containing protein 3	0.93	PGSC0003DMT400022551
Cyt b6-f complex	Cytochrome b6-f complex iron-sulfur subunit	-0.36	PGSC0003DMT400035747
	Cytochrome b6	-0.61	PGSC0003DMT400049986
Photosystem I	Reaction center V	-1.00	PGSC0003DMT400057281
	P700 chlorophyll a apoprotein A1	-1.01	PGSC0003DMT400041230
	P700 chlorophyll a apoprotein A1	-0.73	PGSC0003DMT400013730
	Thylakoid membrane phosphoprotein 14 kDa	-0.68	PGSC0003DMT400029398
	Reaction center subunit	-0.43	PGSC0003DMT400014861
	16kDa membrane protein	-0.74	PGSC0003DMT400015075
	Subunit III	-0.73	PGSC0003DMT400054480
	Subunit XI	-0.55	PGSC0003DMT400071154
	Subunit XI	-0.58	PGSC0003DMT400071155
	Reaction center subunit X psaK	0.66	PGSC0003DMT400052829
Ferredoxin-NADP reductase	leaf-type isozyme	-0.37	PGSC0003DMT400009192
	root-type isozyme	0.05	PGSC0003DMT400030830
	root-type isozyme	-0.30	PGSC0003DMT400010484
F-type H+-transporting ATPase	Subunit alpha	0.83	PGSC0003DMT400021839
	Subunit beta	-0.58	PGSC0003DMT400002642
	Subunit gamma	-0.41	PGSC0003DMT400042499
	Subunit gamma	0.18	PGSC0003DMT400071659
	Subunit delta	-0.45	PGSC0003DMT400043672
	Subunit epsilon	-0.46	PGSC0003DMT400064608
	Subunit a	-0.21	PGSC0003DMT400045540
	Subunit b	-0.66	PGSC0003DMT400052738
	Subunit b	-0.54	PGSC0003DMT400052777
	Subunit c	0.64	PGSC0003DMT400035317

When looking at the pathway of carbon fixation in the Cavin-Benson-Cycle, the picture looked more divers compared to the photosynthetic light reaction (Table 7). The key enzyme Rubisco consists of large and small subunits. The large subunit is encoded in the chloroplast genome. The genes encoding the small subunits are located within the nuclear genome and comprise a small gene family (Andersson, 2008; Fritz et al., 1993). Gene expression of *Rubisco* subunits was not significantly different in leaves under heat stress compared to leaves from control conditions (see Table 7). Among the significantly upregulated entities was *Rubisco activase 1*, which was represented by four transcripts (PGSC0003DMT400028764-7). Rubisco activase is required for the removal of sugar phosphates blocking the active site of Rubisco (Nagarajan and Gill, 2018). Three other entities representing two genes annotated as *Rubisco activase* were not substantially differently regulated in stressed leaves vs. control leaves.

The genes encoding two enzymes catalyzing the reduction phase of the Calvin-Benson-Cycle, namely *phosphoglycerate kinase* and *glyceraldehyde 3-phosphate dehydrogenase* were slightly upregulated in heat-treated potato leaves compared to leaves grown under ambient conditions. The gene expression of enzymes involved in the regeneration phase of the Calvin-Benson-Cycle was very divers and further complicated by the number of isoenzymes present (Table 7).

Another interesting gene was found among the significantly down-regulated entities in the category "Photosynthesis"; *cytosolic Fructose-1,6-bisphosphatase* (*cyFBPase*) (Table A 1). CyFBPase catalyzes one of the key steps of photosynthetic sucrose synthesis and its transcriptional down-regulation could indicate a decrease in sucrose synthesis for export (see Zrenner et al. 1996).

Table 7: Transcriptional changes of components of the Calvin-Benson-Cycle in potato leaves in response to elevated temperatures when compared to control treated leaves at day 54 after planting. Entities were chosen according to MapMan (http://mapman.gabipd.org/) and Metacyc (http://www.plantcyc.org). Red color indicates up-regulated features while blue color indicates down-regulated features. Fold-change values are log2 transformed. Colors saturate at +/-1.3 log2 FC. See next page.

Results

Calvin Cycle			
Phase	Description	log2 FC	Transcript ID
Carboxylation	Ribulose bisphosphate carboxylase large chain	0,03	PGSC0003DMT400083063
	Ribulose bisphosphate carboxylase small chain	2,17	PGSC0003DMT400010489
	Ribulose bisphosphate carboxylase small chain 2C, chloroplastic	-0,38	PGSC0003DMT400032977
	Ribulose bisphosphate carboxylase small chain 2C, chloroplastic	-0,32	PGSC0003DMT400032975
	Ribulose bisphosphate carboxylase small chain 2C, chloroplastic	-0,31	PGSC0003DMT400032978
	Ribulose bisphosphate carboxylase small chain 1, chloroplastic	-0,39	PGSC0003DMT400050381
	Ribulose bisphosphate carboxylase small chain C, chloroplastic	-0,08	PGSC0003DMT400062138
	Ribulose bisphosphate carboxylase small chain 2A, chloroplastic	0,15	PGSC0003DMT400067904
	Ribulose bisphosphate carboxylase small chain 2B, chloroplastic	-0,33	PGSC0003DMT400067907
	Ribulose bisphosphate carboxylase small chain 2B, chloroplastic	0,13	PGSC0003DMT400067906
	Ribulose bisphosphate carboxylase/oxygenase activase 1, chloroplastic	4,32	PGSC0003DMT400028767
	Ribulose bisphosphate carboxylase/oxygenase activase 1, chloroplastic	4,33	PGSC0003DMT400028766
	Ribulose bisphosphate carboxylase/oxygenase activase 1, chloroplastic	1,48	PGSC0003DMT400028765
	Ribulose bisphosphate carboxylase/oxygenase activase 1, chloroplastic	1,40	PGSC0003DMT400028764
	Ribulose bisphosphate carboxylase/oxygenase activase, chloroplast	-0,03	PGSC0003DMT400036879
	Ribulose bisphosphate carboxylase/oxygenase activase, chloroplast	-0,01	PGSC0003DMT400036878
	Ribulose bisphosphate carboxylase/oxygenase activase, chloroplastic	-0,25	PGSC0003DMT400049256
	Rubisco activase	0,69	PGSC0003DMT400091016
	Ribulose-1,5 bisphosphate carboxylase/oxygenase large subunit N-methyltransferase, chloroplastic	0,82	PGSC0003DMT400072873
	Ribulose-1,5 bisphosphate carboxylase/oxygenase large subunit N-methyltransferase, chloroplastic	-0,10	PGSC0003DMT400073004
	Ribulose-1,5 bisphosphate carboxylase/oxygenase large subunit N-methyltransferase, chloroplastic	0,83	PGSC0003DMT400073003
Reduction	Phosphoglycerate kinase	0,30	PGSC0003DMT400009905
	Phosphoglycerate kinase	0,21	PGSC0003DMT400009906
	Phosphoglycerate kinase	0,59	PGSC0003DMT400009908
	Phosphoglycerate kinase	0,26	PGSC0003DMT400056869
	Phosphoglycerate kinase	-0,44	PGSC0003DMT400056870
	Phosphoglycerate kinase	0,14	PGSC0003DMT400056871
	Glyceraldehyde-3-phosphate dehydrogenase B subunit	0,25	PGSC0003DMT400025881
	Glyceraldehyde-3-phosphate dehydrogenase A, chloroplastic	0,23	PGSC0003DMT400030050
	Glyceraldehyde-3-phosphate dehydrogenase B subunit	0,24	PGSC0003DMT400075608
	Glyceraldehyde-3-phosphate dehydrogenase	0,65	PGSC0003DMT400087142
Regeneration	Triosephosphate isomerase, chloroplastic	0,76	PGSC0003DMT400004041
	Triosephosphate isomerase, chloroplastic	1,71	PGSC0003DMT400004042
	Triosephosphate isomerase, chloroplastic	-0,14	PGSC0003DMT400011335
	Triosephosphate isomerase, chloroplastic	0,80	PGSC0003DMT400030013
	Fructose-bisphosphate aldolase	0,39	PGSC0003DMT400006894
	Fructose-bisphosphate aldolase	-0,10	PGSC0003DMT400006895
	Fructose-bisphosphate aldolase	0,35	PGSC0003DMT400008102
	Fructose-bisphosphate aldolase	0,30	PGSC0003DMT400008103
	Fructose-bisphosphate aldolase	0,07	PGSC0003DMT400009126
	Fructose-bisphosphate aldolase	-0,45	PGSC0003DMT400009127
	Fructose-bisphosphate aldolase	0,56	PGSC0003DMT400031351
	Fructose-bisphosphate aldolase	-0,10	PGSC0003DMT400057332
	Fructose-bisphosphate aldolase	-0,06	PGSC0003DMT400068571
	Fructose-bisphosphate aldolase	-0,36	PGSC0003DMT400068572
	Fructose-bisphosphate aldolase	-0,28	PGSC0003DMT400068573
	Fructose-bisphosphate aldolase	-0,16	PGSC0003DMT400072631
	Fructose-bisphosphate aldolase	0,56	PGSC0003DMT400072632
	Fructose-bisphosphate aldolase	-0,69	PGSC0003DMT400078519
	Fructose-bisphosphate aldolase	1,27	PGSC0003DMT400078520
	Chloroplast fructose-1,6-bisphosphatase I	0,00	PGSC0003DMT400049394
	Fructose-1,6-bisphosphatase	-0,31	PGSC0003DMT400049395
	Fructose-1,6-bisphosphatase	-0,39	PGSC0003DMT400052463
	Transketolase 1	-0,16	PGSC0003DMG400007019
	Transketolase	1,40	PGSC0003DMG400014756
	Transketolase, chloroplastic	-0,33	PGSC0003DMG400022088
	Chloroplast sedoheptulose-1,7-bisphosphatase	-0,21	PGSC0003DMT400069750
	Chloroplast sedoheptulose-1,7-bisphosphatase	-0,11	PGSC0003DMT400069751
	Ribulose-phosphate 3-epimerase, chloroplastic	-0,21	PGSC0003DMT400050255
	Ribulose-phosphate 3-epimerase, chloroplastic	-0,31	PGSC0003DMT400050256
	Ribose-5-phosphate isomerase	0,35	PGSC0003DMT400015282
	Ribose-5-phosphate isomerase	0,06	PGSC0003DMT400050076
	Ribose 5-phosphate isomerase	-0,10	PGSC0003DMT400054453
	Ribose 5-phosphate isomerase	-0,10	PGSC0003DMT400054453
	Ribose 5-phosphate isomerase	-0,10	PGSC0003DMT400054453
	Ribose-5-phosphate isomerase	-0,33	PGSC0003DMT400078358
	Phosphoribulokinase	-0,37	PGSC0003DMT400024090

3.3.5.2 Analysis of SP6A expression and co-regulated entities

SP6A has been proposed to be a mobile signal which is expressed in leaves under conditions favoring tuber-induction and transported to the stolons to induce tuberization (Navarro et al., 2011). Its' expression has been shown in various tissues like the leaf, stolon and potato tuber (Navarro et al. 2011). Heat stress is expected to inhibit tuberization which should be reflected in the expression of *SP6A*. Expression of *SP6A* in leaves was analyzed in the microarray samples (Figure 18) and confirmed the results obtained by qRT-PCR analysis (Figure 15). Under control conditions, *SP6A* expression increased over time while it was inhibited by the heat treatment on day 54 and recovered after cessation of the heat period as can be seen on day 68.
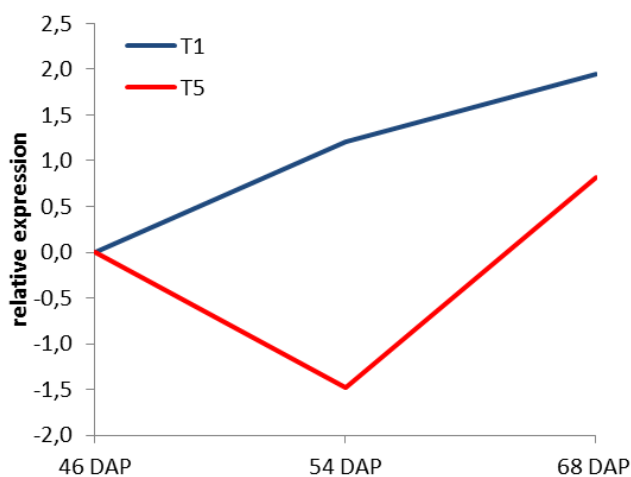
Figure 18: Expression of *SP6A* in microarray samples taken from leaf tissue at different time-points. *SP6A* expression is visible over the experimental time-course beginning with the time-point before the beginning of the heat treatment (46 DAP). SP6A expression under control conditions is represented by the blue line. *SP6A* expression in Treatment 5 is represented by the red line.

A co-expression analysis was conducted to identify entities with a similar expression pattern as *SP6A*. Therefore, a k-means cluster analysis was combined with a Pearson co-expression analysis. Twelve k-means clusters were built and the cluster containing *SP6A* was compared to the resulting list of the Pearson co-expression analysis which was conducted using a correlation coefficient of at least 0.6. The overlap of both analyses consisted of 205 entities (Table A 2). A functional analysis based on MapMan categories (Thimm et al., 2004) showed an enrichment of entities within several categories. Overrepresented categories harbored entities involved in "development", "signaling", "miscellaneous", "carbohydrate metabolism", "DNA", "amino acid metabolism" and "photosynthesis" (Figure 19). The categories "Biodegradation of Xenobiotics" and "metal handling" are each represented by one co-

expressed entity but due to the low number of entities in these categories on the chip, they are relatively overrepresented.
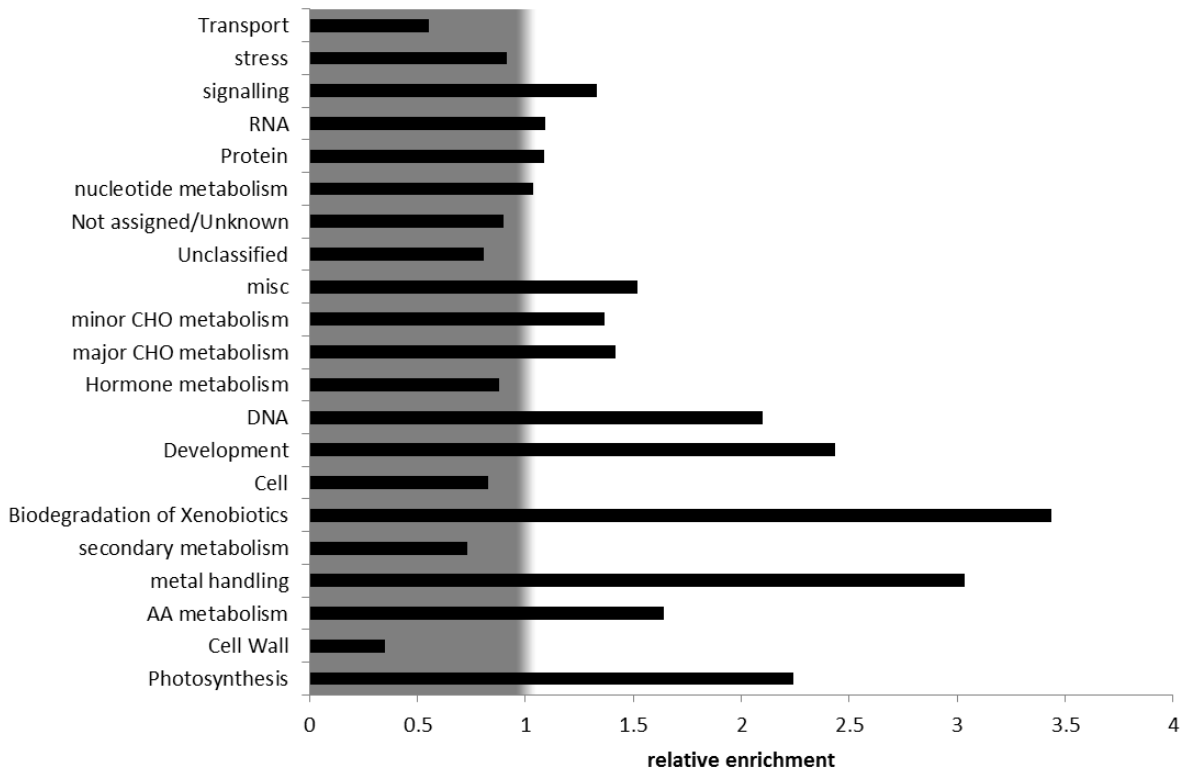
Figure 19: Relative enrichment of functional categories of genes co-expressed with *SP6A* in leaves of Agria plants. Categorization was based on MapMan categories (Thimm et al., 2004). Relative enrichment was calculated by dividing the percentage of co-regulated entities within a particular functional group by the percentage of all entities within the respective category relative to the entire array.

Among the 205 co-expressed entities were several transcription factors. A GRAS family TF (PGSC0003DMT400023877) encoding a SCARECROW-like protein was retrieved, whose homolog in *Arabidopsis thaliana* has been described to function in the signal transduction of Phytochrome A (Torres-Galea et al., 2013). Furthermore, the MADS-box transcription factor *FBP29* (PGSC0003DMT400003484) was among the co-regulated entities whose *Arabidopsis* homolog AGAMOUS-LIKE 7, APETALA1 regulates the expression of some flowering time genes and is itself activated by Flowering locus D and T (Monniaux et al., 2017; Wigge et al., 2005).

3.3.5.3 Microarray analysis of normal growing tubers and tubers exhibiting second-growth

To study the second-growth phenomenon of tubers under short-term heat-stress in more detail, microarray analysis was conducted. The analysis included tuber samples from two normal growing tubers from control treated potato plants (Treatment 1) as well as two primary and the corresponding secondary tubers from plants which had been subjected to a short period of elevated temperatures with a subsequent regeneration phase (Treatment 5).

First, primary and secondary tubers were compared to normal tubers and to each other by means of a moderated t-test with Benjamini-Hochberg correction. In primary tubers, 2673 entities were found to be significantly up-regulated and 1097 down-regulated compared to normal tubers. In secondary tubers versus normal tubers, 1987 entities were significantly up-regulated and 1699 down-regulated. Up- and down-regulated entities were grouped by functional category and their proportion of up- and down-regulated entities was compared to the relative proportion of the respective category on the microarray. The results of this analysis are displayed in Figure 20.
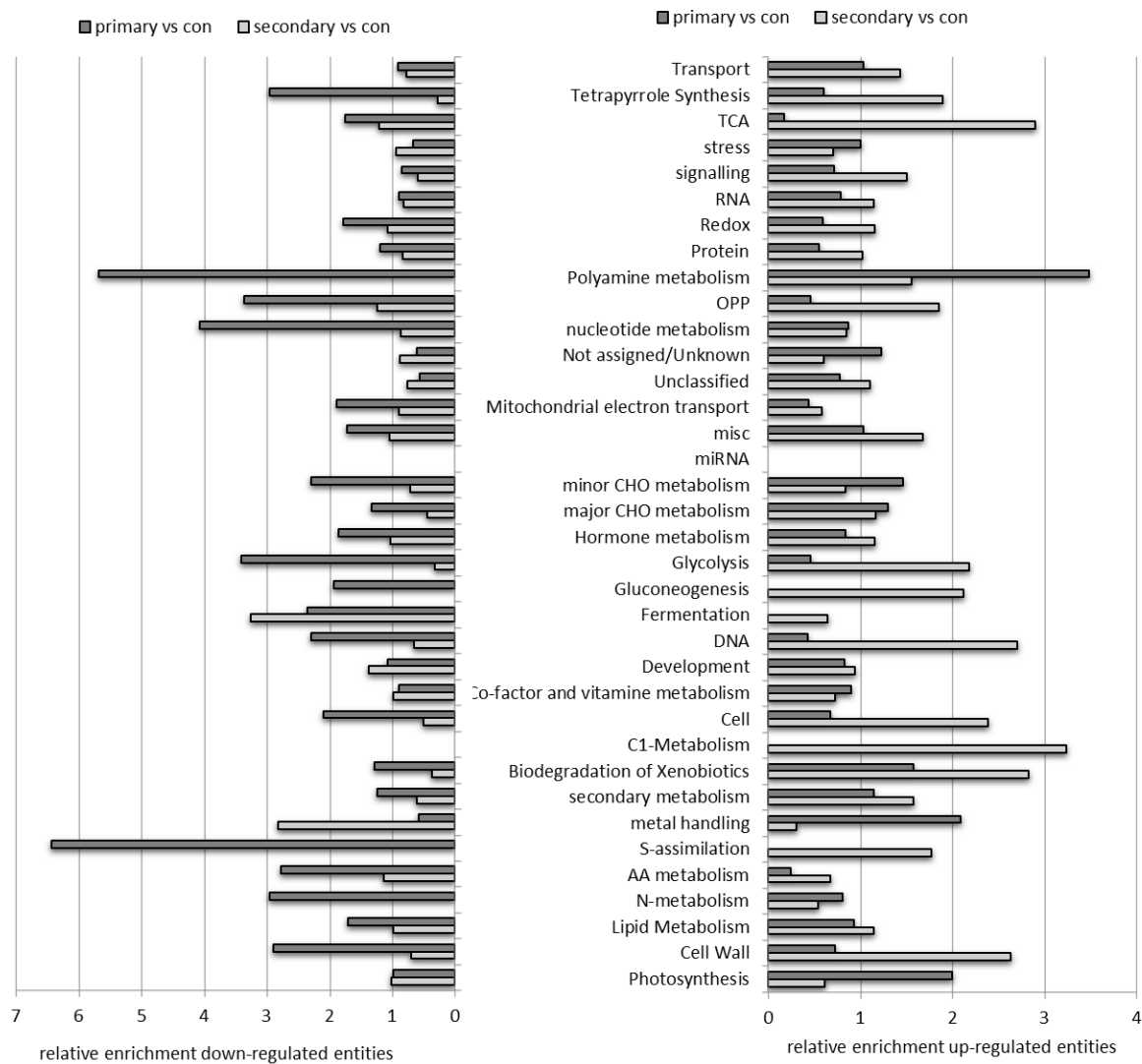
Figure 20 Functional categorization of significantly up- and down-regulated entities in primary (dark grey) and secondary (light grey) tubers compared to normal tubers. Bars indicate relative enrichment of categories in relation to representation of categories on the whole array.

In primary tubers versus control tubers, down-regulation was observed in the categories "Tetrapyrrole synthesis", "oxidative pentose phosphate (OPP)" pathway, "polyamine metabolism", "nucleotide metabolism", "glycolysis", and "S-assimilation" amongst others (Figure 20). Up-regulation was mainly observed in the categories "polyamine metabolism", "photosynthesis" and "metal handling" (Figure 20). Strong metabolic shifts have been described earlier during dormancy release in potato (Liu et al., 2015). Surprisingly, the category "stress" was not among the enriched, which suggests that the recovery phase had been sufficiently long and tuber metabolism was not dominated by stress responses. The transcriptional profile of primary tubers points toward a down-regulation of anabolic processes

like cell wall synthesis, AA-, N, lipid- and nucleotide metabolism which could suggest a role of the primary tuber as substrate donor to the developing secondary tuber.

In secondary tubers versus control tubers, up-regulated entities were especially enriched in the categories "Tricarboxylic acid cycle (TCA)", "Cell", "Cell wall", "DNA" and some other minor metabolic pathways. Down-regulation was observed in the categories "Fermentation" and "metal handling" (Figure 20).

Circadian Clock CONSTANS/SP6A

In leaf samples of potato plants under heat-stress, *SP6A* expression was significantly down-regulated suggesting that tuberization may be inhibited. After cessation of the stress, *SP6A* expression in leaves increased again indicating that tuberization was favored again. The phenomenon of second-growth fits well with this observation. It is hypothesized that the primary tuber stops growing during the heat period and instead of resuming growth after the stress has been relieved, a secondary tuber is formed. A detailed analysis of the regulation of the CONSTANS/SP6A network in primary and secondary tubers revealed that the majority of transcripts was up-regulated in primary tubers and down-regulated in secondary tubers (Table 8).

Table 8: Transcript profile of the CONSTANS/SP6A network in normal tubers from control conditions and primary and secondary tubers from plants subjected to temporal heat stress. Colors highlight up- (red) and down-regulated (blue) genes and saturate at -2 / 2.

ProbeName	Name	Log2 fc primary vs con	Log2 fc secondary vs control	log2 fc secondary vs primary	PrimaryAccession
CUST_44891_PI426222305	Circadian clock-associated FKF1	-0,12	-1,47	-1,36	PGSC0003DMT400051416
CUST_1183_PI426222305	CONSTANS 1	2,10	-0,65	-2,76	PGSC0003DMT400026068
CUST_951_PI426222305	CONSTANS 1	2,04	-1,40	-3,45	PGSC0003DMT400026069
CUST_1249_PI426222305	CONSTANS 2	1,22	0,25	-0,97	PGSC0003DMT400026065
CUST_14166_PI426222305	Flowering locus T protein SP6A	0,34	-3,29	-3,63	PGSC0003DMT400060057
CUST_26089_PI426222305	Flowering locus T SP5G-like	-2,40	-1,67	0,73	PGSC0003DMT400041728
CUST_26285_PI426222305	Flowering locus T SP5G-like	0,70	-0,79	-1,49	PGSC0003DMT400041726
CUST_26183_PI426222305	Flowering locus T SP5G-like	1,49	-0,97	-2,45	PGSC0003DMT400041725
CUST_25680_PI426222305	MYB transcription factor MYB114 (LHY)	1,10	-0,98	-2,08	PGSC0003DMT400029394
CUST_35243_PI426222305	Phytochrome B	-0,18	0,24	0,43	PGSC0003DMT400061712
CUST_39110_PI426222305	Protein GIGANTEA	0,99	-0,88	-1,87	PGSC0003DMT400002842
CUST_45824_PI426222305	Pseudo response regulator (TOC1)	-0,34	-1,92	-1,59	PGSC0003DMT400050252
CUST_28779_PI426222305	Sensory transduction histidine kinase (TOC1)	-0,05	-0,71	-0,66	PGSC0003DMT400083086
CUST_29688_PI426222305	Zinc finger protein CDF1.1	1,15	-0,53	-1,68	PGSC0003DMT400047370
CUST_43585_PI426222305	Zinc finger protein CDF2	1,27	-0,97	-2,23	PGSC0003DMT400064695
CUST_761_PI426222305	Zinc finger protein CDF3	0,63	-1,43	-2,07	PGSC0003DMT400003359
CUST_28689_PI426222305	Dof zinc finger protein CDF4	2,71	0,15	-2,56	PGSC0003DMT400083080
CUST_45817_PI426222305	Dof zinc finger protein CDF5	1,05	-0,74	-1,79	PGSC0003DMT400050273

Starch metabolism

A detailed analysis of starch metabolism was conducted in the tuber samples. As a maker for starch biosynthesis and sink strength, *SuSy4* expression in tubers exhibiting different phenotypes was analyzed. In comparison to normal growing tubers, it became visible that

SuSy4 expression was slightly lower in secondary tubers (log2 fc = -0.38) and much lower in primary tubers (log2 fc = -2.24, Figure 21). Statistical analysis revealed that the difference between primary and secondary tubers was significant (p_{corr} = 0.01) as was the difference between primary and control tubers (p_{corr} < 0.05) indicating that sink strength and starch biosynthesis might be lowest in primary tubers. Overall, in primary tubers, the majority of genes encoding enzymes involved in starch biosynthesis were down-regulated in primary tubers while the majority of genes encoding enzymes involved in starch degradation tended to be up-regulated when compared to control tubers and secondary tubers (Figure 21). This might support the notion that primary tubers cease growing and support secondary tubers with metabolites.

Category	Name	log2 FC 2ndary vs 1ary	log2 FC 1ary vs con	log2 FC 2ndary vs con
starch biosynthesis	SUSY3	-1,96	0,70	-1,26
starch biosynthesis	APL1	-1,42	0,61	-0,81
starch biosynthesis	GPT2.2	-1,05	0,68	-0,37
starch biosynthesis	APS1.1	-1,03	0,31	-0,72
starch biosynthesis	APL2	-0,90	-0,03	-0,93
starch biosynthesis	APS2	-0,61	1,21	0,59
starch biosynthesis	GBSS1	-0,45	-0,24	-0,69
starch biosynthesis	APS1.2	-0,33	-0,23	-0,56
starch biosynthesis	SBE3	-0,22	-0,37	-0,59
starch biosynthesis	SS1	0,06	-0,17	-0,11
starch biosynthesis	APL3	0,22	-0,72	-0,50
starch biosynthesis	PPase	0,39	-0,37	0,02
starch biosynthesis	NTT2	0,43	-0,51	-0,07
starch biosynthesis	SS4	0,56	0,00	0,57
starch biosynthesis	SUSY2	0,61	0,02	0,64
starch biosynthesis	GPT2.1	0,62	-0,83	-0,20
starch biosynthesis	SS5	0,72	-0,88	-0,16
starch biosynthesis	SS3	0,85	-0,94	-0,08
starch biosynthesis	SS2	0,97	-1,32	-0,35
starch biosynthesis	PGI-like2	1,12	-0,59	0,53
starch biosynthesis	SUSY6	1,60	-1,01	0,58
starch biosynthesis	NTT1	1,66	-1,13	0,53
starch biosynthesis	SUSY4	1,86	-2,24	-0,38
starch biosynthesis	PGI	2,01	-0,95	1,07
starch biosynthesis	SUSY7	2,46	0,02	2,48
starch biosynthesis	SUSY1	2,98	-4,31	-1,33
starch biosynthesis	PPase-like	3,72	-2,29	1,43
starch degradation	BAM3.2	-2,97	0,53	-2,44
starch degradation	PHO1b	-2,79	2,53	-0,27
starch degradation	BAM3.1	-2,60	0,63	-1,96
starch degradation	BAM6	-1,90	1,74	-0,16
starch degradation	GWD	-1,64	1,11	-0,53
starch degradation	ISA3	-1,37	0,26	-1,11
starch degradation	AMY23	-1,28	0,33	-0,95
starch degradation	BAM9	-1,08	0,10	-0,98
starch degradation	PHO1a	-1,03	-0,01	-1,04
starch degradation	LSF2	-0,44	-0,05	-0,48
starch degradation	AMY1.2	-0,43	0,51	0,08
starch degradation	LSF1	-0,37	-0,09	-0,46
starch degradation	SEX4	-0,22	-0,84	-1,06
starch degradation	MEX1	-0,14	-0,62	-0,76
starch degradation	ISA2	-0,08	-0,76	-0,84
starch degradation	AMY1.1	-0,04	0,33	0,29
starch degradation	PWD	-0,03	0,31	0,29
starch degradation	BAM4	0,04	0,16	0,20
starch degradation	AMY3	0,17	0,28	0,46
starch degradation	DPE1	0,89	-0,90	-0,11
starch degradation	BAM7	1,29	0,07	1,36
starch degradation	GLT1	1,35	-0,62	0,73
starch degradation	BAM1	2,59	-1,65	0,94
starch degradation	PHO2b	2,82	-0,65	2,17

Figure 21 Comparison of gene expression of enzymes involved in starch metabolism between primary, secondary and control tubers. Values are log2 fold-changes between secondary vs. primary, primary vs. control and secondary vs. control tubers. Colors saturate at -2 (blue) / 2 (red).

Phytohormones

Developmental processes and stress response are regulated by plant hormones. To gain a clearer picture of hormonal regulation of second-growth, gene expression patterns of hormonal pathways were examined closely. 95 differentially regulated entities were found between primary and control tubers of which 50 were up-regulated and 45 down-regulated. The statistical comparison of secondary tubers and control tubers revealed 96 differentially regulated entities (51 up, 45 down). The most pronounced effect was observed when comparing secondary and primary tubers with 212 differentially regulated entities (104 up, 108 down).

In primary tubers, jasmonate metabolism was overrepresented among the down-regulated entities when compared to control tubers. In secondary tubers, brassinosteroid metabolism was overrepresented by the up-regulated entities compared to control tubers. Again, the most pronounced differences were observed between secondary and primary tubers where brassinosteroid, gibberellin and jasmonate metabolism were overrepresented in the up-regulated entities and abscisic acid and cytokinin metabolism in the down-regulated entities (Table 9).

Table 9: Enrichment of differentially regulated entities relative to entities spotted on the microarray. The percentage of up- and down-regulated entities within each category was set in ratio with the percentage of entities spotted on array for the respective category. Overrepresented categories are highlighted in red.

Category	primary vs con		secondary vs con		secondary vs primary	
	relative enrichment up	relative enrichment down	relative enrichment up	relative enrichment down	relative enrichment up	relative enrichment down
abscisic acid	1,13	0,19	0,56	0,56	0,94	2,82
auxin	0,13	0,16	0,08	0,10	0,32	0,24
brassinosteroid	1,11	1,11	3,33	0,00	3,33	1,11
cytokinin	1,01	0,23	0,23	0,34	0,45	2,14
ethylene	0,11	0,09	0,22	0,14	0,30	0,27
gibberelin	0,58	0,96	0,58	0,77	2,31	1,16
jasmonate	0,36	2,17	0,72	1,44	2,53	1,44
salicylic acid	0,30	0,15	0,15	0,44	0,15	0,74

The pronounced down-regulation of jasmonate metabolism in primary tubers was determined by seven entities representing transcripts of six enzymes, namely LEDI-5c protein (PGSC0003DMT400048327), Allene oxide cyclase (PGSC0003DMT400033027), Divinyl ether synthase (PGSC0003DMT400064771, PGSC0003DMT400064772), Fatty acid

hydroperoxide lyase (PGSC0003DMT400002779), Allene oxide synthase 2 (PGSC0003DMT400002934) and Lipoxygenase (PGSC0003DMT400081909).

The consistent overrepresentation of brassinosteroid metabolism in secondary tubers was caused by up-regulation of Transcription factor *BIM1* (PGSC0003DMT400010394), four transcripts of *DWARF1/DIMINUTO* (PGSC0003DMT400054476, PGSC0003DMT400010990, PGSC0003DMT400054478, PGSC0003DMT400030799) and *Delta(7)-sterol-C5(6)-desaturase* (PGSC0003DMT400067881).

Polyamine metabolism

Polyamine metabolism was enriched among the significantly up- and down-regulated entities in primary tubers. Polyamines are molecules which play important roles in the development and physiology of plants (Wimalasekera et al., 2011). Furthermore, they are involved in abiotic stress tolerance (Alcázar et al., 2010). A close analysis of the entire pathway of polyamine biosynthesis showed that *S-adenosylmethionine* (*SAM*) *synthase* and *SAM-decarboxylase* were significantly up-regulated in primary tubers versus control tubers (Figure 22), indicating that the synthesis of Decarboxylated SAM might have been increased. Regulation of further steps of polyamine synthesis was rather ambiguous; however, the degradation of polyamines was likely increased as indicated by a significant up-regulation of *polyamine oxidase* (*PAO*). Interestingly, it was also found that the production of the ethylene precursor 1-aminocyclopropane-1-carboxylic acid (ACC) was up-regulated, while ethylene biosynthesis was not among the up-regulated pathways. ACC is not only the precursor of ethylene, but functions as a signaling molecule on its own (Pattyn et al., 2021).
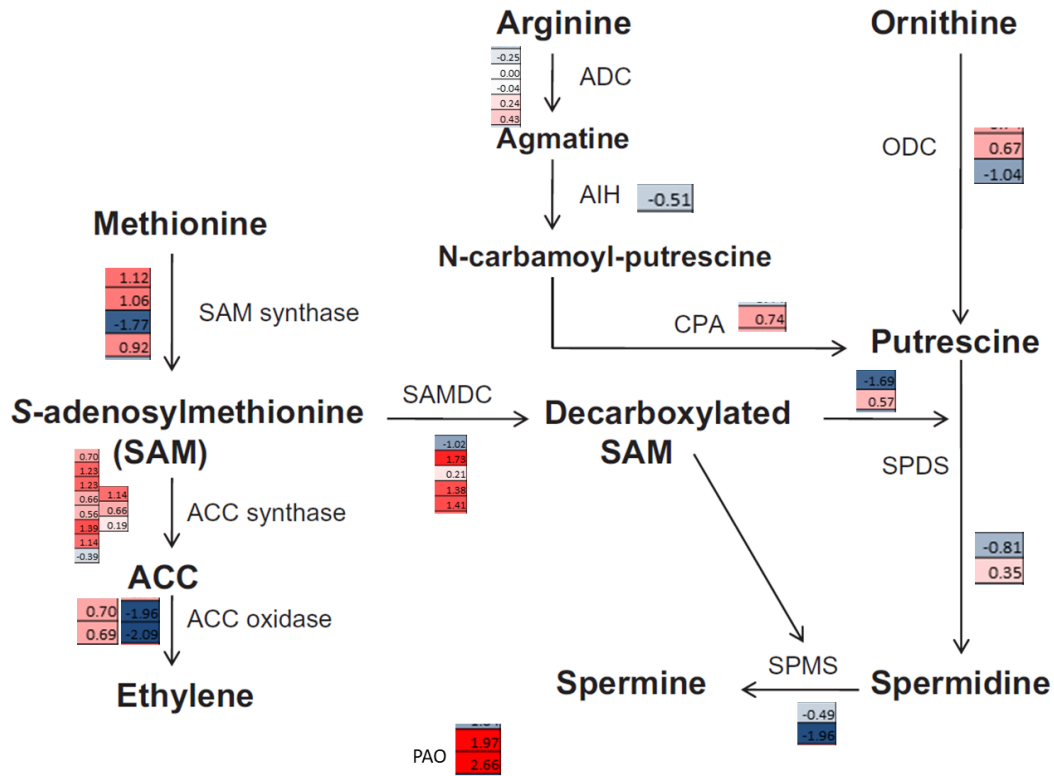
Figure 22 Polyamine biosynthesis pathway and log2 fold-change in gene expression of involved enzymes in primary vs. control tubers. Fold-change values are highlighted in red if up-regulated and in blue if down-regulated (colors saturate at 2.0/-2.0). Figure modified after Wimalasekera et al., 2011.

3.4 Screening of cross-breeding populations regarding their response to heat

Aiming at the identification of the underlying genetic determinants of the different heat response properties of the cultivars Agria, Tomensa, Saturna, Princess and Ramses described in chapter 3.3.1, cross-breeds of different combinations of the cultivars were produced by Solana Research GmbH (Windeby). Parental lines were chosen according to their contrasting heat responses especially concerning the formation of second-growth. In this chapter, the phenotypic analysis of the segregating heat stress response of the offspring and the transcriptional characterization of phenotypic extremes are described.

3.4.1 Establishment of growth conditions suitable for large-scale potato cultivation in phyto-chambers

For the screening of the cross-breeding populations three prerequisites had to be met;

1. They had to be grown in an environment with adaptable conditions
2. Growth conditions should enable the cultivation of a large number of plants simultaneously
3. Growth conditions should support a rapid tuber development.

Adaptable conditions were important to enable the application of heat for defined periods of time and to ensure comparable conditions within one growth period and between cultivation periods. This included the adjustability of light intensity, day length, temperature and humidity. Therefore, cultivation had to be carried out in phyto-chambers, resulting in space restrictions. To overcome these limitations, short-day conditions were applied to the plants resulting in a very early tuber-induction and thus, shorter growth periods. Furthermore, plants were grown in small pots restricting final plant and tuber size but enabling rapid and large-scale potato cultivation.

3.4.2 Phenotyping of three cross-breeding populations

Although the number of plants which could be cultivated simultaneously was increased by the measures described above, space did not suffice for a simultaneous cultivation of all lines. Furthermore, space restrictions prevented the parallel cultivation of plants under differing conditions, i.e., control. Therefore, standardized cultivation conditions were sought enabling successive cultivation periods with high comparability. The course of action included the adjustment of the light intensity in the phyto-chamber and usage of defined amounts of soil per plant. A watering scheme was tried to be established but due to different evaporation-rates as

well as differences in plant growth and water uptake between lines, watering had to be adapted for each plant individually. Furthermore, temperature conditions were slightly changed between the cultivation cycles as described in the chapters below. Consistently, an initial period of 30 days under control temperatures was applied to give the plants time to adapt to their environment and to induce tubers. When tactile tubers had developed, temperatures were increased for a period of 10 days followed by a regenerative phase under normal temperature conditions Figure 23.
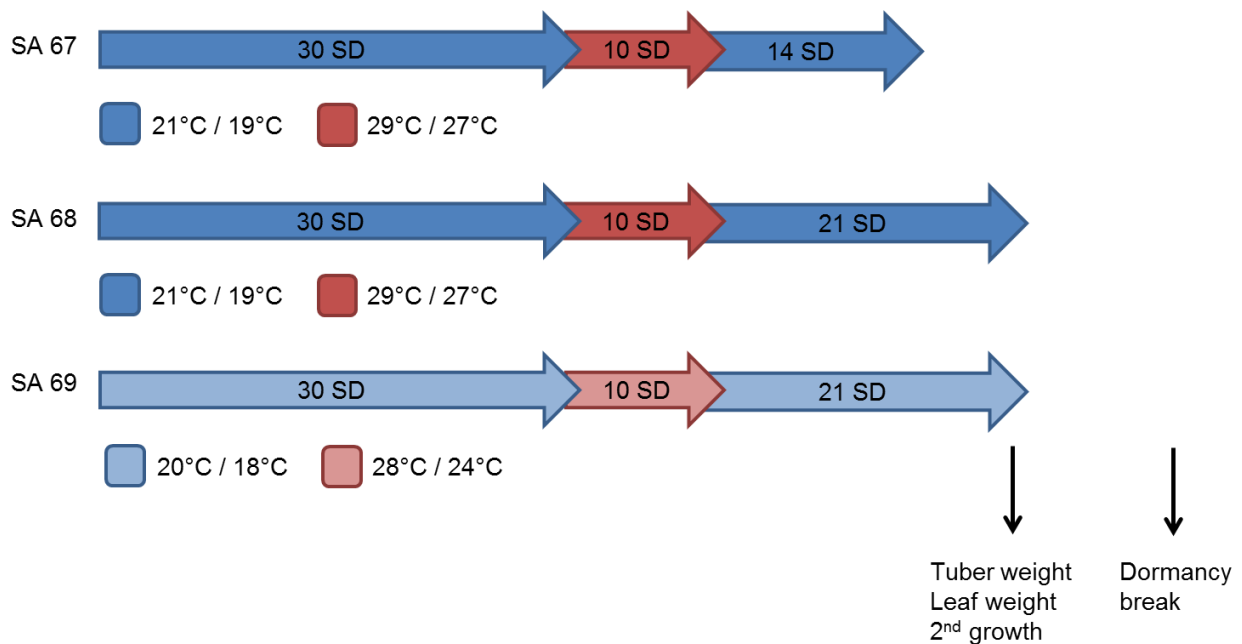
Figure 23: Growth conditions of the cross-breeding populations SA67-69/12 – HotPot. Blue arrows indicate normal temperatures, red arrows indicate elevated temperatures. Day length is indicated by the abbreviation SD (short days). Numbers represent days. Black arrows indicate time-points of physical measurements and visible evaluations of tubers.

At the end of the growth period, plants were harvested and physically evaluated. For this purpose, the parameters leaf weight, tuber weight and tuber phenotype were determined. Afterwards, tubers were stored in cardboard boxes to keep them dry and dark until sprouting.

3.4.2.1   Description of SA67/12 – HotPot (Agria x Saturna)

Crossing of the cultivars Agria and Saturna resulted in the population SA67/12 – HotPot consisting of 77 lines. The growth conditions are depicted in Figure 23 (upper panel). Per line, four plants were grown at the same time to serve as biological replicates. Results of above- and below-ground biomass measurements of population SA67/12 are summarized in Figure 24.
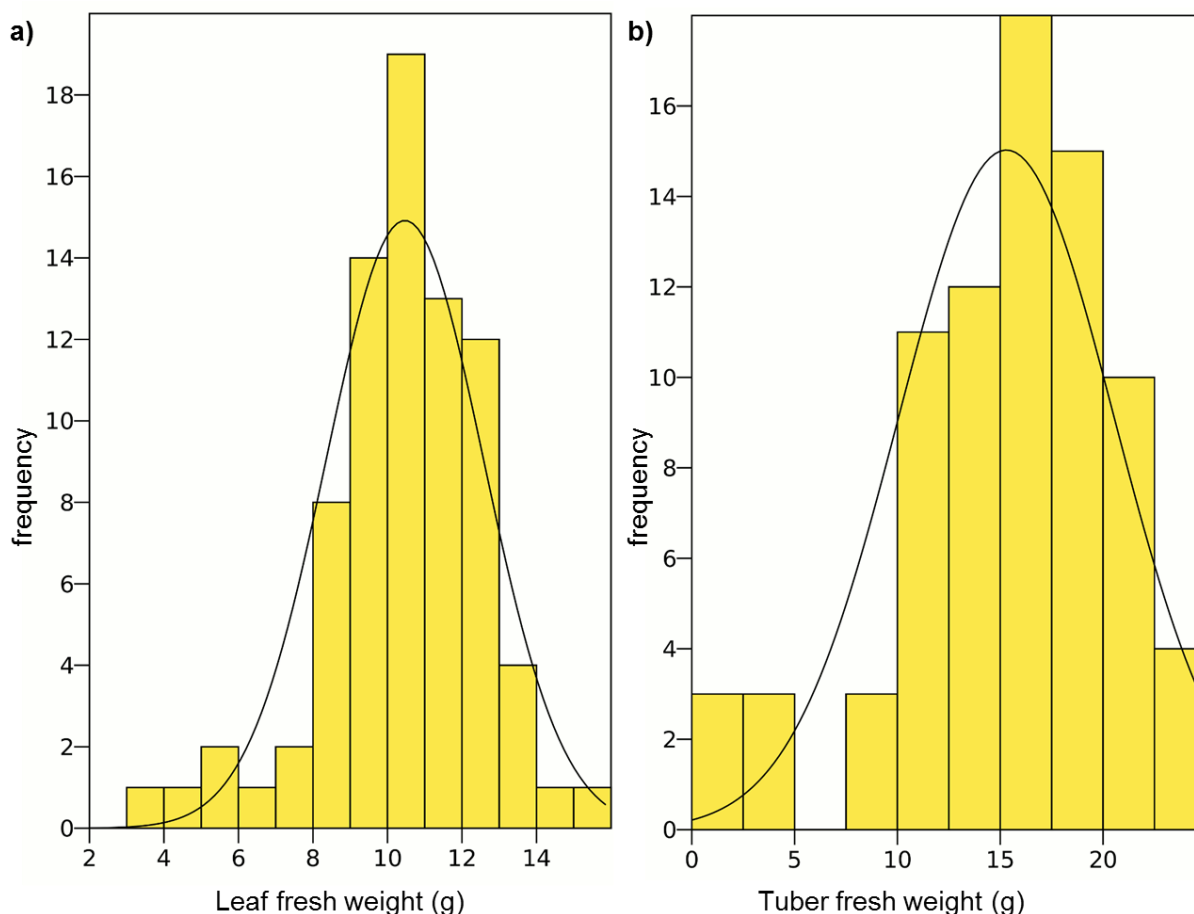
Figure 24: Histograms depicting the distribution of leaf and tuber biomasses across cross-breeds of population SA67/12 – HotPot. To draw the diagrams, each crossing line is represented by the average value of four biological replicates. In total, 79 genotypes were analyzed. The black curve represents the normal distribution.

Regarding leaf fresh weight, biomass distribution among the cross-breeds approached normal distribution (Figure 24a). Average leaf biomass was 10.47 g, with values ranging from 3.17 g in line SA67/12 #43 to 15.17 g in line SA67/12 #45. Both parental strains had leaf biomasses above the population average with 12.7 g in Agria and 13.14 g in Saturna (Figure A 1).

Average tuber biomass of the population was 15.3 g and range was between 1.18 and 24.87 g. Parental lines exhibited average tuber biomasses of 9.7 g (Saturna) and 16.12 g (Agria) (Figure A 1). Distribution of tuber biomasses showed some outliers in the lower range (Figure 24b). Total tuber fresh weight of six lines (SA67/12 #27, 43, 81, 51, 19 and 70) was below 5 g and thus, tubers were very small and hardly allowed for any subsequent rating on second-growth.

Results

Evaluation of the tubers for second-growth phenomena like knobby, chain, bottleneck, elongated and sprouted tubers was done visually. The results are presented in Figure 25 and Table A 3. In contrast to the results obtained from the experiment conducted to describe the parental lines, Agria did not exhibit any second-growth. For Saturna, the case was reversed; while in the initial experiment, only a very low tendency towards second-growth was observed, under the conditions used for the screening, tubers seemed knobby and irregular. In most cases only individual tubers showed one of the second-growth types which, together with the absence of a control treatment, prevented the graduation of the lines into more resistant and susceptible towards heat stress.
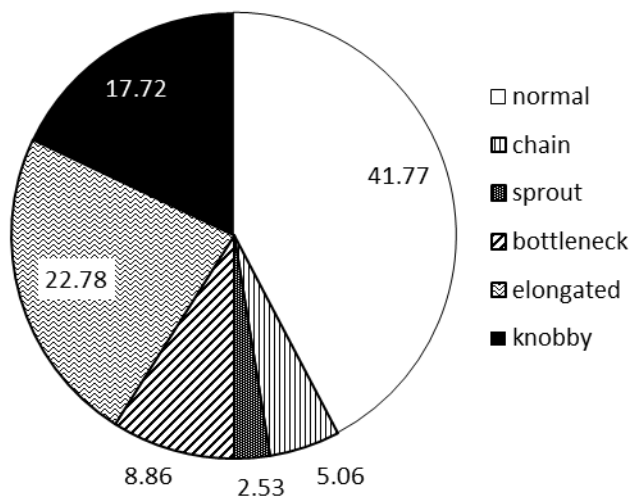
Figure 25: Tuber phenotypes in cross-breeding population SA67/12 – HotPot. Tubers were visually grouped into the second-growth phenotypes. Line #27 was not considered for its very unusual tubers.

The last trait analyzed in the population SA67/12 – HotPot was the duration of dormancy. To evaluate dormancy quantitatively, tubers were analyzed regularly for the formation of sprouts. Sprouted tubers were quantified daily and the day after harvest when 50% of the tubers had sprouted was noted for each line respectively. The Box-Whisker-Plot shows that half of the lines showed sprouting between days 81 and 85. Furthermore, some outliers were detected; lines #64 and #11 sprouted extraordinarily early (days 67 and 75 after harvest respectively) and line # 51 sprouted very late. Line #1 was not an outlier but still among the late sprouting lines (Figure 26).
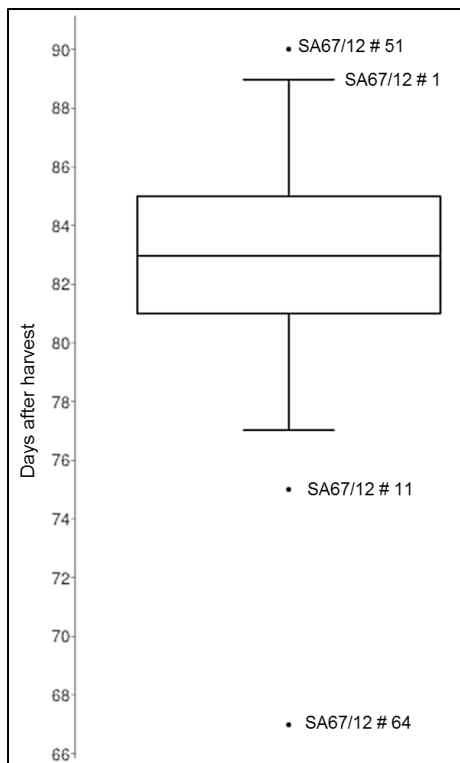
Figure 26: Box-Whisker-Plot representing dormancy break time-points for cross-breeding population SA67/12 – HotPot. For each line, the day when 50% of tubers had sprouted was used for analysis. The online-tool available at www.alcula.com/calculators/statistics/box-plot/ was used to generate the graph.

3.4.2.2 Description of SA68/12 – HotPot (Saturna x Princess)

For the cultivation of the cross-breeding population SA68/12 – HotPot consisting of 66 lines with the parental strains Saturna and Princess, a slightly changed setup was chosen (see Figure 23, middle panel). Four plants per genotype were grown and served as biological replicates. The experimental period was extended for one week of regeneration after the heat period. This was done in anticipation of a clearer outcome regarding second-growth phenotypes. Furthermore, tuber biomass was expected to be higher at harvest avoiding the very low biomasses seen in some lines of SA67/12 – HotPot (Figure A 2).

Average leaf biomass of SA68/12 – HotPot was 11.8 g and ranged between 1.03 g in line #54 and 18.99 g in line #96. Lines # 54 and #31 exhibited the lowest leaf biomasses and can be regarded as outliers (Figure 27a). The parental lines Saturna and Princess had average leaf biomasses of 12.06 g and 13.29 g which were about average.

Analysis of the tuber biomass data showed that on average lines of the crossing population SA68/12 – HotPot had a tuber biomass of 22.58 g. Values ranged from 0.08 g to 32.6 g. The parental lines Saturna and Princess exhibited tuber biomasses of 10.63 and 32.6 g respectively, indicating a favorable biomass allocation towards tubers in Princess (Figure A 2).

Results

Despite the longer growth period, two lines still exhibited very low tuber biomasses (Figure 27b). These were the same two lines exhibiting extraordinarily low leaf weights indicating that they might have a general growth defect (Figure A 2). Nevertheless, on average, lines of population SA68 had higher tuber biomasses than SA67, owing to the extended experimental duration.
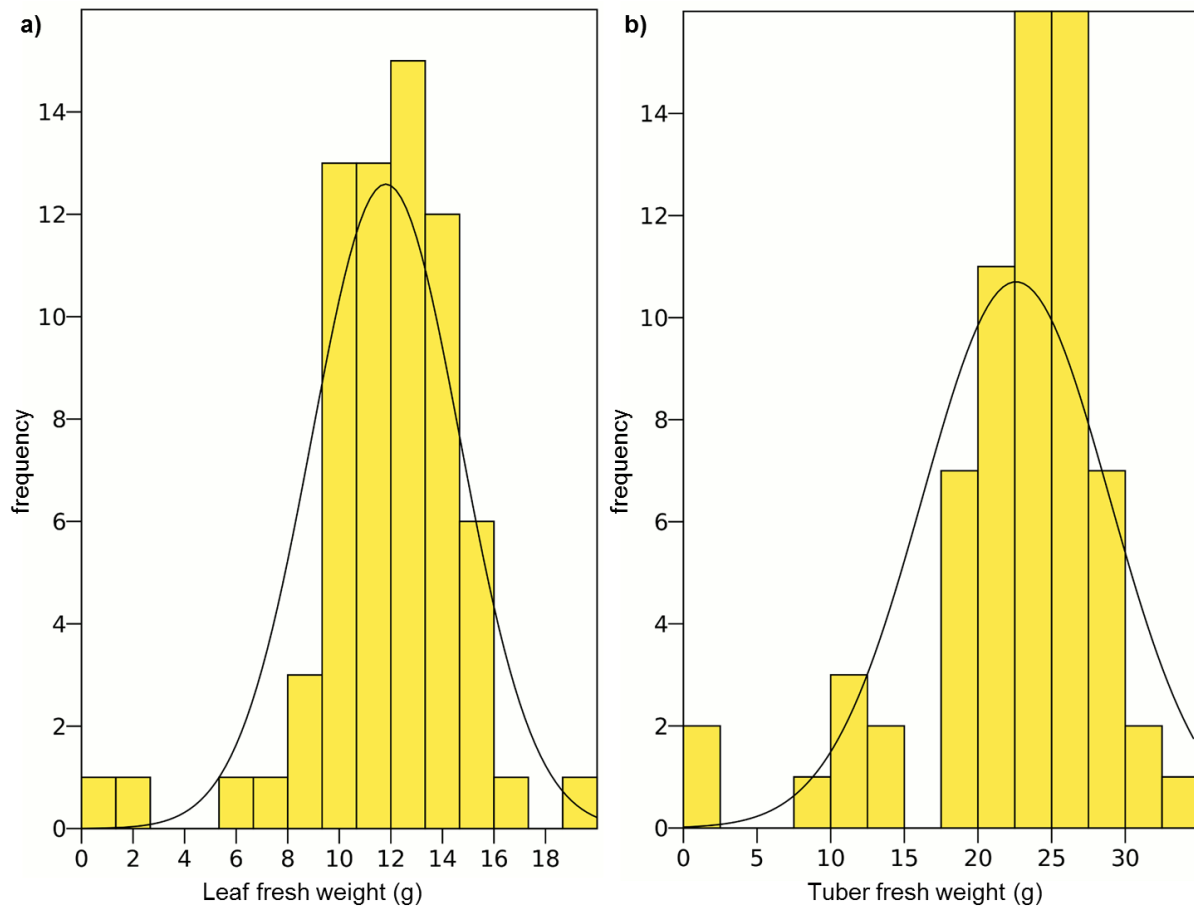
Figure 27: Histograms depicting the distribution of leaf and tuber biomasses across cross-breeds of population SA68/12 – HotPot. To draw the diagrams, each crossing line is represented by the average value of four biological replicates. In total, 68 genotypes were analyzed. The black curve represents the normal distribution.

The occurrence of second-growth phenotypes in the population SA68/12 – HotPot was higher than in SA67. Only 35.3% of the lines exhibited normal looking tubers, while in the other lines at least one tuber with an obvious second-growth type was noted (Figure 28, Table A 4). Moreover, in many lines, more than just a single tuber showed the same phenotype. This finding could be a result of the extended growth period or of the selection of the parental strains Saturna and Princess, both exhibiting tubers with a second-growth phenotype (Table 5).
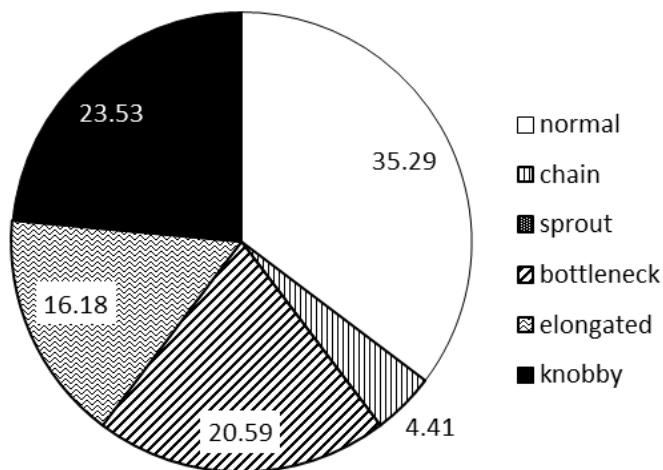
Figure 28: Tuber phenotypes in cross-breeding population SA68/12 – HotPot. The pie chart represents the percentages of lines showing at least one tuber with a second-growth phenotype.

Observing the tubers for dormancy break revealed that in the population SA68 tubers sprouted much earlier than in population SA67. Half of the lines had already shown sprouting in 50% of their tubers after 38 days. Furthermore, the interquartile range was much larger in SA68 than SA67, encompassing a time-span of 12 days during which half of the lines reached 50% sprouted tubers. Only line #5 was identified as an outlier that sprouted significantly later than all other lines (Figure 29).
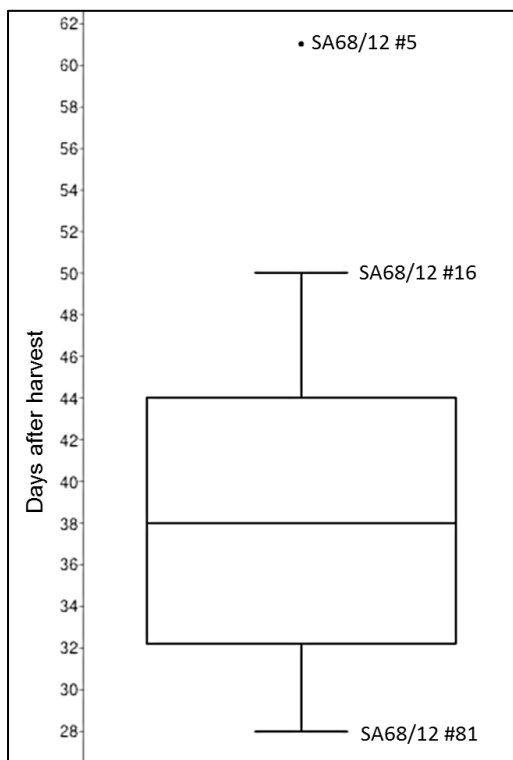
Figure 29: Box-Whisker-Plot representing dormancy break time-points for cross-breeding population SA68/12 – HotPot. For each line, the day when 50% of tubers had sprouted was used for analysis. The online-tool available at www.alcula.com/calculators/statistics/box-plot/ was used to generate the graph.

3.4.2.3 Description of SA69/12 – HotPot (Ramses x Tomensa)

The population SA69/12 – HotPot consisted of 69 lines and was obtained by crossing the cultivars Ramses and Tomensa. In order to characterize the lines, four plants of each line as biological replicates were grown. As depicted in Figure 23, the temperature regime was slightly changed again. Temperatures were decreased from 21°C (day) / 19°C (night) to 20°C / 18°C under control conditions and from 29°C / 27°C to 28°C / 24°C during the heat period.
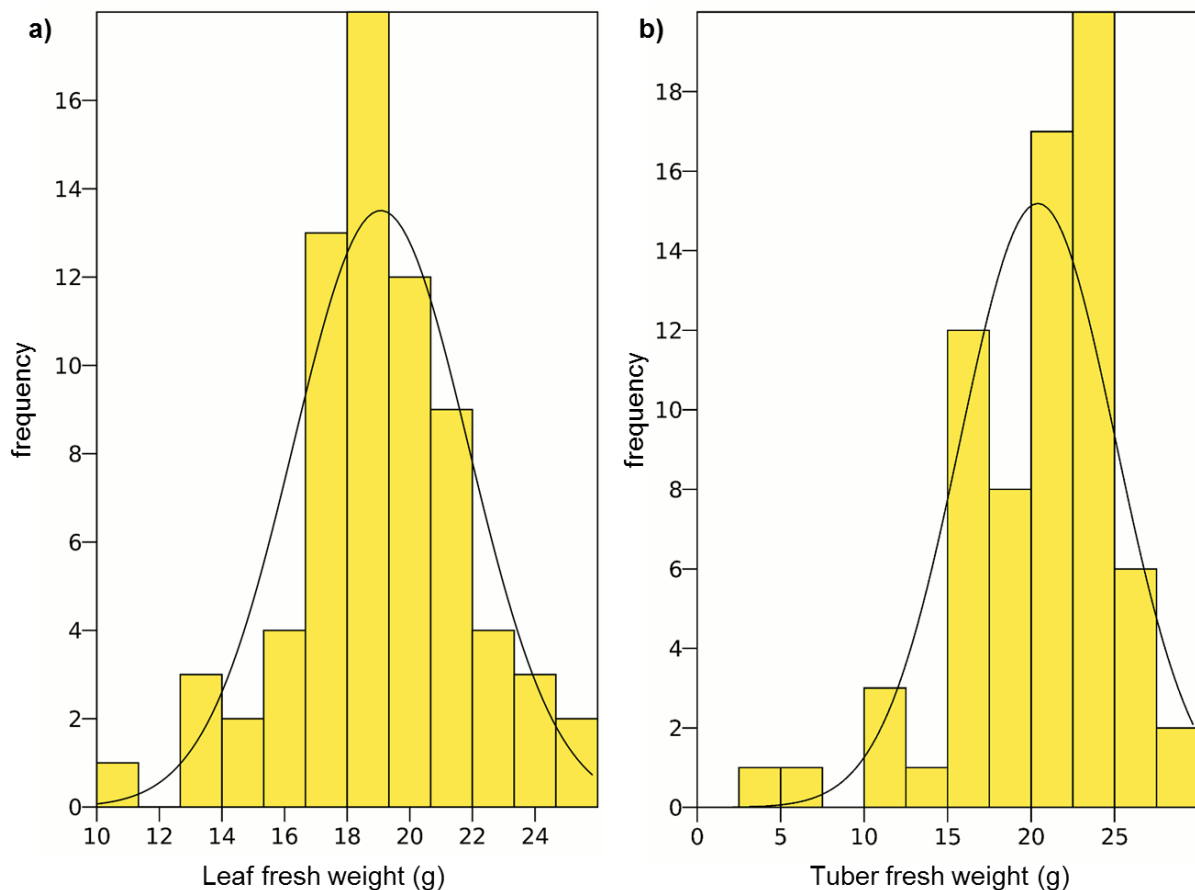
Figure 30: Histograms depicting the distribution of leaf and tuber biomasses across cross-breeds of population SA69/12 – HotPot. To draw the diagrams, each crossing line is represented by the average value of four biological replicates. In total, 71 genotypes were analyzed. The black curve represents the normal distribution.

Analysis of leaf biomass distribution among the lines of population SA69/12 – HotPot showed that the population average was 19.07 g and ranged from 10.4 g to 25.78 g following a normal distribution (Figure 30a). The parental strains Tomensa and Ramses had average leaf weights of 17.97 g and 19.53 g respectively.

Average tuber biomass within cross-breeding population SA69/12 – HotPot was 20.4 g. The lowest tuber yield was 4.52 g and was measured in line #47 which also had the lowest leaf

biomass (Figure 30). Tuber yields in the parental lines were 19.16 g in Tomensa and 24.76 g in Ramses.
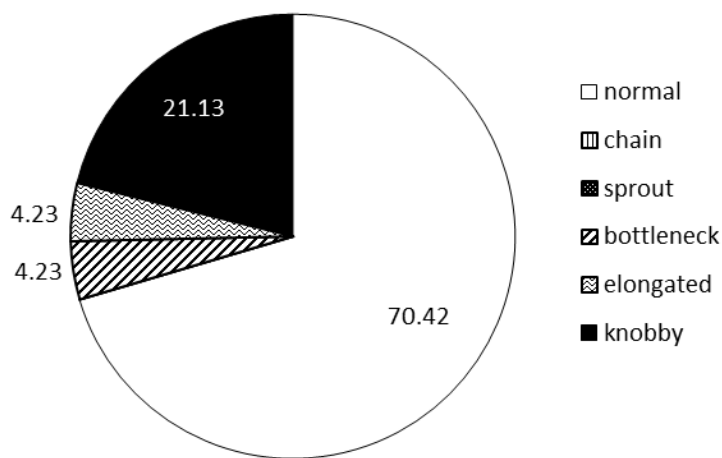
Figure 31: Tuber phenotypes in cross-breeding population SA69/12 – HotPot. The pie chart represents the percentages of lines showing at least one tuber with a second-growth phenotype.

In the cross-breeding lines SA69 only few stress symptoms like second-growth were observed (Figure 31). More than 70% of the lines showed only normal growing tubers without any second-growth phenotype. Furthermore, chain-tubers and sprouting tubers were not detected at all (Table A 5). These results indicate either a stronger resistance of the lines of population SA69 towards heat stress or a lack of stress due to the altered conditions which were milder than for the other two populations (Figure 23 lower panel).

Regarding dormancy in the crossing population SA69/12 – HotPot, it was seen that half of the lines had sprouted 41 days after harvest (Figure 32). This was comparable to population SA68. The interquartile range spanned days 38 to 45 and was in between the other two populations. The parental strains Ramses and Tomensa sprouted on days 40 and 36 after harvest respectively. Three outliers were identified: lines #40 and 50 having a long dormancy period and line #73 exhibiting only a short dormancy period (Figure 32).
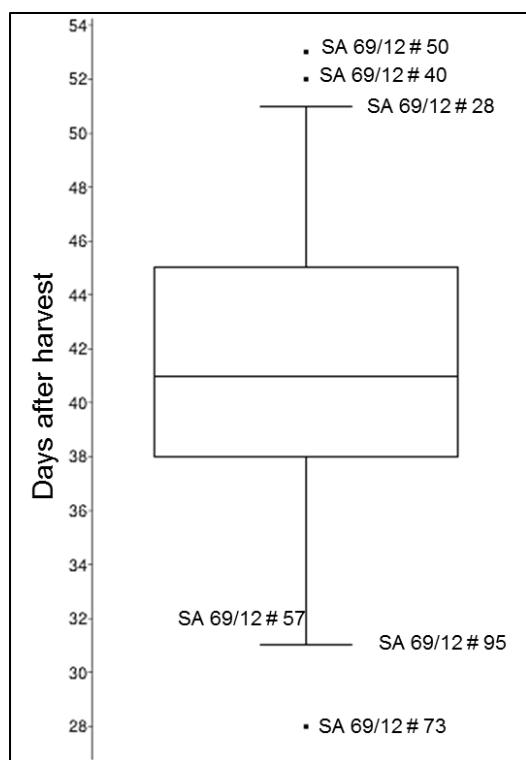
Figure 32: Box-Whisker-Plot representing dormancy break time-points for cross-breeding population SA69/12 – HotPot. For each line, the day when 50% of tubers had sprouted was used for analysis. The online-tool available at www.alcula.com/calculators/statistics/box-plot/ was used to generate the graph.

3.4.3 Dormancy is a stable trait

The phenotyping approach of the cross-breeding populations allowed for the assessment of the traits tuber fresh weight, above-ground biomass and dormancy. Evaluation of heat-induced second-growth on the other side was hardly possible due to the lack of control conditions. Since the formation of certain second-growth types like chain tubers and heat spouting involve bud meristematic activity, it was assumed that the mechanisms underlying second-growth formation and dormancy break could be similar. Therefore, for each cross-breeding population, lines which sprouted very early or very late were cultivated again under controlled conditions and with more replicates (~7-8 per line and condition). Table 10 displays the selected lines and summarizes the outcome of the dormancy length assessments described in 3.4.2.

Table 10: Selected cross-breeding lines and parental strains for re-cultivation to assess sprouting.

population	SA67	SA68	SA69
parental cultivars	Agria x Saturna	Agria x Princess	Ramses x Tomensa
early	#11, #64	#72, #81	#57, #73, #95
late	#1, #51	#5, #16	#28, #50

The selected lines were propagated in tissue culture to enable the cultivation of a higher number of plants and directly compare heat-treated plants to plants grown under control conditions.

3.4.3.1 Re-cultivation of selected lines of cross-breeding populations SA67 and SA68/12 - HotPot

For the re-assessment of the phenotypic characteristics of the selected lines of all three cross-breeding populations, the growth conditions were adapted in order to enable rapid tuber induction by implementing short-day conditions and then enhance the heat stress effect by switching to long-day conditions. The switch was introduced since in the initial experiments with the parental lines (see chapter 3.3.2), which were entirely conducted under long-days, strong effects of the heat treatment regarding the formation of second-growth were seen. Assuming that the day-length would have an influence on the susceptibility of the plants towards heat stress, the conditions depicted in Figure 33 were applied.
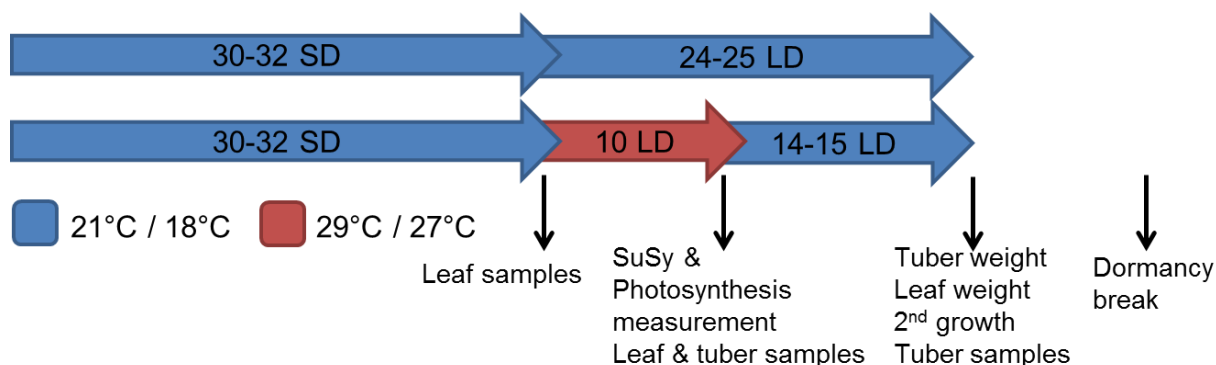
Figure 33: Growth conditions of the selected lines of the cross-breeding populations SA67, SA68 and SA69/12 – HotPot. Blue arrows indicate normal temperatures, red arrows indicate elevated temperatures. Day length is indicated by the abbreviations SD (short days, 8h light) and LD (long days, 16h light). Numbers represent days. Black arrows indicate time-points of physical measurements, sampling and visible evaluations of tubers.

At the end of the 10-day heat period, after a total growth period of 40 days, photosynthesis was measured and samples of leaves and tubers were taken. The final harvest was scheduled two weeks later, after a regeneration period for the stressed plants. At this time-point, leaf and tuber biomasses were assessed and tubers were evaluated for second-growth phenomena. Thereafter, tubers were stored in the dark at room temperature until visible sprouting, which was again monitored.

Lines of populations SA67 and SA68 were grown at the same time-point while lines of SA69 were cultivated separately. Therefore, results are shown for SA67 and 68 together, first.

Results

In order to assess the effect of the heat treatment on tuber starch metabolism, SuSy activity was measured in tubers harvested at the end of the ten-day stress period and compared to control tubers. In the parental lines Saturna, Princess and Agria, the heat treatment significantly decreased SuSy activity when compared to control. In the selected cross-breeding lines, only line SA67#11 exhibited decreased SuSy activity under stress conditions. In this line, the effect was very strong and SuSy activity in stressed tubers was the lowest observed among all lines analyzed. All other cross-breeds showed strong tendencies toward decreased SuSy activity, but statistical significance was not reached (Figure 34).
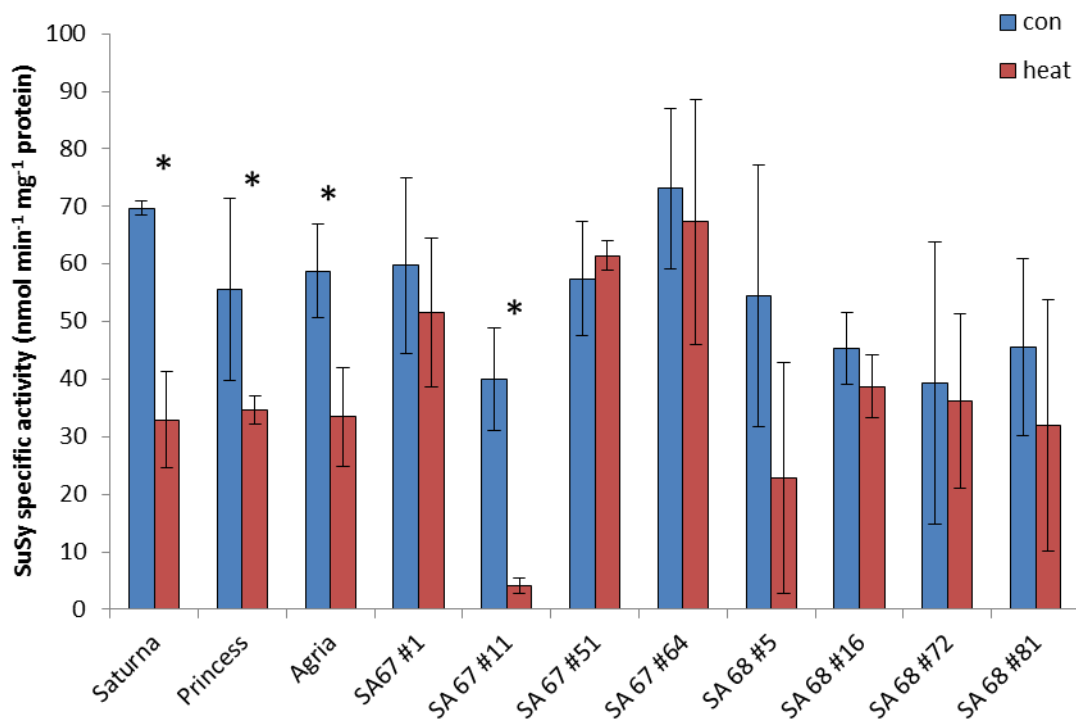
Figure 34: Sucrose Synthase activity in protein extracts from tubers of selected lines of cross-breeding populations SA67 and SA68. Blue bars represent control tubers; red bars represent heat-treated tubers. Error bars represent standard deviation of four (in case of Saturna heat, SA67#51 con and heat, SA68#5 heat only three replicates were obtained, in case of SA67#64 only two) biological replicates. Asterisks mark statistically significant differences ($p < 0.05$) between treatments (Student's t-test).

At the end of the growth period biomasses of leaves and tubers were measured. Analysis of the data showed that tuber yield was significantly diminished in some of the lines due to the stress treatment (Figure 35b). Furthermore, above-ground biomasses were changed in some cases as well (Figure 35a). In contrast to the tuber data, changes in leaf biomasses were found to be both, increased and decreased, when compared to control.
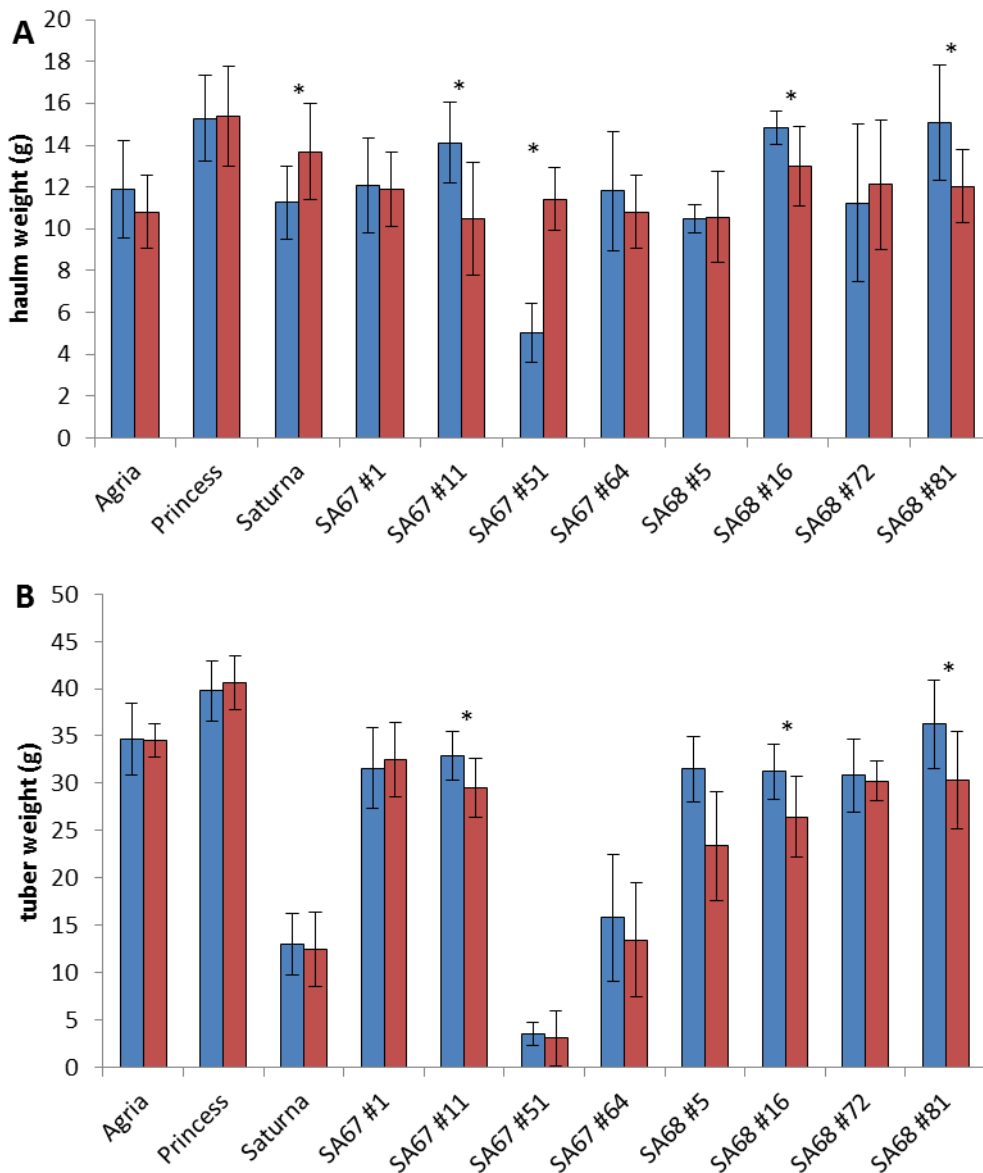
Figure 35: Haulm (A) and tuber (B) weights of selected lines of cross-breeding populations SA67 and SA68. Blue bars represent values from control plants; Red bars represent values from heat-treated plants. Error bars represent standard deviations of eight biological replicates. Asterisks mark statistically significant differences (p < 0.05) between treatments (Student's t-test).

Regarding the formation of second-growth, a few tubers exhibiting phenotypic characteristics of this phenomenon were identified in some of the selected lines. The relative amounts of second-growth tubers are shown in Table 11. The occurrence of second-growth did not correlate with the duration of dormancy. The early sprouting lines SA67#11 and #64 and SA68#72 and #81 showed second-growth in 0-8.6% of tubers under control conditions and in 3.8-7.7% of tubers under stress conditions. On the other side, the late sprouting line SA67#1 showed 20% of tubers with second-growth under control conditions and 0% under stress. The line with the highest rate of second-growth was the parental line Saturna which exhibited

second-growth in 16.7% of tubers under control conditions and 28.6% of tubers under stress. This hints to an increasing effect of the heat treatment on the formation of second-growth in Saturna but not in any of the other lines.

Table 11: Percent of tubers showing second-growth phenotypes in selected lines of cross-breeding populations SA67 and SA68 and the parental strains Agria, Saturna and Princess under control and heat conditions.

	Agria	Princess	Saturna	SA67#1	SA67#11	SA67#51	SA67#64	SA68#5	SA68#16	SA68#72	SA68#81
Con	4.5%	0%	16.7%	20%	8.6%	8.3%	0%	0%	0%	0%	7.4%
Heat	0%	0%	28.6%	0%	3.8%	5%	0%	0%	1.8%	5.2%	7.7%

After tubers were harvested and biomasses assessed, tubers were stored at room temperature in the dark and sprouting was assessed visually on a regular basis. Sprouting time-points for cross-breeding population SA67 were comparable to the first cultivation with lines #11 and #64 exhibiting a shorter dormancy period and lines #1 and #51 showing a longer phase of dormancy. In population SA68, overall sprouting was found to be later than during the first cultivation with no clear difference between "early" and "late" lines. In Saturna, Princess, SA67#1, 11, 64 and SA68#16 and 81, sprouting seemed slightly accelerated in heat-treated tubers when compared to the respective control tubers (Figure 36).
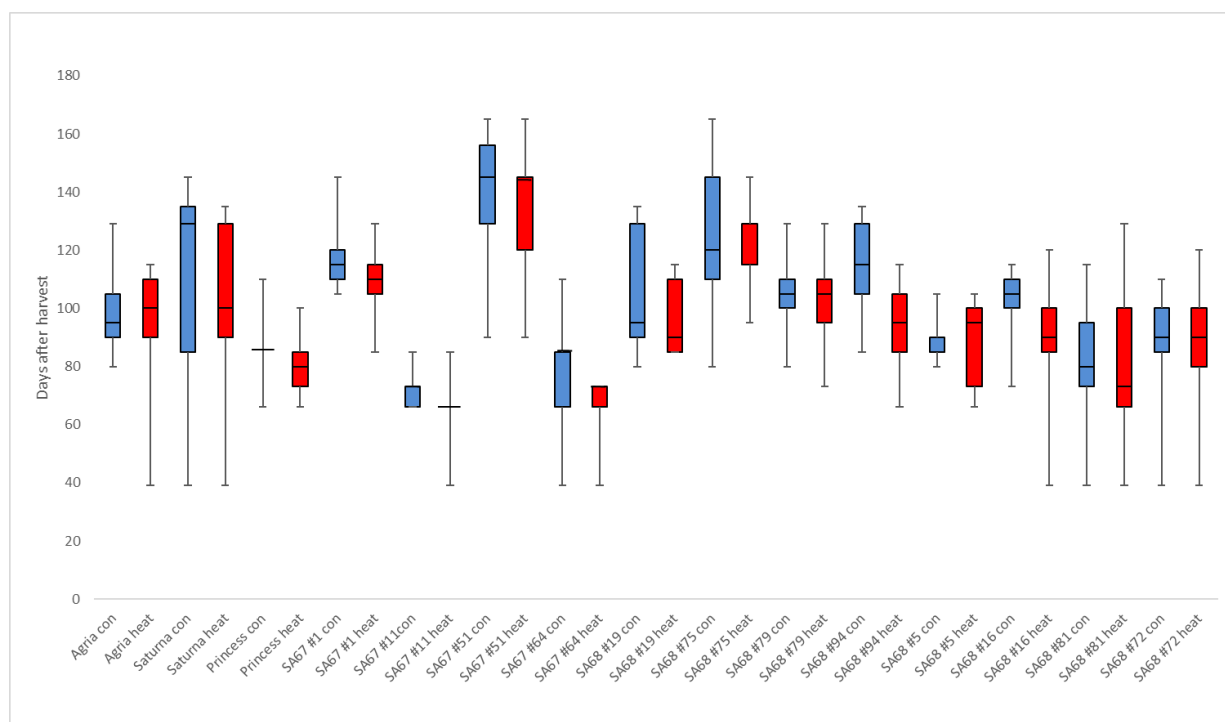
Figure 36: Dormancy length in selected lines of cross-breeding populations SA67 and SA68 as well as the parental strains Agria, Saturna and Princess. Whiskers represent earliest and latest sprouting tubers, boxes represent interquartile ranges. Blue boxes represent control values; Red boxes represent values of heat-treated tubers.

3.4.3.2   Re-cultivation of selected lines of cross-breeding population SA69/12 - HotPot

In selected cross-breeding lines of population SA69, photosynthesis was measured during the last days of the heat period. As expected, transpiration was significantly increased in response to the heat treatment in all lines but Tomensa and SA69 #40 (Figure 37C). With regard to assimilation, decreases due to the heat stress were noted in the parental strain Ramses as well as line #40 (Figure 37A). Electron transport rate was unaffected by the treatment (Figure 37B).
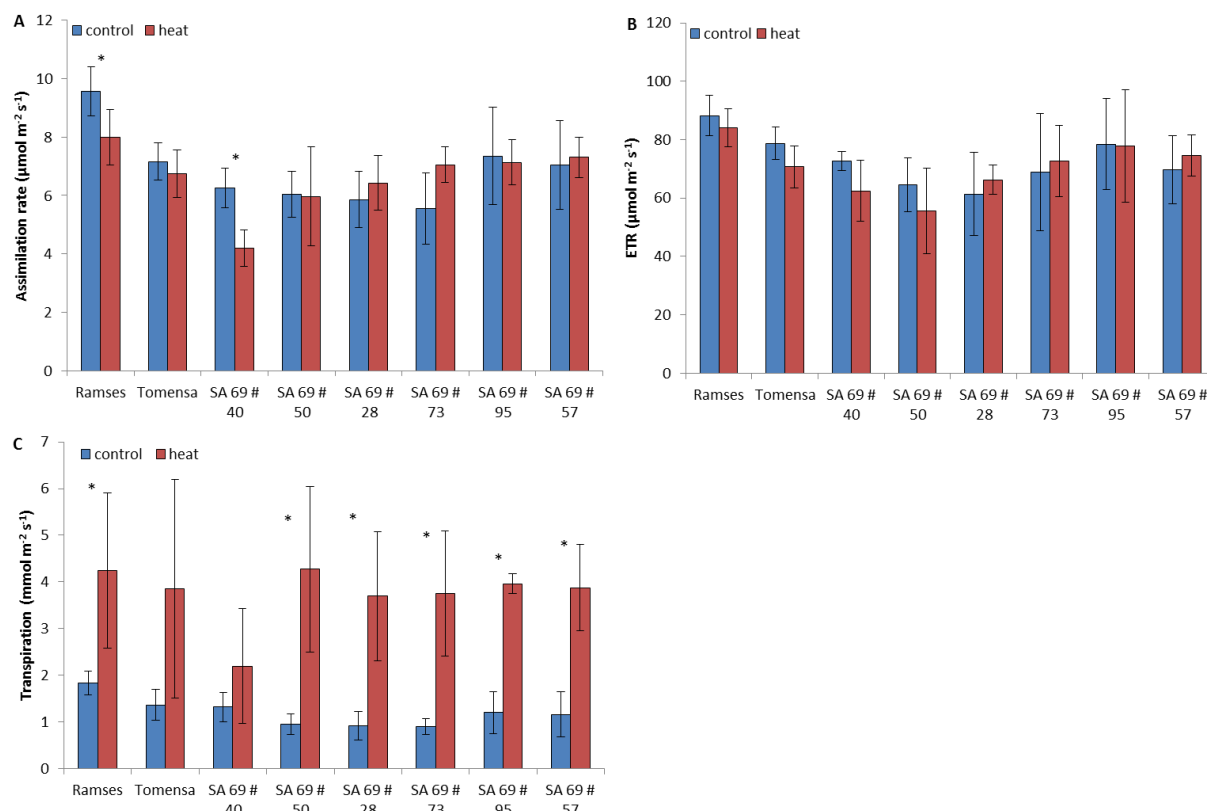
Figure 37 Results of the photosynthesis measurements at the end of the stress period in stressed and control lines of cross-breeding population SA69. A) assimilation rate, B) electron transport rate, C) transpiration. Blue bars represent control plants, red bars represent stressed plants. Error bars represent standard deviations of four biological replicates. Asterisks mark statistically significant differences (p < 0.05) between treatments (Student's t-test).

Measurement of SuSy specific activity in protein extracts of tubers harvested at the end of the heat stress period showed a decrease in activity in response to the heat treatment in the parental strain Ramses as well as the cross-breeding lines SA69#73 and #95 (Figure 38). The values obtained for SA69#95 were very similar to those measured in Ramses under control and stress conditions, respectively. All other lines showed trends towards decreased SuSy activity under heat stress but none of these differences reached statistical significance.
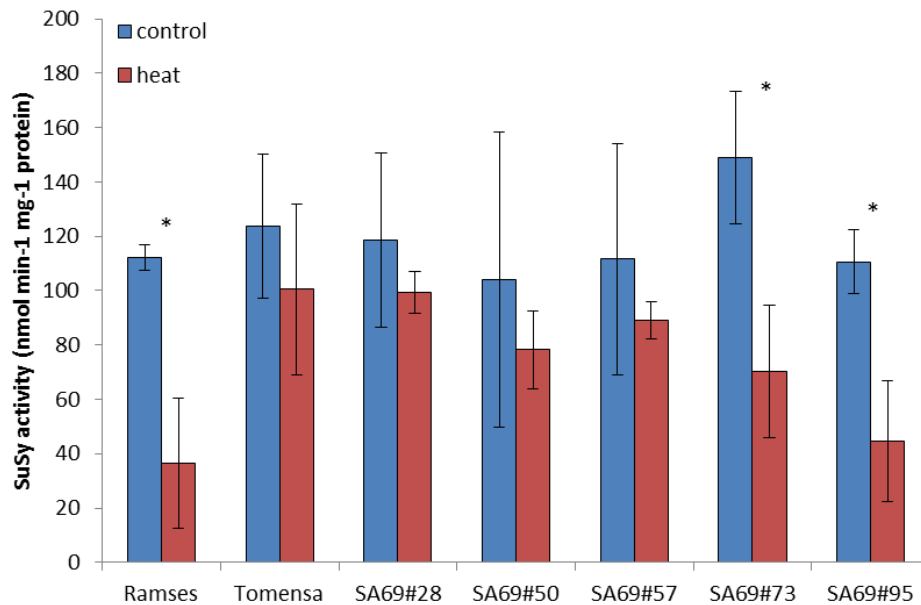
Figure 38: Sucrose Synthase activity in protein extracts from tubers of selected lines of cross-breeding population SA69. Blue bars represent control tubers; red bars represent heat-treated tubers. Error bars represent standard deviation of three to four biological replicates. Asterisks mark statistically significant differences ($p < 0.05$) between treatments (Student's t-test).

In selected cross-breeding lines of population SA69, heat stress led to significantly decreased tuber yields in most of the lines while haulm weights were not significantly affected (Figure 39). The only lines not showing decreased tuber yield due to the heat stress were the parental strain Ramses and line #40, which seems to contradict the results from the photosynthesis measurement where assimilation rates were significantly reduced in response to heat stress compared to control conditions suggesting a lower carbon uptake and, consequently, reduced biomass accumulation.
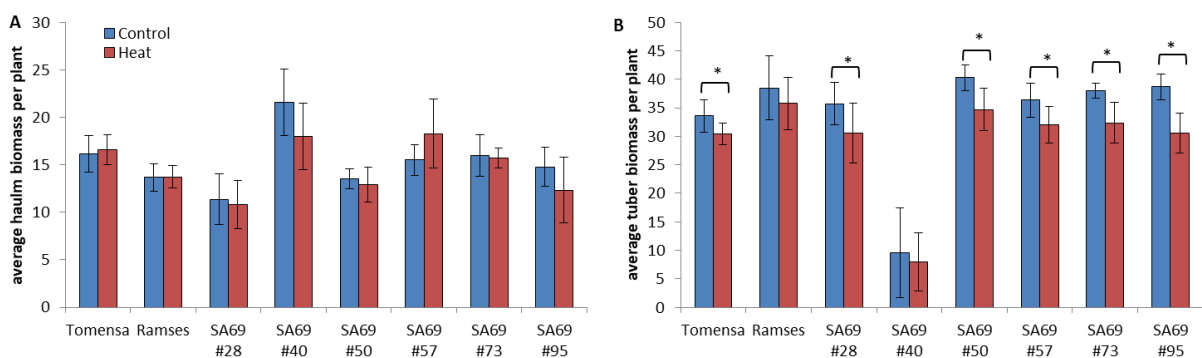
Figure 39: Haulm (A) and tuber (B) weights of selected lines of cross-breeding population SA69 (g). Blue bars represent values from control plants; Red bars represent values from heat-treated plants. Error bars represent standard deviations of seven to eight biological replicates. Asterisks mark statistically significant differences between control and heat-treated plants of the same genotype ($p \leq 0.05$, Student's T-test)

Visual assessment of tuber phenotypes showed an increased proportion of second-growth tubers in heat-treated plants of line #57 in particular (Table 12). Here, second-growth was observed in 2.7% of tubers from control plants and 26.6% of tubers from heat-treated plants. This was surprising given that this line was chosen for its short dormancy period and that it did not show any signs of second-growth during the first cultivation. Furthermore, the parental strain Ramses exhibited about 10% of tubers with second-growth while line #40 showed second-growth irrespective of the treatment with the proportion of second-growth tubers being about the same between control and stressed plants (Table 12).

Table 12: Percent of tubers showing second-growth phenotypes in selected lines of cross-breeding population SA69 and the parental strains Tomensa and Ramses under control and heat conditions.

	Tomensa	Ramses	SA69#28	SA69#40	SA69#50	SA69#57	SA69#73	SA69#95
Con	0%	0%	0%	15.9%	0%	2.7%	0%	0%
Heat	0%	9.6%	0%	18.2%	0%	26.6%	6.3%	4.4%

To identify metabolic differences between the lines, metabolite profiling was conducted from the samples taken at the end of the experimental period. To this end, phosphorylated intermediates as well as amino acids were quantified (Table 13, Figure 40). Lines #40 and #95 were omitted from the analysis of metabolites.

Heat treatment did not cause many effects regarding phosphorylated intermediates. Line #28 showed the most heat-induced differences. 3-Phosphoglycerate (3PG), Phospho-Enolpyruvate (PEP) and Shikimate (Shi) were significantly higher in tubers grown under heat conditions. In the parental line Tomensa, Isocytrate (Icit) was significantly higher in tubers from stressed plants. In line #57, UDP-Glucose (UDPglc) was higher in heat-treated tubers than in control tubers (Table 13).

Regarding the levels of free amino acids, no uniform changes were observed between tubers grown under control conditions and tubers from heat-treated plants (Figure 40). Asparagine (Asn), Serine (Ser) and Threonine (Thr) tended to be higher in heat-treated tubers with the exception of line #73, where they were slightly lower. Line #50 showed the most changes in free amino acids; Asn, Ser, Glutamine (Gln), Thr, Arginine (Arg), Proline (Pro) and Leucine (Leu) were significantly higher under heat treatment than control. In line #57 more diverse changes were observed; Ser, Thr, Alanine (Ala), Valine (Val), Methionine (Met) were higher, while Pro was lower in heat-treated tubers compared to control (Figure 40).

Results

Table 13: Measurement of phosphorylated intermediates. Results are displayed as mean of four biological replicates (nmol/g FW) ± standard deviation. Statistical differences between treatments in tubers of the same line are indicated in bold (t-test assuming unequal variances, p<0.05).

	Tomensa con	Ramses con	SA69 #28 con	SA69 #50 con	SA69 #57 con	SA69 #73 con	Tomensa heat	Ramses heat	SA69 #28 heat	SA69 #50 heat	SA69 #57heat	SA69 #73 heat
Pyr	31.98 ± 4.51	25.57 ± 7.35	34.09 ± 11.11	31.63 ± 6.66	28.44 ± 6.52	35.09 ± 12.54	25.86 ± 7.11	27.65 ± 5.33	33.10 ± 2.77	31.73 ± 10.72	38.49 ± 9.85	33.94 ± 6.74
G1P	43.12 ± 6.46	33.55 ± 13.31	42.42 ± 16.08	52.16 ± 12.55	37.17 ± 7.45	34.11 ± 5.29	47.32 ± 0.26	45.51 ± 20.13	65.91 ± 11.01b	49.95 ± 12.63	37.95 ± 9.79	34.58 ± 5.50
G6P	395.20 ± 89.39	257.77 ± 35.77	329.96 ± 141.40	457.88 ± 42.62	248.93 ± 36.78	252.62 ± 52.08	398.81 ± 66.40	361.72 ± 233.99	517.56 ± 68.01	375.01 ± 79.67	320.72 ± 95.63	281.30 ± 23.08
F6P	118.52 ± 8.94	81.85 ± 18.43	106.09 ± 39.56	136.21 ± 18.14	78.85 ± 10.61	96.81 ± 26.94	133.47 ± 14.60	120.39 ± 53.71	164.38 ± 7.60	136.56 ± 20.69	115.05 ± 36.73	95.31 ± 12.90
M6P	75.14 ± 20.67	43.30 ± 10.17	65.89 ± 26.28	64.62 ± 8.95	48.25 ± 5.18	45.87 ± 4.91	70.59 ± 11.95	58.98 ± 29.60	83.78 ± 18.67	59.76 ± 25.59	60.29 ± 20.93	51.32 ± 7.50
3PG	351.50 ± 82.69	207.84 ± 132.03	**240.67 ± 93.68**	449.36 ± 119.81	219.12 ± 25.86	214.81 ± 41.77	304.43 ± 45.44d	270.42 ± 143.04	**483.82 ± 52.27**	363.79 ± 30.39	286.03 ± 43.57	246.28 ± 22.11
UDPglc	247.04 ± 40.20	185.02 ± 57.43	147.64 ± 91.79	211.62 ± 43.47	**132.56 ± 23.79**	242.66 ± 89.72	213.16 ± 53.98	219.94 ± 68.15	250.20 ± 109.81	256.42 ± 110.31	**198.95 ± 29.60**	245.27 ± 126.25
ADPglc	15.23 ± 12.78	11.62 ± 4.43	8.96 ± 6.34	6.17 ± 2.56	11.98 ± 2.68	16.26 ± 5.88	10.16 ± 8.39	18.01 ± 9.00	8.64 ± 3.29	4.67 ± 1.17	13.17 ± 2.08	15.11 ± 7.05
G16BP	23.61 ± 3.39	19.55 ± 4.89	24.93 ± 3.34	24.60 ± 5.87	19.82 ± 8.70	22.48 ± 4.48	25.20 ± 1.72	29.08 ± 12.75	28.54 ± 11.03	25.18 ± 5.86	26.12 ± 4.87	16.12 ± 8.34
F16BP	0.81 ± 0.22	0.63 ± 0.13	0.98 ± 0.34	1.02 ± 0.34	0.95 ± 0.42	0.99 ± 0.31	0.72 ± 0.90	1.11 ± 0.34	1.03 ± 0.35	1.04 ± 0.19	1.04 ± 0.20	0.91 ± 0.14
PEP	43.76 ± 8.23	24.24 ± 13.00	**29.11 ± 12.38**	44.85 ± 7.70	23.97 ± 5.26	23.86 ± 5.08	36.71 ± 4.00	20.05 ± 17.16	**54.84 ± 4.98**	46.47 ± 8.42	37.94 ± 10.92	29.01 ± 4.25
Cit	17995.39 ± 2161.49	15788.42 ± 1550.34	15666.58 ± 4124.38	21111.12 ± 2399.03	19823.00 ± 3626.89	20740.97 ± 3691.90	21476.70 ± 2079.65	18857.52 ± 7030.67	22969.55 ± 5679.53	19871.15 ± 5218.69	21157.43 ± 2336.93	21461.55 ± 917.29
Icit	**140.37 ± 16.89**	168.12 ± 8.16	288.91 ± 116.46	187.04 ± 70.69	349.58 ± 151.95	267.91 ± 54.09	**230.42 ± 21.84**	182.10 ± 78.07	367.08 ± 80.91	237.39 ± 84.08	137.02 ± 65.65	332.66 ± 51.57
Mal	8947.59 ± 1024.57	9521.75 ± 2637.17	7832.06 ± 1933.03	12859.12 ± 2746.25	16405.76 ± 5682.36	7892.45 ± 1680.95	10088.44 ± 2715.97	11990.94 ± 9347.57	12017.94 ± 1697.28	11354.31 ± 3666.01	15681.62 ± 3146.66	8146.17 ± 1506.97
AMP	126.44 ± 40.39	35.46 ± 4.51	64.35 ± 20.16	104.83 ± 37.69	87.11 ± 22.05	59.00 ± 33.72	92.01 ± 49.13	33.95 ± 11.89	45.41 ± 7.63	50.07 ± 3.59	87.91 ± 36.91	75.50 ± 18.40
ADP	8.75 ± 3.35	34.48 ± 29.92	47.35 ± 27.95	32.31 ± 16.83	6.72 ± 2.45	60.14 ± 38.12	5.65 ± 2.17	93.20 ± 45.11	50.06 ± 24.44	49.37 ± 26.77	13.79 ± 4.73	25.69 ± 12.04
Ru15P2	3829.90 ± 469.12	4681.74 ± 828.46	4314.54 ± 1240.96	4192.83 ± 726.88	5538.93 ± 1618.29	5363.96 ± 1878.71	3297.05 ± 732.30	4536.90 ± 1989.52	5070.15 ± 248.75	3674.75 ± 364.69	6002.24 ± 659.14	6337.90 ± 1099.75
UDP	5.57 ± 3.48	7.00 ± 3.08	7.78 ± 2.53	11.26 ± 4.17	5.04 ± 2.05	22.33 ± 8.84	7.04 ± 3.97	11.56 ± 4.41	12.74 ± 3.02	12.08 ± 2.79	10.12 ± 3.91	13.72 ± 2.15
S6P	6.61 ± 1.43	7.88 ± 3.03	6.54 ± 2.88	4.10 ± 0.71	7.27 ± 4.71	7.55 ± 4.54	5.20 ± 1.04	6.25 ± 2.25	4.50 ± 1.49	4.48 ± 1.50	6.64 ± 1.64	7.81 ± 0.69
T6P	1.61 ± 0.64	1.82 ± 0.70	1.79 ± 0.92	1.41 ± 0.58	2.57 ± 0.67	3.51 ± 2.18	1.75 ± 0.39	2.51 ± 1.00	1.65 ± 0.08	1.39 ± 0.27	2.00 ± 0.29	2.50 ± 1.08
DHAP	55.31 ± 2.00	44.02 ± 19.47	56.43 ± 10.24	64.90 ± 15.66	35.64 ± 7.95	46.99 ± 13.36	47.41 ± 12.01	35.29 ± 35.22	72.23 ± 14.38	65.20 ± 14.91	54.97 ± 14.09	55.00 ± 11.30
aKG	5.00 ± 23.70	4.26 ± 0.13	4.55 ± 3.97	4.34 ± 11.92	3.65 ± 16.31	6.37 ± 3.48	4.51 ± 6.59	4.33 ± 5.35	6.73 ± 1.56	6.90 ± 3.38	10.11 ± 3.61	7.52 ± 4.50
Succ	292.46 ± 102.94	297.36 ± 145.53	358.53 ± 150.10	255.93 ± 106.84	203.86 ± 15.45	499.69 ± 116.03	275.96 ± 46.06	298.67 ± 76.83	310.52 ± 141.86	263.85 ± 69.51	292.76 ± 53.35	307.61 ± 30.27
Fum	121.62 ± 79.05	405.89 ± 178.69	109.43 ± 38.18	357.88 ± 145.18	178.01 ± 155.80	166.52 ± 52.56	151.87 ± 124.35	134.26 ± 339.73	122.67 ± 83.91	260.73 ± 89.30	90.61 ± 14.21	172.37 ± 55.68
E4P	66.44 ± 18.21	36.36 ± 7.97	50.02 ± 21.18	70.81 ± 8.33	38.89 ± 7.46	44.44 ± 15.85	70.06 ± 14.38	32.74 ± 46.96	76.32 ± 17.51	54.21 ± 13.51	45.49 ± 13.71	46.77 ± 12.24
Ppi	5.14 ± 1.21	5.78 ± 1.95	5.85 ± 4.09	6.49 ± 2.00	4.72 ± 0.93	8.38 ± 3.71	4.79 ± 2.00	7.86 ± 3.89	8.36 ± 0.50	8.59 ± 2.43	4.29 ± 0.33	7.90 ± 3.38
UDPNAG	6.57 ± 1.85	6.34 ± 2.48	4.43 ± 6.18	6.49 ± 1.38	5.90 ± 1.54	5.18 ± 0.87	6.01 ± 0.96	6.93 ± 0.71	8.76 ± 1.09	4.85 ± 0.94	5.60 ± 1.38	9.10 ± 2.97
Shik	76.33 ± 7.61	109.38 ± 9.57	**59.48 ± 11.75**	49.55 ± 13.97	91.80 ± 8.74	71.72 ± 27.07	65.60 ± 22.39	87.10 ± 15.10	**93.76 ± 8.93**	49.15 ± 3.68	73.21 ± 7.30	80.09 ± 9.21
ATP	0.91 ± 0.66	5.64 ± 7.13	2.64 ± 1.91	0.83 ± 0.38	0.42 ± 0.18ab	2.33 ± 1.24	1.10 ± 0.52	31.32 ± 28.85	1.71 ± 0.54	1.79 ± 0.69	0.55 ± 0.19	0.79 ± 0.07
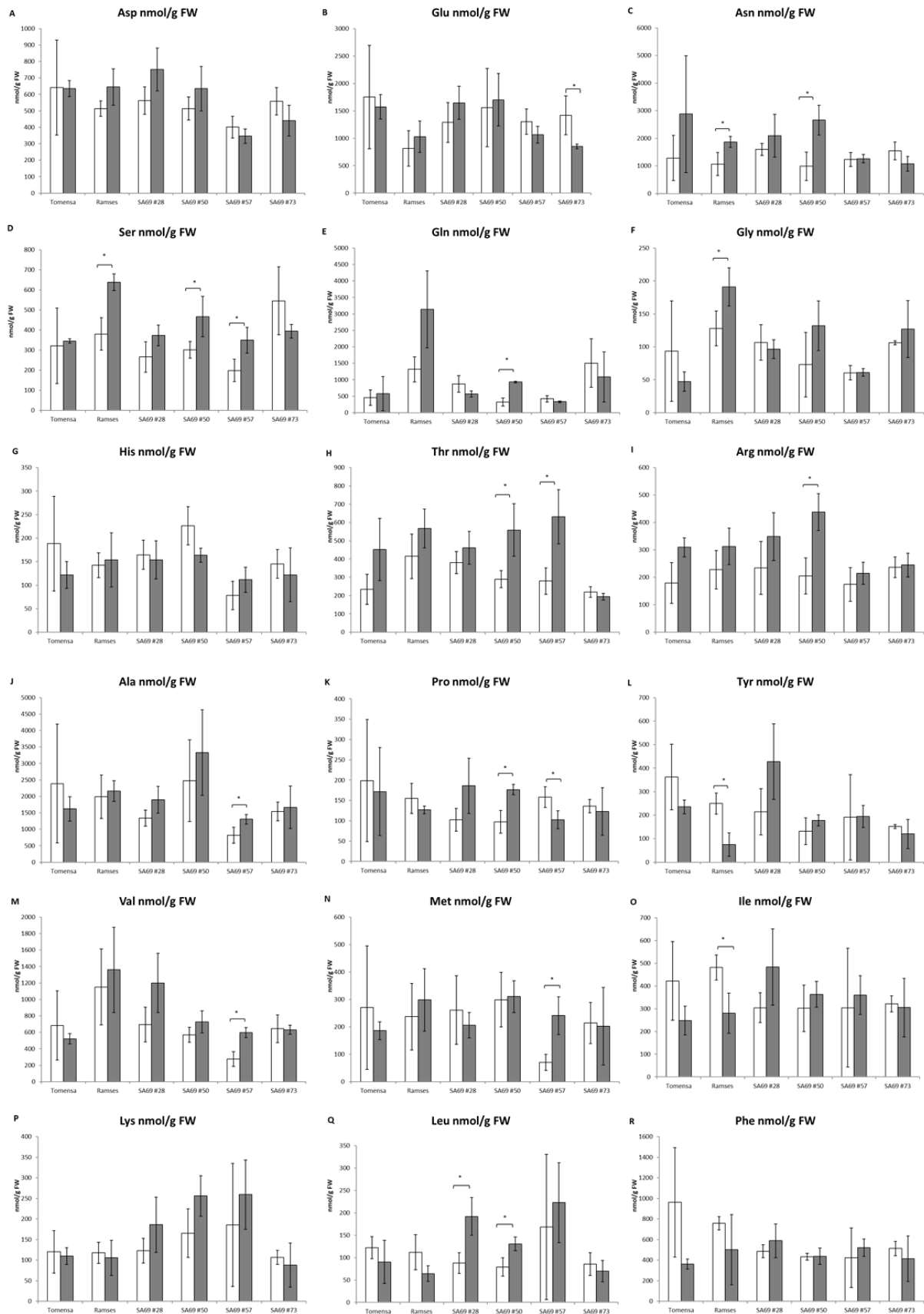
Figure 40 Free Amino Acid contents in tubers of Tomensa, Ramses and crossing-lines # 28, 50, 57 and 73.
Bars indicate mean values of four biological replicates and error bars mark standard deviation. Asterisks
indicate significant differences between tubers grown under control and heat conditions (p < 0.05, t-test).

Results

After harvest, tubers were stored at room temperature to assess sprouting time-points. A tendency towards earlier spouting in tubers of heat-treated plants was visible. This was especially seen in lines #28, 57 and 95 (Figure 41).
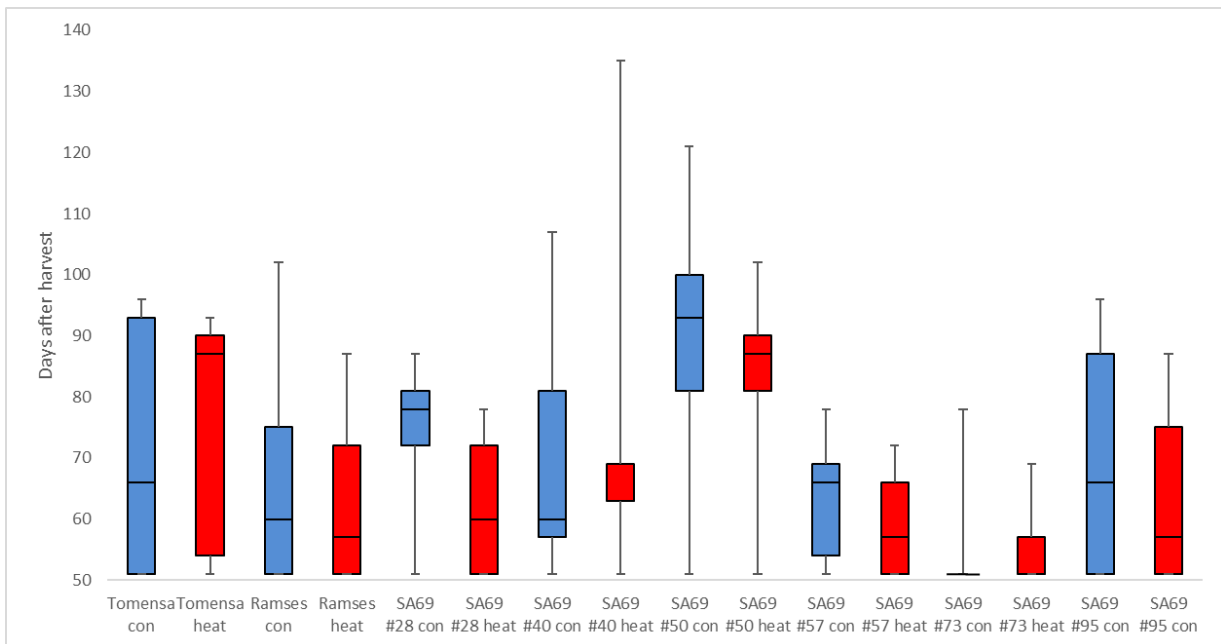
Figure 41: Dormancy length in selected lines of cross-breeding population SA69 as well as the parental strains Tomensa and Ramses. Whiskers represent earliest and latest sprouting tubers, boxes represent interquartile ranges. Blue boxes represent control values; Red boxes represent values of heat-treated tubers.

Based on the data acquired with the cross-breeding lines, it seems that dormancy is a stable trait which can slightly be influenced by heat periods during plant growth. Relatively, dormancy is still similar for one line when compared to the others. This observation suggests that there might be an intrinsic "program" determining the length of dormancy. To test this hypothesis, the parental strains Ramses and Tomensa as well as the cross-breeding lines SA69 #28, 50, 57 and 73 were cultivated a third time to assess for reproducibility and to be able to obtain samples from dormant bud tissue expected to exhibit changes in gene expression that might explain the differences in dormancy.

3.4.3.3 Confirmation of dormancy in selected lines of cross-breeding population SA69/12 - HotPot

For the confirmatory cultivation of selected lines of cross-breeding population SA69/12 – HotPot, lines #40 and #95 were excluded to increase the number of plants of the other lines. Line #40 had proven inappropriate for the assessment of dormancy in the previous cultivations due to very small tuber sizes and overall yields possibly resulting from a delayed tuber

induction. Cultivation conditions were changed towards equinoctial day length (12h light / 12h dark) which was maintained throughout the entire growth period. This was supposed to enable a better characterization of the effects caused by the heat treatment without interference by the day length regimen. Furthermore, pots with higher volumes were used for cultivation to enable tubers to develop properly without space restrictions due to pot size.

The heat period was confined to a length of ten days followed by a two-week regeneration period after which plants were harvested and tuber yields were determined. Tuber yields were increased by approximately 15 grams per plant irrespective of the genotype when compared to the previous cultivation. This can be ascribed to the cultivation conditions (day length, pot size) which favor tuber growth stronger than the conditions used before. Heat treatment significantly reduced tuber yield in the parental strain Ramses and cross-breeding lines #28, 57 and 73 (Figure 42).
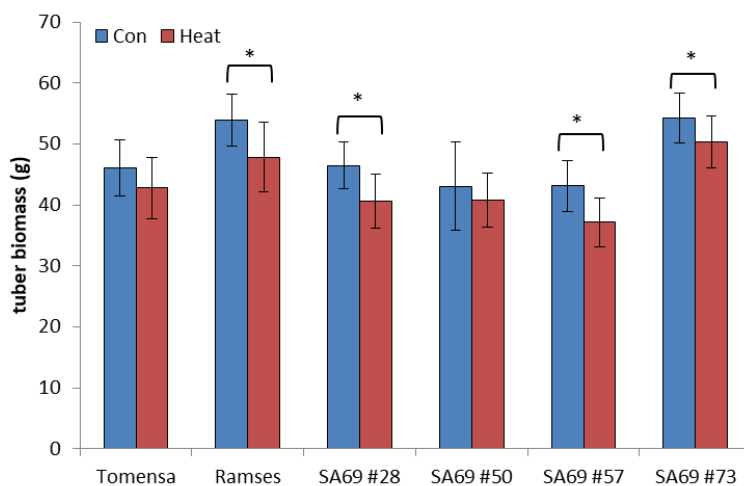
Figure 42: Tuber weights of selected lines of cross-breeding population SA69 (g). Blue bars represent values from control plants; Red bars represent values from heat-treated plants. Error bars represent standard deviations of 15 biological replicates. Asterisks indicate significant differences (p < 0.05, t-test).

After harvest, the tubers were stored at room temperature in the dark for eleven days after which samples were taken from parenchyma tissue underneath the apical bud from randomly chosen tubers. The remaining tubers were further stored until sprouting to confirm dormancy length. Earlier sprouting in response to heat stress during the growth phase was confirmed in lines #28, 50 and 57 (Figure 43). In the parental strains and line #73 dormancy remained unaffected by treatment. Furthermore, it was confirmed, that lines #57 and #73 were early sprouting lines and #28 and #50 were late sprouting lines compared to the parental strains Tomensa and Ramses.
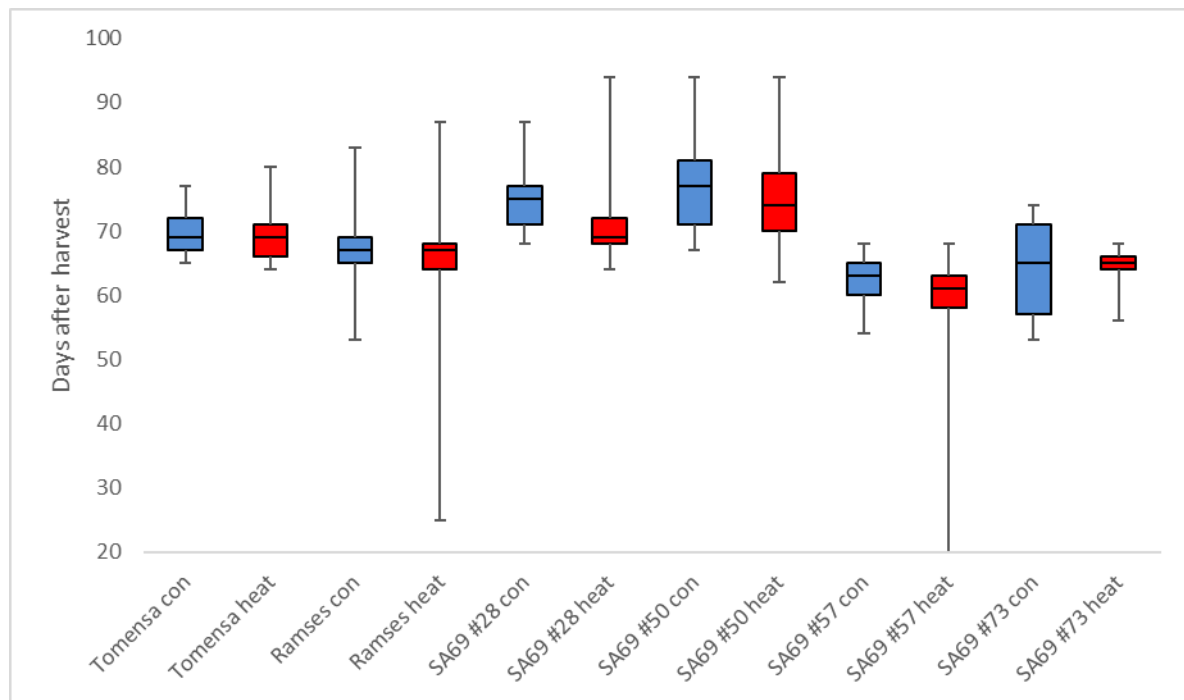
Figure 43: Dormancy length in days after harvest in selected lines of cross-breeding population SA69 and parental strains Tomensa and Ramses after confirmatory cultivation. Whiskers represent earliest and latest sprouting tubers, boxes represent interquartile ranges. Blue boxes represent control values; Red boxes represent values of heat-treated tubers.

3.4.4   Analysis of gene expression patterns in differently sprouting potato lines

In order to gain insight into the underlying regulatory mechanisms controlling dormancy, RNA from selected lines of population SA69/12-HotPot was extracted from parenchyma tissue taken from underneath the apical bud 11 days after harvest to be evaluated via microarray analysis. Per line and condition, four samples were prepared for hybridization. Due to the high number of samples, two different dyes were used to enable hybridization of two samples on one array simultaneously. Using the Genespring software, it is possible to analyze the results separately due to the different dyes.

To gain a first impression of the relationship of different lines, a hierarchical clustering was performed. From the clustering it became obvious that samples were more similar regarding their genotype than treatment (Figure 44). Only lines #28 and 57 could be separated by treatment. All other lines were separated from each other by genotype but the samples within treatments clustered together. This indicated that the heat treatment may not have had a very strong influence on the long term, but genotype played a major role. The clustering also revealed two major arms; one harboring the parental strain Tomensa and the cross-breeding lines #28 and 50 and the other arm harboring the parental strain Ramses and the cross-breeding lines #57 and 73. This result was interesting since one arm included the early

sprouting lines and the other the late sprouting lines, each with a parental line exhibiting intermediate dormancy.
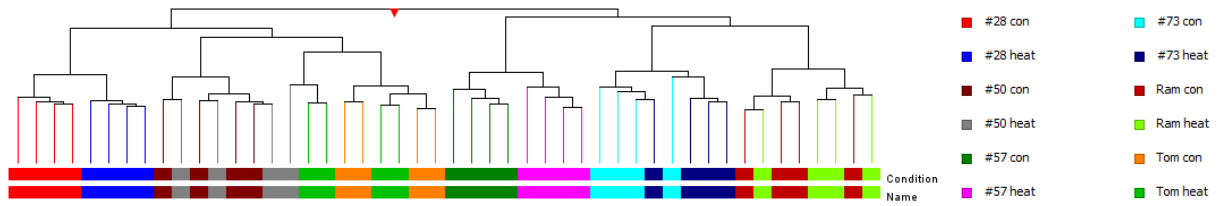
Figure 44 Hierarchical clustering of samples of heat-treated and control tubers according to their gene expression. The clustering algorithm was Euclidean and linkage rule Ward's. Colors were selected per condition and genotype (see legend).

To identify possible factors responsible for the separation of the samples, a principal component analysis (PCA) was performed. From the PCA it was visible that component 1 was responsible for 26.43% of the separation (Figure 45a). In this dimension, samples were separated for the treatment. Values below 0 on the X-axis included heat-treated tuber samples while above 0 the control tubers were located. Component 2, which was responsible for 8.05% of separation, divided the samples by genotype. Interestingly, the largest distance was found between the parental strains which framed the samples of their cross-breeds. Considering component 3, explaining 6.81% of the variation between samples, a clear separation of line #57 was seen (Figure 45b).

a)
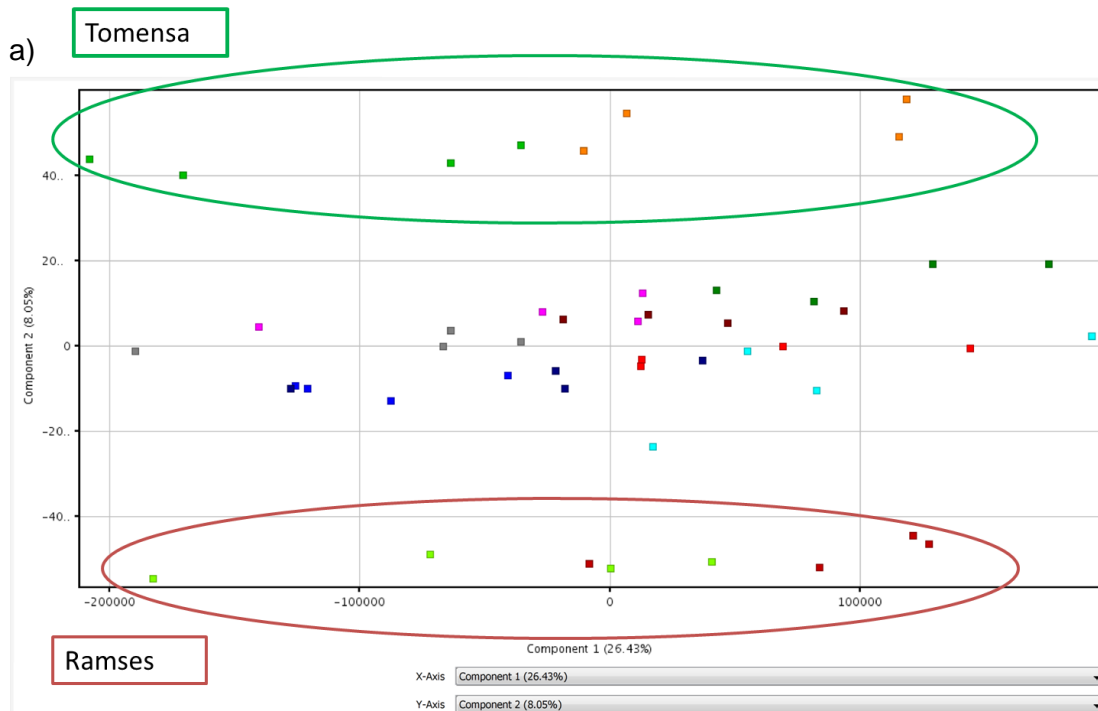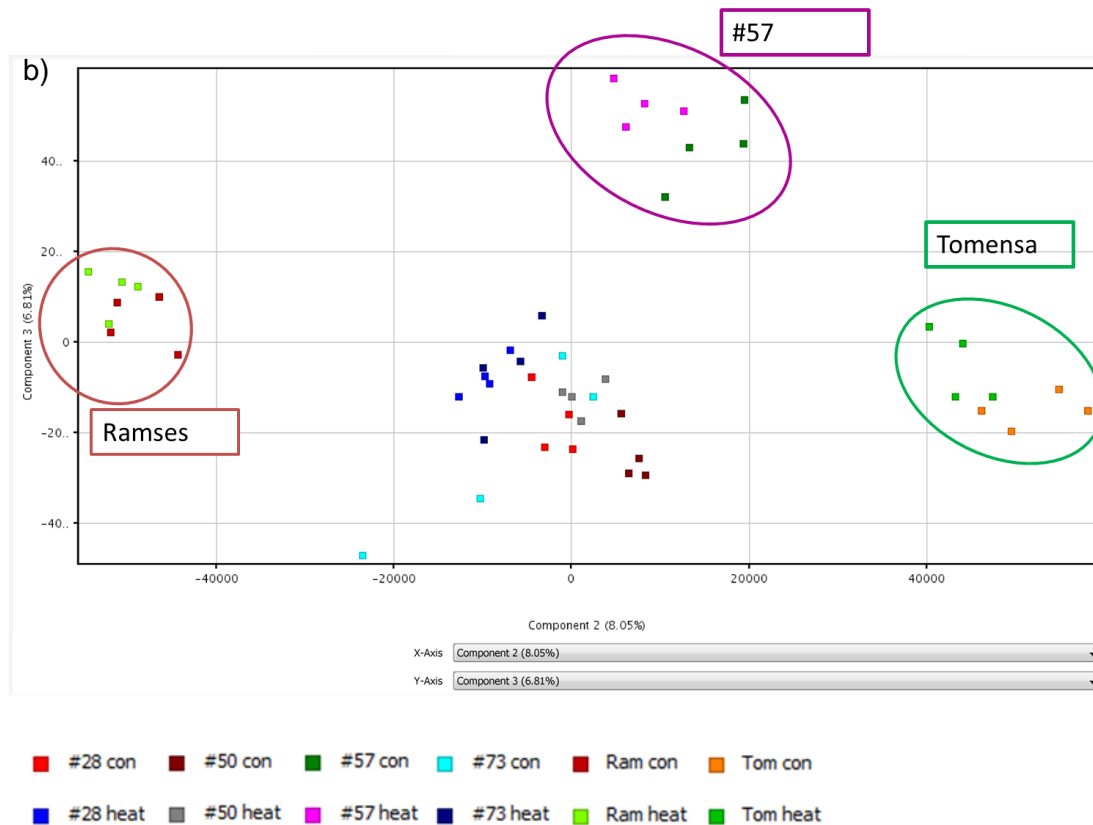
Figure 45: Principal component analysis of microarray samples. a) shows component 1 on the X-axis and component 2 on the Y-axis. b) shows component 2 on the X-axis and component 3 on the Y-axis. The parental strains Tomensa and Ramses as well as line #57 are highlighted by colored circles. Each colored dot represents one sample. Colors are assigned according to genotype and treatment (see legend).

3.4.4.1 Analysis of the effect of heat on tuber transcriptomes of selected lines SA69/12

In a first approach to look at genes which are regulated differentially in tubers grown under heat-stress conditions compared to tubers grown under ambient temperatures, all genotypes were taken together and the conditions were tested against each other (moderated t-test, Benjamini-Hochberg corrected). The resulting list contained 66 differentially regulated transcripts of which 32 were up-regulated and 34 down-regulated (Table A 6).

MapMan categories were analyzed. Regarding the entities which were up-regulated in heat-treated vs control tubers, they were overrepresented in the categories "DNA", "misc", and "stress".

Three of the differentially up-regulated transcripts were in the category "stress". Those were a *small heat shock protein* (PGSC0003DMT400031253), *Heat-shock protein* (PGSC0003DMT400032851) and *Bax inhibitor* (PGSC0003DMT400067509). The category "DNA" was only represented by two up-regulated entities which both map to the same gene *Nucleosome assembly protein 1 4* (PGSC0003DMG402004883).

Furthermore, *Abscisic acid and environmental stress-inducible protein TAS14* (PGSC0003DMT400009069) was found among the significantly up-regulated genes.

Down-regulated entities caused overrepresentation of the categories "secondary metabolism" (one entity), "Development", "DNA" (one entity *F-box and wd40 domain protein*, PGSC0003DMT400043704), "misc", "nucleotide metabolism" (one entity) and "Redox".

The category "Redox" was represented by two transcripts annotated as *glutaredoxin* (PGSC0003DMT400029594, PGSC0003DMT400013649). Within the category "development" five entities mapping to four loci were retrieved: *Nodulin family protein* (PGSC0003DMT400002407), *UPA16* encoding another nodulin family protein (PGSC0003DMT400081210, PGSC0003DMT400081211) *TMS membrane family protein* (PGSC0003DMT400050034) and *Auxin-induced protein 5NG4* (PGSC0003DMT400034864).

3.4.4.2 Analysis of transcriptome in early and late sprouting lines

The cross-breeding lines SA69/12 #28 and #50 were chosen for their long dormancy period, while the lines #57 and #73 exhibited short dormancy phases. The parental lines Tomensa and Ramses exhibited an intermediate duration of dormancy (Figure 43).

In order to determine if any parallels could be drawn to previous findings, expression patterns of selected lines of SA69/12 were compared to gene expression in dormant and sprouting potato buds (Senning, 2010). To this end, identifiers from the list of differentially regulated entities in dormant vs. sprouting buds were "translated" from POCI to CUST microarray. The initial list of differentially expressed entities consisted of 8318 entities. Of these, 3025 were retrieved on the custom 8x60k microarray. Relative expression of those entities was exported and analyzed with the Multi-Experiment Viewer (MEV, Saeed et al., 2003). A hierarchical clustering based on the relative expression of entities uncovered that line #57 clustered together with sprouting buds (Sprouts) while all other lines were found closer to dormant buds (Buds, Figure 46). This indicated that the early-sprouting line #57 might already exhibit a gene expression pattern close to sprouting buds and was different from all other lines. Therefore, a closer look was taken at the transcriptome of line #57
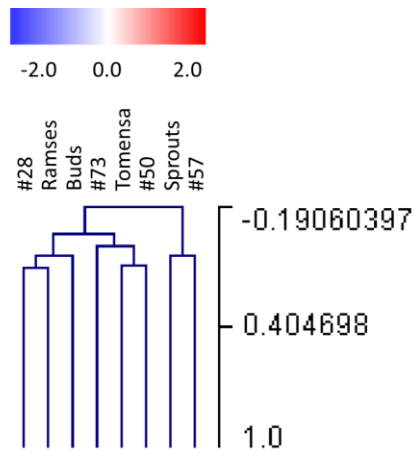
Figure 46 Hierarchical clustering of gene expression data from selected lines SA69/12 and dormant and sprouting buds.

3.4.4.3   Analysis of transcriptome profile of line #57

In order to characterize the differences in gene expression that distinguished line #57 from the other lines, an analysis of variance (ANOVA) was conducted. The resulting list was filtered for entities which were at least 2-fold regulated between line #57 and all other lines. Finally, 250 entities were recovered which were found to be uniquely regulated in line #57 (Table A 7). To get an overview of possible mechanisms and pathways which are affected by the differentially regulated genes in line #57, a functional categorization based on MapMan categories was performed on the genes consistently up- or down-regulated compared to all other lines (Figure 47). Among the categories harboring the down-regulated entities, the most strongly represented were "photosynthesis", "lipid metabolism", "metal handling" „co-factor and vitamin metabolism", „mitochondrial electron transport" and „TCA". Among the categories harboring the up-regulated entities, the most strongly represented were „TCA", „stress", „signaling", „nucleotide metabolism", „mitochondrial electron transport", „major CHO metabolism", „hormone metabolism" and „cell wall".
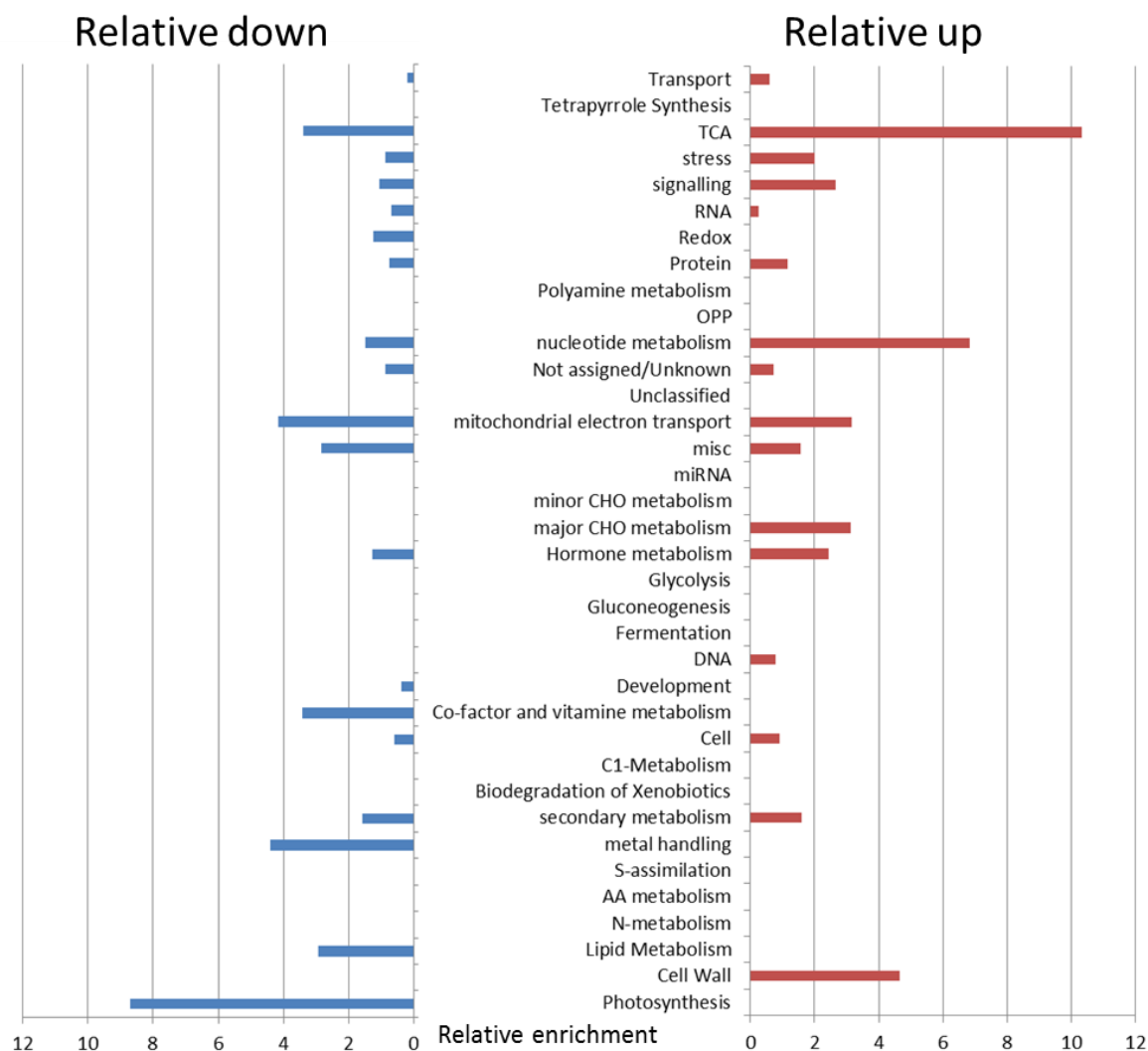
Figure 47 Functional categorization of 250 differentially regulated entities of line #57. Bars represent relative representation of a category compared to its representation on the chip. Blue bars represent categories harboring down-regulated entities; red bars represent categories harboring up-regulated entities.

A closer analysis of the regulated entities within the over-represented categories revealed that 70% of the entities within the category "hormone metabolism" belonged to the ethylene metabolism. Among the up-regulated entities in this category, *1-aminocyclopropane-1-carboxylate oxidase homolog* (*ACO*) was found. ACO is involved in ethylene biosynthesis and catalyzes the last step of ethylene production (Arc et al., 2013). Moreover, within the category "signaling", many *leucine-rich repeat containing receptor-like kinases* (*LRR-RKs*) were retrieved. Most of them were among the up-regulated genes. LRR-RKs are involved in a variety of developmental and defense-related processes (Torii, 2004). Also, among the up-regulated genes was a *Phosphate-responsive 1 family* (*Phi-1*) protein and *NON-PHOTOTROPIC HYPOCOTYL 3* (*NPH3*). Among the down-regulated entities within the category "signaling", light signaling-related transcripts were found namely *PAS/LOV protein* and *Root phototropism*

proteins. Consistently, the auxin-signaling related entities *Auxin response factor 2* (*ARF2*, PGSC0003DMT400037454) and *Auxin-induced protein 6B* (*SAUR*, PGSC0003DMT400086212) were also present among the down-regulated entities characterizing line #57.

3.5 X-ray CT analyses of potato plants under combined heat and drought stress

The results presented in this chapter have been published in the following article:

Van Harsselaar, J.K., Claußen, J., Lübeck, J., Wörlein, N., Uhlmann, N., Sonnewald, U., Gerth, S., 2021. X-Ray CT Phenotyping Reveals Bi-Phasic Growth Phases of Potato Tubers Exposed to Combined Abiotic Stress. Front. Plant Sci. 12, 1–15. https://doi.org/10.3389/fpls.2021.613108

3.5.1 Growth curves of different potato varieties

To investigate how potato tuber growth and morphology respond to combined heat and drought stress, potato tubers were monitored by X-ray CT analysis over their entire growth period at the Fraunhofer Institute for Integrated Circuits in Fürth, Germany. Potato plants were monitored via CT imaging three times per week. After the measurement, the potato tubers were virtually excavated out of the soil (segmented) for each time point. On the segmented tubers the volume and fresh weight of each tuber for each time point was calculated to determine the growth curve over time. Thus, each potato tuber could be tracked over the different measurements and even with slight variation in moisture content of the soil robust tuber tracking and segmentation was possible.

During the first experiment, five different genotypes were measured every second day from day 14 after planting until day 42 after planting. From day 15 after planting until day 29 after planting combined drought and heat stress was applied. The plants had between three and nine tubers. Total tuber volume was calculated for each plant individually as the sum of all tuber volumes of the respective plant at each time-point. Average total tuber volume was then calculated for all plants of the same cultivar. Development of the tuber volumes over the experimental period showed a bi-phasic growth curve in all cultivars tested (Figure 48). Each genotype basically exhibited the same growth dynamic: In the first growth phase, tubers grew until stress treatment was started. Tuber growth stagnated during the combined abiotic stress treatment between days 2 and 16 in all cultivars analyzed. Only very small increments in tuber volumes were observable during the combined stress treatment. After the stress treatment, tubers resumed growth (Van Harsselaar et al. 2021).

The cultivars Diamant and Agria showed the lowest stress response in terms of growth retardation between days 4 and 14 of the experiment which corresponds to days 2 to 12 of the stress treatment. Growth was most affected in this period in the cultivar Ramses. Growth velocity after stress release was highest in Ramses and lowest in Saturna. The cultivars Diamant and Agria showed almost identical growth curves and corresponding growth velocities (Figure 48).
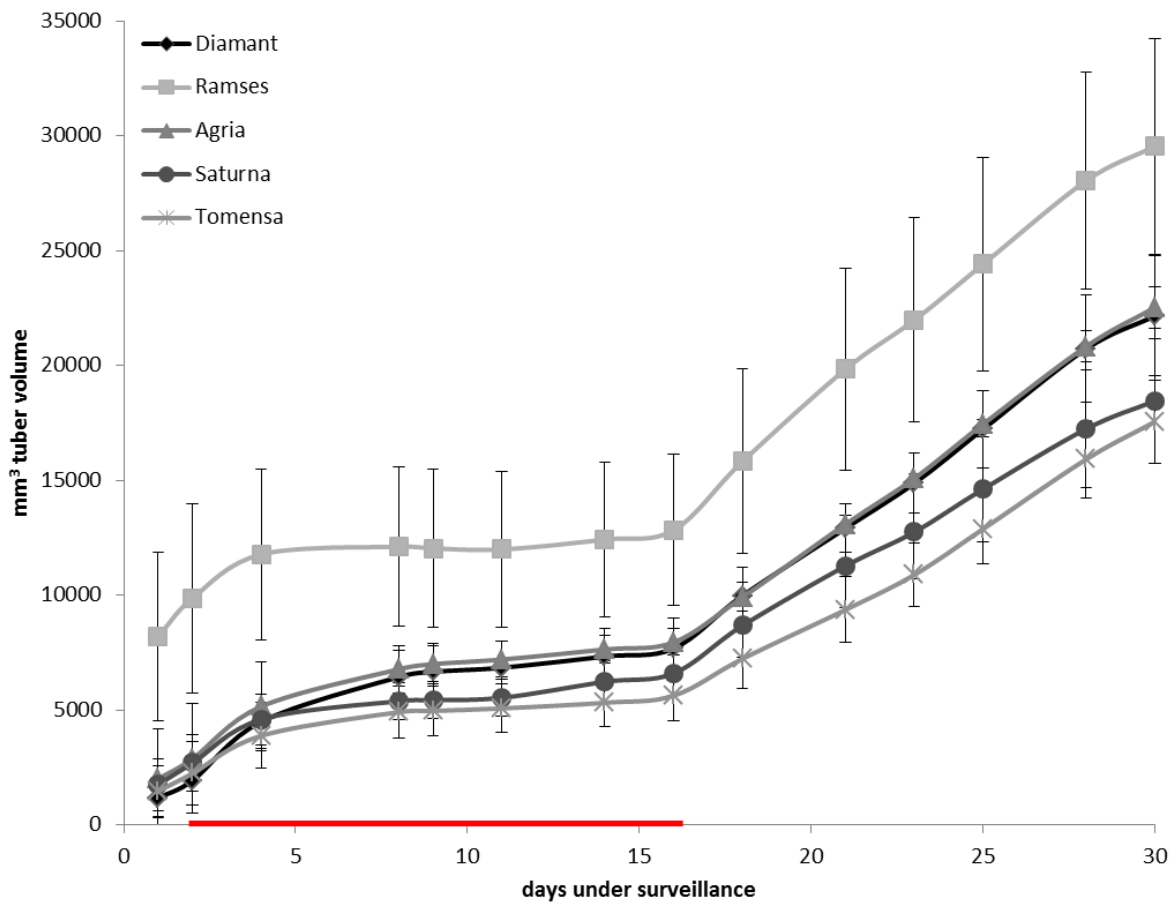
Figure 48: Average tuber volume per plant and genotype over the experimental time-course. Plants were grown in the greenhouse until tuber induction and then transferred to phytochambers under long day conditions. The red line indicates the period of elevated temperature from day two to day 16 (16h light, 29°C, 8h dark, 21°C). Tuber volumes were monitored three times per week in four plants of each of the cultivars; Diamant (diamond), Ramses (square), Agria (triangle), Saturna (circle), Tomensa (cross). Error bars represent standard deviations of four biological replicates.

3.5.2 Tuber growth is inhibited during combined stress but recovers under regenerative conditions

"To investigate whether the bi-phasic growth curve is a response to the combined heat and drought stress, a second experiment with only one genotype but with a control group was conducted. To this end, thirty potato plants of the cultivar Diamant were grown in two phytochambers. Initially, the same temperature regime was applied to all plants until tubers developed i.e., 16 h light at 21°C and 8 h dark at 18°C and 50% humidity during the day and 35% humidity at night. Tuber growth was monitored three times per week in eight pots per group via CT analysis starting at day 21 after planting. Stress treatment was applied to half of the plants when all plants exhibited detectable tubers (starting at day 18 after tuberization).

90

Those plants were subjected to combined heat and drought stress by increasing ambient temperature to 29°C during the day and 21°C during the night and simultaneously decreasing daily water supply to 30 ml per plant per day instead of 50 ml per plant per day for control conditions. This regime was kept for two weeks in the stress group.

A few days after commencement of the stress treatment, tubers in the stressed group of plants ceased growing (Figure 49a). This became visible when average tuber volume per plant was monitored and, moreover, when the average increase in volume per day per plant was investigated (Figure 49b). Four days after the beginning of the stress treatment, a decrease in growth velocity was already measurable and it dropped close to zero at the end of the stress period while tubers in the control group continued growing. In contrast, tubers of plants under control conditions showed constant growth. After releasing the plants from the stress treatment, growth velocity immediately increased to a level similar to that of the control treated plants resulting in a bi-phasic growth pattern (Figure 49 a and b)." (Van Harsselaar et al. 2021).
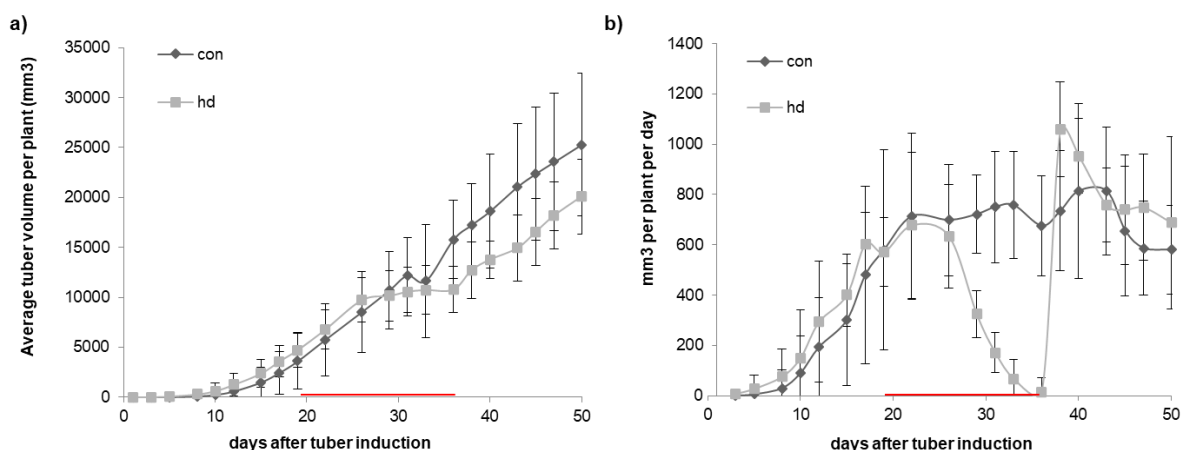
Figure 49: Growth characteristics of potato tubers of cv. Diamant under normal plant growth conditions (dark grey) and under combined heat and drought stress (light grey). a) average tuber volume over the experimental time course, b) average growth velocity of tubers per day in mm³. Error bars represent standard deviations of five to eight plants per treatment and time-point.

3.5.3 Expression of marker genes for abiotic stress confirms combined stress treatment

"To validate that the stress treatment had an effect on tuber physiology, the expression of potential marker genes for stress was investigated. Therefore, tuber samples taken eight days after commencement of the combined stress treatment (TP1), three days after cessation of stress treatment (TP2) and after a 14-day recovery phase at the end of the experiment period (TP3) were subjected to qRT-PCR analysis. Stress-responsive genes were selected from

publications on drought stress and subsequent re-watering in potato stolons (Gong et al., 2015), potato plants exposed to elevated temperatures (Hancock et al., 2014) and combined heat and drought stress in tobacco (Rizhsky et al., 2002).
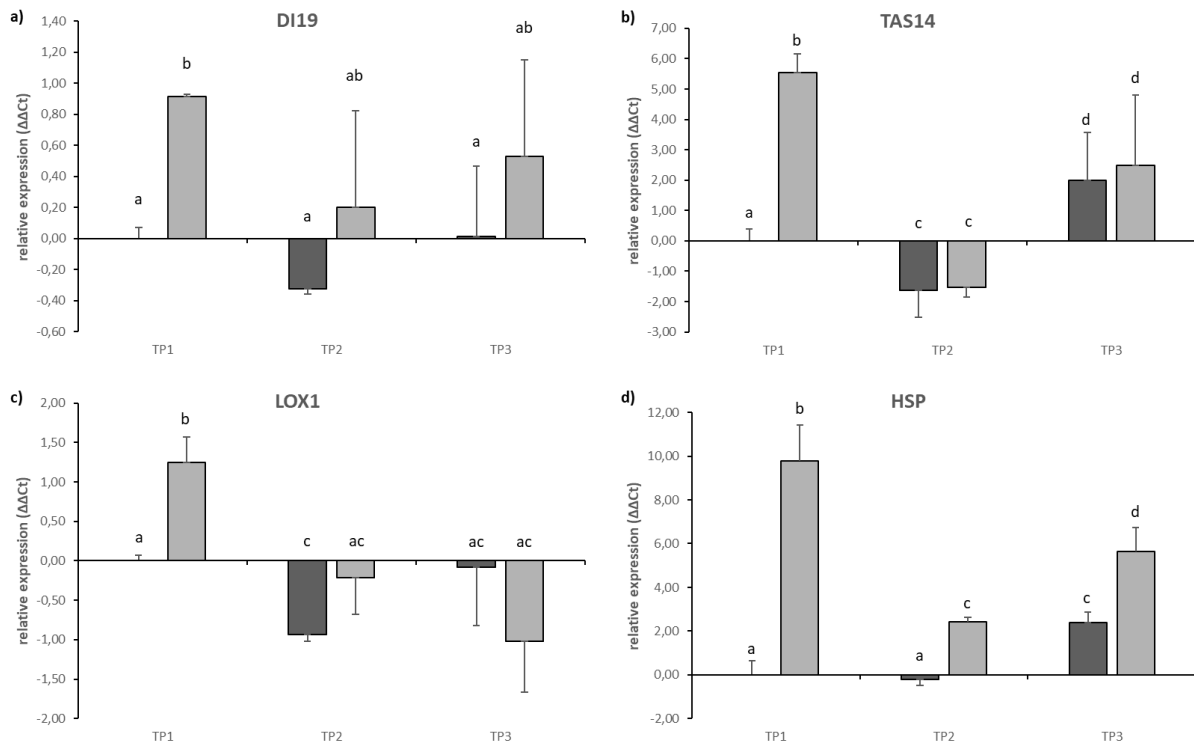
Figure 50: qRT-PCR on stress-responsive gene expression in tuber samples of the potato cultivar Diamant. Results from control treated plants are shown in dark grey, stress treated plant results are shown in light grey. Error bars represent standard deviation of three to four biological replicates. Figure taken from Van Harsselaar et al. 2021.

Gene expression of candidate stress marker genes *drought-induced 19* (*DI19*), *Abscisic acid and environmental stress-inducible protein* (*TAS14*), *Lipoxygenase* (*LOX1*), and *Heat-shock Protein* (*HSP*) was significantly increased during the heat treatment at TP1 when compared to potato tubers grown under control conditions (Figure 50a-d). After relieving the stress from the plants, gene expression of *DI19*, *TAS14* and *LOX1* decreased to control values (Figure 50a-c, TP2 and TP3). The only potential stress marker gene whose expression did not return to control values was a *HSP* whose expression remained significantly above control values until the end of the experimental period although to a lesser extent as during the stress treatment at TP1 (Figure 50d). The expression of *DI19* was significantly increased during the stress treatment but showed a lot of variation after stress release at TP2 and TP3 (Figure 50a) indicating that individual tubers adjust differently to the changed environmental conditions" (Van Harsselaar et al. 2021).

3.5.4 Impact of combined stress on starch metabolism

"Abiotic stress is known to cause yield penalties and quality loss in potato (Levy, 1986, 1985). Since starch content is the main factor determining potato tuber dry matter and an important trait for breeders (Li et al., 2008), the impact of the stress treatment on starch metabolism was investigated. Therefore, SuSy-activity, a marker enzyme for starch biosynthesis (Baroja-Fernández et al., 2009; Zrenner et al., 1995) was measured. In comparison to the control treated plants, SuSy-activity was decreased during the stress treatment and remained low throughout the rest of the experimental period (Figure 51a). In contrast, when measuring starch contents of the tubers at the three time-points, no significant changes were detected (Figure 51b).
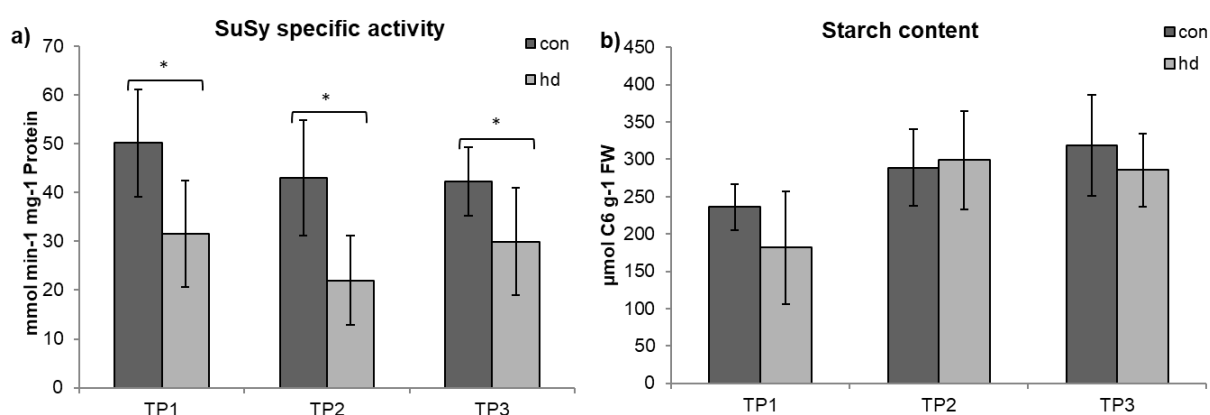
Figure 51: SuSy-activity (a) and starch content (b) of tubers from plants grown under control and combined stress conditions. Dark grey bars represent values from control treated plants; light grey values represent values from stressed plants. Error bars represent standard deviations of nine to ten biological replicates and six to ten biological replicates for SuSy and starch measurements, respectively. *p<0.05 (Student's t-test, figure taken from Van Harsselaar et al., 2021).

To further elucidate the impact of the stress treatment on starch metabolism, mRNA expression of *SuSy4*, the main SuSy isoform in potato tubers (Fu and Park, 1995; Van Harsselaar et al., 2017) and a determinant of sink strength (Zrenner et al., 1995) was evaluated via qRT-PCR analysis. During the stress treatment (TP1) a marked decrease in *SuSy4* expression in comparison to the control group was detected (Figure 52a). After the stress treatment (TP2) *SuSy4* expression recovered to control level. At the end of the experimental period (TP3) *SuSy4* expression in stress treated tubers exceeded the expression in control tubers (Figure 52a). As a second starch metabolism marker, the expression of granule-bound starch synthase (*GBSS*) was analyzed. Similar to *SuSy4*, *GBSS* expression was found to be significantly down-regulated in tubers of the stressed group during the stress treatment (TP1) and to recover to control values after the stress (TP2 and 3, Figure 52b). Additionally, *GPT2.1* expression was analyzed. During the stress treatment and one week after ending the treatment, no effect of

the stress on *GPT2.1* expression could be seen. At the end of the experimental period (TP3), *GPT2.1* expression was slightly, but non-significantly higher in tubers grown under stress conditions than in tubers grown under control conditions (Figure 52c).
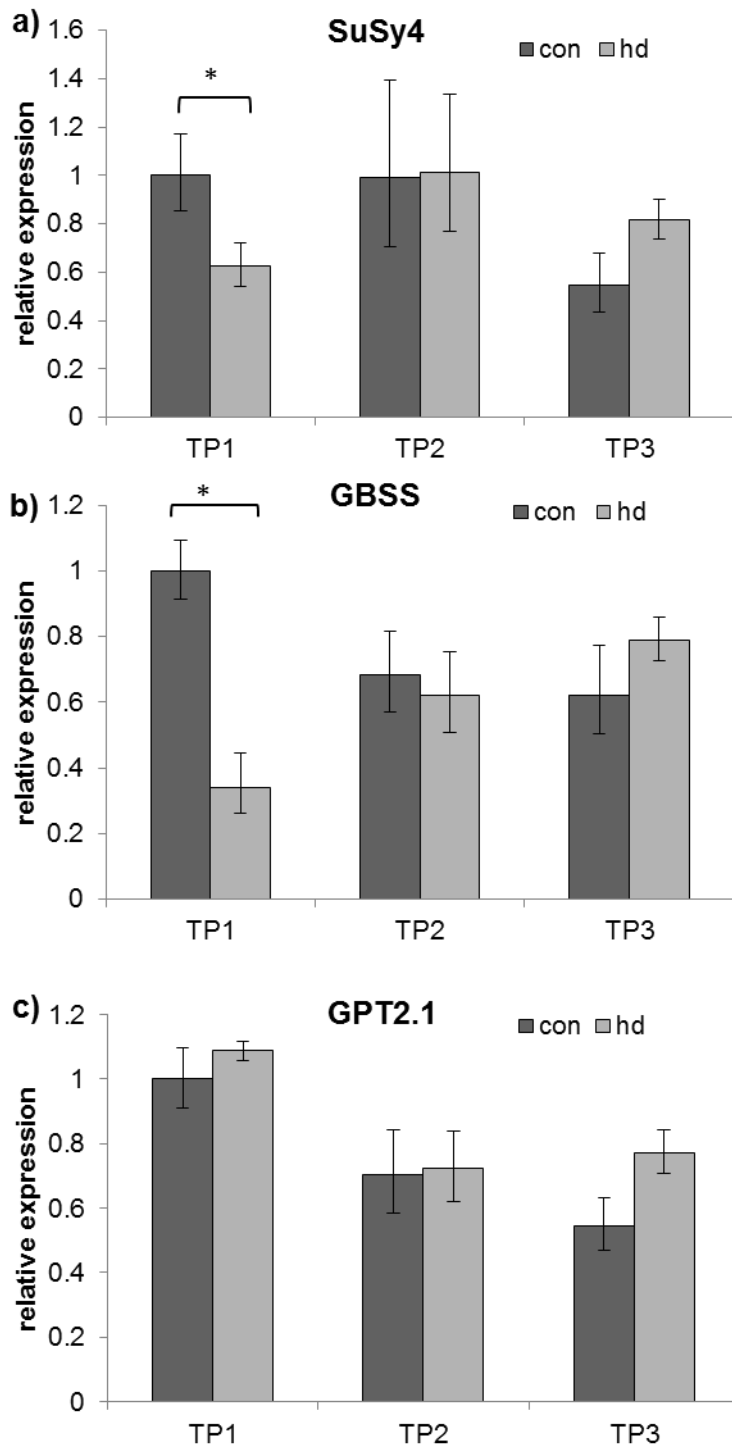
Figure 52: Relative expression of marker genes for starch biosynthesis. A) Sucrose synthase 4 (SuSy4), b) Granule-bound starch synthesis (GBSS) and c) Glucose-6-phosphate translocator 2.1 (GPT2.1). RNA expression was assessed by qRT-PCR with specific primers and normalized to ubi3 expression by ΔΔCt method. Values of control treated plants are shown in dark grey; stressed plants are shown in light grey.

Error bars represent standard deviation of four biological replicates. *p<0.05 (Student's t-test). Figure taken from Van Harsselaar et al., 2021.

In summary, analysis of stress markers and markers for starch biosynthesis show that the biphasic growth curve is due to the combined drought and heat stress response which affects tuber growth and biomass accumulation. Although starch content was not significantly affected by the stress treatment, biochemical and molecular biological parameters suggest an impact on tuber metabolism which is in line with the observation that tuber growth was inhibited by the stress treatment (Figure 49)." (Van Harsselaar et al. 2021).

4 Discussion

4.1 Starch metabolism genes and possible regulators

4.1.1 Genome-wide analysis of starch genes in potato reveals novel isoforms

"Enzymes involved in starch metabolism often belong to gene families encoding several isoenzymes. This work presents a genome-wide analysis of starch genes in potato. A comprehensive BLAST search strategy complemented by motif discovery and comparison to known sequences from *Arabidopsis* was applied aiming at the identification of all "starch gene" loci in potato. We found 81 loci coding for starch metabolism related enzymes belonging to different enzyme classes. Higher plants possess five gene classes encoding starch synthases, designated *GBSS* and *SS1-4* (Zeeman et al., 2010). In rice, two forms of *GBSS* were identified and eight genes encoding the four *SS* classes (Hirose and Terao, 2004). In the potato genome, we confirmed that GBSS which has been reported previously to be responsible for amylose biosynthesis in the starch granule, is encoded by a single gene and is expressed higher in tubers than in leaves (Visser et al., 1989). A second transcript (DMT400003356) annotated as *GBSS2* in the PGSC database had previously been described to possess soluble SS activity (Edwards et al., 1995; Marshall et al., 1996) and was found to be the closest potato homolog to *Arabidopsis SS2* and was therefore consequently designated as SS2. Moreover, it was shown that SS2 plays only a minor role in starch biosynthesis in tubers (Edwards et al., 1995) which is in accordance with our expression analysis showing only a slightly higher expression in tubers compared to leaves although being upregulated during tuber development. In total, seven starch synthases were found in the potato genome (*GBSS*, *SS1-6*) most of which have been described in earlier studies (Abel et al., 1996; Edwards et al., 1995; Kossmann et al., 1999; Larsson et al., 1996; Marshall et al., 1996; Visser et al., 1991, 1989). However, no studies have analyzed the roles of SS5 and SS6 in potato yet, but our gene expression data suggest a possible role for SS5 in potato tuber starch biosynthesis. In contrast, SS6 is expressed to similar levels in leaves and tubers and its expression was not found to change significantly during tuber development (Figure 5). Thus, further analyses are necessary to investigate the function of these genes during starch biosynthesis in potato. A recent publication described the phylogenetic relationship of SS from different plant species, including potato, confirming the presence of a fifth class of SS (H. Liu et al., 2015). In addition the authors found maize *SS5* to be highly expressed during the grain filling stage suggesting a role in starch biosynthesis (H. Liu et al., 2015), which is in agreement with our assumption.

In this study, enzymes were designated regarding to their annotation in *Arabidopsis*. In most cases, this was in accordance with isoform numeration of already described enzymes of potato. One exception concerns the numeration of isoforms within the SBE class where we identified four isoenzymes. Two of them share a very high sequence similarity to each other and have been denoted as *SBE1.1* and *SBE1.2* due to their homology to *Arabidopsis SBE1*. The deduced transcript sequences of these two genes, however, do not correspond to the previously published potato *SBE1* sequences (Khoshnoodi et al., 1996; Larsson et al., 1996; Poulsen and Kreiberg, 1993). The gene product designated *SBE1* in the aforementioned studies corresponds to *SBE3* in this study. It was described as the major SBE isoform in potato tubers and was found to play a role in starch granule formation (Jobling et al., 1999; Khoshnoodi et al., 1996). This is in accordance with the expression profile during tuber development and tissue preference discovered in this study. Until now, only variants of two isoforms, SBE3 and SBE2, have been shown to act as branching enzymes in the amyloplast (Jobling et al., 1999; Larsson et al., 1996). The role of the two potato SBE1 paralogs identified in this study remains unclear. In *Arabidopsis*, SBE1 has an effect on embryogenesis and is essential for plant growth and development (Wang et al., 2010). A direct implication of *At*SBE1 in starch metabolism is not described." (Chapter taken and adapted from Van Harsselaar et al., 2017)

4.1.2 Comparative microarray analysis revealed tissue-specific gene expression

"To identify tuber- and leaf-specifically expressed starch genes different microarray data sets were analyzed. To enable the analysis, specific microarray probes had to be assigned to the different starch genes and their respective isoforms. In general, our findings were in agreement with previously published gene expression analyses and showed a high reproducibility between the two microarray platforms, the POCI 4x44k (Kloosterman et al., 2008) and the Custom 8x60k microarray (Hancock et al., 2014). Tissue-specific expression of enzyme isoforms was for example found for *PHO1a* and *PHO1b*. *PHO1b* appeared to be preferentially expressed in leaves, while *PHO1a* was expressed higher in tubers, which is in accordance with previous findings (Albrecht et al., 2001; Sonnewald et al., 1995). In the case of *AGPase*, most subunits are expressed slightly higher in tubers than in leaves according to our results. However, one isoform, namely *APL1*, was clearly expressed higher in leaves than in tubers. This is in contrast to findings from La Cognata *et al*. (La Cognata et al., 1995) who described tuber-specific expression of *APL1* (designated AGP S3 in their work). The reliability of our results was confirmed by RNA-Seq data and by qRT-PCR using leaf and tuber samples. Genes showing tuber-specific expression were *SuSy4*, *SBE3*, *SS5*, *GPT2.1* and *SEX4*. In contrast to the other tuber-specific isoforms, *SEX4*-specific transcripts were not up-regulated during tuber

development which is consistent with the proposed role of the enzyme in starch degradation (Kotting et al., 2009). The activity of the main SuSy isoform in tubers, SuSy4, is connected to the onset of tuberization (Appeldoorn et al., 1997; Fu and Park, 1995; Viola et al., 2001) and correlates well with transcript and tuber starch accumulation in potato (Zrenner et al., 1995). Accordingly, *SuSy4* overexpression led to an increased starch content and higher tuber yield in potato plants (Baroja-Fernández et al., 2009) supporting its suggested key role in starch metabolism. Similarly, *SBE3* and *GPT2.1* expression have been linked to tuber development and the accompanying accumulation of starch (Ferreira and Sonnewald, 2012; Kaminski et al., 2012; Kossmann et al., 1991). In this context, overexpression of *GPT2.1* together with *NTT* resulted in increased tuber starch content and yield (Zhang et al., 2008) indicating that expression and activity of GPT2.1 are closely related. The similarity between the expression patterns of these enzymes strongly supports the assumption of a coordinated transcriptional regulation of genes within the same pathway (Kossmann et al., 1991). Moreover, these examples confirm that enzymatic activity of SuSy and GPT2.1 nicely correlates with transcript accumulation and that accumulation of starch metabolic enzymes is controlled at the transcriptional level. However, in other species activity of starch metabolic enzymes was shown to be additionally regulated by post-translational mechanisms. For example, phosphorylation of SuSy isoforms was shown to influence sub-cellular localization and protein stability (Koch, 2004). Activity of SBE isoforms was reported to be regulated by protein phosphorylation and redox state (Tetlow and Emes, 2014)." (Chapter taken from Van Harsselaar et al., 2017).

4.1.3 Co-expression analysis reveals candidate regulators of starch biosynthesis

"Co-expression analysis has previously been described to be a suitable tool for the identification of co-regulated genes (Movahedi et al., 2012; Usadel et al., 2009). Assuming that proteins with regulatory functions have to be expressed at the same time or shortly before their target genes, the identification of candidate regulators should be possible by co-expression analysis. The great potential of this strategy has already been demonstrated in several studies including different plant species and tissues (Fu and Xue, 2010; Hirai et al., 2007; Ingkasuwan et al., 2012; Persson et al., 2005). One example is the identification of Rice Starch Regulator 1 (RSR1) by Fu and Xue [15] in a co-expression analysis similar to the approach used in this study. RSR1 was found to be negatively co-expressed with rice starch synthesis genes and was experimentally verified as a modulator of starch gene expression.

In this work, genes that were identified as being tuber-specifically expressed and exhibiting an expression pattern that coincides with starch biosynthesis in the potato tuber were used to search for potential transcriptional regulators, since they are so far not known. The number of genes identified to be co-expressed with *SuSy4*, *GPT2.1* and *SBE3*differed between the two

microarray platforms, and was about 10 times higher in the 8x60k experiments than in those performed with the POCI platform. One reason for this might be the sample selection of the 8x60k platform which basically consists of tuber samples in similar developmental stages while most samples taken from the 4x44k format were originally designed to reflect starch biosynthesis during tuber formation. Therefore, expression profiles derived from experiments using the POCI array were expected to be more specific with respect to the identification of putative regulators of starch biosynthesis in potato tubers. Moreover, we reasoned that co-expression of a regulator with its target genes should occur in all situations. Thus, candidate selection was made after comparing the results of the co-expression analyses of the three query genes in three different platforms each with many individual samples. Eventually we identified 40 genes that are consistently co-regulated with *SuSy4*, *GPT2.1* and *SBE3*. Inspection of co-expressed genes revealed a strong over-representation of genes involved in primary carbon metabolism and development as well as genes encoding storage proteins. Tuber development and storage metabolism are known to be highly associated processes (Kloosterman et al., 2005) which strengthens the significance of the retrieved candidates. Beside this, putative TFs co-expressed with the selected starch genes could be identified. They belong to different classes and none of them has been characterized in potato so far. Clearly, there is a strong enrichment of TFs associated with developmental processes and organogenesis like BOP2, LOB, PTL and LRP.

For *PTL*, a co-expression with *SuSy4* and *GPT2.1* in samples representing different tuber developmental stages could not be confirmed via qRT-PCR and PTL might therefore not be a good candidate for further analysis. The expression profiles obtained by qRT-PCR of the other three TF were in accordance with those of the microarray analysis (Figure 7). Slight variations between qRT-PCR and microarray were found when comparing expression levels of *SuSy4* or *LOB* on "Stage 5" and "grow" from the microarray to "Swollen stolon" and "growing tuber" samples used for qRT-PCR. In the microarray, highest gene expression was seen on "Stage 5", while in the qRT-PCR expression peaked in growing tubers (Figure 7). Nevertheless, an increasing expression level was always associated with tuber formation. A possible explanation for this disagreement might be slightly different developmental stages of the samples used for the analyses. For the microarray defined stages of tuber development were sampled (Ferreira et al., 2010; Kloosterman et al., 2005), while for the qRT-PCR swollen stolons of different developmental stages were pooled. Furthermore, the growing tubers for the microarray experiment were monitored by X-ray CT analysis to determine their growth velocity, while the tubers sampled for qRT-PCR were taken from plants during their growth period, assuming that the tubers were still growing. Despite these small differences between different experiments, expression levels of *LOB*, *TIFY5a* and *WRKY4* correlate well with *SuSy4* and *GPT2.1* (Table 4). Thus, they might be interesting candidates for further analyses.

In *Arabidopsis*, BOP2 and its close homolog BOP1 regulate the expression of LOB-domain containing proteins (Ha et al., 2007). LOB expression has been found in the boundary regions between meristematic tissue and developing lateral organ primordia of the shoot apical meristem and the roots (Shuai et al., 2002). A similar spatial expression is exhibited by LRP1 of *Arabidopsis* which has been shown to be expressed in root primordia in early developmental stages (Smith and Fedoroff, 1995). In maize the localization of LRP in lateral root primordia was confirmed and it was demonstrated that LRP expression was auxin-inducible (Zhang et al., 2015). A link to auxin-signaling may also be established by the closest homolog of potato WRKY4 in *Arabidopsis*. Based on sequence similarity, the closest homolog in *Arabidopsis* is WRKY23 which has been linked to auxin-signaling in root development (Grunewald et al., 2013, 2011). A role of auxin in tuber initiation has been suggested (Roumeliotis et al., 2012) but a direct link to starch biosynthesis is missing. The expression patterns of these TFs suggest that there are interesting candidate genes which may directly or indirectly control starch biosynthesis and that more detailed investigation of their role is worthwhile." (Chapter taken from Van Harsselaar et al., 2017)

4.2   Heat stress has detrimental effects on tuberization

4.2.1   Heat stress leads to reduction in tuber yield and may cause second-growth

Growing different potato varieties under five different temperature regimes enabled the characterization of their responses to heat stress. The experiment confirmed earlier observations that long days and high temperatures have detrimental consequences for tuber development and growth (Van Dam et al., 1996). Early-onset of heat stress before tuber induction inhibited tuberization almost completely in all cultivars tested. Based on yields and tuber sizes it seemed that tuber formation in plants subjected to heat stress before tuberization were only able to form tubers after the stress had been released. In plants subjected to heat treatment during the tuber bulking period, prolonged heat led to heat sprouting and other forms of second-growth while a short period of heat caused second-growth in form of secondary tuber formation and tuber deformations (see Figure 13 and Chapter 3.3.2). Tuber yields, in terms of g per plant and tubers per plant, correlated negatively with the duration of the heat period in all cultivars analyzed, but most consistently in the cultivar Agria. Agria has previously been described as a heat-sensitive variety of potato (Savić et al., 2012) which is in line with the observations made during the heat-stress experiment. Due to its' responsiveness to the different treatments, especially its' susceptibility to second-growth in response to a short heat

period during the tuber bulking phase, plants of the cultivar Agria grown under control and intermittent heat stress conditions were chosen for further analyses.

4.2.2 Leaf transcriptome shows down-regulation of *SP6A* expression as well as photosynthesis under heat stress

SP6A has been identified as a key regulator of tuberization in potato (Navarro et al., 2011). The current model suggests that *SP6A* is transcribed in leaves under conditions that favor tuberization like short days, moderate temperature and low nitrogen supply. In a previous experiment applying moderate temperature stress to potato plants, Hancock et al. (2014) found that *SP6A* expression in leaves was reduced by approximately 50% when compared to leaves under moderate conditions. A very similar observation was described by Hastilestari et al. (2018) in an experiment comparing potato plants subjected to heat conditions. Those findings were confirmed in the work described in this thesis. *SP6A* expression was analyzed by qRT-PCR in leaves of potato plants subjected to heat for different durations and at different developmental stages and compared to control plants. Along with the negative impact on tuber production and yield, heat stress also caused strong reduction of *SP6A* gene expression in leaves of the potato cultivar Agria (Figure 15). This correlation supports the role of SP6A as "tuberigen".

To gain a more detailed insight into gene expression in leaves of potato plants under heat stress, microarray analysis was conducted. The comparison of leaf transcriptomes from plants under heat stress (29/27°C) to leaves from plants grown under control conditions revealed shifts in various metabolic pathways (Figure 17). The most affected functional category was "photosynthesis", which was especially overrepresented among the down-regulated entities. Within this category, a set of *chlorophyll a, b binding proteins* was significantly down-regulated. When looking at entities belonging to the light reaction pathway, it was observed that almost the entire pathway was slightly down-regulated under heat conditions overall (Table 6). This observation is in accordance with previous data obtained with the same cultivar, namely Agria, by Hastilestari et al., 2018 who also found substantial down-regulation of components of photosystem II. In another previous publication on transcriptomic differences between potato plants grown under moderately elevated temperatures (30/20°C) compared to normal temperatures (22/16°C), it was found that photosynthesis was upregulated (Hancock et al., 2014). The difference in these findings might be related to the overall heat-tolerance of the cultivars used for the experiments. While Agria has been described as a heat-sensitive cultivar (Savić et al., 2012), the cultivar Desirée, which has been used by Hancock et al. (2014) exhibits moderate heat-tolerance (Wolf et al., 1991).

Discussion

While gene expression of enzymes involved in the photosynthetic light reaction was for the majority down-regulated in leaves during heat stress (Table 6), the picture looked more complex for the dark reaction or Calvin-Benson-Cycle (Table 7). Transcription of genes encoding enzymes involved in the dark reaction was quite divers and did not follow a clear trend. However, a few statistically significantly up-regulated genes were identified within the Calvin-Benson-Cycle, namely *Rubisco activase 1*, *Rubisco small chain*, *chloroplastic Triosephosphate isomerase*, and *FBP aldolase*. These results are very similar to those described by Hastilestari et al. (2018) who found that entities within photosystem II were mostly down-regulated while some genes encoding enzymes of the Calvin-Benson-Cycle were significantly up-regulated. Among the latter, *Rubisco activase* and *Rubisco small subunit* were found (Hastilestari et al., 2018). It has been hypothesized previously that in higher plants heat-induced decreases of photosynthesis were rather a cause of decreased Rubisco activase activity than due to denaturing of Rubisco (Eckardt and Portis, 1997; Sharkey et al., 2001). While Rubisco activase is considered more heat-labile than Rubisco itself, up-regulation of Rubisco activase expression could be a means of compensation for the decreased activase activity.

Further among the significantly down-regulated entities in the category "Photosynthesis"; was *cyFBPase* (Table A 1). CyFBPase has been shown to regulate photosynthetic sucrose synthesis together with sucrose phosphate synthase (SPS) (Zrenner et al., 1996). Down-regulation of *cyFBPase* indicates a decrease in sucrose synthesis for export which would be expected as a result of decreased photosynthesis under heat stress. The finding that sucrose biosynthetic capacity is diminished during heat stress is in accordance with what has been described by Hastilestari et al., (2018). Reductions in photosynthesis causing lower substrate levels for export to sink tissues might explain the loss in tuber yield which was observed in heat-treated potato plants.

4.2.3 Co-regulation analysis with *SP6A* reveals transcriptional regulators involved in light signaling and development

In order to identify potential transcriptional regulators of or genes regulated by *SP6A*, co-expression analysis was conducted. To find the best matches, k-means clustering was combined with Pearson's correlation analysis. This approach rendered a list of 205 entities which were co-expressed with *SP6A* in leaf samples of potato plants grown under ambient conditions or subjected to a heat-period of one week over a time-course of 22 days (see experimental setup in Figure 10). A closer look at those 205 entities revealed TFs which might play a role in *SP6A* signaling or regulation.

One entity was described as a potential TF belonging to the *GRAS family* (PGSC0003DMT400023877) encoding a SCARECROW-like (SCL) protein. GRAS TFs belong to a major protein family and are specific for plants (Bolle, 2004). GRAS proteins are involved in developmental processes and signaling (Bolle, 2004). The closest homolog of PGSC0003DMT400023877 in *Arabidopsis thaliana* is AT2G04890, SCARECROW-like 21 (SCL21), is supposed to be involved in Phytochrome A signal transduction (Torres-Galea et al., 2013). Among the downstream targets of PhyA are chalcone synthase (chs), rubisco small subunit and chlorophyll a,b binding proteins (Barnes et al., 1995; Jackson et al., 1996; Wu et al., 1996). Interestingly, the gene encoding *Chlorophyll a,b binding protein 3C* was also found among the 205 co-regulated entities.

Another potential TF that was co-expressed with *SP6A* was a *MADS-box TF family protein* (PGSC0003DMT400003484) which has been annotated as *StMADS8* (Gao et al., 2018). MADS-box proteins are downstream targets of FT-proteins like SP6A and are supposed to play a role in flowering and tuberization. Gao et al. (2018) have conducted a co-expression analysis of MADS-box genes with *SP6A* and found that MADS1 and MADS13 were the most likely candidates for downstream signal transduction. *MADS8* gene expression was also investigated by Gao et al. (2018) and found to be highest in roots and flowers, while also being expressed in young tubers, leaves and stolons. According to a BLAST search, the closest homolog of MADS8 in Arabidopsis is AT1G69120 (AGAMOUS-LIKE 7, APETALA1 (AP1)). In Arabidopsis, *AP1* expression is activated by a range of TFs, among which FLOWERING-LOCUS D (FD) and FT have been identified (Monniaux et al., 2017; Wigge et al., 2005). AP1 is a regulator of floral meristem identity and required for the initiation and maintenance of flowering (Han and Jiao, 2015). In potato, it is not yet clear which proteins are responsible for the transduction of signals from SP6A. This MADS-box TF family protein (PGSC0003DMT400003484) seems a well-suited candidate for further investigations into the signaling pathway of tuberization.

4.2.4 Differences in gene expression between primary and secondary tubers

Heat stress can have a major impact on potato tuber induction and development. During the experiments described in chapter 3.3 it was observed that a period of increased temperature during the tuber bulking phase (Treatment 5, see Figure 10) can induce second-growth in various forms like malformation and elongation of tubers, bottleneck tubers and chain tubers. The highest percentage of second-growth was observed in the cultivar Agria under conditions of seven-day heat stress during the tuber bulking period which indicated a high susceptibility of this cultivar toward short periods of heat. The combination of the observations made on

Discussion

tuber morphology under the differing heat treatments suggested that tubers exhibiting second-growth had stopped growing during the heat period and after or during the stress had formed heat sprouts or new stolons. While potatoes of cv. Agria plants which were kept under heat conditions until harvest (Treatment 4) exhibited heat spouts emerging to the surface and forming stems and leaves, tubers of plants subjected to only a short period of heat showed secondary tubers on sprouts/stolons coming from the primary tubers. It seems that after the stress had been relieved, a secondary tuber had formed at the end of the emerging stolon and had grown until harvest. Lugt et al., (1964) made similar observations in their experiments with potato plants subjected to high-temperature conditions (32°C) for one week. They found that primary tubers grew slower during the stress period and started sprouting. Secondary tubers were initiated within the first week after stress release. During the second week after stress release, secondary tubers grew rapidly while primary tubers stopped growing (Lugt et al., 1964).

Tubers of the cultivar Agria from control and seven-day heat treatments (treatments 1 and 5) were chosen for microarray analysis because of their phenotypic response to the stress condition, i.e., the formation of second growth. The analysis of differential gene expression between primary, secondary and normal tubers showed that the *SP6A* signaling network was up-regulated in primary tubers and down-regulated in secondary tubers. The only exception was *SP5G*, which was strongly down-regulated in primary tubers. This was surprising as the network also contains negative regulators of *SP6A* which would be expected to be expressed differently than *SP6A* itself. However, this finding is in line with the observation that *SP5G-like* (PGSC0003DMT400041726) was also among the 205 *SP6A*-co-expressed entities in leaves (Table A 2). The up-regulation of *SP6A* expression in primary tubers could be linked to the development of second-growth. Over-expression of a codon-optimized version of *SP6A* in *S. tuberosum var.* Solara led to massive development of secondary, and even tertiary and quaternary tubers during the storage period after harvest (Lehretz et al., 2019). Thus, SP6A seems to be a strong driver of tuber development, being able to favor secondary tuber growth, which is further strengthened by the observations made in this thesis.

Further characterization of primary tubers by microarray analysis revealed that gene expression of enzymes involved in starch metabolism pointed towards a decrease in starch biosynthesis and an increase in starch degradation (see chapter 3.3.5.3). When looking at the expression of the marker-gene for starch biosynthesis *SuSy4*, a pronounced decrease was observed indicating a reduction of sink strength. *SuSy4* expression is also correlated with tuber growth velocity (Ferreira et al., 2010) which supports the hypothesis that primary tubers stopped growing during the stress period and didn't resume growth after stress release. In secondary tubers, *SuSy4* expression was relatively high suggesting that these tubers were still actively growing. A remaining question about second-growth is where secondary tubers get

their substrates for growth from. It has been proposed from measurements of specific gravity that the primary tuber stops growing when second-growth takes place and that it serves a passive role, like a stem or stolon, as long as the above-ground potato plant is still alive (Lugt, 1960). After the foliage has died, the specific gravity of primary tuber declines, indicating substrate catabolism in primary tubers (Lugt, 1960). If these substrates are transferred to the secondary tubers has not been analyzed and would be an interesting question for future research.

Primary tubers were characterized by strong representation of polyamine metabolism among the significantly up- and down-regulated entities. While polyamines are involved in many developmental processes and stress response of plants (Alcázar et al., 2010, 2006; Wimalasekera et al., 2011), the microarray data didn't suggest an upregulation of polyamine compounds like spermine or putrescine since their biosynthetic enzymes weren't differentially regulated on the transcriptional level. From the transcriptional data it rather seemed like SAM synthesis from methionine was up-regulated and the subsequent decarboxylation step catalyzed by SAMDC was also overexpressed. Furthermore, transcription of the enzyme catalyzing the production of ACC from SAM, ACC Synthase (ACS), was up-regulated, which could indicate a link to ethylene signaling (Pattyn et al., 2021)

Significant changes between normal and primary and secondary tubers were also observed within the category "Hormone metabolism". Primary tubers were characterized by a down-regulation of Jasmonic acid (JA) biosynthetic enzymes' genes. While JA is rather known for its role in wound and stress response than tuber development (Wasternack and Hause, 2013), it has been suggested to play a role in tuberization, too (Begum et al., 2022; Pelacho and Mingo-Castel, 1991; Sohn et al., 2011). During heat stress, an up-regulation of the JA biosynthesis pathway could be expected in potato tubers (Kazan, 2015). However, in the experiment described herein, primary tubers were analyzed two weeks after stress release and microarray analysis did not reveal an over-representation of genes involved in stress-response. Therefore, it seems possible that there could be a role for JA in second-growth development.

Secondary tubers were characterized by an over-representation of brassinosteroid metabolism. Brassinosteroids regulate plant growth and development such as cell elongation, flowering and senescence among others (Clouse, 2011). Currently, the role of brassinosteroids in tuberization is unclear; however, one of the up-regulated genes, *DWARF1/DIMINUTO*, is supposed to have a role in plant sterol metabolism and to influence brassinosteroid levels (Katsarou et al., 2016). DWARF1/DIMINUTO was also identified as a candidate for having a role in regulating tuber shape or tuberization (Katsarou et al., 2016). The results described in this thesis point toward a possible role of brassinosteroids and jasmonate in second-growth formation.

4.3 Analysis of dormancy and transcription profiles in cross-breeding lines

4.3.1 Optimization of growth-conditions of cross-breeding lines

In order to screen the cross-breeding lines, growth conditions were established enabling short growth-periods and space-saving cultivation of the plants. Short-day conditions led to tuber formation within 30 days in the great majority of lines. As effects of heat on tuber phenotype and dormancy were to be studied, the presence of tubers was the prerequisite to start the heat treatment. The growth conditions, i.e., short-days, applied for the screening of the cross-breeding lines led to rapid development of tubers within one month. Extending the recovery period after the stress phase from two weeks (as applied to SA67/12 – HotPot) to three weeks (applied to SA68 and SA69/12-HotPot) led to larger tubers at harvest (compare Figure A 1, Figure A 2, Figure A 3). Larger tubers were advantageous because they are easier to sample. Furthermore, especially for late tuberizing lines, which otherwise exhibit only very small, immature tubers, those conditions lead to more mature tubers. Thus, growth conditions were suitable for screening of large quantities of potato plants in a controlled environmental setting.

During the screening of the cross-breeding populations, short-day conditions were applied during the entire experimental period (Figure 23). While this led to rapid tuber formation, it seemed to suppress the formation of second-growth. A reason for this could be the strong drive toward tuber formation elicited by short-day conditions which overwrote the tuber formation inhibiting signal from the heat stress. Such a strong day-length dependent effect was not expected in the lines analyzed during the experiments, as they were cross-bred from cultivars which are adapted to long days. It has been hypothesized that the pathways for temperature and day-length control of tuberization converge at some point (Rodríguez-Falcón et al., 2006). This common regulation might have led to the observed strong effect of day-length in comparison to the effect of elevated temperatures, resulting in a majority of normally shaped tubers rather than induction of second-growth.

4.3.2 Dormancy of cross-breeding populations in relation to growth-conditions

Dormancy has been defined as 'the absence of visible growth in any plant structure containing a meristem' (Lang et al., 1987) and more recently as 'the inability to initiate growth from meristems (and other organs and cells with the capacity to resume growth) under favorable conditions' (Rohde and Bhalerao, 2007). Dormancy in potato tubers is thought to be established during tuber formation in the meristems contained in the eyes of the tuber. The duration of the dormancy period is dependent on endogenous factors within the meristems themselves (endodormancy) and on environmental conditions (ecodormancy) (Lang et al., 1987). Furthermore, pre-harvest conditions have an influence on the length of tuber dormancy.

In this context, growth under short-day conditions results in shorter dormancy than growth under long-day conditions. Likewise, high temperatures and water shortages during plant cultivation lead to shorter dormancy periods (reviewed by Claassens and Vreugdenhil, 2000 and Sonnewald and Sonnewald, 2014). The same factors influencing dormancy length lead to the induction of second-growth, which shares many of the characteristics of dormancy break. Therefore, dormancy was assessed in the cross-breeding populations as a suspected marker for their susceptibility to second-growth.

Tuber dormancy of cross-breeding lines was analyzed in tubers harvested from two to three experiments. Plants were cultivated and, after harvest, tubers were kept at room temperature in the dark and the time-point of sprouting was monitored. While the length of the dormancy period differed between the experiments – likely resulting from a combination of storage conditions and day-length variations between experiments - the time-point of dormancy break for each line relative to the other lines remained similar indicating an intrinsic mechanism determining the length of the dormancy-period, i.e., endodormancy.

4.3.3 Early sprouting is associated with transcriptional regulation of ethylene biosynthesis and light signaling

During the screening of the cross-breeding populations, a special emphasis was on second-growth phenomena of tubers. However, as mentioned above, it seemed that the tuberization signal in response to the short-day conditions during plant cultivation was stronger than the inhibitory effect of the heat application. As dormancy period duration could be related to the proneness to second-growth, this characteristic was used for further evaluation of the genotypes. Line SA69/12 #57 had a short dormancy period and its' gene expression profile from under-eye tissue clustered with sprouting tuber buds. Furthermore, when growth conditions were adapted to include a combination of heat and long days, a high percentage of tubers exhibiting second-growth was observed in this line. Gene-expression analysis revealed that ethylene-related genes were over-represented among differentially regulated genes in line #57. Ethylene, together with Absicic acid, is involved in the establishment of dormancy. However, ethylene is not needed to maintain dormancy of potato buds (Suttle, 2004). It has been suggested that short-term exposure to ethylene would induce sprouting prematurely, but that extended periods of ethylene exposure inhibit sprout growth (Rylski et al., 1974). In contrast, transgenic tubers exhibiting a delayed onset of sprouting were shown to overexpress entities belonging to the ethylene pathway (Hartmann et al., 2011). If ethylene has a role in dormancy break or sprout outgrowth and how it could function is currently unknown and deserves further consideration.

Discussion

Light signaling-related transcripts were found among the up- and down-regulated entities, namely *Phi-1* and *NPH3* as well as *PAS/LOV protein* and *Root phototropism proteins*, respectively. Heat stress has been shown earlier to cause a phototropism reaction in the above-ground parts of the potato plant, i.e., stem elongation via increased internodal distances (Hastilestari et al., 2018). In this thesis, a thermo-morphogenic response was observed in the below-ground tubers via the formation of second-growth and the longer-term influence on dormancy. This is in line with the similarities between the transcriptional profiles observed in leaves by Hastilestari et al. (2018) and the tuber samples described herein, i.e., down-regulation of *PAS/LOV protein* (homolog to AT2G02710) and up-regulation of *NPH3*. Phototropism involves auxin-signaling which was represented among the 250 uniquely regulated entities by *Auxin-induced protein 6B* (*SAUR*) and *Auxin response factor 2* (*ARF2*), which were both down-regulated. While the relevance of Auxin for plants development and growth and for phototropic responses is acknowledged, its' role in tuber dormancy and sprouting is currently unknown (Sonnewald and Sonnewald, 2014). From the data presented in this thesis it can be hypothesized, that auxin and ethylene may have functions in the regulation of dormancy at an early time-point before visible bud outgrowth.

4.3.4 Analysis of longer-term heat effect on gene expression in cross-breeding lines

66 differentially expressed entities were found between samples of heat-treated tubers compared to tubers from control conditions. Among these 66 entities, *TAS14* was retrieved among the significantly up-regulated entities. *TAS14* was used as a marker for abiotic stress in potato tubers in the experiments described in chapter 3.5.3 and its' possible relevance is discussed in chapter 4.4.2. The results of this microarray analysis add another indication for a role of TAS14 in abiotic stress response. However, the timing differed between the experiments, as *TAS14* had not been suspected to indicate past stress exposure on the longer term. The notion that the stress period was still measurable in gene expression pattern was further supported by the up-regulation of some heat-shock proteins. The long-term consequences of heat stress on gene expression patterns in potato tubers deserve more attention in future research.

Among the down-regulated entities, within the category "development", *nodulin family proteins* as well as *Auxin-induced protein 5NG4* were retrieved. Interestingly, similar findings were reported by Hastilestari et al. (2018) who connected the down-regulation of these genes to the decrease in tuber weight resulting from abiotic stress treatment.

4.4 Influence of combined heat and drought stress on tuber growth and starch metabolism

4.4.1 X-ray CT analysis revealed that combined heat and drought stress affects tuber growth

"In this study, potato tuber development from initiation until harvest was monitored by X-ray CT analysis in stressed plants and plants grown under ambient conditions. […] We chose combined heat and drought stress since these abiotic stresses are likely to occur in parallel in the context of global climate change (Ahuja et al., 2010; Hijmans, 2003). We applied the stress treatment after tuber induction, when tubers were detectable by CT, in order to avoid delaying or even completely inhibiting tuber formation. Such detrimental effects of heat and drought have been described previously (Aliche et al., 2020; Dahal et al., 2019; Jackson, 1999; Luitel et al., 2015). X-ray CT analysis revealed that tuber growth is inhibited during combined elevated temperature and drought stress and can resume after the stress has been terminated. The growth arrest as calculated from the X-ray data led to significantly lower tuber biomasses in stressed plants at the end of the stress treatment compared to control plants. After cessation of the stress, tubers started growing again and were only slightly smaller than control tubers at the end of the experimental period.

Due to the early timing of the stress treatment directly after tuber induction, it seems that tubers were able to recover from the implications of the stress treatment on biomass accumulation. This was also seen in an early study on the effects of individual heat and drought stress on tuber development (Levy, 1985) where early stress, imposed when tubers were small, reduced tuber yield and dry matter accumulation only slightly. Heat or drought stress applied during the tuber bulking stage had a more deleterious effect on tuber yield (Levy, 1986, 1985). Moreover, in our experimental setup plants were still immature at the end of the experimental period, exhibiting only small tubers and low overall tuber biomass. How our findings translate to potato plants grown to maturity requires further trials." (Van Harsselaar et al. 2021).

4.4.2 Stress Markers Respond to the combined Heat and Drought Treatment

"Genes which have previously been shown to respond with differential expression during abiotic stress were selected from the literature (Gong et al., 2015; Rizhsky et al., 2002) in order to confirm that the stress led to a response in the potato tubers. Gong et al. (2015) analyzed gene transcription in stolon tips of potato plants grown under control conditions, drought stress and after re-watering. They found that *TAS14* was 4.7-fold up-regulated after 3 days of drought treatment and 8.2-fold down-regulated after re-watering when compared to stolons from plants grown under control conditions. In our study, *TAS14* expression in tubers was almost 50-fold

upregulated after 8 days of combined drought and heat stress but had returned to values similar to control 3 days after stress release. This indicated that *TAS14* might be suitable as a marker for stress in potato tubers. However, further characterization of its expression profile in different plant organs and under differing conditions is needed to confirm its suitability as a stress marker. Support for the role of TAS14 during abiotic stress comes from experiments in tomato, where stable overexpression of TAS14 led to improved long-term drought tolerance (Muñoz-Mayor et al., 2012).

Rizhsky et al. (2002) examined gene expression patterns under different stress conditions as well as their combinations in tobacco plants. A combination of drought and heat stress led to significant increases in gene expression of *DI19* and *Lox1*, by 34- and 6.7-fold, respectively. DI19 has also been described in rice as a key regulator during drought stress and drought tolerance (Wang et al., 2014). In the present study, *DI19* and *Lox1* were induced significantly, but to a far lesser extent than in those previous studies, in tubers during combined stress treatment compared to tubers grown under control conditions. It appears that these two transcripts are not suitable as markers for combined heat and drought stress in potato tubers.

Heat-shock protein (DMT400032851) which was strongly elevated in potato tubers during combined heat and drought stress compared to control, has previously been found in a microarray analysis among 2,886 differentially expressed genes in potato tubers of the cultivar Desirée during mild heat (Hancock et al., 2014). In the experiment by Hancock et al. (2014), potato plants were subjected to elevated temperature (30°C during the day / 20°C during the night) for 1 week and expression patterns over a time course of 20 h were compared to tubers grown under ambient conditions (22°C / 16°C). HSP was found to be upregulated approximately 12-fold on average over time (range 0.8–30.8-fold) during elevated temperature. The strong induction which we have determined for *HSP* could be a result of the additional drought treatment and the different methodology (qRT-PCR vs. microarray analysis). Thus, *HSP* might be an appropriate marker for combined heat and drought stress in potato tubers but further validation is recommended." (Van Harsselaar et al. 2021).

4.4.3 Combined Heat and Drought Stress Has a Negative Influence on Expression of Genes Encoding Enzymes Involved in Starch Biosynthesis

"Heat and drought are abiotic stress factors influencing many developmental and physiological processes. In potato plants, both factors, alone or in combination, affect tuberization and starch accumulation associated therewith (Bodlaender, 1963; Gawronska et al., 1992; Wolf et al., 1990). Depending on the timing of the occurrence of these disruptive environmental conditions, tuberization can be inhibited completely or tuber bulking can be disturbed (Tang et al., 2018). Furthermore, carbon partitioning can be altered by transient exposure of potato plants to heat

stress leading to reduced starch and increased reducing sugar contents of tubers (Busse et al., 2019). We have seen a disturbance of tuber bulking which was confirmed by analysis of mRNA expression of *SuSy4* as well as specific activity of SuSy, a marker for starch biosynthesis, in tuber samples. Increased SuSy expression and activity has been associated with increased starch and total yield (Baroja-Fernández et al., 2009). Under adverse conditions like heat, *SuSy4* expression and SuSy activity have been shown decrease (Hastilestari et al., 2018).

GPT2.1 has been identified as the tuber-specifically expressed GPT2 isoform (Van Harsselaar et al., 2017), whose expression is strongly associated to processes linked to starch biosynthesis and correlates to *SuSy4* expression (Ferreira et al., 2010). Therefore, we hypothesized that *GPT2.1* expression would decrease during stress treatment. However, gene expression analysis of *GPT2.1* revealed no significant differences between stressed tuber samples and tubers grown under control conditions. This is consistent with the gene expression data from tuber samples under elevated temperatures published by Hancock et al. (2014) and Hastilestari et al. (2018) where *GPT2.1* was not among the differentially regulated genes.

Granule-bound starch synthase is the starch synthase isoform responsible for amylose-synthesis (Visser et al., 1989). Expression of *GBSS* was found to be significantly downregulated in potato tuber during combined heat and drought stress in our qRT-PCR analysis. Similarly, in the microarray experiment by Hancock et al. (2014), *GBSS* expression was downregulated significantly in the tuber samples from plants grown under elevated temperature. This seems consistent with an overall decrease of starch biosynthesis in potato tubers under heat and drought stress. In our experiment, *SuSy4* and *GBSS* expression recovered to levels of tubers grown under control conditions after the stress conditions were released. Similar observations were reported by Chen et al. (2020) in potato leaves during re-watering after a dehydration period, where most genes which were differentially expressed during the dehydration period reversed their expression during re-watering." (Van Harsselaar et al. 2021).

5 Material and Methods

5.1 Chemicals, enzymes and consumables

Unless stated otherwise, chemicals, enzymes and consumables were purchased from Carl Roth GmbH & Co. KG (Karlsruhe), Sigma-Aldrich (St. Louis, USA), Fermentas GmbH (St. Leon-Rot), Applichem GmbH (Darmstadt), Roche Diagnostics GmbH (Mannheim), Bio-Rad (München), GE Healthcare (Freiburg), New England Biolabs GmbH (Frankfurt am Main), Merck (Darmstadt), Stratagene (Amsterdam, Netherlands), Whatman (Maidstone, England), Thermo Fisher Scientific (Carlsbad, USA), Agilent Technologies (Santa Clara, USA) and VWR International GmbH (Darmstadt), Materials and soil for plant cultivation were obtained from Bayerische Gärtnereigenossenschaft e.G. Nürnberg. Kits for the extraction of DNA fragments from agarose gels were obtained from Qiagen (Hilden).

5.2 Oligonucleotides

Oligonucleotides were obtained from Metabion International AG (Martinsried) and Eurofins MWG Operon (Ebersberg). Primers for quantitative real-time PCR analysis were deduced by using the NCBI Primer-BLAST online tool (Ye et al., 2012) to have a product length ranging from 70–150 bp and a melting temperature from 59–61°C. Target genes and sequences are listed in Table 14.

Table 14: Oligonucleotide primers used in this thesis

Primer name	Transcript ID	Sequence	Amplicon length (bp)
qPCR SBE3 fwd	PGSC0003DMT400025846	5'-TCAGGAGCGGTCTTGGGATA-3'	102
qPCR SBE3 rev		5'-TCATCGGTCAAAACAGCGGA-3'	
qPCR SS5 fwd	PGSC0003DMT400078688	5'-GCAAAGTTTCGTTGCAGCAG-3'	89
qPCR SS5 rev		5'-TGCAGGTAAATCTTCAACCAGAGT-3'	
qPCR SuSy4 fwd	PGSC0003DMT400007506	5'-ATGAACCGAGTGAGGAATGG-3'	155
qPCR SuSy4 rev		5'-GCTGGACCACCGTGATTAGT-3'	
qPCR BAM3 fwd	PGSC0003DMT400004686	5'-AGCACCTAGAAGAGTCCACAAG-3'	98
qPCR BAM3 rev		5'-CAGGGAGGCAAAGATTGGCA-3'	
qPCR BAM3-like f	PGSC0003DMT400052839	5'-GTTCGTGAAACGTGGGGTTG-3'	81
qPCR BAM3-like r		5'-GAGCAATTCGCGCTATGTGG-3'	
qPCR AMY1 fwd	PGSC0003DMT400020591	5'-ACTGATTCAACCTTCTGCGGT-3'	117
qPCR AMY1 rev		5'-TCTGCTTCCCTTCAATGGCTT-3'	
qPCR GLT1 fwd	PGSC0003DMT400067884	5'-GGTGAACCGTAGGTGTGCAA-3'	109
qPCR GLT1 rev		5'-TGCAGTTTCTGATTTACACTACGAA-3'	

qPCR NTT1 fwd	PGSC0003DMT400014304	5'-TCCGGAGGAGCCTTGATACA-3'	86
qPCR NTT1 rev		5'-AGGAGCACACCTCCAAGGTA-3'	
qPCR GPT2.1 fwd	PGSC0003DMT400013500	5'-TGGCTGCTGGCTCTCTTATG-3'	109
qPCR GPT2.1 rev		5'-TGAGCCACAGCAACAGGAAA-3'	
qPCR BAM4 fwd	PGSC0003DMT400031627	5'-TCACAGAAGACAGCTCGGAC-3'	119
qPCR BAM4 rev		5'-GCCCACTCACGCATTCCTAT-3'	
qPCR AGPaseL2 f	PGSC0003DMT400041215	5'-TGTGTGCTAGTATGAAGGGCA-3'	115
qPCR AGPaseL2 r		5'-CGGACCCCAAAACCCTTGTT-3'	
qPCR MEX1 fwd	Sotub04g024480.1.1	5'-TTCCATGGCTGGGGATGTTC-3'	93
qPCR MEX1 rev		5'-GCACAACAACCACTTCCGTC-3'	
qPCR LSF2 fwd	PGSC0003DMT400074765	5'-CAGGGAGCTACTTATGATTTGGC-3'	93
qPCR LSF2 rev		5'-CCAATCTGCTACATCCGCGA-3'	
qPCR GWD3 fwd	PGSC0003DMT400042818	5'-GTCTGTGGGGTGTCTTCTGT-3'	89
qPCR GWD3 rev		5'-TGAACCTTCTCAGTAGATGATCCAG-3'	
qPCR SEX4 fwd	PGSC0003DMT400039423	5'-GCCGATCACTTCTCCCAACA-3'	109
qPCR SEX4 rev		5'-ACCGGAGAACCTCTTCCGTA-3'	
qPCR APL3 fwd	PGSC0003DMT400001935	5'-CGGGGAGAAGATCAGAGGGA-3'	113
qPCR APL3 rev		5'-CAGAGTAAGCAACCCCAGGT-3'	
qPCR APL1 fwd	PGSC0003DMT400023304	5'-TGCTTCAATGGGAGTTTACGTCT-3'	116
qPCR APL1 rev		5'-ATTCTTTGGTGGAGGCAGGG-3'	
qPCR GBSS fwd	PGSC0003DMT400031568	5'-CTCACACAGCTCAACAAGTGC-3'	78
qPCR GBSS rev		5'-GTGAAGCTGTGATGCTTGCC-3'	
qPCR TIFY fwd	PGSC0003DMT400002991	5'-TGGCTCCGATCCATTGTTTGT-3'	143
qPCR TIFY rev		5'-GTTGCTACCTAGCGCCATCA-3'	
qPCR LOB fwd	PGSC0003DMT400032877	5'-GCTACCAATGCTGATTTGATGAGA-3'	145
qPCR LOB rev		5'-CATCTGCTTCAGGGTTATTGTTCC-3'	
qPCR WRKY4 fwd	PGSC0003DMT400023368	5'-TTCGGATCCTCTATGCATGTGT-3'	72
qPCR WRKY4 rev		5'-ACAAAGTGAAACGGAAGGACTACT-3'	
qPCR PTL fwd	PGSC0003DMT400007016	5'-GTATGAGATGGTGATGGGACTGG-3'	95
qPCR PTL rev		5'-TAAGGAACTCATGTTGGTGGTGG-3'	
qPCR Sp6a fwd	PGSC0003DMT400060057	5'-ACAGTGTATGCCCCAGGTTG-3'	87
qPCR Sp6a rev		5'-AACAGCTGCAACAGGCAATC-3'	
qPCR Dl19 fwd	PGSC0003DMT400011781	5'-CCAGTGCAGATCCTGATCCC-3'	130
qPCR Dl19 rev		5'-GCGCTTTCTTGTGTTGAGCA-3'	
qPCR LOX1 fwd	Sotub01g036960.1.1	5'-CAGAGCCAGGAAGTGCAGAG-3'	161
qPCR LOX1 rev		5'-TGAATCATTCTGCCCCAGGTAA-3'	
qPCR TAS14 fwd	PGSC0003DMT400009069	5'-TAACACCTGTTGTGCCTCCA-3'	186
qPCR TAS14 rev		5'-CTTGGTTGCCGTATTGTGCC-3'	
SS543 StHSP_5'	PGSC0003DMT400032851	5'-GAAACACCTCAAGCTCATTGC-3'	119
SS544 StHSP_3'		5'-TCTTCTGCTTTCCACTTTCCA-3'	
EF1alpha f	PGSC0003DMT400020969	5'-CCCTCAGACAAGCCACTCC-3'	80
EF1alpha r		5'-ACACGACCAACAGGCACAG-3'	
qPCR Ubi fwd	L22576 (Kloosterman et al. 2005)	5'-TTCCGACACCATCGACAATGT-3'	105
qPCR Ubi rev		5'-CGACCATCCTCAAGCTGCTT-3'	

5.3 Plant material and cultivation

Potato plants (*Solanum tuberosum* L.) were obtained from Bioplant (Ebstorf), KWS Potato BV (Nagele, Netherlands), and SAKA Pflanzenzucht GmbH & Co. KG (Windeby) and were propagated in tissue culture at 21°C and 50 % humidity on Murashige Skoog (MS) medium supplemented with 2% (w/v) sucrose, appropriate phytohormones and antibiotics under a 16 h light/ 8 h dark regime (Murashige and Skoog, 1962).

For experimental procedures, plantlets were transferred to individual, soil containing, pots either in the greenhouse or into phyto-chambers (Plant Master, CLF Plant Climatics, Emersacker). For cultivation in the greenhouse, plants were transferred to 3.5 l pots (Ø 20 cm, height 15.5 cm). Conditions were 16h light with additional illumination (250-300 µmol m^{-2} s^{-1}) at 21°C and 8 h dark at 18°C and a relative humidity of 50% until harvest, unless stated otherwise. For cultivation in phytochambers, plants were treated as described below.

5.3.1 Heat stress experiments with parental lines of S. tuberosum

For heat stress experiments with cultivars Tomensa, Ramses, Princess, Saturna and Agria, plants were transferred to 3.5 l pots (Ø 20 cm, height 15.6 cm). For the heat treatment, plants grown for 6.5 weeks in the greenhouse were transferred to a phytochamber for a 7-day period under 16 h light (250-400 µmol m^{-2} s^{-1}) at 29°C and 8 h dark at 27°C and a relative humidity of 70%. Subsequently, plants were transferred back to greenhouse conditions for 2 weeks of recovery. Leaf samples for microarray analysis of control and heat-treated plants were taken after 6.5 (before heat), 7.5 (end of heat period) and 9.5 (harvest) weeks from five leaves of five individual plants per replicate with a size 5 cork borer. Tuber parenchyma samples were taken after 9.5 weeks from tubers looking normal and tubers showing a second growth phenotype (primary and secondary tubers) from individual tubers of different plants with a size 5 cork borer and a slicer.

5.3.2 Screenings of cross-breeding populations

For screenings of cross-breeding populations, plants were transferred to 0.51 l pots (Ø 10.5 cm, height 9 cm). 200 g soil was used per pot which was watered with a 0.25% solution of Previcur N (Bayer CropScience) on the day before plants were transferred. For each line, four plants were cultivated which were distributed evenly in the phytochamber. Conditions were slightly adapted for each cross-breeding population:

SA67/12 – HotPot (77 lines and parental lines Agria and Saturna) was grown under short day conditions (8 h light / 16 h dark) at 21°C day / 19°C night temperatures for 30 days, then subjected to 10 days of increased temperatures of 29°C day / 27°C night, followed by a regeneration period of 14 days at 21°C day / 19°C night.

SA68/12 -HotPot (66 lines and parental lines Saturna and Princess) was grown under similar conditions as SA67/12 – HotPot, but the regeneration period was extended by 7 days to 21 days.

SA69/12 – HotPot (69 lines and parental lines Ramses and Tomensa) was cultivated under slightly lower temperatures: 20°C day / 18°C night during initial growth and regeneration and 28°C day / 24°C night during the period of elevated temperatures. Apart from that, the conditions were identical to SA68/12 -HotPot.

At harvest, tuber and leaf weights were measured and potatoes were visually assessed for second-growth. After harvest, tubers were stored and evaluated regularly until dormancy break.

5.3.3 Confirmatory experiments with cross-breeding populations

Selected lines of all three cross-breeding populations were propagated in tissue culture and cultivated again in the phytochambers in two groups; one group that was subjected to a heat stress period and one control group. Plants of both groups were first grown under short-day conditions (8 h light / 16 h dark) at 21°C day / 18°C night for 30-32 days. Then, day length was increased to 16 h day / 8 h night for both groups, while at the same time, for one half of the plants, temperatures were increased to 29°C day / 27°C night for a duration of 10 days. Afterwards, temperatures were returned to 21°C day / 18°C night for another 14-15 days.

Samples were taken at different time-points during the growth period: leaf samples were taken at the end of the initial period of ambient temperatures, before the onset of heat. At the end of the heat period, tuber and leaf samples were taken and photosynthesis and transpiration were measured. SuSy activity was measured from tuber parenchyma samples. At the end of the experimental period, leaves and tubers were weighed, tuber samples were taken and tubers were visually analyzed to second-growth phenomena before being stored in cardboard boxes in the dark at room temperature and regularly assessed for sprouting. In the population SA69/12 – HotPot metabolite profiling was conducted from the samples taken at the end of the experimental period. Phosphorylated intermediates as well as amino acids were quantified.

The final experiments with the selected lines of cross-breeding population SA69/12 – HotPot were done under the following conditions: equinoctial day length (12h light / 12h dark) which was maintained throughout the entire growth period. Temperatures were 21°C day / 18°C night for the initial 30 days, then increased to 29°C day / 27°C night for 10 days, then decreased again for the regeneration period of 14 days. Furthermore, pots with higher volumes (1.5 l) were used for cultivation to enable tubers to develop properly without space restrictions due to pot size.

Tuber samples from tissue underneath the apical eyes were taken from tubers after 11 days of storage in the dark and at room temperature with a size 4 cork borer and slicer. For each biological replicate, material from four tubers were pooled. The rest of the unprobed tubers were further stored until dormancy break.

5.3.4 Combined heat and drought stress experiments in growth chambers at the Fraunhofer Institute for Integrated Circuits

"For experiments at the Fraunhofer Institute for Integrated Circuits potato plants were transferred to 1.5 l pots containing sieved soil (Ø 15 cm, height 11.7 cm, Einheitserde Classic ED73; sieve grid 0.5 cm) and placed in plant growth chambers (Conviron, Winnipeg, Canada) under conditions of 16h light at 21°C and 8h dark at 18°C and 50% humidity during the day and 35% humidity at night. Plants were watered daily and tuber growth was monitored by X-ray CT three times per week. In the experiment with the cultivar Diamant, 30 plants were used of which 16 were monitored by X-ray CT analysis. In the first experiment, four plants each of the cultivars Agria, Saturna, Tomensa, Ramses and Diamant were monitored at the same time. When tubers were detectable via CT, combined heat and drought stress was applied by increasing the temperature to 29°C during the light period and 21°C during the dark period and reducing the amount of water given to each plant from 50 to 30 ml/day. In the second experiment with the cultivar Diamant, 30 plants were used of which 16 were monitored by CT analysis. After tuber initiation, as determined by CT monitoring, drought and mild heat stresses were applied to half of the plants for 2 weeks while the other half of the plants served as control group. The control group was watered with 50 ml per day/plant for the whole time while the stress group was subjected to the conditions described above.

Tuber samples from the experiment with the cultivar Diamant were taken at three time points; (1) 8 days after initialization of the stress period, when the tubers had stopped growing (TP1), (2) 3 days after the stress period, when the tubers had started growing again (TP2), and (3) at the end of the experimental period, 2 weeks after the end of the stress phase (TP3). At each time point five plants per treatment were harvested and the leaf and tuber biomass were measured with a laboratory balance. At the first time-point, 10 plants (five per condition) were harvested which had not been monitored by CT analysis. At the second time-point, two plants per condition had not been subjected to CT analysis, while the other three sampled plants had been monitored. At the end of the experimental period the remaining 10 plants which had been monitored via CT imaging were harvested and biomass was determined. At each time point and condition, 10 tubers were selected for sampling. Samples were immediately frozen in liquid nitrogen and stored at -80°C until further use." (Van Harsselaar et al., 2021).

5.4   X-Ray Computer Tomography (CT) Imaging

X-ray CT imaging was conducted at the Fraunhofer Institute for Integrated Circuits as described in Van Harsselaar et al., 2021.

5.5   Measurement of Photosynthesis and Transpiration

Photosynthesis and transpiration were determined using a combined gas exchange chlorophyll fluorescence imaging system (GFS-3000, Walz, Effeltrich). Measurements were taken during the confirmatory experiments with the cross-breeding populations at the end of the 10-day heat-treatment and the same time-point in control plants. To this end, fully expanded leaves were fixed into the device and measurements conducted at 400 µL L^{-1} CO_2 and illumination of 400 µmol m^{-2} s^{-1}.

5.6   Protein extraction for measurement of Sucrose Synthase activity

For the measurement of enzyme activities, proteins were extracted in enzyme extraction buffer (25 mM HepesKOH pH 7.0, 12 mM $MgCl_2$, 0.5 mM Na-EDTA, 8 mM DTT, 0.1 mM Pefabloc, 0.1% (v/v) Triton X-100, 15% glycerine) after grinding with a mortar in liquid nitrogen. Samples were centrifuged for 20 minutes at 13000 rpm at 4°C and supernatants were collected into new tubes and thereby measuring their volume.

Protein content was measured using Bradford reagent (Bradford Protein Assay, BioRad, Munich, (Bradford, 1976)). Therefore, protein extracts were incubated for 5 minutes with Bradford reagent following manufacturer`s instructions and subsequently the extinction was determined photometrically at 595 nm. Protein concentrations were calculated with the help of a BSA standard curve.

For the measurement of Sucrose Synthase activity, 25 µl of protein extract was mixed with 175 µl of measurement buffer (100 mM Tris HCl pH 6.3, 200 mM sucrose, 5 mM DTT, 3 mM MgAc, 5 mM NaF, 2 mM Pyrophosphate (PP$_i$), 500 µM   NAD, 1 U/ml UGPase, 1 U/ml Glucose-6-Phosphat-Dehydrogenase (G6PDH), 0,5 U/ml Phosphoglucomutase (PGM)) in microtiter plates at 4°C. Plates were placed in a multititer plate reader (EL808, BIO-TEK) and enzyme kinetics were measured at 340 nm for a time period of at least 30 minutes. Activity was calculated as UDP-glucose forming activity per minute per mg total protein.

5.7   Determination of starch content

Starch was extracted from tuber or leaf samples as described by Müller-Röber et al. (1992).

Starch was quantified from tuber samples as described in (Van Harsselaar et al., 2021).

5.8 Measurement of phosphorylated metabolites and amino acids

Metabolite extraction for the measurement of amino acids and phosphorylated intermediates was performed with perchloric acid as described previously (Horst et al., 2010). Phosphorylated intermediates were determined by utilizing ion chromatography connected with an ICS3000 HPLC system (Dionex, Idstein) and detection using a QTrap 3200 Triple-Quadrupole mass spectrometer (Applied Biosystems, Foster City, USA) with a turboV ion source (Applied Biosystems) operated in multiple reactions monitoring (MRM) mode. The perchloric acid extracts were also used for the determination of free amino acids. To this end, reversed-phase HPLC with fluorescence detection was utilized after derivatization of the samples with AQC/Accq-Taq (6-aminoquinolyl-N-hydroxysuccinimidylcarbamate).

5.9 RNA extraction

RNA extraction from plant tissues essentially followed the protocol of Logemann et al. (1987). RNA concentration was determined using the ND-1000 spectrophotometer (NanoDrop Technologies).

5.10 DNAse treatment of RNA and cDNA synthesis

Two µg of total RNA were treated with DNase I (Thermo Scientific) prior to reverse transcription using oligo(dT)^{18} primers and RevertAid™ H minus first strand cDNA synthesis kit (Thermo Scientific) according to the manufacturer's instructions.

5.11 Quantitative real-time PCR

For relative quantification of transcripts, qRT-PCR analyses were performed using the AriaMX (Agilent Technologies) or Mx3000P (Stratagene) qPCR system in combination with the Brilliant II SYBR® Green QPCR Master Mix (Agilent Technologies). The master mix contained 2 µl forward primer (200 nM), 2 µl reverse primer (200 nM), 10 µl SYBR Mix I, 1 µl of cDNA and Nuclease-free water up to 20 µl. Elongation Factor 1α (EF1α) or Ubi3 (L22576, Kloosterman et al., 2005) expression was used for normalization of target gene expression. The thermal profile was as follows: 1 cycle 10 min at 95°C for DNA polymerase activation followed by 40 cycles of 30 s at 95°C, 30 s 60°C and 30 s 72°C and subsequently a melting curve.

5.12 Microarray analysis

5.12.1 Microarray hybridization and scanning

Microarray experiments were conducted with the 8x60k microarray (Agilent Technologies) described in Hancock et al., (2014). RNA was isolated as described in chapter 5.9. and purified using the RNeasy Purification Kit (Qiagen). Quality was controlled on the Agilent 2100 Bioanalyzer utilizing the Agilent RNA 600 Nano Kit. cDNA and cRNA analysis and labelling were conducted according to the Single-color (Heat experiment with cultivar Agria) or Two-Color (heat experiment with cross-breeding lines SA69/12) Microarray-Based Gene Expression Analysis protocol (Agilent) using the low input quick amp labelling kit (Agilent). For the two-color labeling, samples from control conditions were labelled with Cy3 and heat-treated samples with Cy5. The same genotypes were hybridized on the same arrays. Microarrays were hybridized for 17h at 65°C and subsequently washed according to manufacturer's recommendations. Chips were scanned with the Agilent DNA Microarray-Scanner with extended dynamic range at high resolution. Data sets were extracted with the feature extraction software (Agilent Technologies) using a standard protocol.

5.12.2 Microarray data extraction and analysis

For microarray data analysis, data files were imported as single channel data into the software GeneSpring 12.6.1 (Agilent Technologies). Samples were normalized applying default settings comprising log2 transformation, normalization to the 75th percentile and feature baseline correction to the median of all samples. The latter was adapted to the control samples in the experiment with S. tuberosum *cv.* Agria, where baseline correction was done to leaves before onset of stress for leaf samples and to "normal" tubers from control conditions for tuber samples.

5.12.2.1 Analysis of combined experimental data for the identification of leaf- and tuber-specifically expressed genes

As described in Van Harsselaar et al., 2017, samples from leaves and tubers (including stolons and sprouts) were grouped as either "leaf" or "tuber" tissue. This was done for experimental data from the POCI 4x44k platform and the 8x60k platform separately. "Subsequently, the ratio between leaf and tuber was calculated giving the fold-change difference in gene expression between the two tissues for all individual starch genes. Genes exhibiting an average absolute fold-change above ten were regarded as being tissue-specifically expressed.

For co-expression analyses, Pearson's correlation with a cut-off value of ≥0.8 was applied on all entities after filtering on entities that have been detected in at least one condition. Starch

genes found to be highly expressed in tubers, which were SuSy4, SBE3, GPT2.1, were used as queries. If more than one valid probe was available, all probes were used as queries for the correlation and the resulting lists were reconciled using Venn-diagrams. Only entities correlating with all query features representing the same gene were considered." (Van Harsselaar et al., 2017).

5.12.2.2 Analysis of microarray data from heat stress experiment with S. tuberosum cv. Agria and selected lines of cross-breeding population SA69/12

Microarray data from heat stress experiments with S. tuberosum cv. Agria and with selected lines of cross-breeding population SA69/12 was filtered on "flags" (detected). Subsequently, features showing changes in expression of more than two-fold were selected for further analysis. A volcano plot (moderated t-test) with Benjamini-Hochberg multiple test correction was applied to retrieve features which were statistically significantly ($p ≤ 0.05$) and at least 2-fold regulated between conditions. Annotations were used as described on the SpudDB website (http://spuddb.uga.edu/index.shtml) or according to the closest *Arabidopsis thaliana* homolog. Functional categorization was based on MapMan categories (Thimm et al., 2004) as provided by Hancock et al., (2014) in a descriptive file for the 8x60k microarray.

5.12.2.3 Availability of microarray data

The datasets produced in the course of this thesis are available in the ArrayExpress repository (www.ebi.ac.uk/arrayexpress), under accession numbers E-MTAB-4805 (experiments described in chapter 3.3.5) and E-MTAB-11723 (experiments described in chapter 3.4.4).

6 References

Abel, G.J.W.W., Springer, F., Willmitzer, L., Kossmann, J., 1996. Cloning and functional analysis of a cDNA encoding a novel 139 kDA starch synthase from potato (Solanum tuberosum L.). Plant J. 10, 981–991. https://doi.org/10.1046/j.1365-313X.1996.10060981.x

Abelenda, A., Cruz-oro, E., Franco-zorrilla, M., Abelenda, A., Cruz-oro, E., 2016. Potato StCONSTANS-like1 Suppresses Storage Organ Formation by Directly Activating the FT-like StSP5G Repressor 872–881. https://doi.org/10.1016/j.cub.2016.01.066

Abelenda, J.A., Bergonzi, S., Oortwijn, M., Sonnewald, S., Du, M., Visser, R.G.F., Sonnewald, U., Bachem, C.W.B., 2019. Source-Sink Regulation Is Mediated by Interaction of an FT Homolog with a SWEET Protein in Potato. Curr. Biol. 29, 1178-1186.e6. https://doi.org/10.1016/j.cub.2019.02.018

Abelenda, J.A., Navarro, C., Prat, S., 2014. Flowering and tuberization: A tale of two nightshades. Trends Plant Sci. 19, 115–122. https://doi.org/10.1016/j.tplants.2013.09.010

Abelenda, J.A., Navarro, C., Prat, S., 2011. From the model to the crop: Genes controlling tuber formation in potato. Curr. Opin. Biotechnol. 22, 287–292. https://doi.org/10.1016/j.copbio.2010.11.013

Ahuja, I., Vos, R.C.H. De, Bones, A.M., Hall, R.D., 2010. Plant molecular stress responses face climate change. Trends Plant Sci. 15, 664–674. https://doi.org/10.1016/j.tplants.2010.08.002

Albrecht, T., Koch, A., Lode, A., Greve, B., Schneider-Mergener, J., Steup, M., 2001. Plastidic (Pho1-type) phosphorylase isoforms in potato (Solanum tuberosum L.) plants: Expression analysis and immunochemical characterization. Planta 213, 602–613. https://doi.org/10.1007/s004250100525

Alcázar, R., Altabella, T., Marco, F., Bortolotti, C., Reymond, M., Koncz, C., Carrasco, P., Tiburcio, A.F., 2010. Polyamines: Molecules with regulatory functions in plant abiotic stress tolerance. Planta 231, 1237–1249. https://doi.org/10.1007/s00425-010-1130-0

Alcázar, R., Marco, F., Cuevas, J.C., Patron, M., Ferrando, A., Carrasco, P., Tiburcio, A.F., Altabella, T., 2006. Involvement of polyamines in plant response to abiotic stress. Biotechnol. Lett. 28, 1867–1876. https://doi.org/10.1007/s10529-006-9179-3

Aliche, E.B., Theeuwen, T.P.J.M., Oortwijn, M., Visser, R.G.F., van der Linden, C.G., 2020. Carbon partitioning mechanisms in POTATO under drought stress. Plant Physiol.

References

Biochem. 146, 211–219. https://doi.org/10.1016/j.plaphy.2019.11.019

Andersson, I., 2008. Catalysis and regulation in Rubisco. J. Exp. Bot. 59, 1555–1568. https://doi.org/10.1093/jxb/ern091

Appeldoorn, N.J.G., De Bruijn, S.M., Koot-Gronsveld, E. a. M., Visser, R.G.F., Vreugdenhil, D., Plas, L.H.W. Van Der, 1999. Developmental changes in enzymes involved in the conversion of hexose phosphate and its subsequent metabolites during early tuberization of potato. Plant, Cell Environ. 22, 1085–1096. https://doi.org/10.1046/j.1365-3040.1999.00473.x

Appeldoorn, N.J.G., De Bruijn, S.M., Koot-Gronsveld, E.A.M., Visser, R.G.F., Vreugdenhil, D., Van der Plas, L.H.W., 1997. Developmental changes of enzymes involved in conversion of sucrose to hexose-phosphate during early tuberisation of potato. Planta 202, 220–226. https://doi.org/10.1007/s004250050122

Arc, E., Sechet, J., Corbineau, F., Rajjou, L., Marion-poll, A., 2013. ABA crosstalk with ethylene and nitric oxide in seed dormancy and germination 4, 1–19. https://doi.org/10.3389/fpls.2013.00063

Bahaji, A., Li, J., Sánchez-López, Á.M., Baroja-Fernández, E., Muñoz, F.J., Ovecka, M., Almagro, G., Montero, M., Ezquer, I., Etxeberria, E., Pozueta-Romero, J., 2014. Starch biosynthesis, its regulation and biotechnological approaches to improve crop yields. Biotechnol. Adv. 32, 87–106. https://doi.org/10.1016/j.biotechadv.2013.06.006

Bailey, T.L., Elkan, C., 1994. Fitting a mixture model by expectation maximization to discover motifs in biopolymers. Proc. Second Int. Conf. Intell. Syst. Mol. Biol. 28–36.

Banerjee, A.K., Chatterjee, M., Yu, Y., Suh, S.G., Miller, W.A., Hannapel, D.J., 2006. Dynamics of a mobile RNA of potato involved in a long-distance signaling pathway. Plant Cell 18, 3443–3457. https://doi.org/10.1105/tpc.106.042473

Barnes, S.A., Quaggio, R.B., Chua, N.H., 1995. Phytochrome signal-transduction: characterization of pathways and isolation of mutants. Philos. Trans. R. Soc. Lond. B. Biol. Sci. 350, 67–74. https://doi.org/10.1098/rstb.1995.0139

Baroja-Fernández, E., Muñoz, F.J., Montero, M., Etxeberria, E., Sesma, M.T., Ovecka, M., Bahaji, A., Ezquer, I., Li, J., Prat, S., Pozueta-Romero, J., 2009. Enhancing sucrose synthase activity in transgenic potato (Solanum tuberosum L.) tubers results in increased levels of starch, ADPglucose and UDPglucose and total yield. Plant Cell Physiol. 50, 1651–1662. https://doi.org/10.1093/pcp/pcp108

Begum, S., Jing, S., Yu, L., Sun, X., Wang, E., Abu Kawochar, M., Qin, J., Liu, J., Song, B., 2022. Modulation of JA signalling reveals the influence of StJAZ1-like on tuber initiation

and tuber bulking in potato. Plant J. 109, 952–964. https://doi.org/10.1111/tpj.15606

Bhogale, S., Mahajan, A.S., Natarajan, B., Rajabhoj, M., Thulasiram, H. V., Banerjee, A.K., 2014. MicroRNA156: A Potential Graft-Transmissible MicroRNA That Modulates Plant Architecture and Tuberization in Solanum tuberosum ssp. andigena. Plant Physiol. 164, 1011–1027. https://doi.org/10.1104/pp.113.230714

Birch, P.R.J., Bryan, G., Fenton, B., Gilroy, E.M., Hein, I., Jones, J.T., Prashar, A., Taylor, M.A., Torrance, L., Toth, I.K., 2012. Crops that feed the world 8: Potato: Are the trends of increased global production sustainable?, Food Security. https://doi.org/10.1007/s12571-012-0220-1

Bodlaender, K.B.A., 1963. Influence of Temperature, Radiation and Photoperiod on Development and Yield. The Growth of the Potato 199–210.

Bodlaender, K.B.A., Lugt, C., Marinus, J., 1964. The induction of second-growth in potato tubers. Eur. Potato J. 7, 57–71.

Bolle, C., 2004. The role of GRAS proteins in plant signal transduction and development. Planta 218, 683–692. https://doi.org/10.1007/s00425-004-1203-z

Bou-Torrent, J., Martínez-García, J.F., García-Martínez, J.L., Prat, S., 2011. Gibberellin a 1 metabolism contributes to the control of photoperiod-mediated tuberization in potato. PLoS One 6. https://doi.org/10.1371/journal.pone.0024458

Bradford, M., 1976. A rapid and sensitive method for the quantitation of microgram quantities of protein utilizing the principle of protein-dye binding. Anal. Biochem. 248–54.

Busse, J.S., Wiberley-Bradford, A.E., Bethke, P.C., 2019. Transient heat stress during tuber development alters post-harvest carbohydrate composition and decreases processing quality of chipping potatoes. J. Sci. Food Agric. 99, 2579–2588. https://doi.org/10.1002/jsfa.9473

Chen, H., Banerjee, A.K., Hannapel, D.J., 2004. The tandem complex of BEL and KNOX partners is required for transcriptional repression of ga20ox1. Plant J. 38, 276–284. https://doi.org/10.1111/j.1365-313X.2004.02048.x

Chen, X., Salamini, F., Gebhardt, C., 2001. A potato molecular-function map for carbohydrate metabolism and transport. Theor. Appl. Genet. 102, 284–295. https://doi.org/10.1007/s001220051645

Chen, Y., Li, C., Yi, J., Yang, Y., Lei, C., Gong, M., 2020. Transcriptome response to drought, rehydration and re-dehydration in potato. Int. J. Mol. Sci. 21. https://doi.org/10.3390/ijms21010159

References

Cheng, L., Wang, Y., Liu, Y., Zhang, Q., Gao, H., Zhang, F., 2018. Comparative proteomics illustrates the molecular mechanism of potato (Solanum tuberosum L.) tuberization inhibited by exogenous gibberellins in vitro. Physiol. Plant. 163, 103–123. https://doi.org/10.1111/ppl.12670

Cho, M.H., Lim, H., Shin, D.H., Jeon, J.S., Bhoo, S.H., Park, Y. Il, Hahn, T.R., 2011. Role of the plastidic glucose translocator in the export of starch degradation products from the chloroplasts in Arabidopsis thaliana. New Phytol. 190, 101–112. https://doi.org/10.1111/j.1469-8137.2010.03580.x

Ciais, P., Reichstein, M., Viovy, N., Granier, a, Ogée, J., Allard, V., Aubinet, M., Buchmann, N., Bernhofer, C., Carrara, a, Chevallier, F., De Noblet, N., Friend, a D., Friedlingstein, P., Grünwald, T., Heinesch, B., Keronen, P., Knohl, a, Krinner, G., Loustau, D., Manca, G., Matteucci, G., Miglietta, F., Ourcival, J.M., Papale, D., Pilegaard, K., Rambal, S., Seufert, G., Soussana, J.F., Sanz, M.J., Schulze, E.D., Vesala, T., Valentini, R., Ciais, P., Reichstein, M., Viovy, N., Granier, a, Oge, J., 2005. Europe-wide reduction in primary productivity caused by the heat and drought in 2003. Nature 437, 529–533. https://doi.org/10.1038/nature03972

Claassens, M.M.J., Vreugdenhil, D., 2000. Is dormancy breaking of potato tubers the reverse of tuber initiation? Potato Res. 43, 347–369. https://doi.org/10.1007/BF02360540

Clouse, S.D., 2011. Brassinosteroid signal transduction: From receptor kinase activation to transcriptional networks regulating plant development. Plant Cell 23, 1219–1230. https://doi.org/10.1105/tpc.111.084475

Cook, E.R., Seager, R., Cane, M.A., Stahle, D.W., 2007. North American drought: Reconstructions, causes, and consequences. Earth-Science Rev. 81, 93–134. https://doi.org/10.1016/j.earscirev.2006.12.002

D'Hulst, C., Mérida, Á.́, 2010. The priming of storage glucan synthesis from bacteria to plants: Current knowledge and new developments. New Phytol. 188, 13–21. https://doi.org/10.1111/j.1469-8137.2010.03361.x

Dahal, K., Li, X.Q., Tai, H., Creelman, A., Bizimungu, B., 2019. Improving potato stress tolerance and tuber yield under a climate change scenario – a current overview. Front. Plant Sci. 10. https://doi.org/10.3389/fpls.2019.00563

De Jong, H., 2016. Impact of the Potato on Society. Am. J. Potato Res. 93, 415–429. https://doi.org/10.1007/s12230-016-9529-1

Deblonde, P.M.K., Ledent, J.F., 2001. Effects of moderate drought conditions on green leaf number, stem height, leaf length and tuber yield of potato cultivars. Eur. J. Agron. 14, 31–

41. https://doi.org/10.1016/S1161-0301(00)00081-2

Eckardt, N.A., Portis, A.R., 1997. Heat denaturation profiles of ribulose-1,5-bisphosphate carboxylase/oxygenase (Rubisco) and Rubisco activase and the inability of Rubisco activase to restore activity of heat-denatured Rubisco. Plant Physiol. 113, 243–248. https://doi.org/10.1104/pp.113.1.243

Edner, C., Li, J., Albrecht, T., Mahlow, S., Hejazi, M., Hussain, H., Kaplan, F., Guy, C., Smith, S.M., Steup, M., Ritte, G., 2007. Glucan, Water Dikinase Activity Stimulates Breakdown of Starch Granules by Plastidial β-Amylases. Plant Physiol. 145, 17–28. https://doi.org/10.1104/pp.107.104224

Edwards, A., Marshall, J., Sidebottom, C., Visser, R.G., Smith, A.M., Martin, C., 1995. Biochemical and molecular characterization of a novel starch synthase from potato tubers. Plant J. 8, 283–294.

European cultivated potato database, 2017. No Title [WWW Document]. URL www.europotato.org

FAO, 2021. Food and Agriculture Organisation of the United Nations [WWW Document]. URL https://www.fao.org/faostat/en/#data/QCL (accessed 12.11.21).

Feike, D., Seung, D., Graf, A., Bischof, S., Ellick, T., Coiro, M., Soyk, S., Eicke, S., Mettler-Altmann, T., Lu, K.-J.J., Trick, M., Zeeman, S.C., Smith, A.M., 2016. The starch granule-associated protein EARLY STARVATION1 is required for the control of starch degradation in Arabidopsis thaliana leaves. Plant Cell 28, 1472–1489. https://doi.org/10.1105/tpc.16.00011

Fernandez-Pozo, N., Menda, N., Edwards, J.D., Saha, S., Tecle, I.Y., Strickler, S.R., Bombarely, A., Fisher-York, T., Pujar, A., Foerster, H., Yan, A., Mueller, L.A., 2015. The Sol Genomics Network (SGN)-from genotype to phenotype to breeding. Nucleic Acids Res. 43, D1036–D1041. https://doi.org/10.1093/nar/gku1195

Fernie, A.R., Willmitzer, L., 2001. Molecular and Biochemical Triggers of Potato Tuber Development. Plant Physiol. 127, 1459–1465. https://doi.org/10.1104/pp.010764

Ferreira, S.J., Senning, M., Sonnewald, S., Kessling, P.-M., Goldstein, R., Sonnewald, U., 2010. Comparative transcriptome analysis coupled to X-ray CT reveals sucrose supply and growth velocity as major determinants of potato tuber starch biosynthesis. BMC Genomics 11, 93. https://doi.org/10.1186/1471-2164-11-93

Ferreira, S.J., Sonnewald, U., 2012. The mode of sucrose degradation in potato tubers determines the fate of assimilate utilization. Front. Plant Sci. 3, 23. https://doi.org/10.3389/fpls.2012.00023

References

Fritz, C.C., Wolter, F.P., Schenkemeyer, V., Herget, T., Schreier, P.H., 1993. The gene family encoding the ribulose-(1,5)-bisphosphate carboxylase/oxygenase (Rubisco) small subunit of potato. Gene 137, 271–274. https://doi.org/10.1016/0378-1119(93)90019-Y

Fu, F.-F.F., Xue, H.-W.W., 2010. Coexpression analysis identifies Rice Starch Regulator1, a rice AP2/EREBP family transcription factor, as a novel rice starch biosynthesis regulator. Plant Physiol. 154, 927–938. https://doi.org/10.1104/pp.110.159517

Fu, H., Park, W.D., 1995. Sink- and vascular-associated sucrose synthase functions are encoded by different gene classes in potato. Plant Cell 7, 1369–85. https://doi.org/10.1105/tpc.7.9.1369

Gao, H., Wang, Z., Li, S., Hou, M., Zhou, Y., Zhao, Y., Li, G., Zhao, H., Ma, H., 2018. Genome-wide survey of potato MADS-box genes reveals that StMADS1 and StMADS13 are putative downstream targets of tuberigen StSP6A. BMC Genomics 19, 1–20. https://doi.org/10.1186/s12864-018-5113-z

Gawronska, H., Thornton, M.K., Dwelle, R.B., B., D.R., Dwelle, R.B., 1992. Influence of heat stress on dry matter production and photoassimilate partitioning by four potato clones. Am. Potato J. 69.

Gong, L., Zhang, H., Gan, X., Zhang, L., Chen, Y., Nie, F., Shi, L., Li, M., Guo, Z., Zhang, G., Song, Y., 2015. Transcriptome profiling of the potato (Solanum tuberosum L.) plant under drought stress and water-stimulus conditions. PLoS One 10, 1–20. https://doi.org/10.1371/journal.pone.0128041

González-Schain, N.D., Díaz-Mendoza, M., Zurczak, M., Suárez-López, P., Żurczak, M., Suárez-López, P., Zurczak, M., Suárez-López, P., 2012. Potato CONSTANS is involved in photoperiodic tuberization in a graft-transmissible manner. Plant J. 70, 678–690. https://doi.org/10.1111/j.1365-313X.2012.04909.x

Grunewald, W., De Smet, I., De Rybel, B., Robert, H.S., van de Cotte, B., Willemsen, V., Gheysen, G., Weijers, D., Friml, J., Beeckman, T., 2013. Tightly controlled WRKY23 expression mediates Arabidopsis embryo development. EMBO Rep. 14, 1136–42. https://doi.org/10.1038/embor.2013.169

Grunewald, W., Smet, I. De, Lewis, D.R., Löfke, C., Jansen, L., Goeminne, G., Bosschea, R. Vanden, Karimi, M., Rybela, B. De, Vanholmea, B., Teichmannf, T., Boerjana, W., Montagub, M.C.E. Van, Gheysenc, G., Mudaye, G.K., Frimla, J., Beeckman, T., 2011. Transcription factor WRKY23 assists auxin distribution patterns during Arabidopsis root development through local control on flavonol biosynthesis. Proc. Natl. Acad. Sci. U. S. A. 109, 1554–1559. https://doi.org/10.1073/pnas.1121134109/-/DCSupplemental.www.pnas.org/cgi/doi/10.1073/pnas.1121134109

Ha, C.M., Jun, J.H., Nam, H.G., Fletcher, J.C., 2007. BLADE-ON-PETIOLE 1 and 2 control Arabidopsis lateral organ fate through regulation of LOB domain and adaxial-abaxial polarity genes. Plant Cell 19, 1809–1825. https://doi.org/10.1105/tpc.107.051938

Hammes, P.S., De Jager, J.A., 1990. Net photosynthetic rate of potato at high temperatures. Potato Res. 33, 515–520. https://doi.org/10.1007/BF02358030

Han, Y., Jiao, Y., 2015. APETALA1 establishes determinate floral meristem through regulating cytokinins homeostasis in Arabidopsis. Plant Signal. Behav. 10, 10–12. https://doi.org/10.4161/15592324.2014.989039

Hancock, R.D., Morris, W.L., Ducreux, L.J.M.M., Morris, J.A., Usman, M., Verrall, S.R., Fuller, J., Simpson, C.G., Zhang, R., Hedley, P.E., Taylor, M.A., 2014. Physiological, biochemical and molecular responses of the potato (Solanum tuberosum L.) plant to moderately elevated temperature. Plant. Cell Environ. 37, 439–50. https://doi.org/10.1111/pce.12168

Hannapel, D.J., Sharma, P., Lin, T., Banerjee, A.K., 2017. The multiple signals that control tuber formation. Plant Physiol. 174, 845–856. https://doi.org/10.1104/pp.17.00272

Hartmann, A., 2012. Investigating the Role of Cytokinin and Beta-1 , 3-Glucanases in Potato Tuber Dormancy and Sprouting. Friedrich-Alexander-Universität Erlangen-Nürnberg, Lehrstuhl für Biochem.

Hartmann, A., Senning, M., Hedden, P., Sonnewald, U., Sonnewald, S., 2011. Reactivation of meristem activity and sprout growth in potato tubers require both cytokinin and gibberellin. Plant Physiol. 155, 776–96. https://doi.org/10.1104/pp.110.168252

Hastilestari, B.R., Lorenz, J., Reid, S., Hofmann, J., Pscheidt, D., Sonnewald, U., Sonnewald, S., 2018. Deciphering source and sink responses of potato plants (Solanum tuberosum L.) to elevated temperatures. Plant Cell Environ. 41, 2600–2616. https://doi.org/10.1111/pce.13366

Hejazi, M., Fettke, J., Haebel, S., Edner, C., Paris, O., Frohberg, C., Steup, M., Ritte, G., 2008. Glucan, water dikinase phosphorylates crystalline maltodextrins and thereby initiates solubilization. Plant J. 55, 323–334. https://doi.org/10.1111/j.1365-313X.2008.03513.x

Helle, S., Bray, F., Verbeke, J., Devassine, S., Szydlowski, N., Emes, M.J., 2018. Proteome Analysis of Potato Starch Reveals the Presence of New Starch Metabolic Proteins as Well as Multiple Protease Inhibitors 9, 1–14. https://doi.org/10.3389/fpls.2018.00746

Hijmans, R.J., 2003. The effect of climate change on global potato production. Am. J. Potato Res. 80, 271–279. https://doi.org/10.1007/BF02855363

Hirai, M.Y., Sugiyama, K., Sawada, Y., Tohge, T., Obayashi, T., Suzuki, A., Araki, R., Sakurai,

References

N., Suzuki, H., Aoki, K., Goda, H., Nishizawa, O.I., 2007. Omics-based identification of Arabidopsis Myb transcription factors regulating aliphatic glucosinolate biosynthesis 104.

Hirose, T., Terao, T., 2004. A comprehensive expression analysis of the starch synthase gene family in rice (Oryza sativa L.). Planta 220, 9–16. https://doi.org/10.1007/s00425-004-1314-6

Hirsch, C.D., Hamilton, J.P., Childs, K.L., Cepela, J., Crisovan, E., Vaillancourt, B., Hirsch, C.N., Habermann, M., Neal, B., Buell, C.R., 2014. Spud DB: A Resource for Mining Sequences, Genotypes, and Phenotypes to Accelerate Potato Breeding. Plant Genome 7. https://doi.org/10.3835/plantgenome2013.12.0042

Horst, R.J., Doehlemann, G., Wahl, R., Hofmann, J., Schmiedl, A., Kahmann, R., Kamper, J., Sonnewald, U., Voll, L.M., 2010. Ustilago maydis infection strongly alters organic nitrogen allocation in maize and stimulates productivity of systemic source leaves. Plant Physiol. 152, 293–308. https://doi.org/10.1104/pp.109.147702

Ingkasuwan, P., Netrphan, S., Prasitwattanaseree, S., Tanticharoen, M., Bhumiratana, S., Meechai, A., Chaijaruwanich, J., Takahashi, H., Cheevadhanarak, S., 2012. Inferring transcriptional gene regulation network of starch metabolism in Arabidopsis thaliana leaves using graphical Gaussian model. BMC Syst. Biol. 6, 100. https://doi.org/10.1186/1752-0509-6-100

Jackson, S.D., 1999. Multiple Signaling Pathways Control Tuber Induction in Potato. Plant Physiol. 119, 1–8. https://doi.org/10.1104/pp.119.1.1

Jackson, S.D., Heyer, A., Dietze, J., Prat, S., 1996. Phytochrome B mediates the photoperiodic control of tuber formation in potato. Plant J. 9, 159–166. https://doi.org/10.1046/j.1365-313X.1996.09020159.x

Jackson, S.D., James, P., Prat, S., Thomas, B., 1998. Phytochrome B affects the levels of a graft-transmissible signal involved in tuberization. Plant Physiol. 117, 29–32. https://doi.org/10.1104/pp.117.1.29

Jackson, S.D., Prat, S., 1996. Control of tuberisation in potato by gibberellins and phytochrome B. Physiol. Plant. 98, 407–412. https://doi.org/10.1034/j.1399-3054.1996.980224.x

Jobling, S. a., Schwall, G.P., Westcott, R.J., Sidebottom, C.M., Debet, M., Gidley, M.J., Jeffcoat, R., Safford, R., 1999. A minor form of starch branching enzyme in potato (Solanum tuberosum L.) tubers has a major effect on starch structure: Cloning and characterisation of multiple forms of SBE A. Plant J. 18, 163–171. https://doi.org/10.1046/j.1365-313X.1999.00441.x

Jørgensen, M., Stensballe, A., Welinder, K.G., 2011. Extensive post-translational processing

of potato tuber storage proteins and vacuolar targeting. FEBS J. 278, 4070–4087. https://doi.org/10.1111/j.1742-4658.2011.08311.x

Jung, J.H., Seo, Y.H., Pil, J.S., Reyes, J.L., Yun, J., Chua, N.H., Park, C.M., 2007. The GIGANTEA-regulated microRNA172 mediates photoperiodic flowering independent of CONSTANS in Arabidopsis. Plant Cell 19, 2736–2748. https://doi.org/10.1105/tpc.107.054528

Jupe, F., Pritchard, L., Etherington, G.J., MacKenzie, K., Cock, P.J., Wright, F., Sharma, S.K., Bolser, D., Bryan, G.J., Jones, J.D., Hein, I., 2012. Identification and localisation of the NB-LRR gene family within the potato genome. BMC Genomics 13, 75. https://doi.org/10.1186/1471-2164-13-75

Kaminski, K.P., Petersen, A.H., Sønderkær, M., Pedersen, L.H., Pedersen, H., Feder, C., Nielsen, K.L., 2012. Transcriptome analysis suggests that starch synthesis may proceed via multiple metabolic routes in high yielding potato cultivars. PLoS One 7, e51248. https://doi.org/10.1371/journal.pone.0051248

Katsarou, K., Wu, Y., Zhang, R., Bonar, N., Morris, J., Hedley, P.E., Bryan, G.J., Kalantidis, K., Hornyik, C., 2016. Insight on genes affecting tuber development in potato upon potato spindle tuber viroid (PSTVd) infection. PLoS One 11, 1–17. https://doi.org/10.1371/journal.pone.0150711

Kazan, K., 2015. Diverse roles of jasmonates and ethylene in abiotic stress tolerance. Trends Plant Sci. 20, 219–229. https://doi.org/10.1016/j.tplants.2015.02.001

Kearse, M., Moir, R., Wilson, A., Stones-Havas, S., Cheung, M., Sturrock, S., Buxton, S., Cooper, A., Markowitz, S., Duran, C., Thierer, T., Ashton, B., Meintjes, P., Drummond, A., 2012. Geneious Basic: An integrated and extendable desktop software platform for the organization and analysis of sequence data. Bioinformatics 28, 1647–1649. https://doi.org/10.1093/bioinformatics/bts199

Kersey, P.J., Allen, J.E., Armean, I., Boddu, S., Bolt, B.J., Carvalho-Silva, D., Christensen, M., Davis, P., Falin, L.J., Grabmueller, C., Humphrey, J., Kerhornou, A., Khobova, J., Aranganathan, N.K., Langridge, N., Lowy, E., McDowall, M.D., Maheswari, U., Nuhn, M., Ong, C.K., Overduin, B., Paulini, M., Pedro, H., Perry, E., Spudich, G., Tapanari, E., Walts, B., Williams, G., Tello-Ruiz, M., Stein, J., Wei, S., Ware, D., Bolser, D.M., Howe, K.L., Kulesha, E., Lawson, D., Maslen, G., Staines, D.M., 2015. Ensembl Genomes 2016: more genomes, more complexity. Nucleic Acids Res. 1–7. https://doi.org/10.1093/nar/gkv1209

Khoshnoodi, J., Blennow, a, Ek, B., Rask, L., Larsson, H., 1996. The multiple forms of starch-branching enzyme I in Solanum tuberosum. Eur. J. Biochem. 242, 148–155.

References

Kloosterman, B., Abelenda, J.A., Gomez, M.D.M.C., Oortwijn, M., De Boer, J.M., Kowitwanich, K., Horvath, B.M., Van Eck, H.J., Smaczniak, C., Prat, S., Visser, R.G.F., Bachem, C.W.B., 2013. Naturally occurring allele diversity allows potato cultivation in northern latitudes. Nature 495, 246–250. https://doi.org/10.1038/nature11912

Kloosterman, B., De Koeyer, D., Griffiths, R., Flinn, B., Steuernagel, B., Scholz, U., Sonnewald, S., Sonnewald, U., Bryan, G.J., Prat, S., Bánfalvi, Z., Hammond, J.P., Geigenberger, P., Nielsen, K.L., Visser, R.G.F., Bachem, C.W.B., 2008. Genes driving potato tuber initiation and growth: identification based on transcriptional changes using the POCI array. Funct. Integr. Genomics 8, 329–40. https://doi.org/10.1007/s10142-008-0083-x

Kloosterman, B., Navarro, C., Bijsterbosch, G., Lange, T., Prat, S., Visser, R.G.F., Bachem, C.W.B., 2007. StGA2ox1 is induced prior to stolon swelling and controls GA levels during potato tuber development. Plant J. 52, 362–73. https://doi.org/10.1111/j.1365-313X.2007.03245.x

Kloosterman, B., Vorst, O., Hall, R.D., Visser, R.G.F., Bachem, C.W., 2005. Tuber on a chip: differential gene expression during potato tuber development. Plant Biotechnol. J. 3, 505–19. https://doi.org/10.1111/j.1467-7652.2005.00141.x

Koch, K., 2004. Sucrose metabolism: regulatory mechanisms and pivotal roles in sugar sensing and plant development. Curr. Opin. Plant Biol. 7, 235–46. https://doi.org/10.1016/j.pbi.2004.03.014

Kondhare, K.R., Natarajan, B., Banerjee, A.K., 2020. Molecular signals that govern tuber development in potato. Int. J. Dev. Biol. 64, 133–140. https://doi.org/10.1387/ijdb.190132ab

Kondhare, K.R., Vetal, P. V., Kalsi, H.S., Banerjee, A.K., 2019. BEL1-like protein (StBEL5) regulates CYCLING DOF FACTOR1 (StCDF1) through tandem TGAC core motifs in potato. J. Plant Physiol. 241. https://doi.org/10.1016/j.jplph.2019.153014

Kossmann, J., Abel, G.J.W.W., Springer, F., Lloyd, J.R., Willmitzer, L., 1999. Cloning anf functional analysis of a cDNA encoding a starch synthase from potato (Solanum tuberosum L.) that is predominantly expressed inleaf tissue. Planta 208, 503–511. https://doi.org/10.1046/j.1365-313X.1996.10060981.x

Kossmann, J., Visser, R.G.F., Müller-Röber, B.T., Willmitzer, L., Sonnewald, U., 1991. Cloning and expression analysis of a potato cDNA that encodes branching enzyme evidence for co-expression of starch biosynthetic genes. MGG Mol. Gen. Genet. 230, 39–44. https://doi.org/10.1007/BF00290648

Kötting, O., Kossmann, J., Zeeman, S.C., Lloyd, J.R., 2010. Regulation of starch metabolism:

the age of enlightenment? Curr. Opin. Plant Biol. 13, 320–328. https://doi.org/10.1016/j.pbi.2010.01.003

Kotting, O., Santelia, D., Edner, C., Eicke, S., Marthaler, T., Gentry, M.S., Comparot-Moss, S., Chen, J., Smith, A.M., Steup, M., Ritte, G., Zeeman, S.C., 2009. STARCH-EXCESS4 Is a Laforin-Like Phosphoglucan Phosphatase Required for Starch Degradation in Arabidopsis thaliana. Plant Cell Online 21, 334–346. https://doi.org/10.1105/tpc.108.064360

Krauss, A., Marschner, H., 1984. Growth rate and carbohydrate metabolism of potato tubers exposed to high temperatures. Potato Res. 27, 297–303.

Krauss, A., Marschner, H., 1982. Influence of nitrogen nutrition, daylength and temperature on contents of gibberellic and abscisic acid and on tuberization in potato plants. Potato Res. 25, 13–21. https://doi.org/10.1007/BF02357269

Kumar, D., Wareing, P.F., 1974. Studies on Tuberization of Solanum Andigena II. Growth Hormones and Tuberization. New Phytol. 73, 833–840. https://doi.org/10.1111/j.1469-8137.1974.tb01311.x

Kumar, D., Wareing, P.F., 1973. Studies on tuberization in Solanum Anidgena: I evidence for the existence and movement of a specific tuberization stimulus. New Phytol. 73, 833–840.

La Cognata, U., Willmitzer, L., Müller-Röber, B., 1995. Molecular cloning and characterization of novel isoforms of potato ADP-glucose pyrophosphorylase. Mol. Gen. Genet. 246, 538–548. https://doi.org/10.1007/BF00298960

Lang, G.A., Early, J.D., Martin, G.C., Darnell, R.L., 1987. Endo-, para-, and ecodormancy: physiological terminology and classification for dormancy research. Hort Sci. 22, 371–377.

Larsson, C.T., Hofvander, P., Ek, B., Rask, L., Larsson, H.H., Khoshnoodi, J., Ek, B., Rask, L., Larsson, H.H., 1996. Three isoforms of starch synthase and two isoforms of branching enzyme are present in potato tuber starch. Plant Sci. 117, 9–16. https://doi.org/10.1016/0168-9452(96)04408-1

Lehretz, G.G., Sonnewald, S., Hornyik, C., Corral, J.M., Sonnewald, U., 2019. Post-transcriptional Regulation of FLOWERING LOCUS T Modulates Heat-Dependent Source-Sink Development in Potato. Curr. Biol. 29, 1614-1624.e3. https://doi.org/10.1016/j.cub.2019.04.027

Levy, D., 1986. Genotypic variation in the response of potatoes (Solanum tuberosum L.) to high ambient temperatures and water deficit. F. Crop. Res. 15, 85–96.

References

Levy, D., 1985. The response of potatoes to a single transient heat or drought stress imposed at different stages of tuber growth. Potato Res. 28, 415–424. https://doi.org/10.1007/BF02357516

Levy, D., Veilleux, R.E., 2007. Adaptation of potato to high temperatures and salinity-a review. Am. J. Potato Res. 84, 487–506. https://doi.org/10.1007/BF02987885

Li, L., Paulo, M.-J.J., Strahwald, J., Lübeck, J., Hofferbert, H.-R.R., Tacke, E., Junghans, H., Wunder, J., Draffehn, A., van Eeuwijk, F., Gebhardt, C., 2008. Natural DNA variation at candidate loci is associated with potato chip color, tuber starch content, yield and starch yield. Theor. Appl. Genet. 116, 1167–81. https://doi.org/10.1007/s00122-008-0746-y

Lin, T., Sharma, P., Gonzalez, D.H., Viola, I.L., Hannapel, D.J., 2013. The impact of the long-distance transport of a BEL1-like messenger RNA on development. Plant Physiol. 161, 760–772. https://doi.org/10.1104/pp.112.209429

Liu, B., Zhang, N., Wen, Y., Jin, X., Yang, J., Si, H., Wang, D., 2015. Transcriptomic changes during tuber dormancy release process revealed by RNA sequencing in potato. J. Biotechnol. 198, 17–30. https://doi.org/10.1016/j.jbiotec.2015.01.019

Liu, H., Yu, G.G.G.G., Wei, B., Wang, Y., Zhang, J., Hu, Y., Liu, Y., Yu, G.G.G.G., Zhang, H., Huang, Y., 2015. Identification and phylogenetic analysis of a novel starch synthase in maize. Front. Plant Sci. 6, 1013. https://doi.org/10.3389/fpls.2015.01013

Lloyd, J.R., Kossmann, J., 2015. Transitory and storage starch metabolism: two sides of the same coin? Curr. Opin. Biotechnol. 32, 143–148. https://doi.org/10.1016/j.copbio.2014.11.026

Logemann, J., Schell, J., Willmitzer, L., 1987. Improved Method for the Isolation of RNA from Plant Tissues. Anal. Biochem. 163, 16–20.

Lu, Y., Gehan, J.P., Sharkey, T.D., 2005. Daylength and circadian effects on starch degradation and maltose metabolism. Plant Physiol. 138, 2280–2291. https://doi.org/10.1104/pp.105.061903

Lu, Y., Sharkey, T.D., 2004. The role of amylomaltase in maltose metabolism in the cytosol of photosynthetic cells. Planta 218, 466–473. https://doi.org/10.1007/s00425-003-1127-z

Lugt, C., 1960. Second-growth phenomena. Eur. Potato J. 3.

Lugt, C., Bodlaender, K.B.A., Goodijk, G., 1964. Observations on the induction of second-growth in potato tubers. Eur. Potato J. 7, 219–227. https://doi.org/10.1007/BF02368253

Luitel, B.P., Khatri, B.B., Choudhary, D., Paudel, B.P., Jung-Sook, S., Hur, O.-S., Baek, H.J., Cheol, K.H., Yul, R.K., 2015. Growth and Yield Characters of Potato Genotypes Grown

in Drought and Irrigated Conditions of Nepal. Int. J. Appl. Sci. Biotechnol. 3, 513–519. https://doi.org/10.3126/ijasbt.v3i3.13347

Machackova, I., Konstantinova, T.N., Sergeeva, L.I., Lozhnikova, V.N., Golyanovskaya, S.A., Dudko, N.D., Eder, J., Aksenova, N.P., 1998. Photoperiodic Control of Growth, Development and Phytohormone Balance in Solanum tuberosum. Physiol. Plant. 102, 272–278.

Marshall, J., Sidebottom, C.M., Debet, M., Martin, C., Smith, A.M., Edwards, A., J, M., C, S., M, D., C, M., Am, S., a, E., 1996. Identification of the major starch synthase in the soluble fraction of pea embryos. Plant Cell 8, 1121.

Martin, A., Adam, H., Díaz-Mendoza, M., Zurczak, M., González-Schain, N.D., Suárez-López, P., Żurczak, M., González-Schain, N.D., Suárez-López, P., 2009. Graft-transmissible induction of potato tuberization by the microRNA miR172. Development 136, 2873–81. https://doi.org/10.1242/dev.031658

Menzel, C.M., 1980. Tuberization in potato at high temperatures: Responses to gibberellin and growth inhibitors. Ann. Bot. 46, 259–265. https://doi.org/10.1093/oxfordjournals.aob.a085916

Monniaux, M., McKim, S.M., Cartolano, M., Thévenon, E., Parcy, F., Tsiantis, M., Hay, A., 2017. Conservation vs divergence in LEAFY and APETALA1 functions between Arabidopsis thaliana and Cardamine hirsuta. New Phytol. 216, 549–561. https://doi.org/10.1111/nph.14419

Morris, W.L., Hancock, R.D., Ducreux, L.J.M.M., Morris, J.A., Usman, M., Verrall, S.R., Sharma, S.K., Bryan, G., Mcnicol, J.W., Hedley, P.E., Taylor, M.A., 2014. Day length dependent restructuring of the leaf transcriptome and metabolome in potato genotypes with contrasting tuberization phenotypes. Plant, Cell Environ. 37, 1351–1363. https://doi.org/10.1111/pce.12238

Movahedi, S., Van Bel, M., Heyndrickx, K.S., Vandepoele, K., 2012. Comparative co-expression analysis in plant biology. Plant. Cell Environ. 35, 1787–98. https://doi.org/10.1111/j.1365-3040.2012.02517.x

Müller-Röber, B., Sonnewald, U., Willmitzer, L., 1992. Inhibition of the ADP-glucose pyrophosphorylase in transgenic potatoes leads to sugar-storing tubers and influences tuber formation and expression of tuber storage protein genes. EMBO J. 11, 1229–38.

Muñoz-Mayor, A., Pineda, B., Garcia-Abellán, J.O., Antón, T., Garcia-Sogo, B., Sanchez-Bel, P., Flores, F.B., Atarés, A., Angosto, T., Pintor-Toro, J.A., Moreno, V., Bolarin, M.C., 2012. Overexpression of dehydrin tas14 gene improves the osmotic stress imposed by

References

drought and salinity in tomato. J. Plant Physiol. 169, 459–468. https://doi.org/10.1016/j.jplph.2011.11.018

Nagarajan, R., Gill, K.S., 2018. Evolution of Rubisco activase gene in plants. Plant Mol. Biol. 96, 69–87. https://doi.org/10.1007/s11103-017-0680-y

Nakamura, Y., 2015. Starch. Springer Japan. https://doi.org/10.1007/978-4-431-55495-0_9

Navarro, C., Abelenda, J. a., Cruz-Oró, E., Cuéllar, C. a., Tamaki, S., Silva, J., Shimamoto, K., Prat, S., 2011. Control of flowering and storage organ formation in potato by FLOWERING LOCUS T. Nature 478, 119–122. https://doi.org/10.1038/nature10431

Niittylä, T.T.T., Messerli, G.G.G., Trevisan, M., Chen, J., Smith, A.M., Zeeman, S.C., 2004. A previously unknown maltose transporter essential for starch degradation in leaves. Science 303, 87–89. https://doi.org/10.1126/science.1091811

Ohdan, T., Francisco, P.B., Sawada, T., Hirose, T., Terao, T., Satoh, H., Nakamura, Y., 2005. Expression profiling of genes involved in starch synthesis in sink and source organs of rice. J. Exp. Bot. 56, 3229–3244. https://doi.org/10.1093/jxb/eri292

Pattyn, J., Vaughan-Hirsch, J., Van de Poel, B., 2021. The regulation of ethylene biosynthesis: a complex multilevel control circuitry. New Phytol. 229, 770–782. https://doi.org/10.1111/nph.16873

Pelacho, A.M., Mingo-Castel, A.M., 1991. Jasmonic acid induces tuberization of potato stolons cultured in Vitro. Plant Physiol. 97, 1253–1255. https://doi.org/10.1104/pp.97.3.1253

Persson, S., Wei, H., Milne, J., Page, G.P., Somerville, C.R., 2005. Identification of genes required for cellulose synthesis by regression analysis of public microarray data sets 102.

PGRDEU Pflanzengenetische Ressourcen in Deutschland [WWW Document], 2017. URL http://pgrdeu.genres.de

Plantenga, F.D.M., Heuvelink, E., Rienstra, J.A., Visser, R.G.F., Bachem, C.W.B., Marcelis, L.F.M., 2019. Coincidence of potato CONSTANS (StCOL1) expression and light cannot explain night-break repression of tuberization. Physiol. Plant. 167, 250–263. https://doi.org/10.1111/ppl.12885

Poulsen, P., Kreiberg, J.D., 1993. Starch branching enzyme cDNA from Solanum tuberosum. Plant Physiol. 102, 1053–4.

proplanta® Das Informationszentrum für die Landwirtschaft, 2017. No Title [WWW Document]. URL www.proplanta.de

Rizhsky, L., Liang, H., Mittler, R., 2002. The combined effect of drought stress and heat shock on gene expression in tobacco. Plant Phisiology 130, 1143–1151.

https://doi.org/10.1104/pp.006858.then

Robertson, T.M., Alzaabi, A.Z., Robertson, M.D., Fielding, B.A., 2018. Starchy carbohydrates in a healthy diet: The role of the humble potato. Nutrients 10. https://doi.org/10.3390/nu10111764

Rodríguez-Falcón, M., Bou, J., Prat, S., 2006. Seasonal control of tuberization in potato: conserved elements with the flowering response. Annu. Rev. Plant Biol. 57, 151–80. https://doi.org/10.1146/annurev.arplant.57.032905.105224

Rohde, A., Bhalerao, R.P., 2007. Plant dormancy in the perennial context. Trends Plant Sci. 12, 217–223. https://doi.org/10.1016/j.tplants.2007.03.012

Roldán, I., Wattebled, F., Mercedes Lucas, M., Delvalé, D., Planchot, V., Jiménez, S., Pérez, R., Ball, S., D'Hulst, C., Mérida, Á., Rold??n, I., Wattebled, F., Mercedes Lucas, M., Delvall??, D., Planchot, V., Jim??nez, S., P??rez, R., Ball, S., D'Hulst, C., M??rida, ??ngel, Roldán, I., Wattebled, F., Mercedes Lucas, M., Delvallé, D., Planchot, V., Jiménez, S., Pérez, R., Ball, S., D'Hulst, C., Mérida, Á., Delvalé, D., Planchot, V., Jiménez, S., Pérez, R., Ball, S., D'Hulst, C., Mérida, Á., 2007. The phenotype of soluble starch synthase IV defective mutants of Arabidopsis thaliana suggests a novel function of elongation enzymes in the control of starch granule formation. Plant J. 49, 492–504. https://doi.org/10.1111/j.1365-313X.2006.02968.x

Ross, H.A., Davies, H. V, Burch, L.R., Viola, R., Mcrae, D., Ro, H. a, Viola, R., 1994. Developmental changes in carbohydrate content and sucrose degrading enzymes in tuberising stolons of potato { Solatium tuberosum) 748–756. https://doi.org/10.1034/j.1399-3054.1994.900418.x

Roumeliotis, E., Kloosterman, B., Oortwijn, M., Kohlen, W., Bouwmeester, H.J., Visser, R.G.F., Bachem, C.W.B., 2012. The effects of auxin and strigolactones on tuber initiation and stolon architecture in potato. J. Exp. Bot. 63, 4539–4547. https://doi.org/10.1093/jxb/ers132

Roumeliotis, E., Kloosterman, B., Oortwijn, M., Visser, R.G.F., Bachem, C.W.B., 2013. The PIN family of proteins in potato and their putative role in tuberization. Front. Plant Sci. 4, 524. https://doi.org/10.3389/fpls.2013.00524

Ruan, Y.-L., 2014. Sucrose metabolism: gateway to diverse carbon use and sugar signaling. Annu. Rev. Plant Biol. 65, 33–67. https://doi.org/10.1146/annurev-arplant-050213-040251

Rylski, I., Rappaport, L., Pratt, H.K., 1974. Dual Effects of Ethylene Potato Dormancy and Sprout Growth '. Plant Phisiology 53, 658–662.

References

Saeed, A.I., Sharov, V., White, J., Li, J., Liang, W., Bhagabati, N., Braisted, J., Klapa, M., Currier, T., Thiagarajan, M., Sturn, A., Snuffin, M., Rezantsev, A., Popov, D., Ryltsov, A., Kostukovich, E., Borisovsky, I., Liu, Z., Vinsavich, A., Trush, V., Quackenbush, J., 2003. TM4: A free, open-source system for microarray data management and analysis. Biotechniques 34, 374–378. https://doi.org/10.2144/03342mt01

Salvucci, M.E., Crafts-Brandner, S.J., 2004. Relationship between the heat tolerance of photosynthesis and the thermal stability of rubisco activase in plants from contrasting thermal environments. Plant Physiol. 134, 1460–1470. https://doi.org/10.1104/pp.103.038323

Santelia, D., Kotting, O., Seung, D., Schubert, M., Thalmann, M., Bischof, S., Meekins, D. a., Lutz, a., Patron, N., Gentry, M.S., Allain, F.H.-T., Zeeman, S.C., 2011. The Phosphoglucan Phosphatase Like Sex Four2 Dephosphorylates Starch at the C3-Position in Arabidopsis. Plant Cell 23, 4096–4111. https://doi.org/10.1105/tpc.111.092155

Sarkar, D., 2008. The signal transduction pathways controlling in planta tuberization in potato: an emerging synthesis. Plant Cell Rep. 27, 1–8.

Savić, J., Dragićević, I., Pantelić, D., Oljača, J., Momćilović, I., 2012. Expression of small heat shock proteins and heat tolerance in potato (Solanum tuberosum L.). Arch. Biol. Sci. 64, 135–144. https://doi.org/10.2298/ABS1201135S

Schwarte, S., Wegner, F., Havenstein, K., Groth, D., Steup, M., Tiedemann, R., 2015. Sequence variation, differential expression, and divergent evolution in starch-related genes among accessions of Arabidopsis thaliana, Plant Molecular Biology. https://doi.org/10.1007/s11103-015-0293-2

Senning, M., 2010. Untersuchungen zur Regulation der Kartoffelknollendormanz. Friedrich-Alexander Univerität Erlangen-Nürnberg.

Seung, D., Soyk, S., Coiro, M., Maier, B.A., Eicke, S., Zeeman, S.C., 2015. PROTEIN TARGETING TO STARCH Is Required for Localising GRANULE-BOUND STARCH SYNTHASE to Starch Granules and for Normal Amylose Synthesis in Arabidopsis. PLoS Biol. 13, 1–29. https://doi.org/10.1371/journal.pbio.1002080

Sharkey, T.D., Badger, M.R., Andrews, T.J., 2001. Increased heat sensitivity of photosynthesis in tobacco plants with reduced Rubisco activase 147–156.

Sharma, P., Lin, T., Hannapel, D.J., 2016. Targets of the *StBEL5* Transcription Factor Include the FT Ortholog *StSP6A*. Plant Physiol. 170, 310–324. https://doi.org/10.1104/pp.15.01314

She, K.-C., Kusano, H., Koizumi, K., Yamakawa, H., Hakata, M., Imamura, T., Fukuda, M., Naito, N., Tsurumaki, Y., Yaeshima, M., Tsuge, T., Matsumoto, K., Kudoh, M., Itoh, E., Kikuchi, S., Kishimoto, N., Yazaki, J., Ando, T., Yano, M., Aoyama, T., Sasaki, T., Satoh, H., Shimada, H., 2010. A novel factor FLOURY ENDOSPERM2 is involved in regulation of rice grain size and starch quality. Plant Cell 22, 3280–94. https://doi.org/10.1105/tpc.109.070821

Shuai, B., Reynaga-Pena, C.G., Springer, P.S., Reynaga-pen, C.G., Springer, P.S., 2002. The LATERAl ORGAN BOUNDARIES gene defines a novel, plant-specific gene family. Plant Physiol. 129, 747–761. https://doi.org/10.1104/pp.010926.1

Singh, A., Siddappa, S., Bhardwaj, V., Singh, B.B.P.B., Kumar, D., Singh, B.B.P.B., 2015. Expression profiling of potato cultivars with contrasting tuberization at elevated temperature using microarray analysis. Plant Physiol. Biochem. 97, 108–116. https://doi.org/10.1016/j.plaphy.2015.09.014

Smith, D.L., Fedoroff, N. V, 1995. LRP1, a gene expressed in lateral and adventitious root primordia of Arabidopsis. Plant Cell 7, 735–745. https://doi.org/10.1105/tpc.7.6.735

Smith, S.M., Fulton, D.C., Chia, T., Thorneycroft, D., Chapple, A., Dunstan, H., Hylton, C., Zeeman, S.C., Smith, A.M., 2004. Diurnal changes in the transcriptome encoding enzymes of starch metabolism provide evidence for both transcriptional and posttranscriptional regulation of starch metabolism in Arabidopsis leaves. Plant Physiol. 136, 2687–2699. https://doi.org/10.1104/pp.104.044347

Sohn, H.B., Lee, H.Y., Seo, J.S., Jung, C., Jeon, J.H., Kim, J.H., Lee, Y.W., Lee, J.S., Cheong, J.J., Choi, Y. Do, 2011. Overexpression of jasmonic acid carboxyl methyltransferase increases tuber yield and size in transgenic potato. Plant Biotechnol. Rep. 5, 27–34. https://doi.org/10.1007/s11816-010-0153-0

Solana GmbH, 2017. Sortenkatalog [WWW Document]. URL www.solana.de

Sonnewald, S., Sonnewald, U., 2014. Regulation of potato tuber sprouting. Planta 239, 27–38. https://doi.org/10.1007/s00425-013-1968-z

Sonnewald, U., Basner, A., Greve, B., Steup, M., 1995. A second L-type isozyme of potato glucan phosphorylase: cloning, antisense inhibition and expression analysis. Plant Mol. Biol. 27, 567–576. https://doi.org/10.1007/BF00019322

Sonnewald, U., Kossmann, J., 2013. Starches-from current models to genetic engineering. Plant Biotechnol. J. 11, 223–232. https://doi.org/10.1111/pbi.12029

Sparla, F., Costa, A., Schiavo, F. Lo, Pupillo, P., Trost, P., 2006. Redox Regulation of a Novel Plastid-Targeted b-Amylase. Plant Physiol. 141, 840–850.

References

https://doi.org/10.1104/pp.106.079186.of

Spooner, D.M., McLean, K., Ramsay, G., Waugh, R., Bryan, G.J., 2005. A single domestication for potato based on multilocus amplified fragment length polymorphism genotyping. Proc. Natl. Acad. Sci. U. S. A. 102, 14694–14699. https://doi.org/10.1073/pnas.0507400102

Stitt, M., Zeeman, S.C., 2012. Starch turnover: pathways, regulation and role in growth. Curr. Opin. Plant Biol. 15, 282–92. https://doi.org/10.1016/j.pbi.2012.03.016

Struik, P.C., Vreugdenhil, D., Eck, H.J., Bachem, C.W., Visser, R.G.F.F., Van Eck, H.J., Bachem, C.W., Visser, R.G.F.F., Eck, H.J., Bachem, C.W., Visser, R.G.F.F., 1999. Physiological and genetic control of tuber formation. Potato Res. 42, 313–331. https://doi.org/10.1007/BF02357860

Sun, C., Palmqvist, S., Olsson, H., Borén, M., Ahlandsberg, S., Jansson, C., 2003. A Novel WRKY Transcription Factor , SUSIBA2 , Participates in Sugar Signaling in Barley by Binding to the Sugar-Responsive Elements of the iso1 Promoter. Plant Cell 15, 2076–2092. https://doi.org/10.1105/tpc.014597.cess

Suttle, J.C., 2004. Physiological regulation of potato tuber dormancy. Am. J. Potato Res. 81, 253–262. https://doi.org/10.1007/BF02871767

Tanaka, M., Takahata, Y., Nakayama, H., Nakatani, M., Tahara, M., 2009. Altered carbohydrate metabolism in the storage roots of sweet potato plants overexpressing the SRF1 gene, which encodes a Dof zinc finger transcription factor. Planta 230, 737–46. https://doi.org/10.1007/s00425-009-0979-2

Tang, R., Niu, S., Zhang, G., Chen, G., Haroon, M., Yang, Q., Rajora, O.P., Li, X.Q., 2018. Physiological and growth responses of potato cultivars to heat stress. Botany 96, 897–912. https://doi.org/10.1139/cjb-2018-0125

Tao, G.Q., Letham, D.S., Yong, J.W.H., Zhang, K., John, P.C.L., Schwartz, O., Wong, S.C., Farquhar, G.D., 2010. Promotion of shoot development and tuberisation in potato by expression of a chimaeric cytokinin synthesis gene at normal and elevated CO2 levels. Funct. Plant Biol. 37, 43–54. https://doi.org/10.1071/FP07032

Tenorio, G., Orea, A., Romero, J.M., Mérida, Á.́, 2003. Oscillation of mRNA level and activity of granule-bound starch synthase I in Arabidopsis leaves during the day/night cycle. Plant Mol. Biol. 51, 949–958. https://doi.org/10.1023/A:1023053420632

Teo, C.J., Takahashi, K., Shimizu, K., Shimamoto, K., Taoka, K.I., 2017. Potato tuber induction is regulated by interactions between components of a tuberigen complex. Plant Cell Physiol. 58, 365–374. https://doi.org/10.1093/pcp/pcw197

Tetlow, I.J., Emes, M.J., 2014. A review of starch-branching enzymes and their role in

amylopectin biosynthesis. IUBMB Life 66, 546–58. https://doi.org/10.1002/iub.1297

Tetlow, I.J., Morell, M.K., Emes, M.J., 2004. Recent developments in understanding the regulation of starch metabolism in higher plants. J. Exp. Bot. https://doi.org/10.1093/jxb/erh248

Thimm, O., Bläsing, O., Gibon, Y., Nagel, A., Meyer, S., Krüger, P., Selbig, J., Müller, L.A., Rhee, S.Y., Stitt, M., 2004. MAPMAN: A user-driven tool to display genomics data sets onto diagrams of metabolic pathways and other biological processes. Plant J. 37, 914–939. https://doi.org/10.1111/j.1365-313X.2004.02016.x

Tiessen, A., Hendriks, J.H.M.M., Stitt, M., Branscheid, A., Gibon, Y., Farré, E.M., Geigenberger, P., 2002. Starch Synthesis in Potato Tubers Is Regulated by Post-Translational Redox Modification of ADP-Glucose Pyrophosphorylase : A Novel Regulatory Mechanism Linking Starch Synthesis to the Sucrose Supply. Plant Cell 14, 2191–2213. https://doi.org/10.1105/tpc.003640.2192

Torii, K.U., 2004. Leucine-Rich Repeat Receptor Kinases in Plants : Structure , Function , and Signal Transduction Pathways 234, 1–46.

Torres-Galea, P., Hirtreiter, B., Bolle, C., 2013. Two GRAS proteins, SCARECROW-LIKE21 and PHYTOCHROME A SIGNAL TRANSDUCTION1, function cooperatively in phytochrome A signal transduction. Plant Physiol. 161, 291–304. https://doi.org/10.1104/pp.112.206607

Usadel, B., Obayashi, T., Mutwil, M., Giorgi, F.M., Bassel, G.W., Tanimoto, M., Chow, A., Steinhauser, D., Persson, S., Provart, N.J., 2009. Co-expression tools for plant biology: Opportunities for hypothesis generation and caveats. Plant, Cell Environ. 32, 1633–1651. https://doi.org/10.1111/j.1365-3040.2009.02040.x

Van Dam, J., Kooman, P.L., Struik, P.C., 1996. Effects of temperature and photoperiod on early growth and final number of tubers in potato (Solanum tuberosum L .). Potato Res. 39, 51–62.

Van Den Berg, J.H., Struick, P.C., Ewing, E.E., 1990. One-leaf cuttings as a model to study second growth in the potato (Solanum tuberosum) Plant. Ann. Bot. 66, 273–280.

Van Harsselaar, J.K., Claußen, J., Lübeck, J., Wörlein, N., Uhlmann, N., Sonnewald, U., Gerth, S., 2021. X-Ray CT Phenotyping Reveals Bi-Phasic Growth Phases of Potato Tubers Exposed to Combined Abiotic Stress. Front. Plant Sci. 12, 1–15. https://doi.org/10.3389/fpls.2021.613108

Van Harsselaar, J.K., Lorenz, J., Senning, M., Sonnewald, U., Sonnewald, S., 2017. Genome-wide analysis of starch metabolism genes in potato (Solanum tuberosum L.). BMC

References

Genomics 18, 1–18. https://doi.org/10.1186/s12864-016-3381-z

Viola, R., Roberts, a G., Haupt, S., Gazzani, S., Hancock, R.D., Marmiroli, N., Machray, G.C., Oparka, K.J., 2001. Tuberization in potato involves a switch from apoplastic to symplastic phloem unloading. Plant Cell 13, 385–98.

Visser, R.G.F., Hergersberg, M., Van Der Leij, F.R.R., Jacobsen, E., Witholt, B., Feenstra, W.J.J., 1989. Molecular cloning and partial characterization of the gene for granule-bound starch synthase from a wildtype and an amylose-free potato (Solanum tuberosum L.). Plant Sci. 64, 185–192. https://doi.org/10.1016/0168-9452(89)90023-X

Visser, R.G.F., Stolte, A., Jacobsen, E., 1991. Expression of a chimaeric granule-bound starch synthase-GUS gene in transgenic potato plants. Plant Mol. Biol. 17, 691–699. https://doi.org/10.1007/BF00037054

Wang, L., Yu, C., Chen, C., He, C., Zhu, Y., Huang, W., 2014. Identification of rice Di19 family reveals OsDi19-4 involved in drought resistance. Plant Cell Rep. 33, 2047–2062. https://doi.org/10.1007/s00299-014-1679-3

Wang, P., Grimm, B., 2015. Organization of chlorophyll biosynthesis and insertion of chlorophyll into the chlorophyll-binding proteins in chloroplasts. Photosynth. Res. 126, 189–202. https://doi.org/10.1007/s11120-015-0154-5

Wang, X., Xue, L., Sun, J., Zuo, J., 2010. The Arabidopsis BE1 gene, encoding a putative glycoside hydrolase localized in plastids, plays crucial roles during embryogenesis and carbohydrate metabolism. J. Integr. Plant Biol. 52, 273–288. https://doi.org/10.1111/j.1744-7909.2010.00930.x

Wasternack, C., Hause, B., 2013. Jasmonates: Biosynthesis, perception, signal transduction and action in plant stress response, growth and development. An update to the 2007 review in Annals of Botany. Ann. Bot. 111, 1021–1058. https://doi.org/10.1093/aob/mct067

Weise, S.E., Weber, A.P.M., Sharkey, T.D., 2004. Maltose is the major form of carbon exported from the chloroplast at night. Planta 218, 474–482. https://doi.org/10.1007/s00425-003-1128-y

Werij, J.S., Furrer, H., van Eck, H.J., Visser, R.G.F., Bachem, C.W.B., 2012. A limited set of starch related genes explain several interrelated traits in potato. Euphytica 186, 501–516. https://doi.org/10.1007/s10681-012-0651-y

Wigge, P.A., Kim, M.C., Jaeger, K.E., Busch, W., Schmid, M., Lohmann, J.U., Weigel, D., 2005. Integration of spatial and temporal information during floral induction in Arabidopsis. Science (80-.). 309, 1056–1059. https://doi.org/10.1126/science.1114358

Wimalasekera, R., Tebartz, F., Scherer, G.F.E., 2011. Polyamines, polyamine oxidases and nitric oxide in development, abiotic and biotic stresses. Plant Sci. 181, 593–603. https://doi.org/10.1016/j.plantsci.2011.04.002

Wolf, S., Marani, A., Rudich, J., 1991. Effect of Temperature on Carbohydrate Metabolism in Potato Plants. J. Exp. Bot. 42, 619–625.

Wolf, S., Olesinski, A.A., Rudich, J., Marani, A., 1990. Effect of high temperature on photosynthesis in potatoes. Ann. Bot. 65, 179–185. https://doi.org/10.1093/oxfordjournals.aob.a087922

Wu, Y., Hiratsuka, K., Neuhaus, G., Chua, N.H., 1996. Calcium and cGMP target distinct phytochrome-responsive elements. Plant J. 10, 1149–54. https://doi.org/10.1046/j.1365-313x.1996.10061149.x

Xu, X., Pan, S., Cheng, S., Zhang, B., Mu, D., Ni, P., Zhang, G., Yang, S., Li, R., Wang, J., Orjeda, G., Guzman, F., Torres, M., Lozano, R., Ponce, O., Martinez, D., De la Cruz, G., Chakrabarti, S.K., Patil, V.U., Skryabin, K.G., Kuznetsov, B.B., Ravin, N. V., Kolganova, T. V., Beletsky, A. V., Mardanov, A. V., Di Genova, A., Bolser, D.M., Martin, D.M.A.A., Li, G., Yang, Y., Kuang, H., Hu, Q., Xiong, X., Bishop, G.J., Sagredo, B., Mejía, N., Zagorski, W., Gromadka, R., Gawor, J., Szczesny, P., Huang, S., Zhang, Z., Liang, C., He, J., Li, Y., He, Y., Xu, J., Zhang, Y., Xie, B., Du, Y., Qu, D., Bonierbale, M., Ghislain, M., del Rosario Herrera, M., Giuliano, G., Pietrella, M., Perrotta, G., Facella, P., O'Brien, K., Feingold, S.E., Barreiro, L.E., Massa, G.A., Diambra, L., Whitty, B.R., Vaillancourt, B., Lin, H., Massa, A.N., Geoffroy, M., Lundback, S., DellaPenna, D., Robin Buell, C., Sharma, S.K., Marshall, D.F., Waugh, R., Bryan, G.J., Destefanis, M., Nagy, I., Milbourne, D., Thomson, S.J., Fiers, M., Jacobs, J.M.E.E., Nielsen, K.L.K.L.K.L., Sønderkær, M., Iovene, M., Torres, G.A., Jiang, J., Veilleux, R.E., Bachem, C.W.B.B., de Boer, J., Borm, T., Kloosterman, B., van Eck, H., Datema, E., te Lintel Hekkert, B., Goverse, A., Van Ham, R.C.H.J.H.J., Visser, R.G.F.F., Skryabin, G., Kuznetsov, B.B., Ravin, N. V., Kolganova, T. V., Beletsky, A. V., Mardanov, A. V., Di Genova, A., Bolser, D.M., Martin, D.M.A.A., Li, G., Yang, Y., Kuang, H., Hu, Q., Xiong, X., Bishop, G.J., Sagredo, B., Mejía, N., Zagorski, W., Gromadka, R., Gawor, J., Szczesny, P., Huang, S., Zhang, Z., Liang, C., He, J., Li, Y., He, Y., Xu, J., Zhang, Y., Xie, B., Du, Y., Qu, D., Bonierbale, M., Ghislain, M., Herrera, M.D.R., Giuliano, G., Pietrella, M., Perrotta, G., Facella, P., O'Brien, K., Feingold, S.E., Barreiro, L.E., Massa, G.A., Diambra, L., Whitty, B.R., Vaillancourt, B., Lin, H., Massa, A.N., Geoffroy, M., Lundback, S., DellaPenna, D., Buell, C.R., Sharma, S.K., Marshall, D.F., Waugh, R., Bryan, G.J., Destefanis, M., Nagy, I., Milbourne, D., Thomson, S.J., Fiers, M., Jacobs, J.M.E.E., Nielsen, K.L.K.L.K.L., Sønderkær, M., Iovene, M., Torres, G.A., Jiang, J., Veilleux, R.E., Bachem, C.W.B.B., de Boer, J., Borm, T., Kloosterman, B.,

References

van Eck, H., Datema, E., Hekkert, B.L., Goverse, A., Van Ham, R.C.H.J.H.J., Visser, R.G.F.F., Skryabin, K.G., Kuznetsov, B.B., Ravin, N. V., Kolganova, T. V., Beletsky, A. V., Mardanov, A. V., Di Genova, A., Bolser, D.M., Martin, D.M.A.A., Li, G., Yang, Y., Kuang, H., Hu, Q., Xiong, X., Bishop, G.J., Sagredo, B., Mejía, N., Zagorski, W., Gromadka, R., Gawor, J., Szczesny, P., Huang, S., Zhang, Z., Liang, C., He, J., Li, Y., He, Y., Xu, J., Zhang, Y., Xie, B., Du, Y., Qu, D., Bonierbale, M., Ghislain, M., del Rosario Herrera, M., Giuliano, G., Pietrella, M., Perrotta, G., Facella, P., O'Brien, K., Feingold, S.E., Barreiro, L.E., Massa, G.A., Diambra, L., Whitty, B.R., Vaillancourt, B., Lin, H., Massa, A.N., Geoffroy, M., Lundback, S., DellaPenna, D., Robin Buell, C., Sharma, S.K., Marshall, D.F., Waugh, R., Bryan, G.J., Destefanis, M., Nagy, I., Milbourne, D., Thomson, S.J., Fiers, M., Jacobs, J.M.E.E., Nielsen, K.L.K.L.K.L., Sønderkær, M., Iovene, M., Torres, G.A., Jiang, J., Veilleux, R.E., Bachem, C.W.B.B., de Boer, J., Borm, T., Kloosterman, B., van Eck, H., Datema, E., te Lintel Hekkert, B., Goverse, A., Van Ham, R.C.H.J.H.J., Visser, R.G.F.F., Skryabin, G., Kuznetsov, B.B., Ravin, N. V., Kolganova, T. V., Beletsky, A. V., Mardanov, A. V., Di Genova, A., Bolser, D.M., Martin, D.M.A.A., Li, G., Yang, Y., Kuang, H., Hu, Q., Xiong, X., Bishop, G.J., Sagredo, B., Mejía, N., Zagorski, W., Gromadka, R., Gawor, J., Szczesny, P., Huang, S., Zhang, Z., Liang, C., He, J., Li, Y., He, Y., Xu, J., Zhang, Y., Xie, B., Du, Y., Qu, D., Bonierbale, M., Ghislain, M., Herrera, M.D.R., Giuliano, G., Pietrella, M., Perrotta, G., Facella, P., O'Brien, K., Feingold, S.E., Barreiro, L.E., Massa, G.A., Diambra, L., Whitty, B.R., Vaillancourt, B., Lin, H., Massa, A.N., Geoffroy, M., Lundback, S., DellaPenna, D., Buell, C.R., Sharma, S.K., Marshall, D.F., Waugh, R., Bryan, G.J., Destefanis, M., Nagy, I., Milbourne, D., Thomson, S.J., Fiers, M., Jacobs, J.M.E.E., Nielsen, K.L.K.L.K.L., Sønderkær, M., Iovene, M., Torres, G.A., Jiang, J., Veilleux, R.E., Bachem, C.W.B.B., de Boer, J., Borm, T., Kloosterman, B., van Eck, H., Datema, E., Hekkert, B.L., Goverse, A., Van Ham, R.C.H.J.H.J., Visser, R.G.F.F., 2011. Genome sequence and analysis of the tuber crop potato. Nature 475, 189–195. https://doi.org/10.1038/nature10158

Xu, X., Van Lammeren, A.A.M., Vermeer, E., Vreugdenhil, D., 1998a. the role of gibberellin, abscisic acid, and sucrose in the regulation of potato tuber formation in vitro. Plant Physiol. 117, 575–584. https://doi.org/10.1104/pp.117.2.575

Xu, X., Vreugdenhil, D., Lammeren, A.A.M., 1998b. Cell division and cell enlargement during potatoes tuber formation. J. Exp. Bot. 49, 573–582.

Ye, J., Coulouris, G., Zaretskaya, I., Cutcutache, I., Rozen, S., Madden, T.L., 2012. Primer-BLAST: A tool to design target-specific primers for polymerase chain reaction. BMC Bioinformatics 13, 134. https://doi.org/10.1186/1471-2105-13-134

Zeeman, S.C., Kossmann, J., Smith, A.M., 2010. Starch: its metabolism, evolution, and

biotechnological modification in plants. Annu. Rev. Plant Biol. 61, 209–34. https://doi.org/10.1146/annurev-arplant-042809-112301

Zhang, L., Häusler, R.E., Greiten, C., Hajirezaei, M.R., Haferkamp, I., Neuhaus, H.E., Flügge, U.I., Ludewig, F., 2008. Overriding the co-limiting import of carbon and energy into tuber amyloplasts increases the starch content and yield of transgenic potato plants. Plant Biotechnol. J. 6, 453–464. https://doi.org/10.1111/j.1467-7652.2008.00332.x

Zhang, Y., Behrens, I. Von, Zimmermann, R., Ludwig, Y., Hey, S., Hochholdinger, F., 2015. LATERAL ROOT PRIMORDIA 1 of maize acts as a transcriptional activator in auxin signalling downstream of the Aux/IAA gene rootless with undetectable meristem 1. J. Exp. Bot. 66, 3855–3863. https://doi.org/10.1093/jxb/erv187

Zhu, Y., Cai, X.-L., Wang, Z.-Y., Hong, M.-M., 2003. An interaction between a MYC protein and an EREBP protein is involved in transcriptional regulation of the rice Wx gene. J. Biol. Chem. 278, 47803–11. https://doi.org/10.1074/jbc.M302806200

Zrenner, R., Krause, K.P., Apel, P., Sonnewald, U., 1996. Reduction of the cytosolic fructose-1,6-bisphosphatase in transgenic potato plants limits photosynthetic sucrose biosynthesis with no impact on plant growth and tuber yield. Plant J. 9, 671–681. https://doi.org/10.1046/j.1365-313X.1996.9050671.x

Zrenner, R., Salanoubat, M., Willmitzer, L., Sonnewald, U., 1995. Evidence of the crucial role of sucrose synthase for sink strength using transgenic potato plants (Solanum tuberosum L.). plant J. 7, 97–107.

7 Appendix

Table A 1: Differentially expressed genes (n=1554) in potato leaves under heat stress conditions compared to leaves from control conditions (p≤0.05, fold-change ≥2).

ProbeName	p	FC (abs) Day 54 heat vs con	Regulation	PrimaryAccession	UniRef based putative functional annotation	functional category
CUST_41954_PI426222305	0,024	2,054	up	PGSC0003DMT400080276	Hydroxymethylglutaryl-CoA lyase	AA metabolism
CUST_14966_PI426222305	0,005	3,330	up	PGSC0003DMT400057174	Imidazole glycerol phosphate synthase subunit hisf	AA metabolism
CUST_14556_PI426222305	0,012	3,242	up	PGSC0003DMT400066599	Methylcrotonoyl-CoA carboxylase beta chain, mitochondrial	AA metabolism
CUST_8216_PI426222305	0,013	3,185	up	PGSC0003DMT400030117	Branched-chain-amino-acid aminotransferase	AA metabolism
CUST_46355_PI426222305	0,005	11,903	up	PGSC0003DMT400074719	Aromatic amino acid decarboxylase 1B	AA metabolism
CUST_15284_PI426222305	0,014	2,325	up	PGSC0003DMT400057095	Serine acetyltransferase	AA metabolism
CUST_14766_PI426222305	0,033	2,462	up	PGSC0003DMT400066601	Methylcrotonoyl-CoA carboxylase beta chain, mitochondrial	AA metabolism
CUST_3041_PI426222305	0,029	2,037	up	PGSC0003DMT400000043	Enoyl-CoA-hydratase	AA metabolism
CUST_30632_PI426222305	0,032	2,178	up	PGSC0003DMT400018589	CXE carboxylesterase	Biodegradation of Xenobiotics
CUST_40328_PI426222305	0,019	2,357	up	PGSC0003DMT400048357	Pepper esterase	Biodegradation of Xenobiotics
CUST_13490_PI426222305	0,032	2,186	up	PGSC0003DMT400017619	Lactoylglutathione lyase	Biodegradation of Xenobiotics
CUST_3227_PI426222305	0,011	6,871	up	PGSC0003DMT400000389	Gibberellin receptor GID1	Biodegradation of Xenobiotics
CUST_19793_PI426222305	0,006	3,838	up	PGSC0003DMT400064056	Lactoylglutathione lyase	Biodegradation of Xenobiotics
CUST_32607_PI426222305	0,023	2,598	up	PGSC0003DMT400022555	Formate dehydrogenase, mitochondrial	C1-metabolism
CUST_950_PI426222305	0,009	3,246	up	PGSC0003DMT400001303	Formate dehydrogenase, mitochondrial	C1-metabolism
CUST_31131_PI426222305	0,011	2,877	up	PGSC0003DMT400068907	Formate dehydrogenase	C1-metabolism
CUST_6929_PI426222305	0,003	3,621	up	PGSC0003DMT400026563	F-box family protein	Cell
CUST_36003_PI426222305	0,000	51,488	up	PGSC0003DMT400080935	Peptidylprolyl isomerase	Cell
CUST_20760_PI426222305	0,013	7,171	up	PGSC0003DMT400011905	Kinesin	Cell
CUST_20535_PI426222305	0,012	8,108	up	PGSC0003DMT400097622	F-box family protein	Cell
CUST_15214_PI426222305	0,037	3,276	up	PGSC0003DMT400056962	Actin, macronuclear	Cell
CUST_48363_PI426222305	0,021	3,803	up	PGSC0003DMT400013717	Formin 1	Cell
CUST_30547_PI426222305	0,002	4,344	up	PGSC0003DMT400007954	SH3 domain-containing protein 3	Cell
CUST_50592_PI426222305	0,038	2,045	up	PGSC0003DMT400022381	Aberrant large forked product	Cell
CUST_12580_PI426222305	0,008	4,568	up	PGSC0003DMT400063740	Conserved gene of unknown function	Cell
CUST_5579_PI426222305	0,036	3,463	up	PGSC0003DMT400007011	Ania-6a type cyclin	Cell
CUST_16223_PI426222305	0,019	2,735	up	PGSC0003DMT400031354	Conserved gene of unknown function	Cell
CUST_24996_PI426222305	0,011	3,957	up	PGSC0003DMT400074851	65-kDa microtubule-associated protein 8	Cell
CUST_12368_PI426222305	0,017	3,060	up	PGSC0003DMT400063739	Phloem protein 2-B15	Cell
CUST_38123_PI426222305	0,006	3,045	up	PGSC0003DMT400054872	Conserved gene of unknown function	Cell
CUST_44907_PI426222305	0,035	2,795	up	PGSC0003DMT400058660	PLE	Cell
CUST_2497_PI426222305	0,042	2,089	up	PGSC0003DMT400028659	Conserved gene of unknown function	Cell
CUST_12348_PI426222305	0,007	3,567	up	PGSC0003DMT400063738	Conserved gene of unknown function	Cell
CUST_33644_PI426222305	0,010	2,428	up	PGSC0003DMT400078760	AAR2 protein family	Cell
CUST_47448_PI426222305	0,029	3,998	up	PGSC0003DMT400064881	Dehydration-responsive protein RD22	Cell Wall
CUST_26351_PI426222305	0,039	4,648	up	PGSC0003DMT400051441	Pectin acetylesterase	Cell Wall
CUST_47063_PI426222305	0,007	5,580	up	PGSC0003DMT400079601	Polygalacturonase-1 non-catalytic subunit beta	Cell Wall
CUST_2143_PI426222305	0,050	29,296	up	PGSC0003DMT400027117	Arabinogalactan protein 3	Cell Wall
CUST_12788_PI426222305	0,029	5,473	up	PGSC0003DMT400063245	Polygalacturonase-1 non-catalytic subunit beta	Cell Wall
CUST_44067_PI426222305	0,045	8,457	up	PGSC0003DMT400056143	Pectinacetylesterase	Cell Wall
CUST_47066_PI426222305	0,021	21,942	up	PGSC0003DMT400079599	Polygalacturonase-1 non-catalytic subunit beta	Cell Wall
CUST_47458_PI426222305	0,023	3,983	up	PGSC0003DMT400064879	Dehydration-responsive protein RD22	Cell Wall
CUST_47053_PI426222305	0,004	4,080	up	PGSC0003DMT400079565	Polygalacturonase non-catalytic subunit AroGP3	Cell Wall
CUST_31293_PI426222305	0,018	2,893	up	PGSC0003DMT400034854	Cellulose synthase	Cell Wall
CUST_16123_PI426222305	0,003	4,450	up	PGSC0003DMT400031330	BURP domain-containing protein	Cell Wall
CUST_51480_PI426222305	0,044	4,703	up	PGSC0003DMT400034177	Beta-D-glucan exohydrolase	Cell Wall
CUST_40136_PI426222305	0,033	2,402	up	PGSC0003DMT400015233	Hydrolase, hydrolyzing O-glycosyl compounds	Cell Wall
CUST_47017_PI426222305	0,023	3,039	up	PGSC0003DMT400079602	Polygalacturonase-1 non-catalytic subunit beta	Cell Wall
CUST_36758_PI426222305	0,050	4,040	up	PGSC0003DMT400004139	Protein COBRA	Cell Wall
CUST_34070_PI426222305	0,009	2,794	up	PGSC0003DMT400030625	Fe-S metabolism associated domain-containing protein	Co-factor and vitamine metabolism
CUST_12065_PI426222305	0,024	2,054	up	PGSC0003DMT400076648	UV-induced protein uvi31	Co-factor and vitamine metabolism
CUST_31672_PI426222305	0,014	2,411	up	PGSC0003DMT400035159	Naphthoate synthase	Co-factor and vitamine metabolism
CUST_42427_PI426222305	0,010	3,705	up	PGSC0003DMT400022567	Patatin-05	Development
CUST_45156_PI426222305	0,022	2,191	up	PGSC0003DMT400081230	NAC domain-containing protein 21/22	Development
CUST_31049_PI426222305	0,009	2,485	up	PGSC0003DMT400040299	Chloroplast envelope protein 1	Development
CUST_25173_PI426222305	0,021	4,752	up	PGSC0003DMT400014815	Plant cell wall protein SITFR88	Development
CUST_31000_PI426222305	0,022	2,273	up	PGSC0003DMT400040303	Chloroplast envelope protein 1	Development
CUST_45846_PI426222305	0,012	3,501	up	PGSC0003DMT400054084	ECP63 protein	Development
CUST_42397_PI426222305	0,043	2,823	up	PGSC0003DMT400036586	Patatin-2-Kuras 4	Development
CUST_6039_PI426222305	0,008	2,582	up	PGSC0003DMT400010706	TOR (TARGET OF RAPAMYCIN); 1-phosphatidylinositol-3-kinase/ protein binding	Development
CUST_8207_PI426222305	0,027	2,394	up	PGSC0003DMT400075435	Caleosin	Development
CUST_17603_PI426222305	0,009	10,390	up	PGSC0003DMT400001470	Pentatricopeptide repeat-containing protein	Development
CUST_27486_PI426222305	0,026	5,137	up	PGSC0003DMT400024505	WD-repeat protein	Development
CUST_11363_PI426222305	0,007	4,173	up	PGSC0003DMT400010672	GTP binding protein	Development
CUST_28264_PI426222305	0,010	12,068	up	PGSC0003DMT400096337	Caleosin	Development

Appendix

CUST_40601_PI426222305	0,048	3,227	up	PGSC0003DMT400073944	Transducin family protein	Development
CUST_50339_PI426222305	0,024	3,734	up	PGSC0003DMT400045865	Ce-LEA	Development
CUST_4350_PI426222305	0,049	10,419	up	PGSC0003DMT400020923	KiTH-2	Development
CUST_14773_PI426222305	0,030	3,113	up	PGSC0003DMT400066737	F-box and wd40 domain protein	DNA
CUST_33912_PI426222305	0,018	2,226	up	PGSC0003DMT400012516	Nucleosome assembly protein 1 4	DNA
CUST_34809_PI426222305	0,046	2,260	up	PGSC0003DMT400009751	Histone H2A	DNA
CUST_1995_PI426222305	0,037	3,655	up	PGSC0003DMT400072269	Alpha/beta fold family protein hydrolase	DNA
CUST_36851_PI426222305	0,000	14,948	up	PGSC0003DMT400094453	Replication protein A1	DNA
CUST_33852_PI426222305	0,018	2,301	up	PGSC0003DMT400012517	Nucleosome assembly protein 1 4	DNA
CUST_30774_PI426222305	0,029	3,028	up	PGSC0003DMT400002471	Exonuclease	DNA
CUST_6874_PI426222305	0,013	7,773	up	PGSC0003DMT400090970	Histone H2A	DNA
CUST_5651_PI426222305	0,036	2,222	up	PGSC0003DMT400007009	Gene of unknown function	DNA
CUST_16560_PI426222305	0,042	4,772	up	PGSC0003DMT400069295	Type I inositol polyphosphate 5-phosphatase	DNA
CUST_6521_PI426222305	0,021	2,260	up	PGSC0003DMT400014626	Endonuclease/exonuclease/phosphatase family protein	DNA
CUST_31694_PI426222305	0,045	25,181	up	PGSC0003DMT400035193	Leafy cotyledon1	DNA
CUST_14399_PI426222305	0,024	2,939	up	PGSC0003DMT400066736	F-box and wd40 domain protein	DNA
CUST_21658_PI426222305	0,015	3,727	up	PGSC0003DMT400051078	Uracil-DNA glycosylase	DNA
CUST_25623_PI426222305	0,012	2,795	up	PGSC0003DMT400029242	Glyceraldehyde-3-phosphate dehydrogenase	Glycolysis
CUST_30038_PI426222305	0,020	3,261	up	PGSC0003DMT400065452	6-phosphofructokinase 7	Glycolysis
CUST_27474_PI426222305	0,006	27,462	up	PGSC0003DMT400095815	Phosphofructokinase	Glycolysis
CUST_49485_PI426222305	0,012	4,558	up	PGSC0003DMT400016844	Pyruvate kinase	Glycolysis
CUST_5641_PI426222305	0,004	5,847	up	PGSC0003DMT400023097	Desacetoxyvindoline 4-hydroxylase	hormone metabolism
CUST_36814_PI426222305	0,014	2,708	up	PGSC0003DMT400004081	Auxin-induced SAUR	hormone metabolism
CUST_25593_PI426222305	0,022	3,759	up	PGSC0003DMT400029281	Gibberellin 2-oxidase 1	hormone metabolism
CUST_33138_PI426222305	0,043	12,277	up	PGSC0003DMT400067582	Leucoanthocyanidin dioxygenase	hormone metabolism
CUST_38802_PI426222305	0,013	7,687	up	PGSC0003DMT400015411	Adenylate isopentenyltransferase	hormone metabolism
CUST_49240_PI426222305	0,020	3,334	up	PGSC0003DMT400059595	Gibberellin 3beta-hydroxylase3	hormone metabolism
CUST_25363_PI426222305	0,015	2,349	up	PGSC0003DMT400034487	ERF transcription factor 5	hormone metabolism
CUST_13691_PI426222305	0,005	3,663	up	PGSC0003DMT400084210	Jasmonic acid-amino acid-conjugating enzyme	hormone metabolism
CUST_28527_PI426222305	0,049	3,883	up	PGSC0003DMT400009900	Leucoanthocyanidin dioxygenase	hormone metabolism
CUST_33223_PI426222305	0,020	3,129	up	PGSC0003DMT400067580	Leucoanthocyanidin dioxygenase	hormone metabolism
CUST_25425_PI426222305	0,016	2,371	up	PGSC0003DMT400034490	ERF transcription factor 5	hormone metabolism
CUST_32322_PI426222305	0,049	2,471	up	PGSC0003DMT400012593	Squalene monooxygenase	hormone metabolism
CUST_31575_PI426222305	0,015	2,820	up	PGSC0003DMT400042658	Gibberellin 20 oxidase	hormone metabolism
CUST_12834_PI426222305	0,021	2,697	up	PGSC0003DMT400062877	Gonadotropin beta chain	hormone metabolism
CUST_25907_PI426222305	0,010	4,032	up	PGSC0003DMT400051610	Gene of unknown function	hormone metabolism
CUST_25205_PI426222305	0,046	2,074	up	PGSC0003DMT400014932	ACC synthase	hormone metabolism
CUST_17774_PI426222305	0,014	6,871	up	PGSC0003DMT400066846	ERF1	hormone metabolism
CUST_29604_PI426222305	0,045	3,813	up	PGSC0003DMT400075949	Sensor histidine kinase	hormone metabolism
CUST_5759_PI426222305	0,025	2,891	up	PGSC0003DMT400023095	Desacetoxyvindoline 4-hydroxylase	hormone metabolism
CUST_33229_PI426222305	0,002	11,485	up	PGSC0003DMT400067586	Leucoanthocyanidin dioxygenase	hormone metabolism
CUST_15513_PI426222305	0,014	2,407	up	PGSC0003DMT400073718	2-oxoglutarate-dependent dioxygenase	hormone metabolism
CUST_39901_PI426222305	0,012	4,361	up	PGSC0003DMT400047553	Carotenoid cleavage dioxygenase 4	hormone metabolism
CUST_31483_PI426222305	0,007	4,169	up	PGSC0003DMT400073345	Conserved gene of unknown function	hormone metabolism
CUST_22740_PI426222305	0,034	3,104	up	PGSC0003DMT400078051	20G-Fe(II) oxidoreductase	hormone metabolism
CUST_31490_PI426222305	0,014	3,906	up	PGSC0003DMT400073342	Conserved gene of unknown function	hormone metabolism
CUST_16579_PI426222305	0,001	13,312	up	PGSC0003DMT400092730	SAUR family protein	hormone metabolism
CUST_25796_PI426222305	0,004	9,081	up	PGSC0003DMT400051813	Auxin-induced in root cultures protein 12	hormone metabolism
CUST_2757_PI426222305	0,033	2,344	up	PGSC0003DMT400048327	LEDI-5c protein	hormone metabolism
CUST_36880_PI426222305	0,017	5,699	up	PGSC0003DMT400067535	ATERF-2/ATERF2/ERF2	hormone metabolism
CUST_31587_PI426222305	0,014	4,452	up	PGSC0003DMT400073343	Conserved gene of unknown function	hormone metabolism
CUST_34115_PI426222305	0,002	4,516	up	PGSC0003DMT400019726	GAST1 protein	hormone metabolism
CUST_41489_PI426222305	0,035	2,470	up	PGSC0003DMT400021600	Auxin efflux carrier	hormone metabolism
CUST_49947_PI426222305	0,014	2,690	up	PGSC0003DMT400071184	C-8,7 sterol isomerase	hormone metabolism
CUST_31570_PI426222305	0,008	3,265	up	PGSC0003DMT400073341	Conserved gene of unknown function	hormone metabolism
CUST_44595_PI426222305	0,007	7,585	up	PGSC0003DMT400013401	Glycerophosphodiester phosphodiesterase	Lipid Metabolism
CUST_47706_PI426222305	0,045	3,253	up	PGSC0003DMT400061255	Fatty acid desaturase	Lipid Metabolism
CUST_47348_PI426222305	0,037	2,070	up	PGSC0003DMT400021395	Triacylglycerol lipase	Lipid Metabolism
CUST_6709_PI426222305	0,040	2,999	up	PGSC0003DMT400014749	Phosphoethanolamine N-methyltransferase	Lipid Metabolism
CUST_13307_PI426222305	0,012	2,819	up	PGSC0003DMT400059370	Diacylglycerol kinase variant B	Lipid Metabolism
CUST_19458_PI426222305	0,048	2,601	up	PGSC0003DMT400072874	Flavonol 4'-sulfotransferase	Lipid Metabolism
CUST_9349_PI426222305	0,026	2,031	up	PGSC0003DMT400023660	Triacylglycerol lipase	Lipid Metabolism
CUST_17090_PI426222305	0,033	2,239	up	PGSC0003DMT400018356	Phosphatidylcholine-sterol acyltransferase	Lipid Metabolism
CUST_44608_PI426222305	0,006	4,261	up	PGSC0003DMT400013402	Glycerophosphodiester phosphodiesterase	Lipid Metabolism
CUST_19268_PI426222305	0,008	3,419	up	PGSC0003DMT400086700	Flavonol 4'-sulfotransferase	Lipid Metabolism
CUST_15064_PI426222305	0,012	2,741	up	PGSC0003DMT400057446	Starch branching enzyme	major CHO metabolism

CUST_8549_PI426222305	0,024	2,044	up	PGSC0003DMT400027659	1,4-alpha-glucan-maltohydrolase	major CHO metabolism
CUST_42396_PI426222305	0,002	6,276	up	PGSC0003DMT400052839	Beta-amylase PCT-BMYI	major CHO metabolism
CUST_24153_PI426222305	0,003	3,943	up	PGSC0003DMT400049045	Sucrose-phosphate synthase isoform C	major CHO metabolism
CUST_36993_PI426222305	0,005	3,230	up	PGSC0003DMT400075057	Ferritin	metal handling
CUST_38840_PI426222305	0,044	5,937	up	PGSC0003DMT400015350	Metal ion binding protein	metal handling
CUST_17425_PI426222305	0,043	3,175	up	PGSC0003DMT400068079	Metal ion binding protein	metal handling
CUST_11762_PI426222305	0,020	12,986	up	PGSC0003DMT400046636	Raffionse synthase 2	minor CHO metabolism
CUST_25290_PI426222305	0,048	8,110	up	PGSC0003DMT400034562	Inositol monophosphatase 3	minor CHO metabolism
CUST_2238_PI426222305	0,045	2,499	up	PGSC0003DMT400072410	3-deoxy-D-manno-octulosonic acid transferase	minor CHO metabolism
CUST_1506_PI426222305	0,027	2,157	up	PGSC0003DMT400003328	Aldose-1-epimerase	minor CHO metabolism
CUST_32242_PI426222305	0,028	2,665	up	PGSC0003DMT400012624	Xylulose kinase	minor CHO metabolism
CUST_35334_PI426222305	0,020	6,588	up	PGSC0003DMT400038402	Aldo-keto reductase	minor CHO metabolism
CUST_18877_PI426222305	0,014	2,224	up	PGSC0003DMT400019145	Aldo-keto reductase	minor CHO metabolism
CUST_45515_PI426222305	0,014	2,182	up	PGSC0003DMT400079681	Conserved gene of unknown function	minor CHO metabolism
CUST_43019_PI426222305	0,023	2,860	up	PGSC0003DMT400018907	Acetylglucosaminyltransferase	misc
CUST_4116_PI426222305	0,037	4,173	up	PGSC0003DMT400008432	Taxane 13-alpha-hydroxylase cytochrome P450	misc
CUST_9829_PI426222305	0,015	2,558	up	PGSC0003DMT400038514	Peroxidase	misc
CUST_45482_PI426222305	0,028	16,076	up	PGSC0003DMT400038056	Dimethylaniline monooxygenase	misc
CUST_50258_PI426222305	0,037	2,048	up	PGSC0003DMT400072053	Short-chain dehydrogenase	misc
CUST_3180_PI426222305	0,028	2,429	up	PGSC0003DMT400000430	Cytochrome P450	misc
CUST_2713_PI426222305	0,013	2,622	up	PGSC0003DMT400080097	Zinc finger protein	misc
CUST_23875_PI426222305	0,007	3,874	up	PGSC0003DMT400032684	UDP-glucuronosyltransferase	misc
CUST_475_PI426222305	0,023	2,028	up	PGSC0003DMT400019561	Cytochrome P450	misc
CUST_5532_PI426222305	0,008	5,147	up	PGSC0003DMT400007080	Cytochrome P450 76A1	misc
CUST_41481_PI426222305	0,022	10,327	up	PGSC0003DMT400021572	2,4-dienoyl-CoA reductase	misc
CUST_38309_PI426222305	0,008	6,845	up	PGSC0003DMT400043673	Cytochrome P450	misc
CUST_33185_PI426222305	0,012	2,999	up	PGSC0003DMT400067682	UDP-glucose:glucosyltransferase	misc
CUST_6481_PI426222305	0,009	4,646	up	PGSC0003DMT400014500	Cytochrome P450	misc
CUST_29084_PI426222305	0,025	2,017	up	PGSC0003DMT400020597	UDP-glucosyltransferase	misc
CUST_24835_PI426222305	0,042	5,853	up	PGSC0003DMT400024073	Cytochrome P450	misc
CUST_49195_PI426222305	0,011	2,829	up	PGSC0003DMT400027786	Adrenodoxin	misc
CUST_17948_PI426222305	0,035	2,488	up	PGSC0003DMT400071059	Glutathione S-transferase T5	misc
CUST_44296_PI426222305	0,005	3,529	up	PGSC0003DMT400010109	Cytochrome P450	misc
CUST_12913_PI426222305	0,024	3,524	up	PGSC0003DMT400063237	Glycosyltransferase UGT90A7	misc
CUST_30880_PI426222305	0,009	5,087	up	PGSC0003DMT400037949	Glycosyltransferase, CAZy family GT8	misc
CUST_33726_PI426222305	0,006	4,325	up	PGSC0003DMT400078577	Phosphatidic acid phosphatase	misc
CUST_47225_PI426222305	0,008	5,662	up	PGSC0003DMT400059008	Exostosin family protein	misc
CUST_18539_PI426222305	0,030	2,439	up	PGSC0003DMT400050768	Amine oxidase	misc
CUST_2311_PI426222305	0,010	5,449	up	PGSC0003DMT400028714	Glutathione S-transferase omega	misc
CUST_36028_PI426222305	0,008	3,614	up	PGSC0003DMT400056301	Conserved gene of unknown function	misc
CUST_14571_PI426222305	0,008	2,466	up	PGSC0003DMT400066576	Phenylpropanoid:glucosyltransferase 1	misc
CUST_18617_PI426222305	0,018	2,509	up	PGSC0003DMT400050769	Amine oxidase	misc
CUST_33153_PI426222305	0,026	3,595	up	PGSC0003DMT400067684	UDP-glucose:glucosyltransferase	misc
CUST_2172_PI426222305	0,002	8,559	up	PGSC0003DMT400072408	Cytochrome P450 76A2	misc
CUST_35934_PI426222305	0,027	2,682	up	PGSC0003DMT400056292	Cytochrome P450 monooxygenase CYP83E9	misc
CUST_33210_PI426222305	0,023	3,033	up	PGSC0003DMT400024615	UDP-glucose:glucosyltransferase	misc
CUST_48560_PI426222305	0,009	3,513	up	PGSC0003DMT400036391	Cytochrome P450	misc
CUST_4073_PI426222305	0,027	2,433	up	PGSC0003DMT400008433	Cytochrome P450	misc
CUST_50223_PI426222305	0,025	7,842	up	PGSC0003DMT400080135	Cytochrome P450	misc
CUST_51593_PI426222305	0,010	3,461	up	PGSC0003DMT400005571	Glutathione S-transferase	misc
CUST_50386_PI426222305	0,026	3,999	up	PGSC0003DMT400072021	Short chain alcohol dehydrogenase	misc
CUST_33216_PI426222305	0,032	2,920	up	PGSC0003DMT400024641	UDP-glucose:glucosyltransferase	misc
CUST_2894_PI426222305	0,040	2,402	up	PGSC0003DMT400000077	Carbonyl reductase	misc
CUST_44414_PI426222305	0,020	2,142	up	PGSC0003DMT400071464	Quinone oxidoreductase	misc
CUST_52567_PI426222305	0,019	2,320	up	PGSC0003DMT400044123	Cytochrome P450	misc
CUST_22879_PI426222305	0,031	6,585	up	PGSC0003DMT400021018	Glucosyltransferase	misc
CUST_32028_PI426222305	0,007	8,981	up	PGSC0003DMT400013258	Polyneuridine-aldehyde esterase	misc
CUST_48349_PI426222305	0,006	3,372	up	PGSC0003DMT400043223	Cytochrome P450	misc
CUST_48315_PI426222305	0,005	2,967	up	PGSC0003DMT400043224	Cytochrome P450	misc
CUST_43044_PI426222305	0,049	2,321	up	PGSC0003DMT400018905	Acetylglucosaminyltransferase	misc
CUST_44642_PI426222305	0,015	2,219	up	PGSC0003DMT400027494	CYP72A58	misc
CUST_48815_PI426222305	0,004	3,955	up	PGSC0003DMT400056090	UDP-glucuronosyltransferase	misc
CUST_48583_PI426222305	0,046	3,155	up	PGSC0003DMT400036399	Flavonoid 3-hydroxylase	misc
CUST_44471_PI426222305	0,037	2,107	up	PGSC0003DMT400019806	Salicylic acid-binding protein 2	misc
CUST_31974_PI426222305	0,034	2,347	up	PGSC0003DMT400013272	Zinc finger protein	misc
CUST_33148_PI426222305	0,016	2,673	up	PGSC0003DMT400024622	UDP-xylose phenolic glycosyltransferase	misc

Appendix

CUST_43917_PI426222305	0,012	2,857	up	PGSC0003DMT400045362	Flavonoid glucoyltransferase UGT73E2	misc
CUST_51622_PI426222305	0,045	3,137	up	PGSC0003DMT400092547	Glucosyl/glucuronosyl transferases	misc
CUST_49739_PI426222305	0,021	3,447	up	PGSC0003DMT400002738	Brassinosteroid hydroxylase	misc
CUST_11853_PI426222305	0,021	2,134	up	PGSC0003DMT400046864	Cytochrome P450 71A4	misc
CUST_2215_PI426222305	0,003	7,358	up	PGSC0003DMT400072645	Cytochrome P450 76A2	misc
CUST_36532_PI426222305	0,002	4,249	up	PGSC0003DMT400064553	Peroxidase	misc
CUST_5746_PI426222305	0,049	3,407	up	PGSC0003DMT400006941	Cytochrome P450 76A1	misc
CUST_14464_PI426222305	0,009	2,462	up	PGSC0003DMT400066575	Phenylpropanoid:glucosyltransferase 1	misc
CUST_4184_PI426222305	0,029	2,977	up	PGSC0003DMT400007619	UDP-glucosyltransferase	misc
CUST_2079_PI426222305	0,011	4,823	up	PGSC0003DMT400028648	UDP-glucuronosyltransferase	misc
CUST_38537_PI426222305	0,014	3,704	up	PGSC0003DMT400001996	Geraniol 10-hydroxylase	misc
CUST_51610_PI426222305	0,006	2,884	up	PGSC0003DMT400005556	Glutathione-S-transferase	misc
CUST_13053_PI426222305	0,046	2,488	up	PGSC0003DMT400063236	Glycosyltransferase UGT90A7	misc
CUST_2636_PI426222305	0,007	2,878	up	PGSC0003DMT400080096	Zinc finger protein	misc
CUST_17565_PI426222305	0,015	19,842	up	PGSC0003DMT400068094	Steroleosin	misc
CUST_18427_PI426222305	0,049	2,199	up	PGSC0003DMT400050771	Amine oxidase	misc
CUST_10492_PI426222305	0,034	2,237	up	PGSC0003DMT400031663	Zinc finger protein	misc
CUST_44647_PI426222305	0,025	2,125	up	PGSC0003DMT400027490	CYP72A58	misc
CUST_7013_PI426222305	0,018	6,605	up	PGSC0003DMT400027906	3-ketoacyl-CoA reductase 2	misc
CUST_33221_PI426222305	0,038	3,122	up	PGSC0003DMT400024628	UDP-xylose phenolic glycosyltransferase	misc
CUST_2205_PI426222305	0,031	2,345	up	PGSC0003DMT400028650	UDP-glucose glucosyltransferase	misc
CUST_33121_PI426222305	0,022	2,227	up	PGSC0003DMT400067683	UDP-xylose phenolic glycosyltransferase	misc
CUST_40062_PI426222305	0,037	4,333	up	PGSC0003DMT400015175	Cytochrome P450	misc
CUST_2343_PI426222305	0,028	9,020	up	PGSC0003DMT400021622	Short chain alcohol dehydrogenase	misc
CUST_50817_PI426222305	0,014	9,255	up	PGSC0003DMT400059655	UDP-glucosyltransferase family 1 protein	misc
CUST_36423_PI426222305	0,047	4,156	up	PGSC0003DMT400079897	Alcohol dehydrogenase	misc
CUST_27028_PI426222305	0,007	2,945	up	PGSC0003DMT400052687	Cytochrome P450 71D7	misc
CUST_23399_PI426222305	0,038	2,412	up	PGSC0003DMT400073811	Pectinesterase inhibitor	misc
CUST_52580_PI426222305	0,040	3,398	up	PGSC0003DMT400017286	Cold-induced glucosyl transferase	misc
CUST_18594_PI426222305	0,021	2,132	up	PGSC0003DMT400042482	Multicopper oxidase	misc
CUST_19021_PI426222305	0,005	3,417	up	PGSC0003DMT400044514	CYP72A57	misc
CUST_48574_PI426222305	0,007	3,285	up	PGSC0003DMT400036392	Cytochrome P450	misc
CUST_28538_PI426222305	0,004	8,403	up	PGSC0003DMT400009964	UDP-glucose:glucosyltransferase	misc
CUST_27682_PI426222305	0,026	2,387	up	PGSC0003DMT400035395	UDP-glucosyltransferase	misc
CUST_51582_PI426222305	0,006	4,341	up	PGSC0003DMT400005542	Glutathione S-transferase	misc
CUST_32045_PI426222305	0,038	3,369	up	PGSC0003DMT400080417	Conserved gene of unknown function	misc
CUST_48561_PI426222305	0,044	3,306	up	PGSC0003DMT400036400	Cytochrome P450 monooxygenase CYP736B	misc
CUST_23913_PI426222305	0,021	2,917	up	PGSC0003DMT400032685	UDP-glucuronosyltransferase	misc
CUST_26951_PI426222305	0,017	2,872	up	PGSC0003DMT400052686	Cytochrome P450 71D7	misc
CUST_12725_PI426222305	0,011	3,403	up	PGSC0003DMT400062870	Mannosyl-oligosaccharide 1,2-alpha-mannosidase IA	misc
CUST_24015_PI426222305	0,006	2,756	up	PGSC0003DMT400032682	2-nitropropane dioxygenase	misc
CUST_36531_PI426222305	0,011	8,331	up	PGSC0003DMT400064525	P18 protein	misc
CUST_4110_PI426222305	0,032	2,313	up	PGSC0003DMT400038256	Taxane 13-alpha-hydroxylase cytochrome P450	misc
CUST_34699_PI426222305	0,020	3,981	up	PGSC0003DMT400001780	Glutathione S-transferase parA	misc
CUST_26792_PI426222305	0,037	2,900	up	PGSC0003DMT400035284	UDP-glucosyltransferase	misc
CUST_34958_PI426222305	0,041	4,962	up	PGSC0003DMT400073020	Zinc finger protein	misc
CUST_51591_PI426222305	0,043	2,194	up	PGSC0003DMT400005561	Glutathione S-transferase	misc
CUST_4270_PI426222305	0,029	2,223	up	PGSC0003DMT400070474	Non-specific lipid-transfer protein	misc
CUST_25836_PI426222305	0,020	5,650	up	PGSC0003DMT400051795	Glycosyltransferase QUASIMODO1	misc
CUST_5527_PI426222305	0,035	7,336	up	PGSC0003DMT400023140	Cytochrome P450	misc
CUST_33157_PI426222305	0,013	5,627	up	PGSC0003DMT400088362	N-hydroxycinnamoyl-CoA:tyramine N-hydroxycinnamoyl transferase THT1-3	misc
CUST_38513_PI426222305	0,043	2,179	up	PGSC0003DMT400001994	Salicylic acid-binding protein 2	misc
CUST_17937_PI426222305	0,007	5,569	up	PGSC0003DMT400006305	Beta-glucosidase 18	misc
CUST_5594_PI426222305	0,001	16,248	up	PGSC0003DMT400023141	Cytochrome P450	misc
CUST_41969_PI426222305	0,047	2,449	up	PGSC0003DMT400022319	D-lactate dehydrogenase	misc
CUST_29570_PI426222305	0,004	12,730	up	PGSC0003DMT400076023	Cytochrome P450	misc
CUST_4985_PI426222305	0,013	3,556	up	PGSC0003DMT400038579	Cytochrome P450	misc
CUST_11909_PI426222305	0,016	3,152	up	PGSC0003DMT400016547	GDSL-like Lipase/Acylhydrolase family protein	misc
CUST_51608_PI426222305	0,003	4,238	up	PGSC0003DMT400005543	Glutathione S-transferase	misc
CUST_18060_PI426222305	0,001	13,044	up	PGSC0003DMT400071057	Glutathione s-transferase	misc
CUST_28582_PI426222305	0,009	3,706	up	PGSC0003DMT400009963	UDP-glucoronosyl/UDP-glucosyl transferase family protein	misc
CUST_48646_PI426222305	0,035	6,585	up	PGSC0003DMT400064984	Glutathione S-transferase T1	misc
CUST_8512_PI426222305	0,001	7,581	up	PGSC0003DMT400029453	Cytochrome P450	misc
CUST_33687_PI426222305	0,014	2,143	up	PGSC0003DMT400078712	Cytochrome-c oxidase	Mitochondrial electron transport
CUST_50285_PI426222305	0,042	2,814	up	PGSC0003DMT400077785	Cytochrome-c oxidase	Mitochondrial electron transport
CUST_1361_PI426222305	0,008	2,533	up	PGSC0003DMT400003262	NADH dehydrogenase	Mitochondrial electron transport

CUST_50190_PI426222305	0,047	2,682	up	PGSC0003DMT400011362	Protein sco1	Mitochondrial electron transport
CUST_2571_PI426222305	0,023	2,067	up	PGSC0003DMT400072516	NADH:cytochrome b5 reductase	N-metabolism
CUST_11982_PI426222305	0,003	8,807	up	PGSC0003DMT400076676	Conserved gene of unknown function	Not assigned/Unknown
CUST_5926_PI426222305	0,020	2,227	up	PGSC0003DMT400056808	Gene of unknown function	Not assigned/Unknown
CUST_49570_PI426222305	0,034	3,285	up	PGSC0003DMT400013664	Conserved gene of unknown function	Not assigned/Unknown
CUST_38036_PI426222305	0,016	3,736	up	PGSC0003DMT400081395	TPR Domain containing protein	Not assigned/Unknown
CUST_30567_PI426222305	0,006	11,271	up	PGSC0003DMT400018721	Gene of unknown function	Not assigned/Unknown
CUST_22759_PI426222305	0,008	2,846	up	PGSC0003DMT400077949	Conserved gene of unknown function	Not assigned/Unknown
CUST_26613_PI426222305	0,040	9,662	up	PGSC0003DMT400000847	Conserved gene of unknown function	Not assigned/Unknown
CUST_22657_PI426222305	0,036	2,759	up	PGSC0003DMT400078135	Conserved gene of unknown function	Not assigned/Unknown
CUST_31134_PI426222305	0,033	2,768	up	PGSC0003DMT400063920	Conserved gene of unknown function	Not assigned/Unknown
CUST_16921_PI426222305	0,039	2,051	up	PGSC0003DMT400046077	Conserved gene of unknown function	Not assigned/Unknown
CUST_34151_PI426222305	0,008	2,805	up	PGSC0003DMT400019739	Gene of unknown function	Not assigned/Unknown
CUST_15646_PI426222305	0,004	3,251	up	PGSC0003DMT400090342	Gene of unknown function	Not assigned/Unknown
CUST_30894_PI426222305	0,034	2,986	up	PGSC0003DMT400037897	Conserved gene of unknown function	Not assigned/Unknown
CUST_32324_PI426222305	0,037	2,268	up	PGSC0003DMT400027544	Conserved gene of unknown function	Not assigned/Unknown
CUST_37489_PI426222305	0,036	2,408	up	PGSC0003DMT400078820	Defensin protein	Not assigned/Unknown
CUST_27039_PI426222305	0,016	3,338	up	PGSC0003DMT400067138	Conserved gene of unknown function	Not assigned/Unknown
CUST_8435_PI426222305	0,016	6,440	up	PGSC0003DMT400029505	Flowering promoting factor-like 1	Not assigned/Unknown
CUST_45562_PI426222305	0,021	4,151	up	PGSC0003DMT400008581	Conserved gene of unknown function	Not assigned/Unknown
CUST_8908_PI426222305	0,002	4,629	up	PGSC0003DMT400013014	ATP binding protein	Not assigned/Unknown
CUST_46609_PI426222305	0,032	4,302	up	PGSC0003DMT400092506	NB-ARC domain containing protein	Not assigned/Unknown
CUST_31268_PI426222305	0,009	2,562	up	PGSC0003DMT400034881	THM18 protein	Not assigned/Unknown
CUST_10556_PI426222305	0,015	3,152	up	PGSC0003DMT400031938	Brain protein 44	Not assigned/Unknown
CUST_39597_PI426222305	0,021	3,362	up	PGSC0003DMT400058777	Gene of unknown function	Not assigned/Unknown
CUST_43561_PI426222305	0,003	3,844	up	PGSC0003DMT400064748	Uncharacterized ACR, COG1678 family protein	Not assigned/Unknown
CUST_7132_PI426222305	0,022	4,335	up	PGSC0003DMT400045611	Methyltransferase/ nucleic acid binding protein	Not assigned/Unknown
CUST_37616_PI426222305	0,016	2,383	up	PGSC0003DMT400049647	Cotton fiber expressed protein 1	Not assigned/Unknown
CUST_3702_PI426222305	0,002	4,262	up	PGSC0003DMT400048846	Gene of unknown function	Not assigned/Unknown
CUST_39601_PI426222305	0,045	3,758	up	PGSC0003DMT400028083	Organ-specific protein P4	Not assigned/Unknown
CUST_21741_PI426222305	0,005	8,313	up	PGSC0003DMT400090715	Zinc-binding family protein	Not assigned/Unknown
CUST_12352_PI426222305	0,000	27,176	up	PGSC0003DMT400063786	RING-H2 finger protein ATL18	Not assigned/Unknown
CUST_52611_PI426222305	0,028	4,341	up	PGSC0003DMT400082139	Gene of unknown function	Not assigned/Unknown
CUST_16666_PI426222305	0,024	2,342	up	PGSC0003DMT400069526	Conserved gene of unknown function	Not assigned/Unknown
CUST_42199_PI426222305	0,022	2,019	up	PGSC0003DMT400038218	Gene of unknown function	Not assigned/Unknown
CUST_7487_PI426222305	0,010	8,272	up	PGSC0003DMT400009455	Gene of unknown function	Not assigned/Unknown
CUST_31432_PI426222305	0,003	4,533	up	PGSC0003DMT400073315	Phospholipid N-methyltransferase	Not assigned/Unknown
CUST_51007_PI426222305	0,007	4,126	up	PGSC0003DMT400089222	Gene of unknown function	Not assigned/Unknown
CUST_14816_PI426222305	0,006	26,522	up	PGSC0003DMT400086180	Gene of unknown function	Not assigned/Unknown
CUST_24270_PI426222305	0,011	5,755	up	PGSC0003DMT400085877	Gene of unknown function	Not assigned/Unknown
CUST_51635_PI426222305	0,032	3,605	up	PGSC0003DMT400034192	Ripening induced protein	Not assigned/Unknown
CUST_46210_PI426222305	0,007	3,816	up	PGSC0003DMT400011421	Lachrymatory-factor synthase	Not assigned/Unknown
CUST_27470_PI426222305	0,023	8,967	up	PGSC0003DMT400056517	Conserved gene of unknown function	Not assigned/Unknown
CUST_13814_PI426222305	0,039	2,649	up	PGSC0003DMT400097608	Gene of unknown function	Not assigned/Unknown
CUST_14860_PI426222305	0,032	2,825	up	PGSC0003DMT400084797	Gene of unknown function	Not assigned/Unknown
CUST_51435_PI426222305	0,050	2,000	up	PGSC0003DMT400034007	Conserved gene of unknown function	Not assigned/Unknown
CUST_51258_PI426222305	0,001	4,571	up	PGSC0003DMT400072117	Disease resistance protein RPS5	Not assigned/Unknown
CUST_45060_PI426222305	0,013	10,920	up	PGSC0003DMT400017248	Conserved gene of unknown function	Not assigned/Unknown
CUST_26064_PI426222305	0,008	3,562	up	PGSC0003DMT400052535	Conserved gene of unknown function	Not assigned/Unknown
CUST_39075_PI426222305	0,033	2,610	up	PGSC0003DMT400008686	Conserved gene of unknown function	Not assigned/Unknown
CUST_35871_PI426222305	0,040	3,168	up	PGSC0003DMT400045904	Integrase core domain containing protein	Not assigned/Unknown
CUST_51397_PI426222305	0,007	7,434	up	PGSC0003DMT400094878	Gene of unknown function	Not assigned/Unknown
CUST_5187_PI426222305	0,007	2,903	up	PGSC0003DMT400004021	Conserved gene of unknown function	Not assigned/Unknown
CUST_51465_PI426222305	0,022	5,459	up	PGSC0003DMT400091678	Gene of unknown function	Not assigned/Unknown
CUST_26393_PI426222305	0,039	3,783	up	PGSC0003DMT400037234	PAR-1c protein	Not assigned/Unknown
CUST_7818_PI426222305	0,032	2,995	up	PGSC0003DMT400025849	BTB/POZ domain-containing protein	Not assigned/Unknown
CUST_8737_PI426222305	0,001	13,047	up	PGSC0003DMT400053997	Conserved gene of unknown function	Not assigned/Unknown
CUST_10006_PI426222305	0,001	6,741	up	PGSC0003DMT400038433	Gene of unknown function	Not assigned/Unknown
CUST_39988_PI426222305	0,036	2,804	up	PGSC0003DMT400030309	Extensin Ext1	Not assigned/Unknown
CUST_30929_PI426222305	0,038	3,872	up	PGSC0003DMT400082415	Early nodulin 75 protein	Not assigned/Unknown
CUST_38240_PI426222305	0,012	2,574	up	PGSC0003DMT400067246	6-phosphogluconolactonase 5, chloroplastic	Not assigned/Unknown
CUST_8883_PI426222305	0,002	4,988	up	PGSC0003DMT400033348	Conserved gene of unknown function	Not assigned/Unknown
CUST_17512_PI426222305	0,048	2,485	up	PGSC0003DMT400068081	Metal ion binding protein	Not assigned/Unknown
CUST_29865_PI426222305	0,020	3,411	up	PGSC0003DMT400097493	Atpob1	Not assigned/Unknown
CUST_9142_PI426222305	0,009	2,979	up	PGSC0003DMT400093660	Gene of unknown function	Not assigned/Unknown
CUST_42246_PI426222305	0,038	3,054	up	PGSC0003DMT400050854	Gene of unknown function	Not assigned/Unknown

Appendix

CUST_44548_PI426222305	0,045	2,294	up	PGSC0003DMT400043068	Conserved gene of unknown function	Not assigned/Unknown
CUST_852_PI426222305	0,036	2,701	up	PGSC0003DMT400001287	Conserved gene of unknown function	Not assigned/Unknown
CUST_49653_PI426222305	0,010	3,939	up	PGSC0003DMT400051227	Conserved gene of unknown function	Not assigned/Unknown
CUST_26539_PI426222305	0,011	15,715	up	PGSC0003DMT400000826	Protein ABIL5	Not assigned/Unknown
CUST_41079_PI426222305	0,002	5,328	up	PGSC0003DMT400097712	TNP2-like transposon protein	Not assigned/Unknown
CUST_38029_PI426222305	0,023	4,041	up	PGSC0003DMT400081308	Gene of unknown function	Not assigned/Unknown
CUST_23256_PI426222305	0,038	3,135	up	PGSC0003DMT400002565	GEX1	Not assigned/Unknown
CUST_44641_PI426222305	0,024	6,699	up	PGSC0003DMT400027465	Sesquiterpene synthase	Not assigned/Unknown
CUST_33782_PI426222305	0,048	4,181	up	PGSC0003DMT400092494	Gene of unknown function	Not assigned/Unknown
CUST_39806_PI426222305	0,042	3,956	up	PGSC0003DMT400095116	Gene of unknown function	Not assigned/Unknown
CUST_5410_PI426222305	0,018	2,194	up	PGSC0003DMT400003935	TSI-1 protein	Not assigned/Unknown
CUST_28951_PI426222305	0,015	5,965	up	PGSC0003DMT400096668	Gene of unknown function	Not assigned/Unknown
CUST_25633_PI426222305	0,026	2,110	up	PGSC0003DMT400029348	S-adenosylmethionine-dependent methyltransferase	Not assigned/Unknown
CUST_37014_PI426222305	0,018	5,438	up	PGSC0003DMT400022213	Gene of unknown function	Not assigned/Unknown
CUST_19429_PI426222305	0,014	2,435	up	PGSC0003DMT400072804	Ankyrin repeat family protein	Not assigned/Unknown
CUST_4334_PI426222305	0,001	8,564	up	PGSC0003DMT400050588	Conserved gene of unknown function	Not assigned/Unknown
CUST_52307_PI426222305	0,023	7,199	up	PGSC0003DMT400039105	Ulp1 protease family, C-terminal catalytic domain containing protein	Not assigned/Unknown
CUST_36819_PI426222305	0,036	2,575	up	PGSC0003DMT400015858	Protein prenyltransferase	Not assigned/Unknown
CUST_535_PI426222305	0,046	4,962	up	PGSC0003DMT400085133	Gene of unknown function	Not assigned/Unknown
CUST_9922_PI426222305	0,042	6,917	up	PGSC0003DMT400003139	Gene of unknown function	Not assigned/Unknown
CUST_50220_PI426222305	0,038	11,572	up	PGSC0003DMT400088010	Mads box protein	Not assigned/Unknown
CUST_23969_PI426222305	0,044	4,479	up	PGSC0003DMT400032636	Conserved gene of unknown function	Not assigned/Unknown
CUST_33090_PI426222305	0,013	3,054	up	PGSC0003DMT400058825	F-box family protein	Not assigned/Unknown
CUST_23475_PI426222305	0,025	2,876	up	PGSC0003DMT400035647	ATP binding protein	Not assigned/Unknown
CUST_42418_PI426222305	0,019	3,855	up	PGSC0003DMT400052890	Gene of unknown function	Not assigned/Unknown
CUST_43573_PI426222305	0,002	4,175	up	PGSC0003DMT400064749	Conserved gene of unknown function	Not assigned/Unknown
CUST_30064_PI426222305	0,037	2,254	up	PGSC0003DMT400003253	Conserved gene of unknown function	Not assigned/Unknown
CUST_10083_PI426222305	0,018	2,646	up	PGSC0003DMT400097544	Gene of unknown function	Not assigned/Unknown
CUST_43905_PI426222305	0,035	3,598	up	PGSC0003DMT400045392	Gag-pol polyprotein	Not assigned/Unknown
CUST_48141_PI426222305	0,016	2,256	up	PGSC0003DMT400091642	Gene of unknown function	Not assigned/Unknown
CUST_3822_PI426222305	0,006	20,915	up	PGSC0003DMT400093950	Gene of unknown function	Not assigned/Unknown
CUST_8957_PI426222305	0,005	6,172	up	PGSC0003DMT400033347	Conserved gene of unknown function	Not assigned/Unknown
CUST_15760_PI426222305	0,020	3,199	up	PGSC0003DMT400057812	Conserved gene of unknown function	Not assigned/Unknown
CUST_44571_PI426222305	0,003	4,627	up	PGSC0003DMT400041324	Gene of unknown function	Not assigned/Unknown
CUST_28912_PI426222305	0,041	3,252	up	PGSC0003DMT400033733	Conserved gene of unknown function	Not assigned/Unknown
CUST_32274_PI426222305	0,030	2,831	up	PGSC0003DMT400012720	Conserved gene of unknown function	Not assigned/Unknown
CUST_15161_PI426222305	0,026	14,782	up	PGSC0003DMT400057385	Conserved gene of unknown function	Not assigned/Unknown
CUST_51899_PI426222305	0,001	14,136	up	PGSC0003DMT400094771	F-box family protein	Not assigned/Unknown
CUST_12045_PI426222305	0,027	2,454	up	PGSC0003DMT400092647	Conserved gene of unknown function	Not assigned/Unknown
CUST_8434_PI426222305	0,022	5,243	up	PGSC0003DMT400086027	Conserved gene of unknown function	Not assigned/Unknown
CUST_29924_PI426222305	0,013	5,847	up	PGSC0003DMT400040598	Gene of unknown function	Not assigned/Unknown
CUST_1204_PI426222305	0,004	3,612	up	PGSC0003DMT400003412	Mitochondrial saccharopine dehydrogenase	Not assigned/Unknown
CUST_41035_PI426222305	0,021	2,028	up	PGSC0003DMT400048862	Gene of unknown function	Not assigned/Unknown
CUST_18824_PI426222305	0,037	2,097	up	PGSC0003DMT400001095	Shugoshin-1	Not assigned/Unknown
CUST_32016_PI426222305	0,010	3,807	up	PGSC0003DMT400083266	Tospovirus resistance protein C	Not assigned/Unknown
CUST_32637_PI426222305	0,008	15,684	up	PGSC0003DMT400095208	Gene of unknown function	Not assigned/Unknown
CUST_31546_PI426222305	0,004	3,527	up	PGSC0003DMT400073316	N-methyltransferase	Not assigned/Unknown
CUST_14102_PI426222305	0,049	5,419	up	PGSC0003DMT400059943	3'(2'),5'-bisphosphate nucleotidase	Not assigned/Unknown
CUST_866_PI426222305	0,004	3,111	up	PGSC0003DMT400003752	Conserved gene of unknown function	Not assigned/Unknown
CUST_11298_PI426222305	0,008	2,709	up	PGSC0003DMT400037700	Conserved gene of unknown function	Not assigned/Unknown
CUST_47826_PI426222305	0,001	8,464	up	PGSC0003DMT400068333	Conserved gene of unknown function	Not assigned/Unknown
CUST_44766_PI426222305	0,009	8,513	up	PGSC0003DMT400096327	Gene of unknown function	Not assigned/Unknown
CUST_22685_PI426222305	0,004	3,128	up	PGSC0003DMT400078044	Lipopolysaccharide-modifying protein	Not assigned/Unknown
CUST_45799_PI426222305	0,022	2,619	up	PGSC0003DMT400050233	Conserved gene of unknown function	Not assigned/Unknown
CUST_25329_PI426222305	0,032	2,031	up	PGSC0003DMT400034690	Transmembrane transporter	Not assigned/Unknown
CUST_49511_PI426222305	0,008	2,941	up	PGSC0003DMT400071905	Hypoxia induced protein conserved region containing protein	Not assigned/Unknown
CUST_21731_PI426222305	0,021	3,688	up	PGSC0003DMT400051180	Conserved gene of unknown function	Not assigned/Unknown
CUST_30088_PI426222305	0,031	2,227	up	PGSC0003DMT400097308	Gag-pol protein	Not assigned/Unknown
CUST_44693_PI426222305	0,006	2,961	up	PGSC0003DMT400045319	Conserved gene of unknown function	Not assigned/Unknown
CUST_39189_PI426222305	0,007	3,753	up	PGSC0003DMT400016710	Gene of unknown function	Not assigned/Unknown
CUST_2346_PI426222305	0,017	3,181	up	PGSC0003DMT400028645	Heparanase	Not assigned/Unknown
CUST_44305_PI426222305	0,006	2,731	up	PGSC0003DMT400010101	Conserved gene of unknown function	Not assigned/Unknown
CUST_49855_PI426222305	0,031	2,090	up	PGSC0003DMT400013114	Conserved gene of unknown function	Not assigned/Unknown
CUST_18670_PI426222305	0,036	6,756	up	PGSC0003DMT400095957	Mads box protein	Not assigned/Unknown
CUST_10553_PI426222305	0,019	3,383	up	PGSC0003DMT400031594	Conserved gene of unknown function	Not assigned/Unknown
CUST_27227_PI426222305	0,015	2,212	up	PGSC0003DMT400059482	Phloem protein 2-B2	Not assigned/Unknown

CUST_12966_PI426222305	0,022	2,367	up	PGSC0003DMT400062923	Conserved gene of unknown function	Not assigned/Unknown
CUST_48135_PI426222305	0,001	11,053	up	PGSC0003DMT400065575	Adaptin ear-binding coat-associated protein	Not assigned/Unknown
CUST_43895_PI426222305	0,047	2,064	up	PGSC0003DMT400091279	Chloroplast lumen common family protein	Not assigned/Unknown
CUST_9730_PI426222305	0,010	5,892	up	PGSC0003DMT400088551	Uniprot|P20840 Saccharomyces cerevisiae YJR004c SAG1 alpha-agglutinin	Not assigned/Unknown
CUST_13972_PI426222305	0,042	2,391	up	PGSC0003DMT400061428	Conserved gene of unknown function	Not assigned/Unknown
CUST_48755_PI426222305	0,029	2,526	up	PGSC0003DMT400091248	Gene of unknown function	Not assigned/Unknown
CUST_12220_PI426222305	0,046	2,427	up	PGSC0003DMT400043149	VAP27	Not assigned/Unknown
CUST_17773_PI426222305	0,003	3,935	up	PGSC0003DMT400066764	Conserved gene of unknown function	Not assigned/Unknown
CUST_46443_PI426222305	0,036	4,292	up	PGSC0003DMT400005896	Conserved gene of unknown function	Not assigned/Unknown
CUST_33511_PI426222305	0,049	2,712	up	PGSC0003DMT400058264	Binding protein	Not assigned/Unknown
CUST_24388_PI426222305	0,020	2,679	up	PGSC0003DMT400062383	Conserved gene of unknown function	Not assigned/Unknown
CUST_34891_PI426222305	0,009	2,611	up	PGSC0003DMT400073078	Conserved gene of unknown function	Not assigned/Unknown
CUST_26472_PI426222305	0,047	2,536	up	PGSC0003DMT400037218	Gene of unknown function	Not assigned/Unknown
CUST_27440_PI426222305	0,006	2,804	up	PGSC0003DMT400070826	Protein EPIDERMAL PATTERNING FACTOR 2	Not assigned/Unknown
CUST_33460_PI426222305	0,006	4,378	up	PGSC0003DMT400058265	Binding protein	Not assigned/Unknown
CUST_19419_PI426222305	0,046	2,242	up	PGSC0003DMT400019466	Gene of unknown function	Not assigned/Unknown
CUST_51545_PI426222305	0,007	4,195	up	PGSC0003DMT400031324	Heterogeneous nuclear ribonucleoprotein A3 2	Not assigned/Unknown
CUST_35474_PI426222305	0,047	3,098	up	PGSC0003DMT400032445	Conserved gene of unknown function	Not assigned/Unknown
CUST_25386_PI426222305	0,033	2,343	up	PGSC0003DMT400034601	ATFP3	Not assigned/Unknown
CUST_1801_PI426222305	0,002	3,711	up	PGSC0003DMT400096585	Gene of unknown function	Not assigned/Unknown
CUST_3704_PI426222305	0,041	4,693	up	PGSC0003DMT400064184	Gene of unknown function	Not assigned/Unknown
CUST_10719_PI426222305	0,031	2,171	up	PGSC0003DMT400031981	Membrane protein	Not assigned/Unknown
CUST_28890_PI426222305	0,017	2,971	up	PGSC0003DMT400019781	Gene of unknown function	Not assigned/Unknown
CUST_49815_PI426222305	0,002	30,659	up	PGSC0003DMT400033778	Gene of unknown function	Not assigned/Unknown
CUST_34008_PI426222305	0,001	5,061	up	PGSC0003DMT400047878	Gene of unknown function	Not assigned/Unknown
CUST_49266_PI426222305	0,003	7,003	up	PGSC0003DMT400085580	Conserved gene of unknown function	Not assigned/Unknown
CUST_22997_PI426222305	0,021	2,523	up	PGSC0003DMT400076776	N-acylneuraminate-9-phosphatase	Not assigned/Unknown
CUST_33592_PI426222305	0,014	6,092	up	PGSC0003DMT400067863	Gene of unknown function	Not assigned/Unknown
CUST_21279_PI426222305	0,004	4,084	up	PGSC0003DMT400020338	Protein EPIDERMAL PATTERNING FACTOR 1	Not assigned/Unknown
CUST_13149_PI426222305	0,005	4,568	up	PGSC0003DMT400089578	Gene of unknown function	Not assigned/Unknown
CUST_18208_PI426222305	0,007	10,590	up	PGSC0003DMT400042213	Conserved gene of unknown function	Not assigned/Unknown
CUST_16413_PI426222305	0,037	3,451	up	PGSC0003DMT400027945	Gene of unknown function	Not assigned/Unknown
CUST_39009_PI426222305	0,007	5,798	up	PGSC0003DMT400091017	Seed maturation protein PM36	Not assigned/Unknown
CUST_45132_PI426222305	0,016	2,996	up	PGSC0003DMT400006111	Gene of unknown function	Not assigned/Unknown
CUST_17732_PI426222305	0,007	3,200	up	PGSC0003DMT400066766	Conserved gene of unknown function	Not assigned/Unknown
CUST_7089_PI426222305	0,025	8,664	up	PGSC0003DMT400095342	Gene of unknown function	Not assigned/Unknown
CUST_11232_PI426222305	0,003	3,756	up	PGSC0003DMT400037754	CONSTANS-like zinc finger protein	Not assigned/Unknown
CUST_34434_PI426222305	0,023	2,236	up	PGSC0003DMT400055614	Gene of unknown function	Not assigned/Unknown
CUST_20022_PI426222305	0,043	3,972	up	PGSC0003DMT400086142	Endonuclease/exonuclease/phosphatase	Not assigned/Unknown
CUST_47612_PI426222305	0,004	4,565	up	PGSC0003DMT400030574	Gene of unknown function	Not assigned/Unknown
CUST_19712_PI426222305	0,020	13,943	up	PGSC0003DMT400061178	Gene of unknown function	Not assigned/Unknown
CUST_50472_PI426222305	0,009	3,465	up	PGSC0003DMT400024848	Ice binding protein	Not assigned/Unknown
CUST_29250_PI426222305	0,034	4,012	up	PGSC0003DMT400004735	Conserved gene of unknown function	Not assigned/Unknown
CUST_24373_PI426222305	0,019	3,397	up	PGSC0003DMT400074140	Glycine rich protein-interacting protein	Not assigned/Unknown
CUST_26571_PI426222305	0,011	2,331	up	PGSC0003DMT400000995	Gene of unknown function	Not assigned/Unknown
CUST_34916_PI426222305	0,025	2,253	up	PGSC0003DMT400073079	Conserved gene of unknown function	Not assigned/Unknown
CUST_37705_PI426222305	0,027	3,538	up	PGSC0003DMT400053645	Conserved gene of unknown function	Not assigned/Unknown
CUST_17172_PI426222305	0,006	5,919	up	PGSC0003DMT400070763	Conserved gene of unknown function	Not assigned/Unknown
CUST_17489_PI426222305	0,050	2,067	up	PGSC0003DMT400068062	Gamma-glutamylcyclotransferase	Not assigned/Unknown
CUST_36397_PI426222305	0,002	7,594	up	PGSC0003DMT400079924	Non-specific lipid-transfer protein	Not assigned/Unknown
CUST_50825_PI426222305	0,035	3,289	up	PGSC0003DMT400022262	Gene of unknown function	Not assigned/Unknown
CUST_4683_PI426222305	0,025	2,839	up	PGSC0003DMT400059509	Cytochrome P450-type monooxygenase 97A29	Not assigned/Unknown
CUST_22898_PI426222305	0,014	3,152	up	PGSC0003DMT400060933	Conserved gene of unknown function	Not assigned/Unknown
CUST_4540_PI426222305	0,038	2,135	up	PGSC0003DMT400020929	Protein SUA5	Not assigned/Unknown
CUST_48030_PI426222305	0,043	2,299	up	PGSC0003DMT400021782	Conserved gene of unknown function	Not assigned/Unknown
CUST_47559_PI426222305	0,020	2,100	up	PGSC0003DMT400027233	Photosystem II 5 kDa protein, chloroplast	Not assigned/Unknown
CUST_22377_PI426222305	0,032	2,937	up	PGSC0003DMT400039397	Gene of unknown function	Not assigned/Unknown
CUST_35511_PI426222305	0,030	2,286	up	PGSC0003DMT400032620	SPX domain-containing membrane protein	Not assigned/Unknown
CUST_18854_PI426222305	0,030	2,539	up	PGSC0003DMT400068256	Conserved gene of unknown function	Not assigned/Unknown
CUST_5366_PI426222305	0,024	2,076	up	PGSC0003DMT400030295	Cyclin-like F-box; F-box protein interaction domain	Not assigned/Unknown
CUST_23513_PI426222305	0,026	2,622	up	PGSC0003DMT400023821	Conserved gene of unknown function	Not assigned/Unknown
CUST_3558_PI426222305	0,005	4,305	up	PGSC0003DMT400064305	Conserved gene of unknown function	Not assigned/Unknown
CUST_34902_PI426222305	0,017	3,677	up	PGSC0003DMT400073241	Aquaporin NIP1;2	Not assigned/Unknown
CUST_37645_PI426222305	0,043	2,034	up	PGSC0003DMT400049656	Conserved gene of unknown function	Not assigned/Unknown
CUST_48052_PI426222305	0,023	2,434	up	PGSC0003DMT400021746	Proline-rich protein	Not assigned/Unknown
CUST_50421_PI426222305	0,006	2,945	up	PGSC0003DMT400010917	NADH ubiquinone oxidoreductase B14 subunit	Not assigned/Unknown

Appendix

CUST_32275_PI426222305	0,029	2,305	up	PGSC0003DMT400012717	Erg28	Not assigned/Unknow n
CUST_52221_PI426222305	0,004	4,075	up	PGSC0003DMT400006289	Cysteine-rich extensin-2	Not assigned/Unknow n
CUST_29742_PI426222305	0,013	3,339	up	PGSC0003DMT400080505	Amino acid transporter family protein	Not assigned/Unknow n
CUST_49510_PI426222305	0,009	2,939	up	PGSC0003DMT400071904	Hypoxia induced protein conserved region containing protein	Not assigned/Unknow n
CUST_44923_PI426222305	0,047	2,096	up	PGSC0003DMT400058616	Protein OBERON 3	Not assigned/Unknow n
CUST_38695_PI426222305	0,012	3,565	up	PGSC0003DMT400094971	Conserved gene of unknow n function	Not assigned/Unknow n
CUST_24297_PI426222305	0,017	3,321	up	PGSC0003DMT400074141	Glycine rich protein-interacting protein	Not assigned/Unknow n
CUST_28941_PI426222305	0,010	8,663	up	PGSC0003DMT400033961	TdcA1-ORF1-ORF2 protein	Not assigned/Unknow n
CUST_11444_PI426222305	0,005	3,829	up	PGSC0003DMT400010653	Conserved gene of unknow n function	Not assigned/Unknow n
CUST_33708_PI426222305	0,023	4,468	up	PGSC0003DMT400067864	Gene of unknow n function	Not assigned/Unknow n
CUST_37575_PI426222305	0,010	2,399	up	PGSC0003DMT400049657	Conserved gene of unknow n function	Not assigned/Unknow n
CUST_50989_PI426222305	0,011	7,960	up	PGSC0003DMT400083999	F-box family protein	Not assigned/Unknow n
CUST_37668_PI426222305	0,016	2,126	up	PGSC0003DMT400049648	Conserved gene of unknow n function	Not assigned/Unknow n
CUST_12747_PI426222305	0,049	5,586	up	PGSC0003DMT400063332	Conserved gene of unknow n function	Not assigned/Unknow n
CUST_8297_PI426222305	0,036	2,251	up	PGSC0003DMT400030201	Conserved gene of unknow n function	Not assigned/Unknow n
CUST_28514_PI426222305	0,047	4,098	up	PGSC0003DMT400055482	Conserved gene of unknow n function	Not assigned/Unknow n
CUST_51672_PI426222305	0,010	6,398	up	PGSC0003DMT400056661	Protein translocase	Not assigned/Unknow n
CUST_24218_PI426222305	0,002	7,761	up	PGSC0003DMT400087471	Gene of unknow n function	Not assigned/Unknow n
CUST_52610_PI426222305	0,022	4,466	up	PGSC0003DMT400082140	GJ10070	Not assigned/Unknow n
CUST_17762_PI426222305	0,006	3,377	up	PGSC0003DMT400066765	Glycine-rich protein	Not assigned/Unknow n
CUST_21609_PI426222305	0,017	2,413	up	PGSC0003DMT400037645	Integrase core domain containing protein	Not assigned/Unknow n
CUST_35965_PI426222305	0,043	2,737	up	PGSC0003DMT400080961	Glycine-rich protein A3	Not assigned/Unknow n
CUST_3116_PI426222305	0,006	11,625	up	PGSC0003DMT400000703	Gene of unknow n function	Not assigned/Unknow n
CUST_9230_PI426222305	0,020	2,373	up	PGSC0003DMT400006431	RWD domain-containing protein	Not assigned/Unknow n
CUST_36040_PI426222305	0,007	3,082	up	PGSC0003DMT400080941	Gene of unknow n function	Not assigned/Unknow n
CUST_35056_PI426222305	0,042	3,011	up	PGSC0003DMT400090246	Gene of unknow n function	Not assigned/Unknow n
CUST_7204_PI426222305	0,038	2,654	up	PGSC0003DMT400071781	Conserved gene of unknow n function	Not assigned/Unknow n
CUST_44639_PI426222305	0,011	4,475	up	PGSC0003DMT400062801	Sesquiterpene synthase	Not assigned/Unknow n
CUST_14762_PI426222305	0,002	4,598	up	PGSC0003DMT400066170	Gene of unknow n function	Not assigned/Unknow n
CUST_16138_PI426222305	0,003	7,779	up	PGSC0003DMT400031355	Gene of unknow n function	Not assigned/Unknow n
CUST_17886_PI426222305	0,029	7,956	up	PGSC0003DMT400071054	Gene of unknow n function	Not assigned/Unknow n
CUST_49571_PI426222305	0,029	3,220	up	PGSC0003DMT400013663	Conserved gene of unknow n function	Not assigned/Unknow n
CUST_43069_PI426222305	0,001	4,693	up	PGSC0003DMT400018861	Acyltransferase	Not assigned/Unknow n
CUST_33051_PI426222305	0,035	2,480	up	PGSC0003DMT400058817	Zinc finger family protein	Not assigned/Unknow n
CUST_38820_PI426222305	0,038	2,048	up	PGSC0003DMT400015418	Gene of unknow n function	Not assigned/Unknow n
CUST_30768_PI426222305	0,048	2,414	up	PGSC0003DMT400089934	Polyadenylation factor subunit	Not assigned/Unknow n
CUST_22127_PI426222305	0,028	2,023	up	PGSC0003DMT400023463	Surfeit locus protein 5 family protein	Not assigned/Unknow n
CUST_37795_PI426222305	0,005	3,022	up	PGSC0003DMT400077009	Conserved gene of unknow n function	Not assigned/Unknow n
CUST_18698_PI426222305	0,034	2,353	up	PGSC0003DMT400001096	Shugoshin-1	Not assigned/Unknow n
CUST_43234_PI426222305	0,002	5,326	up	PGSC0003DMT400002040	Extensin (ext)	Not assigned/Unknow n
CUST_43794_PI426222305	0,017	4,931	up	PGSC0003DMT400040123	An Arabidopsis thaliana chromosome BAC genomic sequence	Not assigned/Unknow n
CUST_27492_PI426222305	0,004	10,340	up	PGSC0003DMT400070909	Gag-pol polyprotein	Not assigned/Unknow n
CUST_27383_PI426222305	0,039	6,876	up	PGSC0003DMT400086799	Conserved gene of unknow n function	Not assigned/Unknow n
CUST_18305_PI426222305	0,008	5,341	up	PGSC0003DMT400042354	Conserved gene of unknow n function	Not assigned/Unknow n
CUST_47400_PI426222305	0,016	2,130	up	PGSC0003DMT400011293	Transferase, transferring glycosyl groups	Not assigned/Unknow n
CUST_45592_PI426222305	0,001	29,086	up	PGSC0003DMT400008580	Conserved gene of unknow n function	Not assigned/Unknow n
CUST_47966_PI426222305	0,013	3,422	up	PGSC0003DMT400074404	Gene of unknow n function	Not assigned/Unknow n
CUST_5577_PI426222305	0,012	4,641	up	PGSC0003DMT400007071	VQ motif-containing protein	Not assigned/Unknow n
CUST_26131_PI426222305	0,020	2,594	up	PGSC0003DMT400041857	Conserved gene of unknow n function	Not assigned/Unknow n
CUST_15154_PI426222305	0,023	2,147	up	PGSC0003DMT400057473	Conserved gene of unknow n function	Not assigned/Unknow n
CUST_3615_PI426222305	0,049	2,163	up	PGSC0003DMT400040793	Conserved gene of unknow n function	Not assigned/Unknow n
CUST_5547_PI426222305	0,007	3,032	up	PGSC0003DMT400007053	Conserved gene of unknow n function	Not assigned/Unknow n
CUST_48784_PI426222305	0,013	2,401	up	PGSC0003DMT400043902	Gene of unknow n function	Not assigned/Unknow n
CUST_36983_PI426222305	0,035	3,454	up	PGSC0003DMT400090640	Integrase core domain containing protein	Not assigned/Unknow n
CUST_32646_PI426222305	0,031	2,366	up	PGSC0003DMT400031531	Calcyclin-binding protein	Not assigned/Unknow n
CUST_31531_PI426222305	0,030	10,139	up	PGSC0003DMT400073400	Conserved gene of unknow n function	Not assigned/Unknow n
CUST_10770_PI426222305	0,014	2,167	up	PGSC0003DMT400031775	Conserved gene of unknow n function	Not assigned/Unknow n
CUST_35916_PI426222305	0,018	2,135	up	PGSC0003DMT400042907	Sorghum bicolor protein targeted either to mitochondria or chloroplast proteins T50848	Not assigned/Unknow n
CUST_38067_PI426222305	0,020	2,075	up	PGSC0003DMT400094978	Integrase core domain containing protein	Not assigned/Unknow n
CUST_47752_PI426222305	0,010	5,225	up	PGSC0003DMT400086241	Conserved gene of unknow n function	Not assigned/Unknow n
CUST_11306_PI426222305	0,001	8,889	up	PGSC0003DMT400007462	Gene of unknow n function	Not assigned/Unknow n
CUST_11898_PI426222305	0,000	12,731	up	PGSC0003DMT400033428	Anti-PCD protein	Not assigned/Unknow n
CUST_48779_PI426222305	0,000	13,143	up	PGSC0003DMT400077271	Gene of unknow n function	Not assigned/Unknow n
CUST_43892_PI426222305	0,005	8,980	up	PGSC0003DMT400091704	Gene of unknow n function	Not assigned/Unknow n
CUST_43085_PI426222305	0,012	2,407	up	PGSC0003DMT400018904	Mo-molybdopterin cofactor sulfurase	Not assigned/Unknow n
CUST_33073_PI426222305	0,032	6,497	up	PGSC0003DMT400016117	Gene of unknow n function	Not assigned/Unknow n

CUST_20347_PI426222305	0,005	4,122	up	PGSC0003DMT400049709	Sulfate transporter	Not assigned/Unknown n
CUST_8149_PI426222305	0,038	3,046	up	PGSC0003DMT400075395	Gene of unknown function	Not assigned/Unknown n
CUST_27615_PI426222305	0,046	3,685	up	PGSC0003DMT400094524	Gene of unknown function	Not assigned/Unknown n
CUST_18252_PI426222305	0,022	4,830	up	PGSC0003DMT400042272	OBP32pep	Not assigned/Unknown n
CUST_35412_PI426222305	0,006	3,810	up	PGSC0003DMT400079441	Conserved gene of unknown function	Not assigned/Unknown n
CUST_29215_PI426222305	0,031	3,939	up	PGSC0003DMT400004734	Conserved gene of unknown function	Not assigned/Unknown n
CUST_29908_PI426222305	0,018	2,860	up	PGSC0003DMT400086953	Zinc knuckle family protein	Not assigned/Unknown n
CUST_8117_PI426222305	0,023	5,307	up	PGSC0003DMT400030106	Anthocyanin acyltransferase	Not assigned/Unknown n
CUST_44294_PI426222305	0,002	6,302	up	PGSC0003DMT400010093	Conserved gene of unknown function	Not assigned/Unknown n
CUST_28293_PI426222305	0,005	4,619	up	PGSC0003DMT400044334	Nucleic acid binding protein	Not assigned/Unknown n
CUST_35796_PI426222305	0,024	2,160	up	PGSC0003DMT400046899	Leucine-rich repeat-containing protein	Not assigned/Unknown n
CUST_19353_PI426222305	0,041	3,009	up	PGSC0003DMT400072777	Alpha/beta hydrolase	Not assigned/Unknown n
CUST_34716_PI426222305	0,027	2,097	up	PGSC0003DMT400001793	PTAC18	Not assigned/Unknown n
CUST_44636_PI426222305	0,022	5,454	up	PGSC0003DMT400027481	Gene of unknown function	Not assigned/Unknown n
CUST_6724_PI426222305	0,001	18,889	up	PGSC0003DMT400036923	Conserved gene of unknown function	Not assigned/Unknown n
CUST_27171_PI426222305	0,025	2,064	up	PGSC0003DMT400026242	Conserved gene of unknown function	Not assigned/Unknown n
CUST_7374_PI426222305	0,006	4,123	up	PGSC0003DMT400052899	Conserved gene of unknown function	Not assigned/Unknown n
CUST_29808_PI426222305	0,045	2,247	up	PGSC0003DMT400088357	Transposon MuDR mudrA	Not assigned/Unknown n
CUST_32251_PI426222305	0,030	2,724	up	PGSC0003DMT400012594	Squalene monooxygenase	Not assigned/Unknown n
CUST_49569_PI426222305	0,000	17,396	up	PGSC0003DMT400013671	Gene of unknown function	Not assigned/Unknown n
CUST_45034_PI426222305	0,025	4,949	up	PGSC0003DMT400027364	Gene of unknown function	Not assigned/Unknown n
CUST_39307_PI426222305	0,043	4,134	up	PGSC0003DMT400085484	C-terminal zinc-finger	Not assigned/Unknown n
CUST_41797_PI426222305	0,006	4,464	up	PGSC0003DMT400015621	Gene of unknown function	Not assigned/Unknown n
CUST_30755_PI426222305	0,009	3,382	up	PGSC0003DMT400097363	F-box protein	Not assigned/Unknown n
CUST_51669_PI426222305	0,019	2,927	up	PGSC0003DMT400056652	Transcription factor	Not assigned/Unknown n
CUST_16069_PI426222305	0,020	4,985	up	PGSC0003DMT400095568	TNP2-like transposon protein	Not assigned/Unknown n
CUST_21598_PI426222305	0,020	11,831	up	PGSC0003DMT400088553	Gene of unknown function	Not assigned/Unknown n
CUST_45466_PI426222305	0,002	11,503	up	PGSC0003DMT400074808	Conserved gene of unknown function	Not assigned/Unknown n
CUST_26641_PI426222305	0,049	2,529	up	PGSC0003DMT400000901	MYB transcription factor	Not assigned/Unknown n
CUST_22809_PI426222305	0,024	3,214	up	PGSC0003DMT400078052	Gene of unknown function	Not assigned/Unknown n
CUST_31707_PI426222305	0,029	3,036	up	PGSC0003DMT400035049	Gene of unknown function	Not assigned/Unknown n
CUST_1956_PI426222305	0,032	3,065	up	PGSC0003DMT400089683	Gag-pol polyprotein	Not assigned/Unknown n
CUST_50037_PI426222305	0,000	14,544	up	PGSC0003DMT400065441	Extracellular matrix glycoprotein pherophorin-V30	Not assigned/Unknown n
CUST_21091_PI426222305	0,020	2,656	up	PGSC0003DMT400020212	Conserved gene of unknown function	Not assigned/Unknown n
CUST_49404_PI426222305	0,007	5,095	up	PGSC0003DMT400074522	Conserved gene of unknown function	Not assigned/Unknown n
CUST_7883_PI426222305	0,046	2,094	up	PGSC0003DMT400025824	Conserved gene of unknown function	Not assigned/Unknown n
CUST_25672_PI426222305	0,039	4,023	up	PGSC0003DMT400029284	Conserved gene of unknown function	Not assigned/Unknown n
CUST_50818_PI426222305	0,015	9,771	up	PGSC0003DMT400083920	Conserved gene of unknown function	Not assigned/Unknown n
CUST_6807_PI426222305	0,000	25,268	up	PGSC0003DMT400036925	Conserved gene of unknown function	Not assigned/Unknown n
CUST_49354_PI426222305	0,014	2,496	up	PGSC0003DMT400056201	Chaperone protein DNAj	Not assigned/Unknown n
CUST_35156_PI426222305	0,019	3,013	up	PGSC0003DMT400021519	Pentatricopeptide repeat-containing protein	Not assigned/Unknown n
CUST_17562_PI426222305	0,001	12,446	up	PGSC0003DMT400068108	Glutamine-rich protein	Not assigned/Unknown n
CUST_21590_PI426222305	0,002	5,148	up	PGSC0003DMT400023943	Conserved gene of unknown function	Not assigned/Unknown n
CUST_20546_PI426222305	0,029	4,679	up	PGSC0003DMT400014142	Gene of unknown function	Not assigned/Unknown n
CUST_17738_PI426222305	0,013	2,318	up	PGSC0003DMT400066762	Conserved gene of unknown function	Not assigned/Unknown n
CUST_3982_PI426222305	0,000	14,740	up	PGSC0003DMT400089636	Gene of unknown function	Not assigned/Unknown n
CUST_24723_PI426222305	0,002	7,290	up	PGSC0003DMT400085483	Conserved gene of unknown function	Not assigned/Unknown n
CUST_3793_PI426222305	0,018	2,647	up	PGSC0003DMT400094715	Early nodulin-75	Not assigned/Unknown n
CUST_16959_PI426222305	0,020	2,084	up	PGSC0003DMT400048286	Nucleic acid binding protein	Not assigned/Unknown n
CUST_6690_PI426222305	0,000	20,829	up	PGSC0003DMT400036922	Conserved gene of unknown function	Not assigned/Unknown n
CUST_24796_PI426222305	0,022	2,133	up	PGSC0003DMT400043964	Blight resistance protein T118	Not assigned/Unknown n
CUST_50425_PI426222305	0,005	3,059	up	PGSC0003DMT400010918	NADH ubiquinone oxidoreductase B14 subunit	Not assigned/Unknown n
CUST_25543_PI426222305	0,047	2,034	up	PGSC0003DMT400029304	Conserved gene of unknown function	Not assigned/Unknown n
CUST_21679_PI426222305	0,049	3,714	up	PGSC0003DMT400076837	Flavonol 4'-sulfotransferase	Not assigned/Unknown n
CUST_52109_PI426222305	0,014	2,716	up	PGSC0003DMT400039128	Defensin protein	Not assigned/Unknown n
CUST_23035_PI426222305	0,023	2,363	up	PGSC0003DMT400060934	Conserved gene of unknown function	Not assigned/Unknown n
CUST_36396_PI426222305	0,028	3,048	up	PGSC0003DMT400054095	Gene of unknown function	Not assigned/Unknown n
CUST_2721_PI426222305	0,018	3,972	up	PGSC0003DMT400080082	Conserved gene of unknown function	Not assigned/Unknown n
CUST_5221_PI426222305	0,032	3,564	up	PGSC0003DMT400009246	Pre-rRNA-processing protein ESF1	Not assigned/Unknown n
CUST_6795_PI426222305	0,020	3,960	up	PGSC0003DMT400036924	Conserved gene of unknown function	Not assigned/Unknown n
CUST_37831_PI426222305	0,031	3,216	up	PGSC0003DMT400096058	Gene of unknown function	Not assigned/Unknown n
CUST_49648_PI426222305	0,008	3,752	up	PGSC0003DMT400016776	Gene of unknown function	Not assigned/Unknown n
CUST_33082_PI426222305	0,011	5,861	up	PGSC0003DMT400094304	Gene of unknown function	Not assigned/Unknown n
CUST_6656_PI426222305	0,022	2,383	up	PGSC0003DMT400036990	Acireductone dioxygenase	Not assigned/Unknown n
CUST_31378_PI426222305	0,022	2,014	up	PGSC0003DMT400035020	Conserved gene of unknown function	Not assigned/Unknown n
CUST_37096_PI426222305	0,005	3,146	up	PGSC0003DMT400020061	Gene of unknown function	Not assigned/Unknown n

CUST_42643_PI426222305	0,034	7,469	up	PGSC0003DMT400093715	Gene of unknown function	Not assigned/Unknown
CUST_13413_PI426222305	0,033	9,770	up	PGSC0003DMT400092658	Gene of unknown function	Not assigned/Unknown
CUST_50908_PI426222305	0,021	2,042	up	PGSC0003DMT400059683	CLE family OsCLE801 protein	Not assigned/Unknown
CUST_3640_PI426222305	0,036	2,014	up	PGSC0003DMT400064196	Conserved gene of unknown function	Not assigned/Unknown
CUST_38267_PI426222305	0,017	2,505	up	PGSC0003DMT400067245	6-phosphogluconolactonase	OPP
CUST_38238_PI426222305	0,021	2,144	up	PGSC0003DMT400067247	6-phosphogluconolactonase	OPP
CUST_1990_PI426222305	0,000	20,023	up	PGSC0003DMT400028767	Ribulose bisphosphate carboxylase/oxygenase activase 1, chloroplastic	Photosynthesis
CUST_2543_PI426222305	0,000	20,170	up	PGSC0003DMT400028766	Ribulose bisphosphate carboxylase/oxygenase activase 1, chloroplastic	Photosynthesis
CUST_1979_PI426222305	0,014	2,788	up	PGSC0003DMT400028765	Ribulose bisphosphate carboxylase/oxygenase activase 1, chloroplastic	Photosynthesis
CUST_19758_PI426222305	0,000	22,181	up	PGSC0003DMT400011522	Chloroplast ferredoxin I	Photosynthesis
CUST_11146_PI426222305	0,014	2,417	up	PGSC0003DMT400078520	Fructose-bisphosphate aldolase	Photosynthesis
CUST_32998_PI426222305	0,005	13,517	up	PGSC0003DMT400019434	Glycolate oxidase	Photosynthesis
CUST_2069_PI426222305	0,016	2,648	up	PGSC0003DMT400028764	Ribulose bisphosphate carboxylase/oxygenase activase 1, chloroplastic	Photosynthesis
CUST_30202_PI426222305	0,018	2,623	up	PGSC0003DMT400012297	Formyltetrahydrofolate deformylase	Photosynthesis
CUST_45347_PI426222305	0,014	4,079	up	PGSC0003DMT400001635	Ubiquitin-protein ligase	Protein
CUST_7853_PI426222305	0,022	2,317	up	PGSC0003DMT400025605	Prolyl endopeptidase	Protein
CUST_27542_PI426222305	0,039	2,519	up	PGSC0003DMT400065969	Glucose acyltransferase	Protein
CUST_2306_PI426222305	0,001	7,331	up	PGSC0003DMT400072406	Brix domain containing protein	Protein
CUST_35032_PI426222305	0,028	2,433	up	PGSC0003DMT400005517	Pentatricopeptide repeat-containing protein	Protein
CUST_7681_PI426222305	0,007	2,770	up	PGSC0003DMT400025910	B2-type cyclin dependent kinase	Protein
CUST_7916_PI426222305	0,038	2,525	up	PGSC0003DMT400053522	Serine carboxypeptidase III	Protein
CUST_24351_PI426222305	0,003	8,576	up	PGSC0003DMT400010965	F-box family protein	Protein
CUST_20661_PI426222305	0,040	4,934	up	PGSC0003DMT400011989	Eukaryotic translation initiation factor 2 gamma subunit	Protein
CUST_30418_PI426222305	0,028	2,833	up	PGSC0003DMT400069956	Pseudouridine synthase	Protein
CUST_30874_PI426222305	0,014	16,453	up	PGSC0003DMT400018829	ATP binding protein	Protein
CUST_30597_PI426222305	0,030	3,613	up	PGSC0003DMT400007973	TA9 protein	Protein
CUST_17259_PI426222305	0,007	4,913	up	PGSC0003DMT400070725	Vacuolar protein sorting protein	Protein
CUST_33576_PI426222305	0,002	13,843	up	PGSC0003DMT400045487	Serine/threonine-protein kinase PBS1	Protein
CUST_21393_PI426222305	0,025	2,125	up	PGSC0003DMT400050818	Serine/threonine protein kinase	Protein
CUST_27572_PI426222305	0,009	2,606	up	PGSC0003DMT400008401	Glucose acyltransferase	Protein
CUST_9625_PI426222305	0,003	6,237	up	PGSC0003DMT400006583	Conserved gene of unknown function	Protein
CUST_515_PI426222305	0,021	6,332	up	PGSC0003DMT400033610	Serine carboxypeptidase	Protein
CUST_12187_PI426222305	0,029	3,907	up	PGSC0003DMT400051560	Proteasome subunit beta type-6	Protein
CUST_35603_PI426222305	0,027	3,813	up	PGSC0003DMT400062255	BRASSINOSTEROID INSENSITIVE 1-associated receptor kinase 1	Protein
CUST_18686_PI426222305	0,030	3,066	up	PGSC0003DMT400001140	Protease	Protein
CUST_3506_PI426222305	0,007	10,193	up	PGSC0003DMT400064314	Cysteine proteinase	Protein
CUST_39326_PI426222305	0,042	2,789	up	PGSC0003DMT400012799	Ubiquitin-conjugating enzyme E2 8	Protein
CUST_34120_PI426222305	0,042	3,786	up	PGSC0003DMT400019728	Chaperonin containing t-complex protein 1, beta subunit, tcpb	Protein
CUST_26416_PI426222305	0,020	2,003	up	PGSC0003DMT400037129	F-box family protein	Protein
CUST_41771_PI426222305	0,004	12,756	up	PGSC0003DMT400015599	F-Box protein	Protein
CUST_20843_PI426222305	0,012	2,783	up	PGSC0003DMT400011662	Mov34-1	Protein
CUST_51668_PI426222305	0,005	5,103	up	PGSC0003DMT400056658	Protein translocase	Protein
CUST_42908_PI426222305	0,017	4,803	up	PGSC0003DMT400097155	F-box family protein	Protein
CUST_44249_PI426222305	0,013	2,433	up	PGSC0003DMT400035505	JmjC domain containing protein	Protein
CUST_24380_PI426222305	0,032	2,127	up	PGSC0003DMT400036066	Conserved gene of unknown function	Protein
CUST_50443_PI426222305	0,008	2,559	up	PGSC0003DMT400065951	HECT; Ubiquitin	Protein
CUST_21325_PI426222305	0,021	2,308	up	PGSC0003DMT400020238	Translation initiation factor	Protein
CUST_32105_PI426222305	0,016	2,254	up	PGSC0003DMT400053922	F-box domain-containing protein	Protein
CUST_9793_PI426222305	0,007	2,615	up	PGSC0003DMT400038500	Subtilisin-like protease	Protein
CUST_49289_PI426222305	0,023	12,305	up	PGSC0003DMT400059084	Ribosomal protein S6 kinase	Protein
CUST_24358_PI426222305	0,013	6,535	up	PGSC0003DMT400074116	Conserved gene of unknown function	Protein
CUST_3584_PI426222305	0,025	2,090	up	PGSC0003DMT400033184	Ubiquitin carboxyl-terminal hydrolase	Protein
CUST_19828_PI426222305	0,018	3,193	up	PGSC0003DMT400061164	Armadillo repeat-containing protein	Protein
CUST_47797_PI426222305	0,018	7,585	up	PGSC0003DMT400019290	ATP binding protein	Protein
CUST_33672_PI426222305	0,041	2,443	up	PGSC0003DMT400078621	Eukaryotic translation initiation factor 5	Protein
CUST_39803_PI426222305	0,024	2,427	up	PGSC0003DMT400067918	50S ribosomal protein L13	Protein
CUST_36883_PI426222305	0,024	4,606	up	PGSC0003DMT400067510	Cell division control protein	Protein
CUST_3646_PI426222305	0,034	2,505	up	PGSC0003DMT400010308	Ubiquitin-protein ligase	Protein
CUST_21107_PI426222305	0,019	7,193	up	PGSC0003DMT400020495	Rnf5	Protein
CUST_52124_PI426222305	0,022	2,155	up	PGSC0003DMT400008825	F-Box protein	Protein
CUST_49812_PI426222305	0,010	4,971	up	PGSC0003DMT400033803	Aspartic proteinase Asp1	Protein
CUST_43469_PI426222305	0,041	2,260	up	PGSC0003DMT400059334	F-box domain-containing protein	Protein
CUST_2037_PI426222305	0,011	2,392	up	PGSC0003DMT400072255	FK506-binding protein	Protein
CUST_24416_PI426222305	0,030	2,200	up	PGSC0003DMT400036067	Zinc metalloproteinase	Protein
CUST_40930_PI426222305	0,018	2,327	up	PGSC0003DMT400079779	Carboxypeptidase type III	Protein
CUST_19737_PI426222305	0,017	2,503	up	PGSC0003DMT400061020	MRNA turnover protein 4 mrt4	Protein

CUST_40945_PI426222305	0,019	2,206	up	PGSC0003DMT400019237	SLF-interacting SKP1	Protein
CUST_19822_PI426222305	0,043	5,457	up	PGSC0003DMT400061080	Importin beta-2 subunit family protein	Protein
CUST_29155_PI426222305	0,001	5,883	up	PGSC0003DMT400030505	Protein Z	Protein
CUST_20707_PI426222305	0,003	3,550	up	PGSC0003DMT400011742	30S ribosomal protein S1, chloroplastic	Protein
CUST_41451_PI426222305	0,028	2,130	up	PGSC0003DMT400061374	60S ribosomal protein L27	Protein
CUST_9500_PI426222305	0,044	2,637	up	PGSC0003DMT400006584	F-box/kelch-repeat protein	Protein
CUST_21311_PI426222305	0,013	7,476	up	PGSC0003DMT400020496	E3 ubiquitin-protein ligase RMA1H1	Protein
CUST_27554_PI426222305	0,019	2,223	up	PGSC0003DMT400013931	Histone deacetylase hda2	Protein
CUST_39705_PI426222305	0,005	2,893	up	PGSC0003DMT400067909	Ubiquitin-associated uba/ubx domain-containing protein	Protein
CUST_26019_PI426222305	0,003	5,556	up	PGSC0003DMT400051957	RNA binding protein	Protein
CUST_35153_PI426222305	0,019	2,416	up	PGSC0003DMT400013477	GTP-binding	Protein
CUST_17203_PI426222305	0,043	3,517	up	PGSC0003DMT400070802	Brix domain-containing protein	Protein
CUST_20725_PI426222305	0,016	2,231	up	PGSC0003DMT400011661	Mov34-1	Protein
CUST_7405_PI426222305	0,021	2,196	up	PGSC0003DMT400025603	Prolyl endopeptidase	Protein
CUST_10455_PI426222305	0,030	2,051	up	PGSC0003DMT400029044	CBL-interacting serine/threonine-protein kinase	Protein
CUST_14198_PI426222305	0,022	9,522	up	PGSC0003DMT400060272	Spotted leaf protein	Protein
CUST_14024_PI426222305	0,016	2,370	up	PGSC0003DMT400060280	10kDa chaperonin (CPN10) protein	Protein
CUST_10552_PI426222305	0,022	4,339	up	PGSC0003DMT400032137	Minor histocompatibility antigen H13	Protein
CUST_6398_PI426222305	0,021	2,553	up	PGSC0003DMT400014772	Tetratricoredoxin	Redox
CUST_41091_PI426222305	0,001	14,442	up	PGSC0003DMT400004360	Ascorbate peroxidase	Redox
CUST_26361_PI426222305	0,028	2,042	up	PGSC0003DMT400037158	Steroid binding protein	Redox
CUST_35138_PI426222305	0,033	3,496	up	PGSC0003DMT400013447	Superoxide dismutase	Redox
CUST_24349_PI426222305	0,021	2,822	up	PGSC0003DMT400074173	Conserved gene of unknown function	Redox
CUST_45838_PI426222305	0,002	4,236	up	PGSC0003DMT400050228	Thioredoxin II	Redox
CUST_33785_PI426222305	0,019	3,180	up	PGSC0003DMT400070923	Superoxide dismutase	Redox
CUST_34431_PI426222305	0,004	3,262	up	PGSC0003DMT400071859	Dead box ATP-dependent RNA helicase	RNA
CUST_824_PI426222305	0,027	2,275	up	PGSC0003DMT400025984	Zinc finger protein	RNA
CUST_1208_PI426222305	0,045	5,613	up	PGSC0003DMT400052239	Conserved gene of unknown function	RNA
CUST_29070_PI426222305	0,001	21,412	up	PGSC0003DMT400020557	DNA binding protein	RNA
CUST_14374_PI426222305	0,039	2,798	up	PGSC0003DMT400060168	Protein 2	RNA
CUST_37101_PI426222305	0,042	2,018	up	PGSC0003DMT400082473	Histone deacetylase	RNA
CUST_19305_PI426222305	0,021	4,091	up	PGSC0003DMT400072891	MADS-box transcription factor	RNA
CUST_14617_PI426222305	0,023	7,075	up	PGSC0003DMT400066647	RNA binding protein	RNA
CUST_22211_PI426222305	0,012	9,805	up	PGSC0003DMT400047622	HD-ZIP	RNA
CUST_3517_PI426222305	0,006	14,922	up	PGSC0003DMT400010235	PHCLF2	RNA
CUST_29659_PI426222305	0,001	17,888	up	PGSC0003DMT400047446	Transcription factor	RNA
CUST_34452_PI426222305	0,005	8,147	up	PGSC0003DMT400055618	DNA binding protein	RNA
CUST_26586_PI426222305	0,020	4,280	up	PGSC0003DMT400000756	Cwf J-like family protein / zinc finger (CCCH-type) family protein	RNA
CUST_4595_PI426222305	0,004	3,093	up	PGSC0003DMT400065585	Zinc finger CCCH domain-containing protein 39	RNA
CUST_48713_PI426222305	0,019	2,703	up	PGSC0003DMT400036286	MYB transcription factor	RNA
CUST_5277_PI426222305	0,042	8,048	up	PGSC0003DMT400009232	Zinc finger protein	RNA
CUST_5367_PI426222305	0,049	2,852	up	PGSC0003DMT400003936	TSI-1 protein	RNA
CUST_47614_PI426222305	0,006	3,265	up	PGSC0003DMT400005206	Nucleic acid binding protein	RNA
CUST_27007_PI426222305	0,021	3,036	up	PGSC0003DMT400067142	Heat shock protein 70 (HSP70)-interacting protein	RNA
CUST_46607_PI426222305	0,016	4,689	up	PGSC0003DMT400027073	Pentatricopeptide repeat-containing protein	RNA
CUST_5084_PI426222305	0,035	2,441	up	PGSC0003DMT400003934	TSI-1 protein	RNA
CUST_3754_PI426222305	0,013	2,441	up	PGSC0003DMT400040786	Conserved gene of unknown function	RNA
CUST_974_PI426222305	0,022	5,951	up	PGSC0003DMT400052057	WRKY transcription factor-b	RNA
CUST_8971_PI426222305	0,001	8,211	up	PGSC0003DMT400092643	RNase Phy3	RNA
CUST_47710_PI426222305	0,025	2,215	up	PGSC0003DMT400061226	Stress-associated protein 10	RNA
CUST_17110_PI426222305	0,015	2,332	up	PGSC0003DMT400018357	RNA binding protein	RNA
CUST_38819_PI426222305	0,022	2,275	up	PGSC0003DMT400015371	Zinc finger protein	RNA
CUST_46134_PI426222305	0,022	2,304	up	PGSC0003DMT400018556	Transcription factor IIIA	RNA
CUST_39033_PI426222305	0,040	2,086	up	PGSC0003DMT400068603	Arginine decarboxylase	RNA
CUST_26574_PI426222305	0,020	3,791	up	PGSC0003DMT400001036	Conserved gene of unknown function	RNA
CUST_46099_PI426222305	0,031	2,110	up	PGSC0003DMT400018555	Transcription factor IIIA	RNA
CUST_42826_PI426222305	0,049	9,205	up	PGSC0003DMT400056558	Pax transcription activation domain interacting protein	RNA
CUST_2194_PI426222305	0,002	5,058	up	PGSC0003DMT400072257	Transcription factor	RNA
CUST_17751_PI426222305	0,001	138,911	up	PGSC0003DMT400067013	Ethylene-responsive transcription factor 13	RNA
CUST_12445_PI426222305	0,021	5,015	up	PGSC0003DMT400085559	Anaerobic basic leucine zipper protein	RNA
CUST_25015_PI426222305	0,020	2,944	up	PGSC0003DMT400056352	WRKY-type DNA binding protein	RNA
CUST_11241_PI426222305	0,024	3,263	up	PGSC0003DMT400037755	Transcription factor	RNA
CUST_3485_PI426222305	0,023	2,142	up	PGSC0003DMT400085930	Agamous-like MADS-box protein AGL62	RNA
CUST_47307_PI426222305	0,026	2,190	up	PGSC0003DMT400074074	Inducer of CBF expression 2 protein	RNA
CUST_42767_PI426222305	0,024	2,317	up	PGSC0003DMT400033741	Transcription factor HBP-1b(C1)	RNA
CUST_19194_PI426222305	0,002	6,263	up	PGSC0003DMT400072889	MADS-box transcription factor	RNA

Appendix

CUST_20786_PI426222305	0,046	2,932	up	PGSC0003DMT400011778	GATA transcription factor	RNA
CUST_4264_PI426222305	0,036	3,366	up	PGSC0003DMT400020802	DNA binding protein	RNA
CUST_35569_PI426222305	0,028	2,097	up	PGSC0003DMT400004671	ATP-dependent helicase	RNA
CUST_37568_PI426222305	0,038	2,800	up	PGSC0003DMT400049663	NAC domain class transcription factor	RNA
CUST_43734_PI426222305	0,050	3,081	up	PGSC0003DMT400076898	Homeobox protein	RNA
CUST_11951_PI426222305	0,014	4,112	up	PGSC0003DMT400085905	Type I MADS box transcription factor	RNA
CUST_22289_PI426222305	0,012	4,215	up	PGSC0003DMT400047621	HD-ZIP	RNA
CUST_23811_PI426222305	0,000	10,271	up	PGSC0003DMT400021164	Transcription factor	RNA
CUST_31032_PI426222305	0,017	2,432	up	PGSC0003DMT400010574	Conserved gene of unknown function	RNA
CUST_8059_PI426222305	0,012	2,217	up	PGSC0003DMT400039974	Myb family transcription factor	RNA
CUST_7788_PI426222305	0,001	6,013	up	PGSC0003DMT400025704	DNA binding protein	RNA
CUST_19446_PI426222305	0,016	5,065	up	PGSC0003DMT400072890	MADS-box transcription factor	RNA
CUST_7406_PI426222305	0,003	4,662	up	PGSC0003DMT400009582	RAD 6	RNA
CUST_9005_PI426222305	0,047	2,057	up	PGSC0003DMT400058187	Ocs element-binding factor	RNA
CUST_8346_PI426222305	0,007	2,665	up	PGSC0003DMT400075434	Pre-mRNA-splicing factor	RNA
CUST_44133_PI426222305	0,001	7,070	up	PGSC0003DMT400055210	AP2 domain-containing transcription factor	RNA
CUST_42330_PI426222305	0,039	4,130	up	PGSC0003DMT400089604	WRKY transcription factor 27	RNA
CUST_11288_PI426222305	0,001	14,353	up	PGSC0003DMT400007351	Myb-like DNA-binding protein	RNA
CUST_761_PI426222305	0,038	3,961	up	PGSC0003DMT400003359	Zinc finger protein	RNA
CUST_44871_PI426222305	0,012	2,383	up	PGSC0003DMT400038867	Sesquiterpene synthase	secondary metabolism
CUST_46393_PI426222305	0,010	11,907	up	PGSC0003DMT400046332	Anthocyanin acyltransferase	secondary metabolism
CUST_25944_PI426222305	0,046	2,214	up	PGSC0003DMT400061768	Aminotransferase ybdL	secondary metabolism
CUST_22712_PI426222305	0,009	15,445	up	PGSC0003DMT400078188	Conserved gene of unknown function	secondary metabolism
CUST_22910_PI426222305	0,021	2,379	up	PGSC0003DMT400076777	Strictosidine synthase	secondary metabolism
CUST_8070_PI426222305	0,021	4,704	up	PGSC0003DMT400075300	Anthranilate N-benzoyltransferase protein	secondary metabolism
CUST_3766_PI426222305	0,000	8,080	up	PGSC0003DMT400013704	Sinapyl alcohol dehydrogenase 2	secondary metabolism
CUST_52018_PI426222305	0,016	2,176	up	PGSC0003DMT400089311	Acyltransferase	secondary metabolism
CUST_30757_PI426222305	0,017	2,378	up	PGSC0003DMT400022103	Tryptophan decarboxylase	secondary metabolism
CUST_44645_PI426222305	0,005	3,861	up	PGSC0003DMT400027448	Sesquiterpene synthase	secondary metabolism
CUST_44634_PI426222305	0,009	3,194	up	PGSC0003DMT400062798	Sesquiterpene synthase	secondary metabolism
CUST_26278_PI426222305	0,037	2,266	up	PGSC0003DMT400041567	ELI3	secondary metabolism
CUST_48210_PI426222305	0,010	2,883	up	PGSC0003DMT400055897	(-)-a-terpineol synthase	secondary metabolism
CUST_10321_PI426222305	0,021	2,489	up	PGSC0003DMT400029079	HQT	secondary metabolism
CUST_18264_PI426222305	0,013	2,199	up	PGSC0003DMT400042325	Isochorismatase	secondary metabolism
CUST_44638_PI426222305	0,020	7,061	up	PGSC0003DMT400027444	Sesquiterpene synthase	secondary metabolism
CUST_42340_PI426222305	0,034	2,102	up	PGSC0003DMT400024575	Gene of unknown function	secondary metabolism
CUST_51530_PI426222305	0,006	3,250	up	PGSC0003DMT400046420	Anthocyanin acyltransferase	secondary metabolism
CUST_43022_PI426222305	0,001	11,963	up	PGSC0003DMT400018860	Acyltransferase	secondary metabolism
CUST_46387_PI426222305	0,002	21,489	up	PGSC0003DMT400036383	Anthocyanin acyltransferase	secondary metabolism
CUST_46039_PI426222305	0,044	2,783	up	PGSC0003DMT400040520	10-hydroxygeraniol oxidoreductase	secondary metabolism
CUST_37813_PI426222305	0,026	3,004	up	PGSC0003DMT400006173	NPH3 (NON-PHOTOTROPIC HYPOCOTYL 3)	signalling
CUST_33535_PI426222305	0,027	2,352	up	PGSC0003DMT400045477	Twin lov protein	signalling
CUST_15843_PI426222305	0,008	2,506	up	PGSC0003DMT400036029	S-locus lectin protein kinase family protein	signalling
CUST_25737_PI426222305	0,010	5,808	up	PGSC0003DMT400029287	P21-rho-binding domain-containing protein	signalling
CUST_20936_PI426222305	0,012	3,355	up	PGSC0003DMT400011936	Mitochondrial pyruvate dehydrogenase kinase isoform 1	signalling
CUST_49771_PI426222305	0,038	2,156	up	PGSC0003DMT400035842	Receptor protein kinase	signalling
CUST_37424_PI426222305	0,022	2,434	up	PGSC0003DMT400010738	Leucine-rich repeat resistance protein	signalling
CUST_9418_PI426222305	0,002	6,163	up	PGSC0003DMT400006376	Calmodulin binding protein	signalling
CUST_24436_PI426222305	0,027	4,440	up	PGSC0003DMT400034271	DUF26 domain-containing protein 2	signalling
CUST_25218_PI426222305	0,005	3,668	up	PGSC0003DMT400014960	Calcineurin B	signalling
CUST_52242_PI426222305	0,004	13,075	up	PGSC0003DMT400014252	Disease resistance protein	signalling
CUST_49093_PI426222305	0,031	2,594	up	PGSC0003DMT400008629	Dual-specific kinase DSK1	signalling
CUST_24283_PI426222305	0,021	4,303	up	PGSC0003DMT400034269	DUF26 domain-containing protein 2	signalling
CUST_11040_PI426222305	0,014	2,467	up	PGSC0003DMT400078489	ATP binding / protein kinase/ protein serine/threonine kinase/ protein tyrosine kinase/ sugar binding	signalling
CUST_25843_PI426222305	0,015	2,421	up	PGSC0003DMT400051855	Nucleolar GTP-binding protein	signalling
CUST_26968_PI426222305	0,007	3,316	up	PGSC0003DMT400067071	Leucine-rich repeat transmembrane protein kinase	signalling
CUST_48074_PI426222305	0,003	6,513	up	PGSC0003DMT400013991	Receptor-kinase	signalling
CUST_41512_PI426222305	0,020	14,437	up	PGSC0003DMT400021586	Phosphatidylinositol-4-phosphate 5-kinase	signalling
CUST_23599_PI426222305	0,045	3,253	up	PGSC0003DMT400015531	Protein SENSITIVITY TO RED LIGHT REDUCED	signalling
CUST_8911_PI426222305	0,010	3,776	up	PGSC0003DMT400096473	Cold shock domain protein 1	stress
CUST_39350_PI426222305	0,002	20,973	up	PGSC0003DMT400030387	Chloroplast small heat shock protein class I	stress
CUST_32031_PI426222305	0,006	5,427	up	PGSC0003DMT400013254	NTGP4	stress
CUST_52106_PI426222305	0,010	3,090	up	PGSC0003DMT400039131	Defensin P322	stress
CUST_42972_PI426222305	0,011	2,452	up	PGSC0003DMT400015734	Heat shock protein	stress
CUST_37535_PI426222305	0,040	2,941	up	PGSC0003DMT400014217	Heat shock protein 83	stress
CUST_12865_PI426222305	0,009	9,766	up	PGSC0003DMT400062882	Heat-shock protein	stress

CUST_15473_PI426222305	0,003	7,892	up	PGSC0003DMT400073689	Small heat-shock protein	stress
CUST_15384_PI426222305	0,013	2,984	up	PGSC0003DMT400073712	Heat shock protein	stress
CUST_13131_PI426222305	0,019	4,751	up	PGSC0003DMT400089913	Low molecular weight heat-shock protein	stress
CUST_15110_PI426222305	0,047	3,797	up	PGSC0003DMT400056985	Chaperone protein DNAj	stress
CUST_35368_PI426222305	0,010	2,994	up	PGSC0003DMT400079419	C2 domain-containing protein	stress
CUST_3884_PI426222305	0,001	14,378	up	PGSC0003DMT400038705	17.6 kD class I small heat shock protein	stress
CUST_39367_PI426222305	0,005	5,622	up	PGSC0003DMT400030386	Chloroplast small heat shock protein class I	stress
CUST_41941_PI426222305	0,002	3,842	up	PGSC0003DMT400026521	Abscisic acid receptor PYL6	stress
CUST_38770_PI426222305	0,031	5,203	up	PGSC0003DMT400015307	Late blight resistance protein homolog R1B-16	stress
CUST_33027_PI426222305	0,003	3,518	up	PGSC0003DMT400058792	DNAJ heat shock N-terminal domain-containing protein	stress
CUST_32676_PI426222305	0,047	3,370	up	PGSC0003DMT400047340	Wound induced protein	stress
CUST_43532_PI426222305	0,011	2,954	up	PGSC0003DMT400002668	Pollen Ole e 1 allergen and extensin	stress
CUST_29397_PI426222305	0,041	28,403	up	PGSC0003DMT400075938	Kunitz-type protease inhibitor KPI-D2.2	stress
CUST_57_PI426222305	0,031	2,422	up	PGSC0003DMT400084231	Universal stress protein family protein	stress
CUST_17502_PI426222305	0,000	199,146	up	PGSC0003DMT400008351	Small heat shock protein, chloroplastic	stress
CUST_1579_PI426222305	0,047	2,027	up	PGSC0003DMT400043631	Conserved gene of unknown function	stress
CUST_3126_PI426222305	0,002	6,016	up	PGSC0003DMT400000245	BCL-2-associated athanogene 6	stress
CUST_39358_PI426222305	0,001	19,591	up	PGSC0003DMT400030385	Chloroplast small heat shock protein class I	stress
CUST_6584_PI426222305	0,006	6,281	up	PGSC0003DMT400036856	Heat shock protein	stress
CUST_31820_PI426222305	0,007	4,486	up	PGSC0003DMT400053116	MLO1	stress
CUST_17217_PI426222305	0,032	4,135	up	PGSC0003DMT400050016	Wound-induced protein WIN1	stress
CUST_39369_PI426222305	0,003	7,309	up	PGSC0003DMT400030380	Chloroplast small heat shock protein class I	stress
CUST_52108_PI426222305	0,011	2,828	up	PGSC0003DMT400039130	Defensin P322	stress
CUST_47234_PI426222305	0,021	2,449	up	PGSC0003DMT400005012	NBS-coding resistance gene analog	stress
CUST_22802_PI426222305	0,000	17,102	up	PGSC0003DMT400078008	17.6 kDa class I heat shock protein	stress
CUST_9375_PI426222305	0,036	4,011	up	PGSC0003DMT400023713	Small heat stress protein class CIII	stress
CUST_2978_PI426222305	0,002	6,398	up	PGSC0003DMT400000247	BCL-2-associated athanogene 6	stress
CUST_13034_PI426222305	0,003	12,832	up	PGSC0003DMT400063164	Rhicadhesin receptor	stress
CUST_15408_PI426222305	0,014	4,784	up	PGSC0003DMT400073713	Heat shock protein	stress
CUST_12528_PI426222305	0,020	3,622	up	PGSC0003DMT400093322	Conserved gene of unknown function	stress
CUST_12548_PI426222305	0,024	2,450	up	PGSC0003DMT400063545	Luminal binding protein	stress
CUST_23797_PI426222305	0,036	7,831	up	PGSC0003DMT400055958	Class II small heat shock protein Le-HSP17.6	stress
CUST_41335_PI426222305	0,014	2,657	up	PGSC0003DMT400008029	Nbs-lrr resistance protein	stress
CUST_39348_PI426222305	0,047	2,112	up	PGSC0003DMT400030382	Chloroplast small heat shock protein class I	stress
CUST_39375_PI426222305	0,004	7,391	up	PGSC0003DMT400088908	Chloroplast small heat shock protein class I	stress
CUST_12396_PI426222305	0,045	2,318	up	PGSC0003DMT400063543	Luminal binding protein	stress
CUST_38423_PI426222305	0,037	3,004	up	PGSC0003DMT400074375	Heat shock protein 90	stress
CUST_22568_PI426222305	0,000	18,054	up	PGSC0003DMT400078202	Hsp20.1 protein	stress
CUST_6946_PI426222305	0,000	15,143	up	PGSC0003DMT400031252	Small heat shock protein	stress
CUST_16339_PI426222305	0,001	9,242	up	PGSC0003DMT400060724	Universal stress protein family protein	stress
CUST_19681_PI426222305	0,001	20,626	up	PGSC0003DMT400053402	Heat-shock protein	stress
CUST_42977_PI426222305	0,019	2,287	up	PGSC0003DMT400015735	Heat shock protein	stress
CUST_39377_PI426222305	0,009	5,055	up	PGSC0003DMT400030381	Chloroplast small heat shock protein class I	stress
CUST_22682_PI426222305	0,001	6,366	up	PGSC0003DMT400078201	17.6 kD class I small heat shock protein	stress
CUST_39416_PI426222305	0,003	6,229	up	PGSC0003DMT400077357	Heat shock protein 70kD	stress
CUST_23794_PI426222305	0,006	5,635	up	PGSC0003DMT400021142	Class II small heat shock protein Le-HSP17.6	stress
CUST_21561_PI426222305	0,000	22,374	up	PGSC0003DMT400023932	Small heat-shock protein homolog protein	stress
CUST_49213_PI426222305	0,008	4,051	up	PGSC0003DMT400044066	Hsp20.1 protein	stress
CUST_44178_PI426222305	0,005	3,567	up	PGSC0003DMT400034080	Conserved gene of unknown function	stress
CUST_22541_PI426222305	0,000	18,919	up	PGSC0003DMT400078006	17.6 kD class I small heat shock protein	stress
CUST_30269_PI426222305	0,001	5,259	up	PGSC0003DMT400012249	Mitochondrial small heat shock protein	stress
CUST_13135_PI426222305	0,001	16,649	up	PGSC0003DMT400007587	Small molecular heat shock protein	stress
CUST_37554_PI426222305	0,037	2,980	up	PGSC0003DMT400014216	Heat shock protein	stress
CUST_16326_PI426222305	0,002	3,929	up	PGSC0003DMT400060736	Peroxisomal small heat shock protein	stress
CUST_6999_PI426222305	0,000	17,998	up	PGSC0003DMT400031253	Small heat shock protein	stress
CUST_48226_PI426222305	0,002	5,963	up	PGSC0003DMT400055930	Furin	stress
CUST_32286_PI426222305	0,005	2,883	up	PGSC0003DMT400027537	SNKR2GH2 protein	stress
CUST_4534_PI426222305	0,008	6,305	up	PGSC0003DMT400007728	DNAJ protein	stress
CUST_22787_PI426222305	0,000	136,570	up	PGSC0003DMT400078007	17.6 kD class I small heat shock protein	stress
CUST_17936_PI426222305	0,026	2,072	up	PGSC0003DMT400032266	Malate dehydrogenase	TCA
CUST_32441_PI426222305	0,042	3,203	up	PGSC0003DMT400033904	Branched chain alpha-keto acid dehydrogenase E1-alpha subunit	TCA
CUST_47883_PI426222305	0,024	4,458	up	PGSC0003DMT400062473	Nectarin-2	TCA
CUST_33300_PI426222305	0,001	12,102	up	PGSC0003DMT400017914	Carbonic anhydrase	TCA
CUST_20652_PI426222305	0,041	2,291	up	PGSC0003DMT400011963	ATP:citrate lyase	TCA
CUST_33248_PI426222305	0,002	18,512	up	PGSC0003DMT400017915	Carbonic anhydrase	TCA
CUST_37115_PI426222305	0,005	2,960	up	PGSC0003DMT400082447	Glutamate-1-semialdehyde 2,1-aminomutase, chloroplastic	tetrapyrrole synthesis

Appendix

CUST_18078_PI426222305	0,049	2,802	up	PGSC0003DMT400071039	Heme-binding protein		tetrapyrrole synthesis
CUST_10261_PI426222305	0,027	2,557	up	PGSC0003DMT400029192	Sodium/potassium/calcium exchanger 6		Transport
CUST_12878_PI426222305	0,008	14,589	up	PGSC0003DMT400062927	Sugar transporter		Transport
CUST_41572_PI426222305	0,009	2,494	up	PGSC0003DMT400021562	Tyrosine-specific transport protein		Transport
CUST_43631_PI426222305	0,030	3,773	up	PGSC0003DMT400091020	Potassium channel NKT1		Transport
CUST_39947_PI426222305	0,005	2,864	up	PGSC0003DMT400076965	ZIP family metal transporter		Transport
CUST_46305_PI426222305	0,004	4,270	up	PGSC0003DMT400034124	Pleiotropic drug resistance protein 1		Transport
CUST_4688_PI426222305	0,008	4,218	up	PGSC0003DMT400073887	Ammonium transporter 1 member 2		Transport
CUST_39931_PI426222305	0,003	4,842	up	PGSC0003DMT400076963	ZIP family metal transporter		Transport
CUST_20391_PI426222305	0,004	5,014	up	PGSC0003DMT400049708	Sulfate transporter		Transport
CUST_7618_PI426222305	0,002	6,125	up	PGSC0003DMT400009599	Phosphatidylinositol transfer III		Transport
CUST_44213_PI426222305	0,020	3,367	up	PGSC0003DMT400035512	Auxin:hydrogen symporter		Transport
CUST_20294_PI426222305	0,005	7,949	up	PGSC0003DMT400049706	Sulfate/bicarbonate/oxalate exchanger and transporter sat-1		Transport
CUST_10800_PI426222305	0,049	4,367	up	PGSC0003DMT400031823	Mitochondrial carrier protein		Transport
CUST_29694_PI426222305	0,025	2,504	up	PGSC0003DMT400080507	Amino acid transporter family protein		Transport
CUST_22937_PI426222305	0,038	2,690	up	PGSC0003DMT400021045	Mitochondrial carrier protein		Transport
CUST_9644_PI426222305	0,002	5,134	up	PGSC0003DMT400032198	TRANSPARENT TESTA 12 protein		Transport
CUST_23923_PI426222305	0,040	2,132	up	PGSC0003DMT400032673	ATP-binding cassette transporter		Transport
CUST_37655_PI426222305	0,011	4,169	up	PGSC0003DMT400049495	Organic cation transporter		Transport
CUST_39449_PI426222305	0,026	2,981	up	PGSC0003DMT400077340	Transporter		Transport
CUST_20341_PI426222305	0,003	5,038	up	PGSC0003DMT400049711	Sulfate/bicarbonate/oxalate exchanger and transporter sat-1		Transport
CUST_23206_PI426222305	0,004	6,745	up	PGSC0003DMT400026636	Inorganic phosphate transporter		Transport
CUST_26870_PI426222305	0,007	3,717	up	PGSC0003DMT400034119	Metal transporter		Transport
CUST_39461_PI426222305	0,046	3,299	up	PGSC0003DMT400019863	Sulfate/bicarbonate/oxalate exchanger and transporter sat-1		Transport
CUST_20309_PI426222305	0,001	9,196	up	PGSC0003DMT400049717	Sulfate transporter		Transport
CUST_3880_PI426222305	0,039	2,158	up	PGSC0003DMT400045125	Phosphate transporter 1		Transport
CUST_43060_PI426222305	0,044	7,324	up	PGSC0003DMT400018880	ATPDR3/PDR3 (PLEIOTROPIC DRUG RESISTANCE 3)		Transport
CUST_38850_PI426222305	0,022	6,567	up	PGSC0003DMT400015301	TRANSPARENT TESTA 12 protein		Transport
CUST_7992_PI426222305	0,021	2,116	up	PGSC0003DMT400039972	Sugar transporter		Transport
CUST_566_PI426222305	0,005	46,153	up	PGSC0003DMT400070558	Sugar transporter		Transport
CUST_15864_PI426222305	0,001	18,304	up	PGSC0003DMT400076361	Vacuolar ATP synthase subunit G plant		Transport
CUST_1435_PI426222305	0,021	2,018	up	PGSC0003DMT400052206	Yellow stripe 1.1		Transport
CUST_13679_PI426222305	0,044	2,079	up	PGSC0003DMT400055748	Oligopeptide transporter OPT family		Transport
CUST_6798_PI426222305	0,004	3,939	up	PGSC0003DMT400014431	Conserved gene of unknown function		Transport
CUST_39355_PI426222305	0,047	2,716	up	PGSC0003DMT400030364	Patellin-6		Transport
CUST_21102_PI426222305	0,014	13,243	up	PGSC0003DMT400090965	Potassium channel tetramerization domain-containing protein		Transport
CUST_44237_PI426222305	0,028	3,361	up	PGSC0003DMT400035511	Auxin:hydrogen symporter		Transport
CUST_30963_PI426222305	0,026	2,625	up	PGSC0003DMT400040284	LATD/NIP		Transport
CUST_28686_PI426222305	0,014	2,238	up	PGSC0003DMT400083070	ABC transporter		Transport
CUST_20381_PI426222305	0,013	8,781	up	PGSC0003DMT400049707	Sulfate/bicarbonate/oxalate exchanger and transporter sat-1		Transport
CUST_26710_PI426222305	0,028	2,067	up	PGSC0003DMT400074952	Amino acid transporter		Transport
CUST_43651_PI426222305	0,016	2,370	up	PGSC0003DMT400030772	Vacuolar cation/proton exchanger 1a		Transport
CUST_22470_PI426222305	0,033	8,351	up	PGSC0003DMT400039495	ABC-2 type transporter family protein		Transport
CUST_39930_PI426222305	0,003	3,946	up	PGSC0003DMT400076962	ZIP family metal transporter		Transport
CUST_49486_PI426222305	0,010	2,788	up	PGSC0003DMT400016849	ATMRP14		Transport
CUST_44202_PI426222305	0,003	4,456	up	PGSC0003DMT400035510	Auxin:hydrogen symporter		Transport
CUST_40641_PI426222305	0,014	6,556	up	PGSC0003DMT400056444	Cation/H(+) antiporter 15		Transport
CUST_39957_PI426222305	0,001	4,560	up	PGSC0003DMT400076964	ZIP family metal transporter		Transport
CUST_22341_PI426222305	0,042	3,476	up	PGSC0003DMT400039400	Purine permease		Transport
CUST_8128_PI426222305	0,021	2,091	up	PGSC0003DMT400039973	Sugar transporter		Transport
CUST_20293_PI426222305	0,004	6,308	up	PGSC0003DMT400049710	Sulfate/bicarbonate/oxalate exchanger and transporter sat-1		Transport
CUST_5658_PI426222305	0,004	4,076	up	PGSC0003DMT400062355	Plastid RNA-binding protein 1		Transport
CUST_39362_PI426222305	0,046	2,129	up	PGSC0003DMT400030365	Patellin-6		Transport
CUST_41100_PI426222305	0,026	2,422	up	PGSC0003DMT400004437	Dead box ATP-dependent RNA helicase		Unclassified
CUST_8377_PI426222305	0,002	5,598	up	PGSC0003DMT400075471	Trans-2-enoyl CoA reductase		Unclassified
CUST_40002_PI426222305	0,002	6,082	up	PGSC0003DMT400093628	Polyadenylation factor subunit		Unclassified
CUST_20960_PI426222305	0,049	3,115	up	PGSC0003DMT400011868	Serine hydroxymethyltransferase		Unclassified
CUST_20115_PI426222305	0,018	6,480	up	PGSC0003DMT400011492	AP2/ERF domain-containing transcription factor		Unclassified
CUST_21651_PI426222305	0,042	2,500	up	PGSC0003DMT400046239	S locus glycoprotein		Unclassified
CUST_43915_PI426222305	0,006	3,052	up	PGSC0003DMT400045390	Protein ALUMINUM SENSITIVE 3		Unclassified
CUST_26972_PI426222305	0,018	2,410	up	PGSC0003DMT400067218	Ethylene response factor 1		Unclassified
CUST_28005_PI426222305	0,007	3,636	up	PGSC0003DMT400082017	D12 oleate desaturase		Unclassified
CUST_11778_PI426222305	0,037	3,032	up	PGSC0003DMT400046624	Cell division cycle protein 48		Unclassified
CUST_17169_PI426222305	0,034	3,944	up	PGSC0003DMT400050018	Wound-induced protein WIN2		Unclassified
CUST_978_PI426222305	0,013	4,123	up	PGSC0003DMT400003544	Paired amphipathic helix protein Sin3-like 1		Unclassified
CUST_7614_PI426222305	0,035	3,585	up	PGSC0003DMT400009475	Adenosine kinase		Unclassified

CUST_25382_PI426222305	0,043	2,444	up	PGSC0003DMT400034502	Pentatricopeptide repeat-containing protein	Unclassified
CUST_52526_PI426222305	0,006	82,952	down	PGSC0003DMT400051586	Histidine decarboxylase	AA metabolism
CUST_27067_PI426222305	0,029	8,508	down	PGSC0003DMT400065841	Pyridoxal-dependent decarboxylase, C-terminal sheet domain containing protein	AA metabolism
CUST_49255_PI426222305	0,001	12,309	down	PGSC0003DMT400019747	Histidine decarboxylase	AA metabolism
CUST_45558_PI426222305	0,020	9,235	down	PGSC0003DMT400062817	Pyridoxal-dependent decarboxylase, C-terminal sheet domain containing protein	AA metabolism
CUST_3136_PI426222305	0,021	2,759	down	PGSC0003DMT400000108	Synaptotagmin	AA metabolism
CUST_45536_PI426222305	0,009	17,147	down	PGSC0003DMT400079729	Ornithine decarboxylase	AA metabolism
CUST_34562_PI426222305	0,002	46,447	down	PGSC0003DMT400036114	Histidine decarboxylase	AA metabolism
CUST_20045_PI426222305	0,009	4,151	down	PGSC0003DMT400049234	Glyoxal oxidase	Biodegradation of Xenobiotics
CUST_2763_PI426222305	0,009	3,533	down	PGSC0003DMT400000390	Gibberellin receptor GID1	Biodegradation of Xenobiotics
CUST_33520_PI426222305	0,010	3,935	down	PGSC0003DMT400045472	Conserved gene of unknown function	Biodegradation of Xenobiotics
CUST_7514_PI426222305	0,019	2,586	down	PGSC0003DMT400025739	Beta-tubulin	Cell
CUST_22771_PI426222305	0,041	2,456	down	PGSC0003DMT400078033	Cdc6	Cell
CUST_1154_PI426222305	0,006	3,138	down	PGSC0003DMT400003687	ATEXO70E1	Cell
CUST_305_PI426222305	0,043	2,186	down	PGSC0003DMT400028119	Conserved gene of unknown function	Cell
CUST_37599_PI426222305	0,028	3,785	down	PGSC0003DMT400049547	Structural molecule	Cell
CUST_15104_PI426222305	0,007	3,896	down	PGSC0003DMT400057119	Chromosome-associated kinesin KIF4A	Cell
CUST_18870_PI426222305	0,013	3,110	down	PGSC0003DMT400001172	Ring zinc finger protein	Cell
CUST_31338_PI426222305	0,018	2,842	down	PGSC0003DMT400034944	Ankyrin	Cell
CUST_12334_PI426222305	0,011	2,632	down	PGSC0003DMT400063541	Formin 11	Cell
CUST_40085_PI426222305	0,047	2,066	down	PGSC0003DMT400015245	Cyclin B1	Cell
CUST_18887_PI426222305	0,011	3,237	down	PGSC0003DMT400001171	Ring zinc finger protein	Cell
CUST_37635_PI426222305	0,025	6,128	down	PGSC0003DMT400049566	Pectinesterase	Cell Wall
CUST_10810_PI426222305	0,007	3,703	down	PGSC0003DMT400031896	Endo-1,4-beta-glucanase	Cell Wall
CUST_47615_PI426222305	0,034	3,398	down	PGSC0003DMT400005202	Lyase	Cell Wall
CUST_39145_PI426222305	0,008	3,783	down	PGSC0003DMT400035577	Pectinesterase	Cell Wall
CUST_39287_PI426222305	0,035	2,239	down	PGSC0003DMT400012809	Endo-beta-1,4-glucanase	Cell Wall
CUST_37685_PI426222305	0,023	6,303	down	PGSC0003DMT400049571	Pectinesterase	Cell Wall
CUST_38986_PI426222305	0,021	3,275	down	PGSC0003DMT400070322	ATCSLA09	Cell Wall
CUST_48380_PI426222305	0,015	2,340	down	PGSC0003DMT400011244	Expansin	Cell Wall
CUST_32658_PI426222305	0,041	2,312	down	PGSC0003DMT400047177	Beta-expansin 3	Cell Wall
CUST_32876_PI426222305	0,016	2,136	down	PGSC0003DMT400080635	UDP-D-xylose 4-epimerase	Cell Wall
CUST_1303_PI426222305	0,007	2,600	down	PGSC0003DMT400032910	Pectate lyase P18	Cell Wall
CUST_37980_PI426222305	0,023	2,260	down	PGSC0003DMT400081388	Pectinesterase	Cell Wall
CUST_22482_PI426222305	0,002	4,109	down	PGSC0003DMT400039385	Pectate lyase	Cell Wall
CUST_39144_PI426222305	0,016	4,072	down	PGSC0003DMT400035624	Phosphomannomutase	Cell Wall
CUST_37681_PI426222305	0,022	6,627	down	PGSC0003DMT400049564	Pectinesterase 3	Cell Wall
CUST_20900_PI426222305	0,035	2,503	down	PGSC0003DMT400011867	UDP-D-glucuronic acid 4-epimerase	Cell Wall
CUST_34188_PI426222305	0,010	4,134	down	PGSC0003DMT400030665	Pectinesterase	Cell Wall
CUST_38996_PI426222305	0,009	3,228	down	PGSC0003DMT400070323	Cellulose synthase-like A1	Cell Wall
CUST_16675_PI426222305	0,003	4,001	down	PGSC0003DMT400069500	Polygalacturonase-1 non-catalytic subunit beta	Cell Wall
CUST_47624_PI426222305	0,027	2,321	down	PGSC0003DMT400005204	Lyase	Cell Wall
CUST_11482_PI426222305	0,007	2,861	down	PGSC0003DMT400010632	Thiamine biosynthesis protein ThiC variant L1	Co-factor and vitamine metabolism
CUST_2887_PI426222305	0,029	2,292	down	PGSC0003DMT400000220	Ethylene-responsive late embryogenesis	Development
CUST_45529_PI426222305	0,011	3,710	down	PGSC0003DMT400079721	Argonaute 1	Development
CUST_16561_PI426222305	0,026	2,070	down	PGSC0003DMT400069511	Nam 1	Development
CUST_39695_PI426222305	0,010	2,909	down	PGSC0003DMT400058763	Conserved gene of unknown function	Development
CUST_15902_PI426222305	0,005	3,677	down	PGSC0003DMT400057803	Conserved gene of unknown function	Development
CUST_43258_PI426222305	0,018	2,868	down	PGSC0003DMT400008929	Nodulin	Development
CUST_14166_PI426222305	0,001	6,432	down	PGSC0003DMT400060057	Flowering locus T protein	Development
CUST_26285_PI426222305	0,010	3,572	down	PGSC0003DMT400041726	Flowering locus T	Development
CUST_36752_PI426222305	0,020	2,165	down	PGSC0003DMT400015812	Nodulin family protein	Development
CUST_4960_PI426222305	0,013	2,609	down	PGSC0003DMT400009432	Senescence-associated protein	Development
CUST_5494_PI426222305	0,034	6,003	down	PGSC0003DMT400022827	Nodulin	Development
CUST_5601_PI426222305	0,009	4,413	down	PGSC0003DMT400022826	Nodulin	Development
CUST_26183_PI426222305	0,004	6,854	down	PGSC0003DMT400041725	Flowering locus T	Development
CUST_17488_PI426222305	0,014	2,211	down	PGSC0003DMT400081212	UPA16	Development
CUST_9079_PI426222305	0,017	2,725	down	PGSC0003DMT400061888	Conserved gene of unknown function	DNA
CUST_48627_PI426222305	0,013	3,942	down	PGSC0003DMT400065027	Histone H3.2	DNA
CUST_45545_PI426222305	0,032	2,494	down	PGSC0003DMT400079711	DNA polymerase epsilon subunit B	DNA
CUST_45531_PI426222305	0,011	2,285	down	PGSC0003DMT400079712	DNA polymerase epsilon subunit B	DNA
CUST_13484_PI426222305	0,013	2,514	down	PGSC0003DMT400017488	DNA topoisomerase 2	DNA
CUST_45517_PI426222305	0,016	2,487	down	PGSC0003DMT400079710	DNA polymerase epsilon subunit B	DNA
CUST_26478_PI426222305	0,026	3,484	down	PGSC0003DMT400037075	Flap endonuclease GEN-like 2	DNA
CUST_10135_PI426222305	0,007	2,923	down	PGSC0003DMT400005594	Minichromosome maintenance factor	DNA
CUST_12705_PI426222305	0,045	3,226	down	PGSC0003DMT400063329	70 kDa subunit of replication protein A	DNA

CUST_10131_PI426222305	0,014	2,965	down	PGSC0003DMT400005593	MCM protein	DNA
CUST_44229_PI426222305	0,017	2,813	down	PGSC0003DMT400035464	Mini-chromosome maintenance protein MCM6	DNA
CUST_48628_PI426222305	0,024	3,190	down	PGSC0003DMT400064996	Histone H3.2	DNA
CUST_50607_PI426222305	0,016	3,584	down	PGSC0003DMT400065513	Isocitrate lyase	Gluconeogenesis
CUST_30643_PI426222305	0,049	2,092	down	PGSC0003DMT400008001	Leucoanthocyanidin dioxygenase	hormone metabolism
CUST_37708_PI426222305	0,017	3,100	down	PGSC0003DMT400004981	Carotenoid cleavage dioxygenase 4	hormone metabolism
CUST_36048_PI426222305	0,008	2,505	down	PGSC0003DMT400058565	Molybdopterin cofactor sulfurase	hormone metabolism
CUST_26807_PI426222305	0,010	2,723	down	PGSC0003DMT400035329	Indole-3-acetic acid-induced protein ARG7	hormone metabolism
CUST_37743_PI426222305	0,005	2,998	down	PGSC0003DMT400004980	Carotenoid cleavage dioxygenase 4	hormone metabolism
CUST_23816_PI426222305	0,015	2,803	down	PGSC0003DMT400055956	1-aminocyclopropane-1-carboxylate oxidase	hormone metabolism
CUST_39191_PI426222305	0,044	2,942	down	PGSC0003DMT400016687	Conserved gene of unknown function	hormone metabolism
CUST_31850_PI426222305	0,043	2,010	down	PGSC0003DMT400031146	Leucoanthocyanidin dioxygenase	hormone metabolism
CUST_38041_PI426222305	0,041	2,551	down	PGSC0003DMT400081401	Ethylene receptor homolog	hormone metabolism
CUST_18115_PI426222305	0,033	3,042	down	PGSC0003DMT400071048	9-cis-epoxycarotenoid dioxygenase	hormone metabolism
CUST_4357_PI426222305	0,023	2,067	down	PGSC0003DMT400002934	Allene oxide synthase 2	hormone metabolism
CUST_37602_PI426222305	0,002	3,925	down	PGSC0003DMT400049504	Transcription factor	hormone metabolism
CUST_43067_PI426222305	0,012	2,781	down	PGSC0003DMT400018924	Conserved gene of unknown function	hormone metabolism
CUST_37717_PI426222305	0,010	3,691	down	PGSC0003DMT400004977	Carotenoid cleavage dioxygenase 4	hormone metabolism
CUST_37718_PI426222305	0,013	3,851	down	PGSC0003DMT400004974	Carotenoid cleavage dioxygenase 4	hormone metabolism
CUST_46194_PI426222305	0,018	2,734	down	PGSC0003DMT400077449	Histidine phosphotransfer protein	hormone metabolism
CUST_37728_PI426222305	0,010	3,788	down	PGSC0003DMT400004978	Carotenoid cleavage dioxygenase 4	hormone metabolism
CUST_50659_PI426222305	0,043	2,397	down	PGSC0003DMT400068625	Indole-3-acetic acid-amido synthetase GH3.3	hormone metabolism
CUST_31862_PI426222305	0,033	2,090	down	PGSC0003DMT400031149	Oxidoreductase	hormone metabolism
CUST_37761_PI426222305	0,010	3,729	down	PGSC0003DMT400004975	Carotenoid cleavage dioxygenase 4a	hormone metabolism
CUST_46185_PI426222305	0,018	11,338	down	PGSC0003DMT400077450	Histidine phosphotransfer protein	hormone metabolism
CUST_31380_PI426222305	0,017	2,147	down	PGSC0003DMT400034972	Acyltransferase	Lipid Metabolism
CUST_23662_PI426222305	0,014	2,186	down	PGSC0003DMT400002337	Long-chain-fatty-acid CoA ligase	Lipid Metabolism
CUST_43405_PI426222305	0,048	2,029	down	PGSC0003DMT400032992	Gene of unknown function	Lipid Metabolism
CUST_39633_PI426222305	0,011	2,395	down	PGSC0003DMT400028048	Acyltransferase	Lipid Metabolism
CUST_15479_PI426222305	0,005	3,891	down	PGSC0003DMT400037473	Phosphoethanolamine N-methyltransferase	Lipid Metabolism
CUST_3080_PI426222305	0,040	2,396	down	PGSC0003DMT400000302	Triacylglycerol lipase	Lipid Metabolism
CUST_31968_PI426222305	0,008	3,051	down	PGSC0003DMT400083252	Cell wall apoplastic invertase	major CHO metabolism
CUST_10538_PI426222305	0,049	2,116	down	PGSC0003DMT400031568	Granule-bound starch synthase 1, chloroplastic/amyloplastic	major CHO metabolism
CUST_30240_PI426222305	0,014	2,148	down	PGSC0003DMT400012125	Glucosyltransferase	major CHO metabolism
CUST_10857_PI426222305	0,038	2,012	down	PGSC0003DMT400031569	Granule-bound starch synthase 1, chloroplastic/amyloplastic	major CHO metabolism
CUST_4964_PI426222305	0,026	3,878	down	PGSC0003DMT400009388	Farnesylated protein (ATFP6)	metal handling
CUST_13471_PI426222305	0,009	3,830	down	PGSC0003DMT400017657	Conserved oligomeric Golgi complex component	minor CHO metabolism
CUST_49755_PI426222305	0,006	3,348	down	PGSC0003DMT400035870	Trehalose-6-phosphate synthase	minor CHO metabolism
CUST_49334_PI426222305	0,006	3,319	down	PGSC0003DMT400056161	Trehalose-6-phosphate synthase	minor CHO metabolism
CUST_48598_PI426222305	0,022	2,689	down	PGSC0003DMT400035991	Trehalose 6-phosphate phosphatase	minor CHO metabolism
CUST_13591_PI426222305	0,022	2,405	down	PGSC0003DMT400017445	Glucosamine-fructose-6-phosphate aminotransferase	minor CHO metabolism
CUST_10795_PI426222305	0,020	2,090	down	PGSC0003DMT400032062	Aldose 1-epimerase	minor CHO metabolism
CUST_26464_PI426222305	0,046	2,830	down	PGSC0003DMT400037148	Sugar isomerase domain-containing protein	minor CHO metabolism
CUST_48848_PI426222305	0,049	2,067	down	PGSC0003DMT400028088	Tyramine N-feruloyltransferase 4/11	misc
CUST_23881_PI426222305	0,021	2,774	down	PGSC0003DMT400032789	Cationic peroxidase	misc
CUST_20952_PI426222305	0,017	3,083	down	PGSC0003DMT400011854	Conserved gene of unknown function	misc
CUST_4604_PI426222305	0,042	2,567	down	PGSC0003DMT400002922	Cytochrome P450 92B1	misc
CUST_24637_PI426222305	0,043	2,686	down	PGSC0003DMT400054391	Reticuline oxidase	misc
CUST_30232_PI426222305	0,005	3,293	down	PGSC0003DMT400089643	Arachidonic acid-induced DEA1	misc
CUST_33115_PI426222305	0,001	6,374	down	PGSC0003DMT400038473	Proline-rich protein	misc
CUST_42655_PI426222305	0,025	2,626	down	PGSC0003DMT400052472	Conserved gene of unknown function	misc
CUST_23011_PI426222305	0,007	3,645	down	PGSC0003DMT400061003	Zeatin O-glucosyltransferase	misc
CUST_9320_PI426222305	0,011	6,338	down	PGSC0003DMT400006459	Zinc finger protein	misc
CUST_49123_PI426222305	0,039	4,903	down	PGSC0003DMT400043474	Gene of unknown function	misc
CUST_41114_PI426222305	0,008	3,406	down	PGSC0003DMT400004447	Peroxidase	misc
CUST_27968_PI426222305	0,036	2,205	down	PGSC0003DMT400081975	Non-specific lipid-transfer protein	misc
CUST_41683_PI426222305	0,016	3,714	down	PGSC0003DMT400014094	Cytochrome P450	misc
CUST_40275_PI426222305	0,020	2,171	down	PGSC0003DMT400036487	Peroxidase	misc
CUST_47564_PI426222305	0,048	2,076	down	PGSC0003DMT400027198	Acidic class II 1,3-beta-glucanase	misc
CUST_1282_PI426222305	0,006	3,068	down	PGSC0003DMT400003644	UDP-glycosyltransferase	misc
CUST_41094_PI426222305	0,005	3,457	down	PGSC0003DMT400004446	Peroxidase	misc
CUST_26973_PI426222305	0,025	2,694	down	PGSC0003DMT400067202	Zinc finger protein	misc
CUST_20316_PI426222305	0,016	2,224	down	PGSC0003DMT400049736	Non-specific lipid-transfer protein	misc
CUST_31135_PI426222305	0,013	4,091	down	PGSC0003DMT400063936	Alcohol dehydrogenase 1	misc
CUST_1129_PI426222305	0,007	3,450	down	PGSC0003DMT400032896	Acetylglucosaminyltransferase	misc
CUST_1242_PI426222305	0,005	3,910	down	PGSC0003DMT400032895	Acetylglucosaminyltransferase	misc

CUST_24573_PI426222305	0,039	6,962	down	PGSC0003DMT400054386	Conserved gene of unknown function	misc
CUST_24665_PI426222305	0,035	5,418	down	PGSC0003DMT400054387	Conserved gene of unknown function	misc
CUST_39017_PI426222305	0,031	2,713	down	PGSC0003DMT400070316	Cytochrome P450 77A1	misc
CUST_4460_PI426222305	0,024	2,816	down	PGSC0003DMT400002923	Cytochrome P450 92B1	misc
CUST_19726_PI426222305	0,031	2,062	down	PGSC0003DMT400053378	Lipid transfer VAS	misc
CUST_4462_PI426222305	0,007	3,299	down	PGSC0003DMT400048145	Amidase family protein	misc
CUST_50228_PI426222305	0,037	3,943	down	PGSC0003DMT400080115	Chloroplast purple acid phosphatase isoform c	misc
CUST_50241_PI426222305	0,010	4,955	down	PGSC0003DMT400080116	Nucleotide pyrophosphatase/phosphodiesterase	misc
CUST_23038_PI426222305	0,035	2,276	down	PGSC0003DMT400021122	Conserved gene of unknown function	Not assigned/Unknown
CUST_30121_PI426222305	0,011	2,320	down	PGSC0003DMT400019529	Conserved gene of unknown function	Not assigned/Unknown
CUST_8573_PI426222305	0,015	4,094	down	PGSC0003DMT400058378	UPF0497 membrane protein 10	Not assigned/Unknown
CUST_22782_PI426222305	0,015	2,405	down	PGSC0003DMT400077995	Conserved gene of unknown function	Not assigned/Unknown
CUST_35687_PI426222305	0,024	2,597	down	PGSC0003DMT400096723	Sporozoite surface protein 2	Not assigned/Unknown
CUST_27864_PI426222305	0,004	3,961	down	PGSC0003DMT400015933	Periaxin	Not assigned/Unknown
CUST_8162_PI426222305	0,006	3,097	down	PGSC0003DMT400039857	Conserved gene of unknown function	Not assigned/Unknown
CUST_31580_PI426222305	0,026	2,165	down	PGSC0003DMT400073423	Gene of unknown function	Not assigned/Unknown
CUST_5049_PI426222305	0,041	2,835	down	PGSC0003DMT400003907	Conserved gene of unknown function	Not assigned/Unknown
CUST_637_PI426222305	0,003	9,408	down	PGSC0003DMT400070567	Sigma factor sigb regulation protein rsbq	Not assigned/Unknown
CUST_5335_PI426222305	0,022	2,639	down	PGSC0003DMT400009428	Conserved gene of unknown function	Not assigned/Unknown
CUST_31525_PI426222305	0,036	2,556	down	PGSC0003DMT400073465	Conserved gene of unknown function	Not assigned/Unknown
CUST_44288_PI426222305	0,038	2,203	down	PGSC0003DMT400010024	Sugar transporter	Not assigned/Unknown
CUST_42051_PI426222305	0,019	4,043	down	PGSC0003DMT400056024	Nonspecific lipid-transfer protein AKCS9	Not assigned/Unknown
CUST_10812_PI426222305	0,019	2,441	down	PGSC0003DMT400031674	Conserved gene of unknown function	Not assigned/Unknown
CUST_50219_PI426222305	0,002	5,841	down	PGSC0003DMT400080134	Conserved gene of unknown function	Not assigned/Unknown
CUST_16370_PI426222305	0,019	2,188	down	PGSC0003DMT400060746	Conserved gene of unknown function	Not assigned/Unknown
CUST_30277_PI426222305	0,036	2,332	down	PGSC0003DMT400012127	Glucosyltransferase	Not assigned/Unknown
CUST_20075_PI426222305	0,014	2,452	down	PGSC0003DMT400049403	Conserved gene of unknown function	Not assigned/Unknown
CUST_31932_PI426222305	0,043	2,297	down	PGSC0003DMT400015915	Conserved gene of unknown function	Not assigned/Unknown
CUST_45306_PI426222305	0,034	2,664	down	PGSC0003DMT400001658	Conserved gene of unknown function	Not assigned/Unknown
CUST_28750_PI426222305	0,042	3,195	down	PGSC0003DMT400083184	Gene of unknown function	Not assigned/Unknown
CUST_52150_PI426222305	0,046	2,462	down	PGSC0003DMT400084899	Glycine-rich protein 2	Not assigned/Unknown
CUST_658_PI426222305	0,013	5,023	down	PGSC0003DMT400055122	Multispanning membrane protein	Not assigned/Unknown
CUST_3966_PI426222305	0,023	2,463	down	PGSC0003DMT400093090	Gene of unknown function	Not assigned/Unknown
CUST_51055_PI426222305	0,037	2,025	down	PGSC0003DMT400030985	Glucosyltransferase	Not assigned/Unknown
CUST_8786_PI426222305	0,010	3,673	down	PGSC0003DMT400041482	Hydroxyproline-rich glycoprotein family protein	Not assigned/Unknown
CUST_15437_PI426222305	0,023	2,295	down	PGSC0003DMT400073731	Conserved gene of unknown function	Not assigned/Unknown
CUST_38625_PI426222305	0,015	3,052	down	PGSC0003DMT400076296	Gene of unknown function	Not assigned/Unknown
CUST_19969_PI426222305	0,017	2,408	down	PGSC0003DMT400049404	Conserved gene of unknown function	Not assigned/Unknown
CUST_5383_PI426222305	0,032	2,092	down	PGSC0003DMT400009365	Conserved gene of unknown function	Not assigned/Unknown
CUST_10333_PI426222305	0,021	3,762	down	PGSC0003DMT400028963	Conserved gene of unknown function	Not assigned/Unknown
CUST_47119_PI426222305	0,007	2,777	down	PGSC0003DMT400041332	ATP binding protein	Not assigned/Unknown
CUST_14756_PI426222305	0,035	2,212	down	PGSC0003DMT400066535	Auxin and ethylene responsive GH3	Not assigned/Unknown
CUST_8470_PI426222305	0,028	2,311	down	PGSC0003DMT400071564	Gene of unknown function	Not assigned/Unknown
CUST_16723_PI426222305	0,042	2,372	down	PGSC0003DMT400069576	DC1 domain containing protein	Not assigned/Unknown
CUST_51804_PI426222305	0,026	2,266	down	PGSC0003DMT400039169	Gene of unknown function	Not assigned/Unknown
CUST_21287_PI426222305	0,027	4,100	down	PGSC0003DMT400020222	Glycine-rich cell wall structural protein 1	Not assigned/Unknown
CUST_50047_PI426222305	0,006	3,475	down	PGSC0003DMT400065443	Gene of unknown function	Not assigned/Unknown
CUST_29331_PI426222305	0,040	2,131	down	PGSC0003DMT400089948	Gene of unknown function	Not assigned/Unknown
CUST_50043_PI426222305	0,009	3,475	down	PGSC0003DMT400065439	Gene of unknown function	Not assigned/Unknown
CUST_41876_PI426222305	0,020	2,900	down	PGSC0003DMT400026442	Conserved gene of unknown function	Not assigned/Unknown
CUST_51112_PI426222305	0,025	3,938	down	PGSC0003DMT400084313	Gene of unknown function	Not assigned/Unknown
CUST_20122_PI426222305	0,011	2,678	down	PGSC0003DMT400090511	Gene of unknown function	Not assigned/Unknown
CUST_35448_PI426222305	0,000	17,469	down	PGSC0003DMT400005823	Mutt domain protein	Not assigned/Unknown
CUST_2770_PI426222305	0,042	2,473	down	PGSC0003DMT400000263	BTB/POZ protein	Not assigned/Unknown
CUST_41781_PI426222305	0,003	5,905	down	PGSC0003DMT400015572	GTP binding protein gamma subunit	Not assigned/Unknown
CUST_42354_PI426222305	0,028	2,181	down	PGSC0003DMT400024564	Hemolysin	Not assigned/Unknown
CUST_3173_PI426222305	0,041	2,178	down	PGSC0003DMT400000170	Chromatin remodeling complex subunit	Not assigned/Unknown
CUST_32089_PI426222305	0,000	9,111	down	PGSC0003DMT400059829	Gene of unknown function	Not assigned/Unknown
CUST_29055_PI426222305	0,040	2,317	down	PGSC0003DMT400020606	Conserved gene of unknown function	Not assigned/Unknown
CUST_2225_PI426222305	0,021	2,261	down	PGSC0003DMT400028570	Putative sulfate transporter	Not assigned/Unknown
CUST_6595_PI426222305	0,019	2,634	down	PGSC0003DMT400014343	X-linked inhibitor of apoptosis protein, xiap	Not assigned/Unknown
CUST_49837_PI426222305	0,024	2,420	down	PGSC0003DMT400028219	UPA23	Not assigned/Unknown
CUST_27950_PI426222305	0,011	2,512	down	PGSC0003DMT400081919	Conserved gene of unknown function	Not assigned/Unknown
CUST_31244_PI426222305	0,002	4,095	down	PGSC0003DMT400034831	Protease inhibitor/seed storage/lipid transfer protein family protein	Not assigned/Unknown
CUST_9503_PI426222305	0,047	2,506	down	PGSC0003DMT400006513	60S ribosomal protein L37	Not assigned/Unknown
CUST_17514_PI426222305	0,022	2,282	down	PGSC0003DMT400001572	Gene of unknown function	Not assigned/Unknown

Appendix

CUST_20607_PI426222305	0,019	2,390	down	PGSC0003DMT400007838	Gene of unknown function	Not assigned/Unknown
CUST_45165_PI426222305	0,024	2,314	down	PGSC0003DMT400081227	Conserved gene of unknown function	Not assigned/Unknown
CUST_32195_PI426222305	0,034	2,340	down	PGSC0003DMT400084824	Gene of unknown function	Not assigned/Unknown
CUST_37463_PI426222305	0,018	2,155	down	PGSC0003DMT400078944	Aldose 1-epimerase	Not assigned/Unknown
CUST_20797_PI426222305	0,016	2,236	down	PGSC0003DMT400011875	Gene of unknown function	Not assigned/Unknown
CUST_2893_PI426222305	0,024	2,358	down	PGSC0003DMT400000235	Conserved gene of unknown function	Not assigned/Unknown
CUST_47603_PI426222305	0,024	2,017	down	PGSC0003DMT400030584	Conserved gene of unknown function	Not assigned/Unknown
CUST_34685_PI426222305	0,035	2,208	down	PGSC0003DMT400001772	Ubiquitin-protein ligase	Not assigned/Unknown
CUST_13596_PI426222305	0,031	2,280	down	PGSC0003DMT400046251	Leucine-rich repeat protein	Not assigned/Unknown
CUST_23931_PI426222305	0,018	2,075	down	PGSC0003DMT400083790	Gamma-gliadin	Not assigned/Unknown
CUST_28026_PI426222305	0,028	3,066	down	PGSC0003DMT400081920	Conserved gene of unknown function	Not assigned/Unknown
CUST_5588_PI426222305	0,007	2,638	down	PGSC0003DMT400022795	Conserved gene of unknown function	Not assigned/Unknown
CUST_23940_PI426222305	0,010	2,765	down	PGSC0003DMT400083791	Periaxin	Not assigned/Unknown
CUST_13465_PI426222305	0,050	2,184	down	PGSC0003DMT400017741	Gene of unknown function	Not assigned/Unknown
CUST_37564_PI426222305	0,011	4,030	down	PGSC0003DMT400049558	Gene of unknown function	Not assigned/Unknown
CUST_1502_PI426222305	0,039	3,383	down	PGSC0003DMT400052058	Conserved gene of unknown function	Not assigned/Unknown
CUST_2901_PI426222305	0,021	4,263	down	PGSC0003DMT400000327	Gene of unknown function	Not assigned/Unknown
CUST_24084_PI426222305	0,001	5,831	down	PGSC0003DMT400083793	Periaxin	Not assigned/Unknown
CUST_3777_PI426222305	0,036	2,129	down	PGSC0003DMT400090569	Gene of unknown function	Not assigned/Unknown
CUST_24051_PI426222305	0,003	3,684	down	PGSC0003DMT400083792	Periaxin	Not assigned/Unknown
CUST_18721_PI426222305	0,035	2,619	down	PGSC0003DMT400001241	Conserved gene of unknown function	Not assigned/Unknown
CUST_28010_PI426222305	0,044	2,026	down	PGSC0003DMT400081995	Ubiquitin ligase SINAT2	Not assigned/Unknown
CUST_17421_PI426222305	0,005	4,423	down	PGSC0003DMT400008367	Conserved gene of unknown function	Not assigned/Unknown
CUST_3167_PI426222305	0,025	4,524	down	PGSC0003DMT400000323	Conserved gene of unknown function	Not assigned/Unknown
CUST_6198_PI426222305	0,009	2,435	down	PGSC0003DMT400072135	Gene of unknown function	Not assigned/Unknown
CUST_7756_PI426222305	0,020	4,018	down	PGSC0003DMT400013202	F-box protein	Not assigned/Unknown
CUST_40487_PI426222305	0,006	3,326	down	PGSC0003DMT400077610	Gene of unknown function	Not assigned/Unknown
CUST_28725_PI426222305	0,028	2,835	down	PGSC0003DMT400083176	Conserved gene of unknown function	Not assigned/Unknown
CUST_27983_PI426222305	0,041	2,669	down	PGSC0003DMT400081922	Cell number regulator 10	Not assigned/Unknown
CUST_31345_PI426222305	0,009	3,271	down	PGSC0003DMT400035024	Conserved gene of unknown function	Not assigned/Unknown
CUST_10821_PI426222305	0,019	2,443	down	PGSC0003DMT400031584	Gene of unknown function	Not assigned/Unknown
CUST_9296_PI426222305	0,018	2,461	down	PGSC0003DMT400058926	Plastid beta-ketoacyl ACP synthase	Not assigned/Unknown
CUST_11703_PI426222305	0,046	2,205	down	PGSC0003DMT400046630	Conserved gene of unknown function	Not assigned/Unknown
CUST_26474_PI426222305	0,024	2,336	down	PGSC0003DMT400037065	Conserved gene of unknown function	Not assigned/Unknown
CUST_11118_PI426222305	0,005	2,834	down	PGSC0003DMT400007334	Conserved gene of unknown function	Not assigned/Unknown
CUST_19019_PI426222305	0,047	3,441	down	PGSC0003DMT400024315	Conserved gene of unknown function	Not assigned/Unknown
CUST_35181_PI426222305	0,008	4,080	down	PGSC0003DMT400021521	Gene of unknown function	Not assigned/Unknown
CUST_44826_PI426222305	0,004	3,526	down	PGSC0003DMT400002273	Quinonprotein alcohol dehydrogenase	Not assigned/Unknown
CUST_30371_PI426222305	0,014	2,328	down	PGSC0003DMT400069999	Conserved gene of unknown function	Not assigned/Unknown
CUST_37975_PI426222305	0,005	3,112	down	PGSC0003DMT400081429	Protein SSM1	Not assigned/Unknown
CUST_49402_PI426222305	0,024	3,666	down	PGSC0003DMT400074505	Glycine-rich cell wall structural protein 1	Not assigned/Unknown
CUST_39422_PI426222305	0,019	6,196	down	PGSC0003DMT400082104	Lipid binding protein	Not assigned/Unknown
CUST_44530_PI426222305	0,015	2,153	down	PGSC0003DMT400043064	Ulp1 protease family, C-terminal catalytic domain containing protein	Not assigned/Unknown
CUST_44836_PI426222305	0,006	3,480	down	PGSC0003DMT400002277	Quinonprotein alcohol dehydrogenase	Not assigned/Unknown
CUST_8206_PI426222305	0,015	3,183	down	PGSC0003DMT400075407	Conserved gene of unknown function	Not assigned/Unknown
CUST_16383_PI426222305	0,008	3,731	down	PGSC0003DMT400060751	Lipid binding protein	Not assigned/Unknown
CUST_17180_PI426222305	0,026	2,495	down	PGSC0003DMT400057920	Adhesive plaque matrix protein	Not assigned/Unknown
CUST_34752_PI426222305	0,008	3,910	down	PGSC0003DMT400009694	Male specific sperm protein	Not assigned/Unknown
CUST_23474_PI426222305	0,032	2,617	down	PGSC0003DMT400064972	Gene of unknown function	Not assigned/Unknown
CUST_21094_PI426222305	0,042	2,073	down	PGSC0003DMT400020111	Metal ion binding protein	Not assigned/Unknown
CUST_27841_PI426222305	0,005	3,474	down	PGSC0003DMT400015939	Gamma-gliadin	Not assigned/Unknown
CUST_44685_PI426222305	0,042	2,987	down	PGSC0003DMT400045316	Conserved gene of unknown function	Not assigned/Unknown
CUST_25918_PI426222305	0,025	3,820	down	PGSC0003DMT400051652	Protein TIFY 4B	Not assigned/Unknown
CUST_20709_PI426222305	0,013	3,427	down	PGSC0003DMT400011949	Metal ion binding protein	Not assigned/Unknown
CUST_36438_PI426222305	0,028	2,884	down	PGSC0003DMT400074524	Gene of unknown function	Not assigned/Unknown
CUST_34129_PI426222305	0,021	3,465	down	PGSC0003DMT400033085	Conserved gene of unknown function	Not assigned/Unknown
CUST_36031_PI426222305	0,017	2,141	down	PGSC0003DMT400046159	Glycine-rich protein	Not assigned/Unknown
CUST_9639_PI426222305	0,017	2,233	down	PGSC0003DMT400006487	Conserved gene of unknown function	Not assigned/Unknown
CUST_13156_PI426222305	0,012	2,387	down	PGSC0003DMT400085260	ORF107c	Not assigned/Unknown
CUST_51153_PI426222305	0,003	4,394	down	PGSC0003DMT400008561	Conserved gene of unknown function	Not assigned/Unknown
CUST_2952_PI426222305	0,041	3,277	down	PGSC0003DMT400000326	Wax synthase	Not assigned/Unknown
CUST_35753_PI426222305	0,028	4,294	down	PGSC0003DMT400046917	Conserved gene of unknown function	Not assigned/Unknown
CUST_25580_PI426222305	0,007	4,104	down	PGSC0003DMT400037283	Conserved gene of unknown function	Not assigned/Unknown
CUST_44226_PI426222305	0,011	2,867	down	PGSC0003DMT400035513	Gene of unknown function	Not assigned/Unknown
CUST_47078_PI426222305	0,022	2,385	down	PGSC0003DMT400086967	Conserved gene of unknown function	Not assigned/Unknown
CUST_52645_PI426222305	0,031	2,537	down	PGSC0003DMT400084487	Dehydrin DH2a	Not assigned/Unknown

CUST_21518_PI426222305	0,030	2,043	down	PGSC0003DMT400093652	Conserved gene of unknown function	Not assigned/Unknown
CUST_2764_PI426222305	0,017	2,426	down	PGSC0003DMT400000324	Conserved gene of unknown function	Not assigned/Unknown
CUST_35815_PI426222305	0,023	4,108	down	PGSC0003DMT400046918	Conserved gene of unknown function	Not assigned/Unknown
CUST_47165_PI426222305	0,006	3,512	down	PGSC0003DMT400089750	Latency-associated nuclear antigen	Not assigned/Unknown
CUST_24301_PI426222305	0,014	3,086	down	PGSC0003DMT400035701	Conserved gene of unknown function	Not assigned/Unknown
CUST_40009_PI426222305	0,014	3,452	down	PGSC0003DMT400030328	Conserved gene of unknown function	Not assigned/Unknown
CUST_40013_PI426222305	0,034	4,354	down	PGSC0003DMT400015185	Transcription factor	Not assigned/Unknown
CUST_31583_PI426222305	0,028	2,927	down	PGSC0003DMT400042522	Gene of unknown function	Not assigned/Unknown
CUST_37974_PI426222305	0,002	3,922	down	PGSC0003DMT400081431	Protein SSM1	Not assigned/Unknown
CUST_3927_PI426222305	0,009	3,103	down	PGSC0003DMT400085243	Gene of unknown function	Not assigned/Unknown
CUST_30375_PI426222305	0,006	3,331	down	PGSC0003DMT400069914	Proline transporter 3	Not assigned/Unknown
CUST_30215_PI426222305	0,047	2,120	down	PGSC0003DMT400012228	P-rich protein EIG-I30	Not assigned/Unknown
CUST_34153_PI426222305	0,009	4,011	down	PGSC0003DMT400033082	Conserved gene of unknown function	Not assigned/Unknown
CUST_4301_PI426222305	0,010	2,623	down	PGSC0003DMT400007760	Conserved gene of unknown function	Not assigned/Unknown
CUST_27982_PI426222305	0,031	2,279	down	PGSC0003DMT400082019	Selenoprotein O	Not assigned/Unknown
CUST_50213_PI426222305	0,025	2,369	down	PGSC0003DMT400080170	RAB7A	Not assigned/Unknown
CUST_31532_PI426222305	0,026	2,345	down	PGSC0003DMT400042533	Conserved gene of unknown function	Not assigned/Unknown
CUST_18578_PI426222305	0,040	5,378	down	PGSC0003DMT400042479	Glycine-rich protein	Not assigned/Unknown
CUST_21838_PI426222305	0,016	3,586	down	PGSC0003DMT400094670	Transcription factor hy5	Not assigned/Unknown
CUST_36651_PI426222305	0,031	2,059	down	PGSC0003DMT400030707	Gene of unknown function	Not assigned/Unknown
CUST_39436_PI426222305	0,001	4,489	down	PGSC0003DMT400082103	Protease inhibitor	Not assigned/Unknown
CUST_51918_PI426222305	0,011	2,704	down	PGSC0003DMT400039040	Non-specific lipid-transfer protein	Not assigned/Unknown
CUST_52625_PI426222305	0,005	5,947	down	PGSC0003DMT400069120	GI11736	Not assigned/Unknown
CUST_7287_PI426222305	0,026	3,271	down	PGSC0003DMT400091990	Gene of unknown function	Not assigned/Unknown
CUST_37576_PI426222305	0,004	3,715	down	PGSC0003DMT400049606	Conserved gene of unknown function	Not assigned/Unknown
CUST_27320_PI426222305	0,010	4,891	down	PGSC0003DMT400088375	Gene of unknown function	Not assigned/Unknown
CUST_2835_PI426222305	0,028	2,303	down	PGSC0003DMT400000236	Conserved gene of unknown function	Not assigned/Unknown
CUST_38370_PI426222305	0,035	2,271	down	PGSC0003DMT400022043	NTGP5	Not assigned/Unknown
CUST_6746_PI426222305	0,012	2,469	down	PGSC0003DMT400014777	Sulfate transporter	Not assigned/Unknown
CUST_49622_PI426222305	0,048	3,462	down	PGSC0003DMT400079867	Gene of unknown function	Not assigned/Unknown
CUST_28380_PI426222305	0,022	2,210	down	PGSC0003DMT400044333	MazG nucleotide pyrophosphohydrolase domain protein	Not assigned/Unknown
CUST_14920_PI426222305	0,011	2,589	down	PGSC0003DMT400056910	Lipid binding protein	Not assigned/Unknown
CUST_13618_PI426222305	0,007	3,355	down	PGSC0003DMT400017671	Conserved gene of unknown function	Not assigned/Unknown
CUST_18482_PI426222305	0,004	6,859	down	PGSC0003DMT400042454	Conserved gene of unknown function	Not assigned/Unknown
CUST_10319_PI426222305	0,018	2,441	down	PGSC0003DMT400029139	Conserved gene of unknown function	Not assigned/Unknown
CUST_35287_PI426222305	0,043	2,310	down	PGSC0003DMT400072118	HyPRP	Not assigned/Unknown
CUST_22537_PI426222305	0,011	2,590	down	PGSC0003DMT400078308	Conserved gene of unknown function	Not assigned/Unknown
CUST_34987_PI426222305	0,035	3,447	down	PGSC0003DMT400053731	Conserved gene of unknown function	Not assigned/Unknown
CUST_32733_PI426222305	0,029	2,050	down	PGSC0003DMT400047266	Conserved gene of unknown function	Not assigned/Unknown
CUST_32501_PI426222305	0,017	2,055	down	PGSC0003DMT400086680	Gibberellin 20-oxidase	Not assigned/Unknown
CUST_5066_PI426222305	0,041	2,162	down	PGSC0003DMT400009393	Self-pruning G-box protein	Not assigned/Unknown
CUST_10772_PI426222305	0,002	5,081	down	PGSC0003DMT400031668	Conserved gene of unknown function	Not assigned/Unknown
CUST_7711_PI426222305	0,016	6,325	down	PGSC0003DMT400025558	Conserved gene of unknown function	Not assigned/Unknown
CUST_5291_PI426222305	0,032	2,126	down	PGSC0003DMT400003839	Conserved gene of unknown function	Not assigned/Unknown
CUST_38031_PI426222305	0,002	3,784	down	PGSC0003DMT400081432	Protein SSM1	Not assigned/Unknown
CUST_49271_PI426222305	0,013	2,891	down	PGSC0003DMT400059128	Gene of unknown function	Not assigned/Unknown
CUST_25824_PI426222305	0,012	3,785	down	PGSC0003DMT400051706	Glycolipid transfer protein	Not assigned/Unknown
CUST_12836_PI426222305	0,036	2,358	down	PGSC0003DMT400063177	Conserved gene of unknown function	Not assigned/Unknown
CUST_788_PI426222305	0,007	14,691	down	PGSC0003DMT400052059	Conserved gene of unknown function	Not assigned/Unknown
CUST_5247_PI426222305	0,025	3,680	down	PGSC0003DMT400009059	Conserved gene of unknown function	Not assigned/Unknown
CUST_19975_PI426222305	0,037	3,394	down	PGSC0003DMT400049257	Conserved gene of unknown function	Not assigned/Unknown
CUST_7025_PI426222305	0,049	2,467	down	PGSC0003DMT400031265	Gene of unknown function	Not assigned/Unknown
CUST_10720_PI426222305	0,026	2,207	down	PGSC0003DMT400031671	Conserved gene of unknown function	Not assigned/Unknown
CUST_51791_PI426222305	0,026	2,803	down	PGSC0003DMT400017057	ASR4	Not assigned/Unknown
CUST_17691_PI426222305	0,043	3,822	down	PGSC0003DMT400066818	Conserved gene of unknown function	Not assigned/Unknown
CUST_7647_PI426222305	0,023	5,226	down	PGSC0003DMT400025559	Conserved gene of unknown function	Not assigned/Unknown
CUST_35508_PI426222305	0,000	17,479	down	PGSC0003DMT400005816	Mutt domain protein	Not assigned/Unknown
CUST_18955_PI426222305	0,022	2,014	down	PGSC0003DMT400024308	Arabinogalactan-protein	Not assigned/Unknown
CUST_51481_PI426222305	0,030	2,145	down	PGSC0003DMT400034175	Conserved gene of unknown function	Not assigned/Unknown
CUST_13467_PI426222305	0,018	2,116	down	PGSC0003DMT400017404	Esterase	Not assigned/Unknown
CUST_29054_PI426222305	0,012	7,526	down	PGSC0003DMT400020512	Gene of unknown function	Not assigned/Unknown
CUST_20169_PI426222305	0,011	3,094	down	PGSC0003DMT400062558	Gene of unknown function	Not assigned/Unknown
CUST_27861_PI426222305	0,003	3,157	down	PGSC0003DMT400015941	Gamma-gliadin	Not assigned/Unknown
CUST_42193_PI426222305	0,044	2,837	down	PGSC0003DMT400038234	RNase H family protein	Not assigned/Unknown
CUST_7422_PI426222305	0,019	2,064	down	PGSC0003DMT400009483	Conserved gene of unknown function	Not assigned/Unknown
CUST_44220_PI426222305	0,016	2,759	down	PGSC0003DMT400035454	Conserved gene of unknown function	Not assigned/Unknown

CUST_45751_PI426222305	0,029	2,382	down	PGSC0003DMT400055683	Wiscott-Aldrich syndrome, C-terminal	Not assigned/Unknown
CUST_10701_PI426222305	0,004	3,523	down	PGSC0003DMT400032175	Conserved gene of unknown function	Not assigned/Unknown
CUST_46558_PI426222305	0,039	2,032	down	PGSC0003DMT400071451	RRNA intron-encoded homing endonuclease	Not assigned/Unknown
CUST_26908_PI426222305	0,002	6,432	down	PGSC0003DMT400067222	Flotillin-1	Not assigned/Unknown
CUST_27954_PI426222305	0,030	3,179	down	PGSC0003DMT400081921	Conserved gene of unknown function	Not assigned/Unknown
CUST_34082_PI426222305	0,002	3,838	down	PGSC0003DMT400047880	Elicitor resposible protein	Not assigned/Unknown
CUST_32103_PI426222305	0,018	2,702	down	PGSC0003DMT400059825	Gene of unknown function	Not assigned/Unknown
CUST_38622_PI426222305	0,013	2,454	down	PGSC0003DMT400076295	Gene of unknown function	Not assigned/Unknown
CUST_42462_PI426222305	0,021	2,181	down	PGSC0003DMT400059173	Conserved gene of unknown function	Not assigned/Unknown
CUST_16603_PI426222305	0,021	2,045	down	PGSC0003DMT400069510	Nam 1	Not assigned/Unknown
CUST_46179_PI426222305	0,021	2,905	down	PGSC0003DMT400085725	Gene of unknown function	Not assigned/Unknown
CUST_30103_PI426222305	0,023	2,091	down	PGSC0003DMT400019530	Conserved gene of unknown function	Not assigned/Unknown
CUST_6097_PI426222305	0,044	2,455	down	PGSC0003DMT400096322	Polyprotein protein	Not assigned/Unknown
CUST_7712_PI426222305	0,041	2,096	down	PGSC0003DMT400025812	25 kDa protein dehydrin	Not assigned/Unknown
CUST_37506_PI426222305	0,011	2,655	down	PGSC0003DMT400078876	Conserved gene of unknown function	Not assigned/Unknown
CUST_12998_PI426222305	0,012	2,809	down	PGSC0003DMT400063325	SP1L	Not assigned/Unknown
CUST_32755_PI426222305	0,047	2,491	down	PGSC0003DMT400047200	Forminotransferase-cyclodeaminase	Not assigned/Unknown
CUST_3505_PI426222305	0,024	2,065	down	PGSC0003DMT400064189	Conserved gene of unknown function	Not assigned/Unknown
CUST_35596_PI426222305	0,011	3,729	down	PGSC0003DMT400004709	Glycine-rich protein	Not assigned/Unknown
CUST_46554_PI426222305	0,004	3,117	down	PGSC0003DMT400071453	Conserved gene of unknown function	Not assigned/Unknown
CUST_5834_PI426222305	0,018	2,362	down	PGSC0003DMT400006858	Conserved gene of unknown function	Not assigned/Unknown
CUST_10836_PI426222305	0,025	2,329	down	PGSC0003DMT400032037	Methanol inducible protein	Not assigned/Unknown
CUST_35417_PI426222305	0,035	2,161	down	PGSC0003DMT400071808	Conserved gene of unknown function	Not assigned/Unknown
CUST_38056_PI426222305	0,003	3,626	down	PGSC0003DMT400081428	Protein SSM1	Not assigned/Unknown
CUST_10598_PI426222305	0,005	3,026	down	PGSC0003DMT400032033	Keratin-associated protein 6-2	Not assigned/Unknown
CUST_50056_PI426222305	0,024	2,764	down	PGSC0003DMT400065437	Gene of unknown function	Not assigned/Unknown
CUST_51366_PI426222305	0,004	4,091	down	PGSC0003DMT400090071	Conserved gene of unknown function	Not assigned/Unknown
CUST_5279_PI426222305	0,018	2,217	down	PGSC0003DMT400003847	Conserved gene of unknown function	Not assigned/Unknown
CUST_38292_PI426222305	0,028	3,293	down	PGSC0003DMT400067282	Gene of unknown function	Not assigned/Unknown
CUST_38054_PI426222305	0,002	3,677	down	PGSC0003DMT400081430	Protein SSM1	Not assigned/Unknown
CUST_47806_PI426222305	0,003	4,402	down	PGSC0003DMT400019315	Gene of unknown function	Not assigned/Unknown
CUST_30249_PI426222305	0,014	5,196	down	PGSC0003DMT400012074	P-rich protein EIG-I30	Not assigned/Unknown
CUST_31829_PI426222305	0,025	2,814	down	PGSC0003DMT400071272	Gene of unknown function	Not assigned/Unknown
CUST_29839_PI426222305	0,038	4,035	down	PGSC0003DMT400033401	Conserved gene of unknown function	Not assigned/Unknown
CUST_25855_PI426222305	0,014	2,466	down	PGSC0003DMT400061760	Conserved gene of unknown function	Not assigned/Unknown
CUST_41356_PI426222305	0,048	2,025	down	PGSC0003DMT400079482	Conserved gene of unknown function	Not assigned/Unknown
CUST_40206_PI426222305	0,009	2,996	down	PGSC0003DMT400005379	Gene of unknown function	Not assigned/Unknown
CUST_16694_PI426222305	0,002	5,256	down	PGSC0003DMT400069530	Hydrogen peroxide-induced 1	Not assigned/Unknown
CUST_19780_PI426222305	0,045	2,503	down	PGSC0003DMT400064115	Conserved gene of unknown function	Not assigned/Unknown
CUST_4614_PI426222305	0,024	2,928	down	PGSC0003DMT400048142	Gene of unknown function	Not assigned/Unknown
CUST_16768_PI426222305	0,018	4,365	down	PGSC0003DMT400069236	Hydrogen peroxide-induced 1	Not assigned/Unknown
CUST_25914_PI426222305	0,024	2,147	down	PGSC0003DMT400051852	Circadian clock coupling factor ZGT	Not assigned/Unknown
CUST_24174_PI426222305	0,027	2,025	down	PGSC0003DMT400017083	Conserved gene of unknown function	Not assigned/Unknown
CUST_26991_PI426222305	0,003	3,691	down	PGSC0003DMT400067224	Gene of unknown function	Not assigned/Unknown
CUST_9243_PI426222305	0,009	2,426	down	PGSC0003DMT400023654	GDP-fucose protein-O-fucosyltransferase 2	Not assigned/Unknown
CUST_44283_PI426222305	0,010	2,937	down	PGSC0003DMT400010086	Conserved gene of unknown function	Not assigned/Unknown
CUST_35482_PI426222305	0,016	2,717	down	PGSC0003DMT400005815	Mutt domain protein	nucleotide metabolism
CUST_52482_PI426222305	0,000	18,228	down	PGSC0003DMT400049095	Mutt domain protein	nucleotide metabolism
CUST_35536_PI426222305	0,015	2,755	down	PGSC0003DMT400005803	Mutt domain protein	nucleotide metabolism
CUST_5516_PI426222305	0,030	2,089	down	PGSC0003DMT400023069	Magnesium dependent soluble inorganic pyrophosphatase	nucleotide metabolism
CUST_1548_PI426222305	0,035	2,042	down	PGSC0003DMT400052217	Ribonucleoside-diphosphate reductase small chain	nucleotide metabolism
CUST_35463_PI426222305	0,000	19,137	down	PGSC0003DMT400005804	Mutt domain protein	nucleotide metabolism
CUST_52483_PI426222305	0,005	3,917	down	PGSC0003DMT400049092	Mutt domain protein	nucleotide metabolism
CUST_52486_PI426222305	0,000	16,334	down	PGSC0003DMT400049094	Mutt domain protein	nucleotide metabolism
CUST_52484_PI426222305	0,000	16,108	down	PGSC0003DMT400049096	Mutt domain protein	nucleotide metabolism
CUST_38129_PI426222305	0,016	2,123	down	PGSC0003DMT400054829	Ribose-phosphate pyrophosphokinase 4	nucleotide metabolism
CUST_37028_PI426222305	0,032	2,066	down	PGSC0003DMT400061952	Fructose-1,6-bisphosphatase, cytosolic	Photosynthesis
CUST_37050_PI426222305	0,035	2,236	down	PGSC0003DMT400061949	Fructose-1,6-bisphosphatase, cytosolic	Photosynthesis
CUST_20983_PI426222305	0,030	2,119	down	PGSC0003DMT400056635	Photosystem I reaction center subunit IV B isoform 2	Photosynthesis
CUST_37071_PI426222305	0,033	2,236	down	PGSC0003DMT400061953	Fructose-1,6-bisphosphatase, cytosolic	Photosynthesis
CUST_47343_PI426222305	0,049	2,077	down	PGSC0003DMT400021392	Chlorophyll a/b binding protein PSII	Photosynthesis
CUST_31288_PI426222305	0,020	3,289	down	PGSC0003DMT400034895	Chlorophyll a-b binding protein 3C, chloroplastic PSII	Photosynthesis
CUST_9470_PI426222305	0,049	2,069	down	PGSC0003DMT400006768	Photosystem I psaH protein	Photosynthesis
CUST_43838_PI426222305	0,010	2,751	down	PGSC0003DMT400040116	Chitinase 1	Photosynthesis
CUST_44514_PI426222305	0,005	5,235	down	PGSC0003DMT400043054	Chlorophyll a-b binding protein 50, chloroplastic	Photosynthesis
CUST_48298_PI426222305	0,026	2,248	down	PGSC0003DMT400002438	NADH dehydrogenase subunit 5, mitochondrial	Photosynthesis

CUST_31403_PI426222305	0,011	2,500	down	PGSC0003DMT400042546	PSI-H	Photosynthesis
CUST_37042_PI426222305	0,032	2,054	down	PGSC0003DMT400061950	Fructose-1,6-bisphosphatase, cytosolic	Photosynthesis
CUST_31307_PI426222305	0,036	2,078	down	PGSC0003DMT400034893	Chlorophyll a-b binding protein 3C PSII	Photosynthesis
CUST_24374_PI426222305	0,044	3,101	down	PGSC0003DMT400010985	Chlorophyll a,b binding protein type I PSII	Photosynthesis
CUST_31296_PI426222305	0,002	11,109	down	PGSC0003DMT400034897	Chlorophyll a-b binding protein 3C, chloroplastic	Photosynthesis
CUST_31364_PI426222305	0,002	9,022	down	PGSC0003DMT400034898	Chlorophyll a-b binding protein 3C, chloroplastic	Photosynthesis
CUST_37033_PI426222305	0,034	2,317	down	PGSC0003DMT400061951	Fructose-1,6-bisphosphatase, cytosolic	Photosynthesis
CUST_31290_PI426222305	0,024	2,370	down	PGSC0003DMT400034892	Chlorophyll a-b binding protein 3C, chloroplastic	Photosynthesis
CUST_31356_PI426222305	0,009	2,718	down	PGSC0003DMT400035007	Chlorophyll a-b binding protein 3C, chloroplastic	Photosynthesis
CUST_14352_PI426222305	0,032	2,262	down	PGSC0003DMT400059995	Chlorophyll a-b binding protein 6A, chloroplastic	Photosynthesis
CUST_31278_PI426222305	0,002	10,283	down	PGSC0003DMT400034896	Chlorophyll a-b binding protein 3C, chloroplastic	Photosynthesis
CUST_39494_PI426222305	0,019	3,032	down	PGSC0003DMT400019031	Chlorophyll a/b-binding protein PS II-Type I	Photosynthesis
CUST_9519_PI426222305	0,016	2,640	down	PGSC0003DMT400006490	SEC13 family protein	Protein
CUST_22576_PI426222305	0,010	5,455	down	PGSC0003DMT400078244	Protein kinase	Protein
CUST_22505_PI426222305	0,035	2,446	down	PGSC0003DMT400039186	Copine	Protein
CUST_15993_PI426222305	0,044	2,271	down	PGSC0003DMT400076435	PHO2	Protein
CUST_25538_PI426222305	0,009	2,506	down	PGSC0003DMT400022424	Calcium ion binding protein	Protein
CUST_13610_PI426222305	0,003	3,877	down	PGSC0003DMT400092874	Subtilisin-like protease	Protein
CUST_41887_PI426222305	0,003	5,601	down	PGSC0003DMT400026507	Cysteine protease	Protein
CUST_9485_PI426222305	0,010	2,650	down	PGSC0003DMT400006609	Protein phosphatase 2C ABI2 homolog	Protein
CUST_15112_PI426222305	0,017	3,072	down	PGSC0003DMT400057326	BTB/POZ domain-containing protein	Protein
CUST_9304_PI426222305	0,007	3,148	down	PGSC0003DMT400006608	Protein phosphatase 2C ABI2 homolog	Protein
CUST_46291_PI426222305	0,044	2,106	down	PGSC0003DMT400092982	F-box domain-containing protein	Protein
CUST_33299_PI426222305	0,042	2,244	down	PGSC0003DMT400017897	Zinc finger protein	Protein
CUST_19122_PI426222305	0,029	2,281	down	PGSC0003DMT400044603	Zinc finger family protein	Protein
CUST_15266_PI426222305	0,012	2,687	down	PGSC0003DMT400057328	BTB/POZ domain-containing protein	Protein
CUST_1316_PI426222305	0,008	2,686	down	PGSC0003DMT400003465	FERONIA receptor-like kinase	Protein
CUST_6698_PI426222305	0,009	7,002	down	PGSC0003DMT400036931	Glycyl-tRNA synthetase	Protein
CUST_34871_PI426222305	0,023	2,209	down	PGSC0003DMT400073070	Sec61 transport protein	Protein
CUST_24597_PI426222305	0,044	2,073	down	PGSC0003DMT400054479	Conserved gene of unknown function	Protein
CUST_29096_PI426222305	0,046	2,069	down	PGSC0003DMT400020698	Protein phosphatase	Protein
CUST_13612_PI426222305	0,015	2,701	down	PGSC0003DMT400017451	Subtilase	Protein
CUST_13460_PI426222305	0,008	2,509	down	PGSC0003DMT400017638	SBT4C protein	Protein
CUST_9997_PI426222305	0,011	5,657	down	PGSC0003DMT400074985	Zinc finger family protein	Protein
CUST_11743_PI426222305	0,047	3,264	down	PGSC0003DMT400046591	F-box family protein	Protein
CUST_41942_PI426222305	0,021	2,739	down	PGSC0003DMT400026494	Cysteine proteinase	Protein
CUST_29658_PI426222305	0,020	2,037	down	PGSC0003DMT400047369	Zinc finger protein	Protein
CUST_9294_PI426222305	0,012	2,489	down	PGSC0003DMT400006610	Protein phosphatase 2C ABI2 homolog	Protein
CUST_37367_PI426222305	0,014	2,695	down	PGSC0003DMT400029631	Not56	Protein
CUST_6707_PI426222305	0,036	2,282	down	PGSC0003DMT400014695	FK506 binding protein	Protein
CUST_9968_PI426222305	0,008	5,599	down	PGSC0003DMT400074981	Zinc finger family protein	Protein
CUST_6760_PI426222305	0,011	2,631	down	PGSC0003DMT400036932	Glycyl-tRNA synthetase	Protein
CUST_29095_PI426222305	0,008	2,543	down	PGSC0003DMT400020577	Serine/threonine-protein kinase	Protein
CUST_9990_PI426222305	0,026	7,285	down	PGSC0003DMT400074983	Zinc finger family protein	Protein
CUST_9186_PI426222305	0,026	2,709	down	PGSC0003DMT400006607	Protein phosphatase 2C ABI2 homolog	Protein
CUST_23879_PI426222305	0,027	2,106	down	PGSC0003DMT400032797	BRASSINOSTEROID INSENSITIVE 1-associated receptor kinase 1	Protein
CUST_51316_PI426222305	0,047	2,165	down	PGSC0003DMT400041343	ATP binding protein	Protein
CUST_31149_PI426222305	0,008	2,892	down	PGSC0003DMT400063857	MAP3Ka	Protein
CUST_18902_PI426222305	0,028	2,362	down	PGSC0003DMT400044605	Zinc finger family protein	Protein
CUST_22827_PI426222305	0,013	5,777	down	PGSC0003DMT400078243	Protein kinase	Protein
CUST_41937_PI426222305	0,003	5,425	down	PGSC0003DMT400026506	Cysteine protease	Protein
CUST_44358_PI426222305	0,038	2,703	down	PGSC0003DMT400009991	Serine protease	Protein
CUST_26712_PI426222305	0,016	3,137	down	PGSC0003DMT400077222	Ser-thr protein kinase	Protein
CUST_41925_PI426222305	0,003	5,237	down	PGSC0003DMT400026505	Cysteine protease	Protein
CUST_41915_PI426222305	0,006	3,443	down	PGSC0003DMT400026464	Cysteine protease	Protein
CUST_9908_PI426222305	0,032	4,155	down	PGSC0003DMT400074984	Zinc finger family protein	Protein
CUST_50956_PI426222305	0,039	3,087	down	PGSC0003DMT400082809	ATP binding / protein kinase/ protein serine/threonine kinase	Protein
CUST_9513_PI426222305	0,046	2,148	down	PGSC0003DMT400006611	Protein phosphatase 2C ABI2 homolog	Protein
CUST_31878_PI426222305	0,018	3,625	down	PGSC0003DMT400053107	Elongation factor	Protein
CUST_10216_PI426222305	0,010	2,764	down	PGSC0003DMT400070670	Protein translocase secy subunit	Protein
CUST_29038_PI426222305	0,045	2,427	down	PGSC0003DMT400020545	Subtilisin-like protease preproenzyme	Protein
CUST_18795_PI426222305	0,017	2,845	down	PGSC0003DMT400001221	RING-H2 finger protein ATL57	Protein
CUST_41932_PI426222305	0,016	2,384	down	PGSC0003DMT400026495	Cysteine protease	Protein
CUST_16796_PI426222305	0,031	2,173	down	PGSC0003DMT400069540	Zinc finger family protein	Protein
CUST_46932_PI426222305	0,025	2,170	down	PGSC0003DMT400048698	F-box/kelch-repeat protein SKIP25	Protein
CUST_29013_PI426222305	0,010	2,465	down	PGSC0003DMT400020578	Serine/threonine-protein kinase	Protein

CUST_42777_PI426222305	0,029	2,588	down	PGSC0003DMT400033762	Protein phosphatase 2A	Protein
CUST_28067_PI426222305	0,009	2,482	down	PGSC0003DMT400004563	Ring finger protein	Protein
CUST_48986_PI426222305	0,009	2,465	down	PGSC0003DMT400056253	Glutaredoxin	Redox
CUST_29153_PI426222305	0,019	3,205	down	PGSC0003DMT400020675	Thioredoxin	Redox
CUST_8472_PI426222305	0,011	2,529	down	PGSC0003DMT400058325	Glutaredoxin, grx	Redox
CUST_23760_PI426222305	0,007	3,259	down	PGSC0003DMT400021232	Heat shock factor protein HSF30	RNA
CUST_39153_PI426222305	0,025	2,044	down	PGSC0003DMT400035592	Auxin response factor 19	RNA
CUST_19511_PI426222305	0,008	2,621	down	PGSC0003DMT400002860	Protein CHMP7	RNA
CUST_43515_PI426222305	0,008	2,564	down	PGSC0003DMT400065377	Zinc finger protein CONSTANS-LIKE 15	RNA
CUST_5560_PI426222305	0,025	2,118	down	PGSC0003DMT400006919	Heat stress transcription factor A3	RNA
CUST_21912_PI426222305	0,003	4,487	down	PGSC0003DMT400093117	Mads box protein	RNA
CUST_46771_PI426222305	0,005	3,663	down	PGSC0003DMT400038273	41 kD chloroplast nucleoid DNA binding protein (CND41)	RNA
CUST_9419_PI426222305	0,024	3,663	down	PGSC0003DMT400006452	DNA binding protein	RNA
CUST_27939_PI426222305	0,011	2,529	down	PGSC0003DMT400081782	Isoform 2 of UPF0496 protein	RNA
CUST_40953_PI426222305	0,013	2,486	down	PGSC0003DMT400019213	Dicer	RNA
CUST_26961_PI426222305	0,011	3,110	down	PGSC0003DMT400052697	Calcium-dependent protein kinase substrate protein	RNA
CUST_44281_PI426222305	0,029	2,181	down	PGSC0003DMT400010004	AT-hook DNA-binding protein	RNA
CUST_49298_PI426222305	0,027	2,688	down	PGSC0003DMT400059117	Lanceolate	RNA
CUST_28830_PI426222305	0,016	3,202	down	PGSC0003DMT400010397	DOF domain class transcription factor	RNA
CUST_30328_PI426222305	0,014	2,179	down	PGSC0003DMT400069733	AP2-domain DNA-binding protein	RNA
CUST_26394_PI426222305	0,023	2,294	down	PGSC0003DMT400037192	Remorin	RNA
CUST_9404_PI426222305	0,012	3,090	down	PGSC0003DMT400006751	AP2 domain class transcription factor	RNA
CUST_19011_PI426222305	0,012	2,864	down	PGSC0003DMT400024272	Nucleic acid binding protein	RNA
CUST_5825_PI426222305	0,031	2,088	down	PGSC0003DMT400006920	Heat stress transcription factor A3	RNA
CUST_51535_PI426222305	0,007	3,812	down	PGSC0003DMT400048964	Zinc finger protein	RNA
CUST_1554_PI426222305	0,033	2,217	down	PGSC0003DMT400026171	BIPINNATA	RNA
CUST_50927_PI426222305	0,035	2,342	down	PGSC0003DMT400013968	HD-ZIP	RNA
CUST_2481_PI426222305	0,012	2,625	down	PGSC0003DMT400072210	DNA binding protein	RNA
CUST_8985_PI426222305	0,047	2,046	down	PGSC0003DMT400048032	Auxin response factor 8-1	RNA
CUST_43614_PI426222305	0,013	3,400	down	PGSC0003DMT400064702	KH domain-containing protein	RNA
CUST_36843_PI426222305	0,043	2,592	down	PGSC0003DMT400086663	SRF-type transcription factor family protein	RNA
CUST_11071_PI426222305	0,037	2,336	down	PGSC0003DMT400078476	Myb-like transcription factor 6	RNA
CUST_24093_PI426222305	0,031	2,172	down	PGSC0003DMT400008944	RNA-binding region-containing protein	RNA
CUST_38246_PI426222305	0,035	2,477	down	PGSC0003DMT400067285	SET domain-containing protein	RNA
CUST_15970_PI426222305	0,046	2,731	down	PGSC0003DMT400076408	Putative ethylene responsive element binding protein 1	RNA
CUST_46236_PI426222305	0,032	3,876	down	PGSC0003DMT400053238	Binding protein	RNA
CUST_47808_PI426222305	0,002	4,415	down	PGSC0003DMT400019296	RAV	RNA
CUST_25234_PI426222305	0,050	2,928	down	PGSC0003DMT400014953	AP2/ERF domain-containing transcription factor	RNA
CUST_50509_PI426222305	0,015	5,013	down	PGSC0003DMT400062081	Homeobox-leucine zipper protein	RNA
CUST_36972_PI426222305	0,023	2,153	down	PGSC0003DMT400068508	DNA binding protein	RNA
CUST_52282_PI426222305	0,017	2,379	down	PGSC0003DMT400020031	Transcription factor	RNA
CUST_36965_PI426222305	0,023	2,129	down	PGSC0003DMT400067504	SET domain protein	RNA
CUST_10462_PI426222305	0,002	4,351	down	PGSC0003DMT400070680	CONSTANS	RNA
CUST_50874_PI426222305	0,025	2,014	down	PGSC0003DMT400071577	S-adenosylmethionine-dependent methyltransferase	RNA
CUST_36375_PI426222305	0,005	3,159	down	PGSC0003DMT400016188	Conserved gene of unknown function	RNA
CUST_11895_PI426222305	0,003	5,065	down	PGSC0003DMT400048639	Transcription factor	RNA
CUST_23812_PI426222305	0,030	2,933	down	PGSC0003DMT400021144	WRKY transcription factor	RNA
CUST_2338_PI426222305	0,017	2,391	down	PGSC0003DMT400072208	Myb RL3	RNA
CUST_25096_PI426222305	0,021	2,477	down	PGSC0003DMT400014952	AP2/ERF domain-containing transcription factor	RNA
CUST_36339_PI426222305	0,021	2,946	down	PGSC0003DMT400074526	CHP-rich zinc finger protein	RNA
CUST_25658_PI426222305	0,006	7,368	down	PGSC0003DMT400029328	WRKY DNA-binding protein	RNA
CUST_24139_PI426222305	0,028	2,241	down	PGSC0003DMT400008945	RNA-binding region-containing protein	RNA
CUST_23868_PI426222305	0,046	2,133	down	PGSC0003DMT400083784	Conserved gene of unknown function	secondary metabolism
CUST_17579_PI426222305	0,005	3,146	down	PGSC0003DMT400081183	Feruloyl transferase	secondary metabolism
CUST_30393_PI426222305	0,004	4,789	down	PGSC0003DMT400069866	Laccase 90a	secondary metabolism
CUST_32704_PI426222305	0,022	3,562	down	PGSC0003DMT400047279	Tryptophan decarboxylase	secondary metabolism
CUST_7635_PI426222305	0,006	3,724	down	PGSC0003DMT400025701	3-hydroxy-3-methylglutaryl coenzyme A reductase	secondary metabolism
CUST_32654_PI426222305	0,016	2,148	down	PGSC0003DMT400047278	Tryptophan decarboxylase	secondary metabolism
CUST_17416_PI426222305	0,006	2,789	down	PGSC0003DMT400081182	Feruloyl transferase	secondary metabolism
CUST_31842_PI426222305	0,027	2,020	down	PGSC0003DMT400031147	Leucoanthocyanidin dioxygenase	secondary metabolism
CUST_30349_PI426222305	0,002	4,846	down	PGSC0003DMT400069728	Laccase 90c	secondary metabolism
CUST_1260_PI426222305	0,019	2,222	down	PGSC0003DMT400025951	Autoinhibited calcium ATPase	signalling
CUST_4703_PI426222305	0,014	2,808	down	PGSC0003DMT400010610	SF16 protein	signalling
CUST_50622_PI426222305	0,024	2,113	down	PGSC0003DMT400065539	Glutamate receptor 3 plant	signalling
CUST_10183_PI426222305	0,038	2,226	down	PGSC0003DMT400030924	Receptor-like kinase CHRK1	signalling
CUST_43825_PI426222305	0,005	7,337	down	PGSC0003DMT400040125	Serine-threonine protein kinase, plant-type	signalling

CUST_42619_PI426222305	0,004	4,579	down	PGSC0003DMT400026813	Serine-threonine protein kinase, plant-type	signalling
CUST_16305_PI426222305	0,015	2,626	down	PGSC0003DMT400060607	Conserved gene of unknown function	signalling
CUST_27302_PI426222305	0,032	3,989	down	PGSC0003DMT400033812	Receptor protein kinase	signalling
CUST_50623_PI426222305	0,026	2,127	down	PGSC0003DMT400065536	Glutamate receptor 3 plant	signalling
CUST_3600_PI426222305	0,015	2,311	down	PGSC0003DMT400040776	Conserved gene of unknown function	signalling
CUST_34957_PI426222305	0,032	2,150	down	PGSC0003DMT400073110	Serine-threonine protein kinase, plant-type	signalling
CUST_50621_PI426222305	0,023	2,246	down	PGSC0003DMT400065535	Glutamate receptor 3 plant	signalling
CUST_15517_PI426222305	0,041	3,759	down	PGSC0003DMT400073675	Conserved gene of unknown function	signalling
CUST_42531_PI426222305	0,032	2,665	down	PGSC0003DMT400079204	Conserved gene of unknown function	signalling
CUST_15463_PI426222305	0,039	3,688	down	PGSC0003DMT400073677	Conserved gene of unknown function	signalling
CUST_27006_PI426222305	0,012	2,408	down	PGSC0003DMT400067204	Phosphatidylinositol-4-phosphate 5-kinase	signalling
CUST_15444_PI426222305	0,033	3,645	down	PGSC0003DMT400073678	Conserved gene of unknown function	signalling
CUST_11816_PI426222305	0,044	2,322	down	PGSC0003DMT400046807	Receptor protein kinase	signalling
CUST_50215_PI426222305	0,034	2,164	down	PGSC0003DMT400080167	RAB7A	signalling
CUST_19083_PI426222305	0,049	2,010	down	PGSC0003DMT400024269	Receptor protein kinase CLAVATA1	signalling
CUST_44609_PI426222305	0,023	2,579	down	PGSC0003DMT400013398	Hcr9-OR3A	signalling
CUST_51417_PI426222305	0,015	3,753	down	PGSC0003DMT400034331	Conserved gene of unknown function	signalling
CUST_27405_PI426222305	0,005	3,050	down	PGSC0003DMT400045690	Conserved gene of unknown function	signalling
CUST_9205_PI426222305	0,019	2,269	down	PGSC0003DMT400023629	Chaperonin Cpn60/TCP-1; Phosphatidylinositol-4-phosphate 5-kinase; Zinc finger, FYVE/PHD-type	signalling
CUST_11711_PI426222305	0,030	2,510	down	PGSC0003DMT400046806	Receptor protein kinase	signalling
CUST_39779_PI426222305	0,027	9,176	down	PGSC0003DMT400067920	UPA22	signalling
CUST_9159_PI426222305	0,009	4,261	down	PGSC0003DMT400058127	Calcium-dependent protein kinase	signalling
CUST_9586_PI426222305	0,024	2,430	down	PGSC0003DMT400006372	Calmodulin binding protein	signalling
CUST_3853_PI426222305	0,020	2,137	down	PGSC0003DMT400013709	Calreticulin	signalling
CUST_20000_PI426222305	0,007	3,274	down	PGSC0003DMT400049439	WD-40 repeat family protein	signalling
CUST_24425_PI426222305	0,026	2,143	down	PGSC0003DMT400022542	Monomeric G-protein	signalling
CUST_11042_PI426222305	0,011	3,140	down	PGSC0003DMT400078562	Receptor kinase	signalling
CUST_11389_PI426222305	0,011	2,757	down	PGSC0003DMT400010659	Serine-threonine protein kinase, plant-type	signalling
CUST_10801_PI426222305	0,018	2,201	down	PGSC0003DMT400031856	Receptor kinase	signalling
CUST_4786_PI426222305	0,012	3,776	down	PGSC0003DMT400010609	SF16 protein	signalling
CUST_20017_PI426222305	0,014	2,876	down	PGSC0003DMT400049216	NtEIG-E80 protein	signalling
CUST_10378_PI426222305	0,022	2,646	down	PGSC0003DMT400070694	Serine-threonine protein kinase, plant-type	signalling
CUST_9119_PI426222305	0,028	2,884	down	PGSC0003DMT400058117	Protein P21	stress
CUST_42803_PI426222305	0,038	2,361	down	PGSC0003DMT400002131	NBS-coding resistance gene analog	stress
CUST_22324_PI426222305	0,002	5,831	down	PGSC0003DMT400039340	Conserved gene of unknown function	stress
CUST_5518_PI426222305	0,023	2,230	down	PGSC0003DMT400006908	Heat shock protein binding protein	stress
CUST_28225_PI426222305	0,037	2,933	down	PGSC0003DMT400044225	Rhicadhesin receptor	stress
CUST_22567_PI426222305	0,007	4,301	down	PGSC0003DMT400078163	Heat shock cognate 70 kDa protein 1	stress
CUST_39773_PI426222305	0,011	2,467	down	PGSC0003DMT400067963	NBS-coding resistance gene protein	stress
CUST_50754_PI426222305	0,028	2,189	down	PGSC0003DMT400049062	Sn-1 protein	stress
CUST_36685_PI426222305	0,006	3,101	down	PGSC0003DMT400004111	Disease resistance response protein	stress
CUST_49124_PI426222305	0,006	3,233	down	PGSC0003DMT400043497	SCUTL2	stress
CUST_19908_PI426222305	0,006	2,860	down	PGSC0003DMT400034089	Leucine-rich repeat-containing protein	stress
CUST_39721_PI426222305	0,023	2,364	down	PGSC0003DMT400020005	Tir-nbs-lrr resistance protein	stress
CUST_48204_PI426222305	0,023	2,839	down	PGSC0003DMT400071638	Resistance protein PSH-RGH7	stress
CUST_50758_PI426222305	0,013	2,230	down	PGSC0003DMT400093098	Sn-1 protein	stress
CUST_47467_PI426222305	0,019	2,052	down	PGSC0003DMT400064779	Conserved gene of unknown function	stress
CUST_8973_PI426222305	0,004	3,327	down	PGSC0003DMT400012936	Conserved gene of unknown function	stress
CUST_31161_PI426222305	0,032	2,510	down	PGSC0003DMT400063922	Conserved gene of unknown function	stress
CUST_15246_PI426222305	0,040	2,146	down	PGSC0003DMT400096975	Tir-nbs resistance protein	stress
CUST_39738_PI426222305	0,031	2,041	down	PGSC0003DMT400067974	TMV resistance protein N	stress
CUST_41104_PI426222305	0,008	2,455	down	PGSC0003DMT400004399	P58IPK	stress
CUST_15208_PI426222305	0,043	4,794	down	PGSC0003DMT400057098	Germin 11-1	stress
CUST_50753_PI426222305	0,002	4,370	down	PGSC0003DMT400059752	Sn-1 protein	stress
CUST_9069_PI426222305	0,018	2,329	down	PGSC0003DMT400012937	Conserved gene of unknown function	stress
CUST_25643_PI426222305	0,043	3,006	down	PGSC0003DMT400037336	Heat shock cognate protein 80	stress
CUST_12002_PI426222305	0,018	2,195	down	PGSC0003DMT400076601	Molecular chaperone Hsp90-1	stress
CUST_9434_PI426222305	0,015	2,620	down	PGSC0003DMT400006724	Malic enzyme	TCA
CUST_9215_PI426222305	0,013	2,701	down	PGSC0003DMT400006726	Malic enzyme	TCA
CUST_35135_PI426222305	0,042	2,152	down	PGSC0003DMT400021489	Succinate dehydrogenase subunit 3	TCA
CUST_9540_PI426222305	0,016	2,637	down	PGSC0003DMT400006725	Malic enzyme	TCA
CUST_49000_PI426222305	0,020	2,613	down	PGSC0003DMT400021923	Auxin influx transport protein	Transport
CUST_46482_PI426222305	0,017	2,418	down	PGSC0003DMT400016339	Oligopeptide transporter OPT family	Transport
CUST_11267_PI426222305	0,010	2,402	down	PGSC0003DMT400078524	GABA-specific permease	Transport
CUST_26132_PI426222305	0,036	2,867	down	PGSC0003DMT400041648	2-oxoglutarate/malate translocator	Transport
CUST_51288_PI426222305	0,011	2,617	down	PGSC0003DMT400016890	Nitrate excretion transporter 1	Transport

Appendix

CUST_16742_PI426222305	0,018	2,532	down	PGSC0003DMT400069660	Nitrate transporter	Transport
CUST_39871_PI426222305	0,027	2,354	down	PGSC0003DMT400047546	White-brown-complex ABC transporter family	Transport
CUST_30345_PI426222305	0,036	4,465	down	PGSC0003DMT400069919	Proline transporter 2	Transport
CUST_35288_PI426222305	0,007	2,832	down	PGSC0003DMT400048535	Sugar transporter	Transport
CUST_30415_PI426222305	0,005	3,346	down	PGSC0003DMT400069916	Proline transporter 3	Transport
CUST_24831_PI426222305	0,049	2,067	down	PGSC0003DMT400045176	P-glycoprotein	Transport
CUST_45029_PI426222305	0,005	5,368	down	PGSC0003DMT400027348	OST3/OST6 family protein	Transport
CUST_30350_PI426222305	0,007	2,842	down	PGSC0003DMT400069917	Proline transporter 3	Transport
CUST_10461_PI426222305	0,017	2,365	down	PGSC0003DMT400070689	Conserved gene of unknown function	Transport
CUST_16782_PI426222305	0,049	3,450	down	PGSC0003DMT400069676	Anion exchanger family protein	Transport
CUST_50630_PI426222305	0,043	2,964	down	PGSC0003DMT400065544	MATE efflux family protein	Transport
CUST_51289_PI426222305	0,015	2,381	down	PGSC0003DMT400016894	Peptide transporter	Transport
CUST_30429_PI426222305	0,004	3,290	down	PGSC0003DMT400069915	Proline transporter 3	Transport
CUST_26433_PI426222305	0,015	2,140	down	PGSC0003DMT400037015	Multidrug resistance pump	Transport
CUST_16183_PI426222305	0,017	2,355	down	PGSC0003DMT400039994	Sugar transporter	Transport
CUST_10182_PI426222305	0,044	2,133	down	PGSC0003DMT400070650	TRANSPARENT TESTA 12 protein	Transport
CUST_51283_PI426222305	0,015	2,777	down	PGSC0003DMT400016889	Peptide transporter	Transport
CUST_48865_PI426222305	0,016	2,428	down	PGSC0003DMT400043270	ATP-binding cassette transporter	Transport
CUST_42795_PI426222305	0,003	3,452	down	PGSC0003DMT400002144	Lysine/histidine transporter	Transport
CUST_49176_PI426222305	0,008	2,878	down	PGSC0003DMT400071749	Sulfate/bicarbonate/oxalate exchanger and transporter sat-1	Transport
CUST_25528_PI426222305	0,044	2,512	down	PGSC0003DMT400029244	Cation diffusion facilitator 9	Transport
CUST_42590_PI426222305	0,019	3,603	down	PGSC0003DMT400026883	Iron-regulated transporter 1	Transport
CUST_47872_PI426222305	0,016	3,027	down	PGSC0003DMT400019424	Peptide transporter	Transport
CUST_45767_PI426222305	0,022	5,272	down	PGSC0003DMT400055694	Amino acid transporter	Transport
CUST_26181_PI426222305	0,040	2,685	down	PGSC0003DMT400041652	Glutamate/malate translocator	Transport
CUST_34063_PI426222305	0,011	2,472	down	PGSC0003DMT400030604	Copper transporter	Transport
CUST_50617_PI426222305	0,035	2,230	down	PGSC0003DMT400065526	Glucose-6-phosphate/phosphate-translocator	Transport
CUST_22804_PI426222305	0,036	2,995	down	PGSC0003DMT400077926	Aquaporin, MIP family, TIP subfamily	Transport
CUST_35580_PI426222305	0,031	2,040	down	PGSC0003DMT400004654	Purine permease	Transport
CUST_50444_PI426222305	0,002	10,640	down	PGSC0003DMT400065948	Potassium channel NKT1	Transport
CUST_49033_PI426222305	0,018	2,077	down	PGSC0003DMT400021855	ATP binding protein	Unclassified
CUST_50949_PI426222305	0,022	2,085	down	PGSC0003DMT400082789	Squamosa promoter binding	Unclassified
CUST_5562_PI426222305	0,009	2,676	down	PGSC0003DMT400006922	Heat stress transcription factor A3	Unclassified
CUST_23776_PI426222305	0,005	3,086	down	PGSC0003DMT400021233	Heat shock factor protein HSF30	Unclassified
CUST_23821_PI426222305	0,005	3,189	down	PGSC0003DMT400021235	Heat shock factor protein HSF30	Unclassified
CUST_34269_PI426222305	0,003	4,834	down	PGSC0003DMT400044918	Flavonol synthase/flavanone 3-hydroxylase	Unclassified
CUST_46200_PI426222305	0,003	9,987	down	PGSC0003DMT400077451	Histidine phosphotransfer protein	Unclassified

Table A 2: 205 co-expressed entities with SP6A resulting from the overlap between k-means clustering and Pearson's correlation (coefficient ≥ 0.6).

ProbeName	PrimaryAccession	UniRef based putative functional annotation	A.t. BLAST hit	Category
CUST_42657_PI426222305	PGSC0003DMT400052381	Prephenate dehydrogenase	AT5G34930.1	AA metabolism
CUST_33144_PI426222305	PGSC0003DMT400067600	Aromatic amino acid decarboxylase 2	AT1G43710.1	AA metabolism
CUST_52526_PI426222305	PGSC0003DMT400051586	Histidine decarboxylase	AT1G43710.1	AA metabolism
CUST_28999_PI426222305	PGSC0003DMT400020612	Gibberellin receptor GID1	AT1G47480.1	Biodegradation of Xenobiotics
CUST_33573_PI426222305	PGSC0003DMT400058197	HIPL1 protein	AT1G74790.1	Cell
CUST_46332_PI426222305	PGSC0003DMT400034146	Tom	AT2G02230.1	Cell
CUST_27936_PI426222305	PGSC0003DMT400081918	Dynein light chain type 1 family protein	AT1G23220.1	Cell
CUST_37599_PI426222305	PGSC0003DMT400049547	Structural molecule	AT5G54110.1	Cell
CUST_39144_PI426222305	PGSC0003DMT400035624	Phosphomannomutase	AT2G45790.1	Cell Wall
CUST_14166_PI426222305	PGSC0003DMT400060057	Flowering locus T protein	AT1G65480.1	Development
CUST_26285_PI426222305	PGSC0003DMT400041726	Flowering locus T	AT4G20370.1	Development
CUST_17488_PI426222305	PGSC0003DMT400081212	UPA16	AT5G50790.1	Development
CUST_15135_PI426222305	PGSC0003DMT400090327	NAC domain protein	AT2G43000.1	Development
CUST_21193_PI426222305	PGSC0003DMT400020387	Senescence-associated protein	AT2G23810.1	Development
CUST_5494_PI426222305	PGSC0003DMT400022827	Nodulin	AT2G37460.1	Development
CUST_4960_PI426222305	PGSC0003DMT400009432	Senescence-associated protein	AT4G35770.1	Development
CUST_5601_PI426222305	PGSC0003DMT400022826	Nodulin	AT2G37460.1	Development
CUST_15902_PI426222305	PGSC0003DMT400057803	Conserved gene of unknown function	AT2G20740.1	Development
CUST_44230_PI426222305	PGSC0003DMT400035465	Mini-chromosome maintenance protein MCM6	AT5G44635.1	DNA
CUST_12705_PI426222305	PGSC0003DMT400063329	70 kDa subunit of replication protein A	AT5G08020.1	DNA
CUST_48627_PI426222305	PGSC0003DMT400065027	Histone H3.2	AT1G09200.1	DNA
CUST_14114_PI426222305	PGSC0003DMT400060472	Histone H4	AT1G07660.1	DNA
CUST_48628_PI426222305	PGSC0003DMT400064996	Histone H3.2	AT1G09200.1	DNA
CUST_44229_PI426222305	PGSC0003DMT400035464	Mini-chromosome maintenance protein MCM6	AT5G44635.1	DNA
CUST_23816_PI426222305	PGSC0003DMT400055956	1-aminocyclopropane-1-carboxylate oxidase	AT1G17020.1	hormone metabolism
CUST_15128_PI426222305	PGSC0003DMT400056893	Molybdenum cofactor sulfurase	AT1G16540.1	hormone metabolism
CUST_43185_PI426222305	PGSC0003DMT400042690	Auxin-induced SAUR	AT1G29510.1	hormone metabolism
CUST_43192_PI426222305	PGSC0003DMT400042745	SAUR family protein	AT5G18080.1	hormone metabolism
CUST_31968_PI426222305	PGSC0003DMT400083252	Cell wall apoplastic invertase	AT1G55120.1	major CHO metabolism
CUST_39315_PI426222305	PGSC0003DMT400012844	Metal ion binding protein	AT2G18196.1	metal handling
CUST_49334_PI426222305	PGSC0003DMT400056161	Trehalose-6-phosphate synthase	AT4G39770.1	minor CHO metabolism
CUST_1242_PI426222305	PGSC0003DMT400032895	Acetylglucosaminyltransferase	AT3G27540.1	misc
CUST_1129_PI426222305	PGSC0003DMT400032896	Acetylglucosaminyltransferase	AT3G27540.1	misc
CUST_24573_PI426222305	PGSC0003DMT400054386	FAD linked oxidase, N-terminal domain containing protein	AT5G44440.1	misc
CUST_51964_PI426222305	PGSC0003DMT400017153	Cytochrome P450 hydroxylase	AT3G26330.1	misc
CUST_10281_PI426222305	PGSC0003DMT400029080	Pectinesterase inhibitor	no Hit	misc
CUST_24665_PI426222305	PGSC0003DMT400054387	Conserved gene of unknown function	AT5G44440.1	misc
CUST_32165_PI426222305	PGSC0003DMT400037628	Flavin monooxygenase	AT5G25620.2	misc
CUST_9399_PI426222305	PGSC0003DMT400023616	GDSL esterase/lipase 5	AT1G53920.1	misc
CUST_41114_PI426222305	PGSC0003DMT400004447	Peroxidase	AT2G37130.1	misc
CUST_41094_PI426222305	PGSC0003DMT400004446	Peroxidase	AT2G37130.1	misc
CUST_20952_PI426222305	PGSC0003DMT400011854	Conserved gene of unknown function	AT2G06025.1	misc
CUST_28243_PI426222305	PGSC0003DMT400044261	Glucosyl/glucuronosyl transferases	AT5G65550.1	misc
CUST_23011_PI426222305	PGSC0003DMT400061003	Zeatin O-glucosyltransferase	AT2G36780.1	misc
CUST_4462_PI426222305	PGSC0003DMT400048145	Amidase family protein	AT4G34880.1	misc
CUST_21974_PI426222305	PGSC0003DMT400042055	Non-specific lipid-transfer protein	AT3G22600.1	misc
CUST_26494_PI426222305	PGSC0003DMT400037139	Nonspecific lipid-transfer protein	AT5G62065.1	misc
CUST_38946_PI426222305	PGSC0003DMT400070296	Transferase, transferring glycosyl groups	AT5G04480.1	misc
CUST_22777_PI426222305	PGSC0003DMT400077994	Conserved gene of unknown function	AT3G55646.1	Not assigned/Unknown
CUST_42471_PI426222305	PGSC0003DMT400090066	EIX receptor 2	AT3G23110.1	Not assigned/Unknown
CUST_26185_PI426222305	PGSC0003DMT400041684	80A08_29	AT5G10320.1	Not assigned/Unknown
CUST_27407_PI426222305	PGSC0003DMT400056515	Gene of unknown function	no Hit	Not assigned/Unknown
CUST_4301_PI426222305	PGSC0003DMT400007760	Conserved gene of unknown function	AT5G22090.1	Not assigned/Unknown
CUST_7025_PI426222305	PGSC0003DMT400031265	Gene of unknown function	no Hit	Not assigned/Unknown
CUST_21287_PI426222305	PGSC0003DMT400020222	Glycine-rich cell wall structural protein 1	AT2G31540.1	Not assigned/Unknown
CUST_22782_PI426222305	PGSC0003DMT400077995	Conserved gene of unknown function	AT3G55646.1	Not assigned/Unknown
CUST_7814_PI426222305	PGSC0003DMT400025836	Pentatricopeptide repeat-containing protein	AT1G76280.3	Not assigned/Unknown
CUST_27954_PI426222305	PGSC0003DMT400081921	Protein PLANT CADMIUM RESISTANCE 2	AT1G14870.1	Not assigned/Unknown
CUST_28026_PI426222305	PGSC0003DMT400081920	Conserved gene of unknown function	AT1G14870.1	Not assigned/Unknown
CUST_34753_PI426222305	PGSC0003DMT400009730	Gene of unknown function	no Hit	Not assigned/Unknown
CUST_17691_PI426222305	PGSC0003DMT400066818	Conserved gene of unknown function	AT4G25170.2	Not assigned/Unknown
CUST_32733_PI426222305	PGSC0003DMT400047266	Conserved gene of unknown function	AT2G14830.1	Not assigned/Unknown
CUST_25580_PI426222305	PGSC0003DMT400037283	Conserved gene of unknown function	no Hit	Not assigned/Unknown
CUST_48651_PI426222305	PGSC0003DMT400065034	Conserved gene of unknown function	no Hit	Not assigned/Unknown
CUST_32260_PI426222305	PGSC0003DMT400092427	Sigma factor sigb regulation protein rsbq	AT3G03990.1	Not assigned/Unknown

Appendix

CUST_32089_PI426222305	PGSC0003DMT400059829	Gene of unknown function	no Hit	Not assigned/Unknown
CUST_47865_PI426222305	PGSC0003DMT400062500	Conserved gene of unknown function	AT5G60680.1	Not assigned/Unknown
CUST_22537_PI426222305	PGSC0003DMT400078308	Conserved gene of unknown function	AT5G02640.1	Not assigned/Unknown
CUST_40084_PI426222305	PGSC0003DMT400015182	Conserved gene of unknown function	AT5G22120.1	Not assigned/Unknown
CUST_13273_PI426222305	PGSC0003DMT400089995	Integrase core domain containing protein	no Hit	Not assigned/Unknown
CUST_43338_PI426222305	PGSC0003DMT400064447	Conserved gene of unknown function	AT1G53035.1	Not assigned/Unknown
CUST_37576_PI426222305	PGSC0003DMT400049606	Conserved gene of unknown function	no Hit	Not assigned/Unknown
CUST_10701_PI426222305	PGSC0003DMT400032175	Late embryogenesis abundant hydroxyproline-rich glycoprotein	AT1G64065.1	Not assigned/Unknown
CUST_50359_PI426222305	PGSC0003DMT400036349	TMV induced protein 1-2	AT2G22170.1	Not assigned/Unknown
CUST_26908_PI426222305	PGSC0003DMT400067222	Flotillin-1	AT5G25250.1	Not assigned/Unknown
CUST_31461_PI426222305	PGSC0003DMT400073455	Tetratricopeptide repeat domain-containing protein	AT5G20190.1	Not assigned/Unknown
CUST_2770_PI426222305	PGSC0003DMT400000263	BTB/POZ protein	AT3G61600.1	Not assigned/Unknown
CUST_20169_PI426222305	PGSC0003DMT400062558	Gene of unknown function	no Hit	Not assigned/Unknown
CUST_8430_PI426222305	PGSC0003DMT400029476	Phylloplanin	AT3G16660.1	Not assigned/Unknown
CUST_3927_PI426222305	PGSC0003DMT400085243	Gene of unknown function	no Hit	Not assigned/Unknown
CUST_35596_PI426222305	PGSC0003DMT400004709	Glycine-rich protein	AT5G47020.1	Not assigned/Unknown
CUST_41356_PI426222305	PGSC0003DMT400079482	Conserved gene of unknown function	AT2G16385.1	Not assigned/Unknown
CUST_9639_PI426222305	PGSC0003DMT400006487	Conserved gene of unknown function	AT1G15215.2	Not assigned/Unknown
CUST_32281_PI426222305	PGSC0003DMT400012584	Gene of unknown function	no Hit	Not assigned/Unknown
CUST_8874_PI426222305	PGSC0003DMT400058036	S-adenosyl-L-methionine-dependent methyltransferase domain-containing protein	AT4G35987.1	Not assigned/Unknown
CUST_10772_PI426222305	PGSC0003DMT400031668	Conserved gene of unknown function	no Hit	Not assigned/Unknown
CUST_44836_PI426222305	PGSC0003DMT400002277	Quinonprotein alcohol dehydrogenase	no Hit	Not assigned/Unknown
CUST_35687_PI426222305	PGSC0003DMT400096723	Sporozoite surface protein 2	no Hit	Not assigned/Unknown
CUST_38880_PI426222305	PGSC0003DMT400037863	EIX receptor 2	AT2G34930.1	Not assigned/Unknown
CUST_20709_PI426222305	PGSC0003DMT400011949	Metal ion binding protein	AT5G23760.1	Not assigned/Unknown
CUST_30375_PI426222305	PGSC0003DMT400069914	Proline transporter 3	AT2G39890.1	Not assigned/Unknown
CUST_15437_PI426222305	PGSC0003DMT400073731	Conserved gene of unknown function	AT5G53830.1	Not assigned/Unknown
CUST_19780_PI426222305	PGSC0003DMT400064115	Conserved gene of unknown function	AT1G09812.1	Not assigned/Unknown
CUST_44826_PI426222305	PGSC0003DMT400002273	Quinonprotein alcohol dehydrogenase	no Hit	Not assigned/Unknown
CUST_39958_PI426222305	PGSC0003DMT400076975	Conserved gene of unknown function	AT5G11840.1	Not assigned/Unknown
CUST_2110_PI426222305	PGSC0003DMT400028701	PHAP2B protein	AT2G28550.3	Not assigned/Unknown
CUST_19969_PI426222305	PGSC0003DMT400049404	Conserved gene of unknown function	AT3G54000.1	Not assigned/Unknown
CUST_18578_PI426222305	PGSC0003DMT400042479	Glycine-rich protein	AT3G23450.1	Not assigned/Unknown
CUST_47113_PI426222305	PGSC0003DMT400092771	Glycosyl transferase, family 8	no Hit	Not assigned/Unknown
CUST_36704_PI426222305	PGSC0003DMT400015788	Gene of unknown function	no Hit	Not assigned/Unknown
CUST_7192_PI426222305	PGSC0003DMT400077250	Gene of unknown function	no Hit	Not assigned/Unknown
CUST_47165_PI426222305	PGSC0003DMT400089750	Latency-associated nuclear antigen	no Hit	Not assigned/Unknown
CUST_31580_PI426222305	PGSC0003DMT400073423	Gene of unknown function	no Hit	Not assigned/Unknown
CUST_21198_PI426222305	PGSC0003DMT400020306	Gene of unknown function	no Hit	Not assigned/Unknown
CUST_25189_PI426222305	PGSC0003DMT400014807	RRNA-processing protein UTP23	AT2G34570.1	Not assigned/Unknown
CUST_35815_PI426222305	PGSC0003DMT400046918	Conserved gene of unknown function	AT5G49800.1	Not assigned/Unknown
CUST_21838_PI426222305	PGSC0003DMT400094670	Transcription factor hy5	AT3G56660.1	Not assigned/Unknown
CUST_45807_PI426222305	PGSC0003DMT400050239	Activating signal cointegrator	AT3G47610.1	Not assigned/Unknown
CUST_27460_PI426222305	PGSC0003DMT400024480	Metal-binding isoprenylated protein	AT4G08570.1	Not assigned/Unknown
CUST_35753_PI426222305	PGSC0003DMT400046917	Conserved gene of unknown function	AT5G49800.1	Not assigned/Unknown
CUST_47806_PI426222305	PGSC0003DMT400019315	Gene of unknown function	no Hit	Not assigned/Unknown
CUST_37974_PI426222305	PGSC0003DMT400081431	Protein SSM1	AT2G32150.1	Not assigned/Unknown
CUST_48318_PI426222305	PGSC0003DMT400043220	Gene of unknown function	no Hit	Not assigned/Unknown
CUST_31583_PI426222305	PGSC0003DMT400042522	Gene of unknown function	no Hit	Not assigned/Unknown
CUST_10720_PI426222305	PGSC0003DMT400031671	Conserved gene of unknown function	no Hit	Not assigned/Unknown
CUST_3442_PI426222305	PGSC0003DMT400041206	Conserved gene of unknown function	AT5G19875.1	Not assigned/Unknown
CUST_10812_PI426222305	PGSC0003DMT400031674	Conserved gene of unknown function	no Hit	Not assigned/Unknown
CUST_35809_PI426222305	PGSC0003DMT400046916	Conserved gene of unknown function	AT5G49800.1	Not assigned/Unknown
CUST_9991_PI426222305	PGSC0003DMT400097500	Gene of unknown function	no Hit	Not assigned/Unknown
CUST_43999_PI426222305	PGSC0003DMT400016478	Aldo/keto reductase	no Hit	Not assigned/Unknown
CUST_52625_PI426222305	PGSC0003DMT400069120	GI11736	AT3G22142.1	Not assigned/Unknown
CUST_40013_PI426222305	PGSC0003DMT400015185	Transcription factor	no Hit	Not assigned/Unknown
CUST_7756_PI426222305	PGSC0003DMT400013202	F-box protein	AT3G10240.1	Not assigned/Unknown
CUST_36438_PI426222305	PGSC0003DMT400074524	Gene of unknown function	no Hit	Not assigned/Unknown
CUST_14323_PI426222305	PGSC0003DMT400060119	Protein YIP1	AT2G36300.1	Not assigned/Unknown
CUST_51153_PI426222305	PGSC0003DMT400008561	Conserved gene of unknown function	no Hit	Not assigned/Unknown
CUST_3687_PI426222305	PGSC0003DMT400064324	Conserved gene of unknown function	no Hit	Not assigned/Unknown
CUST_22770_PI426222305	PGSC0003DMT400077960	Conserved gene of unknown function	AT5G59400.2	Not assigned/Unknown
CUST_43559_PI426222305	PGSC0003DMT400038891	TMV resistance protein N	AT1G27170.1	Not assigned/Unknown
CUST_21088_PI426222305	PGSC0003DMT400020483	Gene of unknown function	no Hit	Not assigned/Unknown
CUST_24808_PI426222305	PGSC0003DMT400024110	Receptor protein kinase	no Hit	Not assigned/Unknown
CUST_36031_PI426222305	PGSC0003DMT400046159	Glycine-rich protein	AT2G05540.1	Not assigned/Unknown
CUST_35536_PI426222305	PGSC0003DMT400005803	Mutt domain protein	AT5G47240.1	nucleotide metabolism
CUST_39427_PI426222305	PGSC0003DMT400077330	Conserved gene of unknown function	AT1G05385.1	Photosynthesis
CUST_31364_PI426222305	PGSC0003DMT400034898	Chlorophyll a-b binding protein 3C, chloroplastic	AT1G29930.1	Photosynthesis
CUST_31296_PI426222305	PGSC0003DMT400034897	Chlorophyll a-b binding protein 3C, chloroplastic	AT1G29930.1	Photosynthesis

CUST_46291_PI426222305	PGSC0003DMT400092982	F-box domain-containing protein	AT1G47790.1	Protein
CUST_18795_PI426222305	PGSC0003DMT400001221	RING-H2 finger protein ATL57	AT2G27940.1	Protein
CUST_51712_PI426222305	PGSC0003DMT400028480	Conserved gene of unknown function	AT1G19390.1	Protein
CUST_10881_PI426222305	PGSC0003DMT400036366	Serine carboxypeptidase III	AT3G45010.1	Protein
CUST_15426_PI426222305	PGSC0003DMT400037526	ATP-dependent Clp protease ATP-binding subunit clpA homolog CD4B, chloroplastic	AT5G50920.1	Protein
CUST_9997_PI426222305	PGSC0003DMT400074985	Zinc finger family protein	AT5G60580.2	Protein
CUST_26712_PI426222305	PGSC0003DMT400077222	Ser-thr protein kinase	AT5G45840.2	Protein
CUST_31149_PI426222305	PGSC0003DMT400063857	MAP3Ka	AT1G53570.1	Protein
CUST_9908_PI426222305	PGSC0003DMT400074984	Zinc finger family protein	AT5G60580.2	Protein
CUST_23275_PI426222305	PGSC0003DMT400073836	E3 ubiquitin ligase PUB14	AT5G37490.1	Protein
CUST_9968_PI426222305	PGSC0003DMT400074981	Zinc finger family protein	AT5G60580.2	Protein
CUST_41753_PI426222305	PGSC0003DMT400015590	Serine-threonine protein kinase, plant-type	AT2G23770.1	Protein
CUST_9527_PI426222305	PGSC0003DMT400023656	26S protease regulatory subunit 7 homolog A	AT1G53750.1	Protein
CUST_9990_PI426222305	PGSC0003DMT400074983	Zinc finger family protein	AT5G60580.2	Protein
CUST_41756_PI426222305	PGSC0003DMT400015591	Serine-threonine protein kinase, plant-type	AT2G33580.1	Protein
CUST_33751_PI426222305	PGSC0003DMT400078804	Sporulation protein RMD5	AT4G37880.1	Protein
CUST_6958_PI426222305	PGSC0003DMT400027889	Prenyl-dependent CAAX protease	AT3G26085.2	Protein
CUST_31878_PI426222305	PGSC0003DMT400053107	Elongation factor	AT2G38560.1	Protein
CUST_3607_PI426222305	PGSC0003DMT400010265	Nucleoporin 98	AT1G10390.1	Protein
CUST_22505_PI426222305	PGSC0003DMT400039186	Copine	AT5G14420.1	Protein
CUST_13610_PI426222305	PGSC0003DMT400092874	Subtilisin-like protease	AT5G67360.1	Protein
CUST_40894_PI426222305	PGSC0003DMT400079820	ATP binding protein	AT3G10420.2	Protein
CUST_34871_PI426222305	PGSC0003DMT400073070	Sec61 transport protein	AT2G34250.1	Protein
CUST_23534_PI426222305	PGSC0003DMT400023877	GRAS family transcription factor	AT2G04890	RNA
CUST_1193_PI426222305	PGSC0003DMT400003484	MADS-box transcription factor FBP29	AT1G69120.1	RNA
CUST_36965_PI426222305	PGSC0003DMT400067504	SET domain protein	AT2G35160.1	RNA
CUST_6673_PI426222305	PGSC0003DMT400014383	MYB	AT1G68320.1	RNA
CUST_40605_PI426222305	PGSC0003DMT400073947	PRP8 protein	AT1G80070.1	RNA
CUST_32691_PI426222305	PGSC0003DMT400047303	Pentatricopeptide repeat-containing protein	AT1G11900.1	RNA
CUST_50509_PI426222305	PGSC0003DMT400062081	Homeobox-leucine zipper protein	AT4G16780.1	RNA
CUST_46195_PI426222305	PGSC0003DMT400011427	Mads box protein	AT2G34440.1	RNA
CUST_46771_PI426222305	PGSC0003DMT400038273	41 kD chloroplast nucleoid DNA binding protein (CND41)	AT5G10770	RNA
CUST_22694_PI426222305	PGSC0003DMT400077935	DNA binding protein	AT5G59830.1	RNA
CUST_28830_PI426222305	PGSC0003DMT400010397	DOF domain class transcription factor	AT5G60850.1	RNA
CUST_47808_PI426222305	PGSC0003DMT400019296	RAV	AT1G25560.1	RNA
CUST_36339_PI426222305	PGSC0003DMT400074526	CHP-rich zinc finger protein	AT2G27660.1	RNA
CUST_2481_PI426222305	PGSC0003DMT400072210	DNA binding protein	AT4G39250.1	RNA
CUST_12063_PI426222305	PGSC0003DMT400076669	WRKY transcription factor	AT4G26640.2	RNA
CUST_23812_PI426222305	PGSC0003DMT400021144	WRKY transcription factor	AT5G26170.1	RNA
CUST_3084_PI426222305	PGSC0003DMT400033211	Forkhead-associated domain-containing protein	AT2G45460.3	RNA
CUST_2338_PI426222305	PGSC0003DMT400072208	Myb RL3	AT4G39250.1	RNA
CUST_41097_PI426222305	PGSC0003DMT400004441	DNA-binding protein S1FA	AT3G09735.1	RNA
CUST_6914_PI426222305	PGSC0003DMT400026583	Remorin 2	AT5G23750.1	RNA
CUST_30393_PI426222305	PGSC0003DMT400069866	Laccase 90a	AT2G40370.1	secondary metabolism
CUST_2216_PI426222305	PGSC0003DMT400072540	Carotenoid isomerase, chloroplastic	AT1G06820.1	secondary metabolism
CUST_34869_PI426222305	PGSC0003DMT400073114	Serine-threonine protein kinase, plant-type	AT3G47090.1	signalling
CUST_50576_PI426222305	PGSC0003DMT400068776	Flagellin-sensing 2	AT5G46330.1	signalling
CUST_42619_PI426222305	PGSC0003DMT400026813	Serine-threonine protein kinase, plant-type	AT5G46330.1	signalling
CUST_27405_PI426222305	PGSC0003DMT400045690	Receptor protein kinase	AT1G35710.1	signalling
CUST_11042_PI426222305	PGSC0003DMT400078562	Receptor kinase	AT5G39030.1	signalling
CUST_6848_PI426222305	PGSC0003DMT400046292	Hcr2-0A	AT1G45616.1	signalling
CUST_42205_PI426222305	PGSC0003DMT400038175	Calmodulin binding protein	AT4G00820.1	signalling
CUST_9586_PI426222305	PGSC0003DMT400006372	Calmodulin binding protein	AT5G57010.1	signalling
CUST_10378_PI426222305	PGSC0003DMT400070694	Serine-threonine protein kinase, plant-type	AT5G48380.1	signalling
CUST_43825_PI426222305	PGSC0003DMT400040125	Serine-threonine protein kinase, plant-type	AT4G29990.1	signalling
CUST_3853_PI426222305	PGSC0003DMT400013709	Calreticulin	AT1G08450.1	signalling
CUST_50753_PI426222305	PGSC0003DMT400059752	Sn-1 protein	AT1G70890.1	stress
CUST_19908_PI426222305	PGSC0003DMT400034089	Leucine-rich repeat-containing protein	AT5G36930.2	stress
CUST_19923_PI426222305	PGSC0003DMT400034090	TMV resistance protein N	AT5G36930.2	stress
CUST_19951_PI426222305	PGSC0003DMT400049441	Heat shock cognate 70 kDa protein 2	AT3G12580.1	stress
CUST_45658_PI426222305	PGSC0003DMT400079343	Disease resistance protein RGA2	AT3G14470.1	stress
CUST_13936_PI426222305	PGSC0003DMT400005135	Cytoplasmic small heat shock protein class I	AT2G14580.1	stress
CUST_45767_PI426222305	PGSC0003DMT400055694	Amino acid transporter	AT5G16740.1	Transport
CUST_30415_PI426222305	PGSC0003DMT400069916	Proline transporter 3	AT2G39890.1	Transport
CUST_30429_PI426222305	PGSC0003DMT400069915	Proline transporter 3	AT2G39890.1	Transport
CUST_37726_PI426222305	PGSC0003DMT400004971	White-brown-complex ABC transporter family	AT1G31770.1	Transport
CUST_34269_PI426222305	PGSC0003DMT400044918	Flavonol synthase/flavanone 3-hydroxylase	AT5G54000.1	Unclassified
CUST_10172_PI426222305	PGSC0003DMT400021703	Endo-1,4-beta-xylanase A	AT4G38650.1	Unclassified
CUST_13436_PI426222305	PGSC0003DMT400062587	Conserved gene of unknown function	not found	Unclassified

Appendix
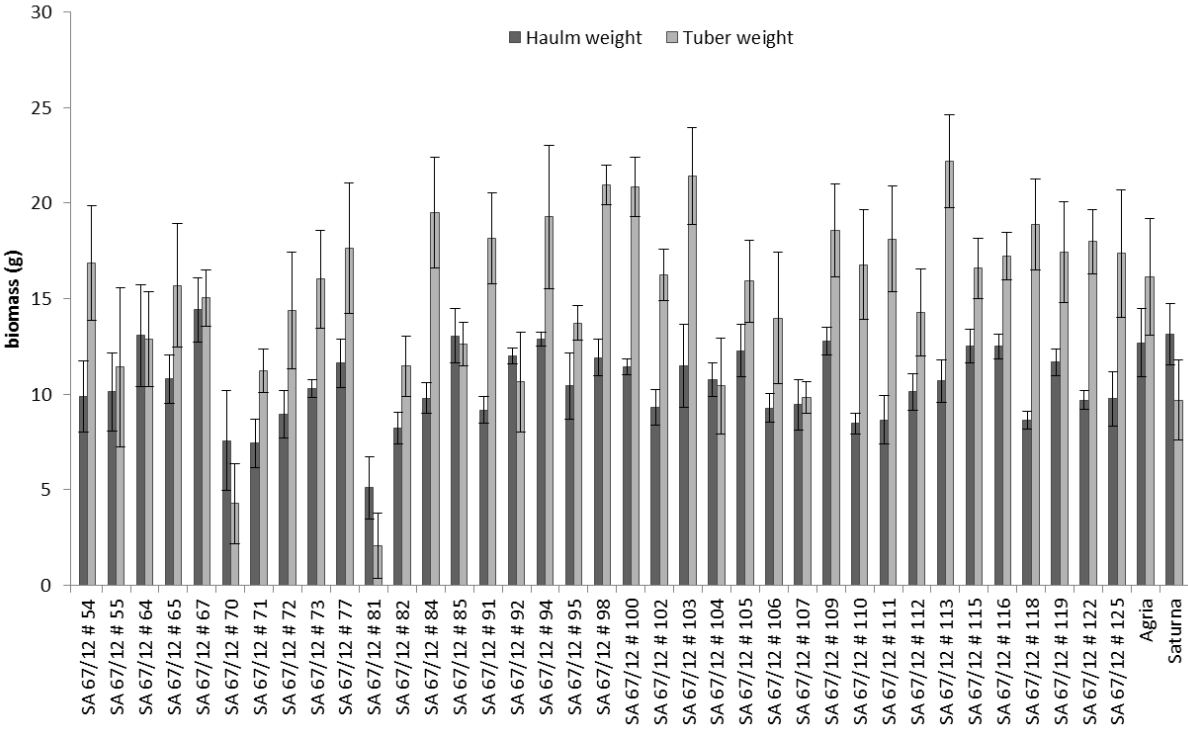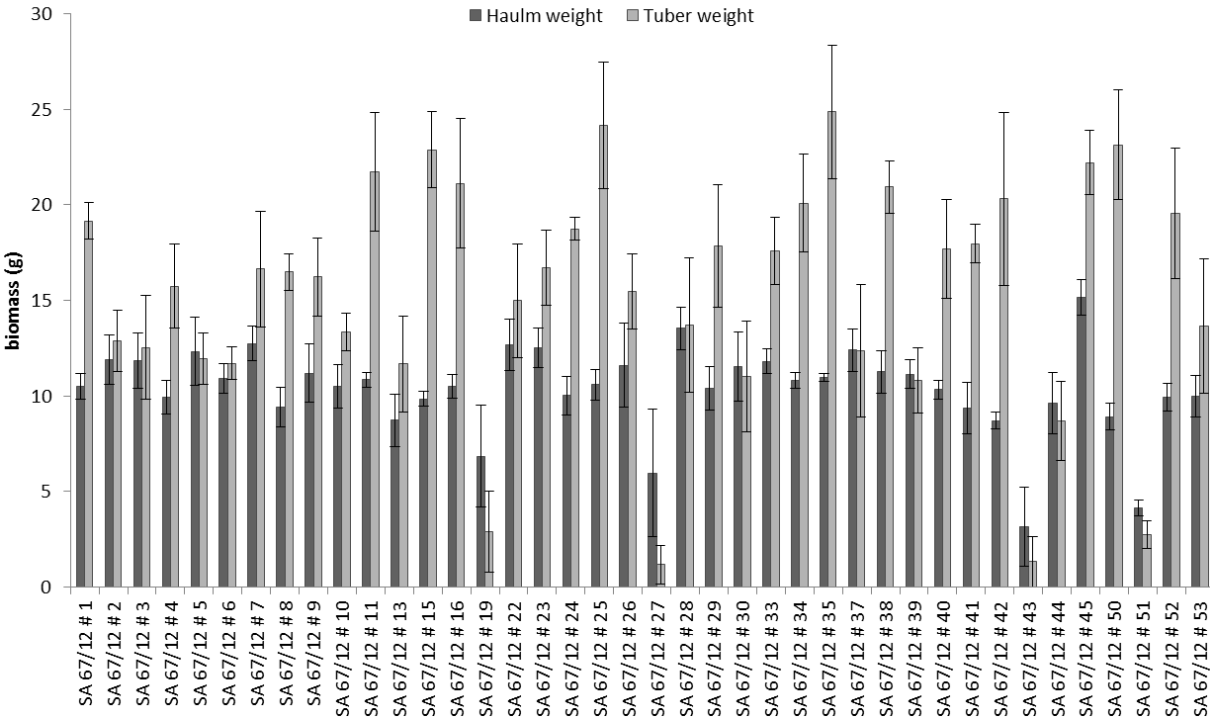
Figure A 1: Bar chart diagram representing average haulm and tuber weights of cross-breeding lines of population SA67/12 – HotPot. Error bars represent standard deviations of four biological replicates.

Table A 3: Second-growth phenotypes in cross-breeding lines of population SA67/12 – HotPot.

Normal growth	Chain tubers	Sprouted tubers	Bottleneck tubers	Elongated tubers	Knobby tubers
4, 5, 8, 11, 13, 15, 16, 22, 23, 29, 34, 37, 38, 39, 40, 42, 44, 50, 51, 64, 65, 67, 71, 72, 73, 77, 82, 94, 105, 112, 116, 119, Agria	19, 52, 70, 102	85, 113	6, 35, 54, 92, 104, 106, 110	3, 7, 9, 24, 26, 30, 33, 43, 55, 84, 91, 95, 98, 107, 111, 115, 118, 125	1, 2, 10, 25, 28, 41, 45, 53, 81, 100, 103, 109, 122, Saturna
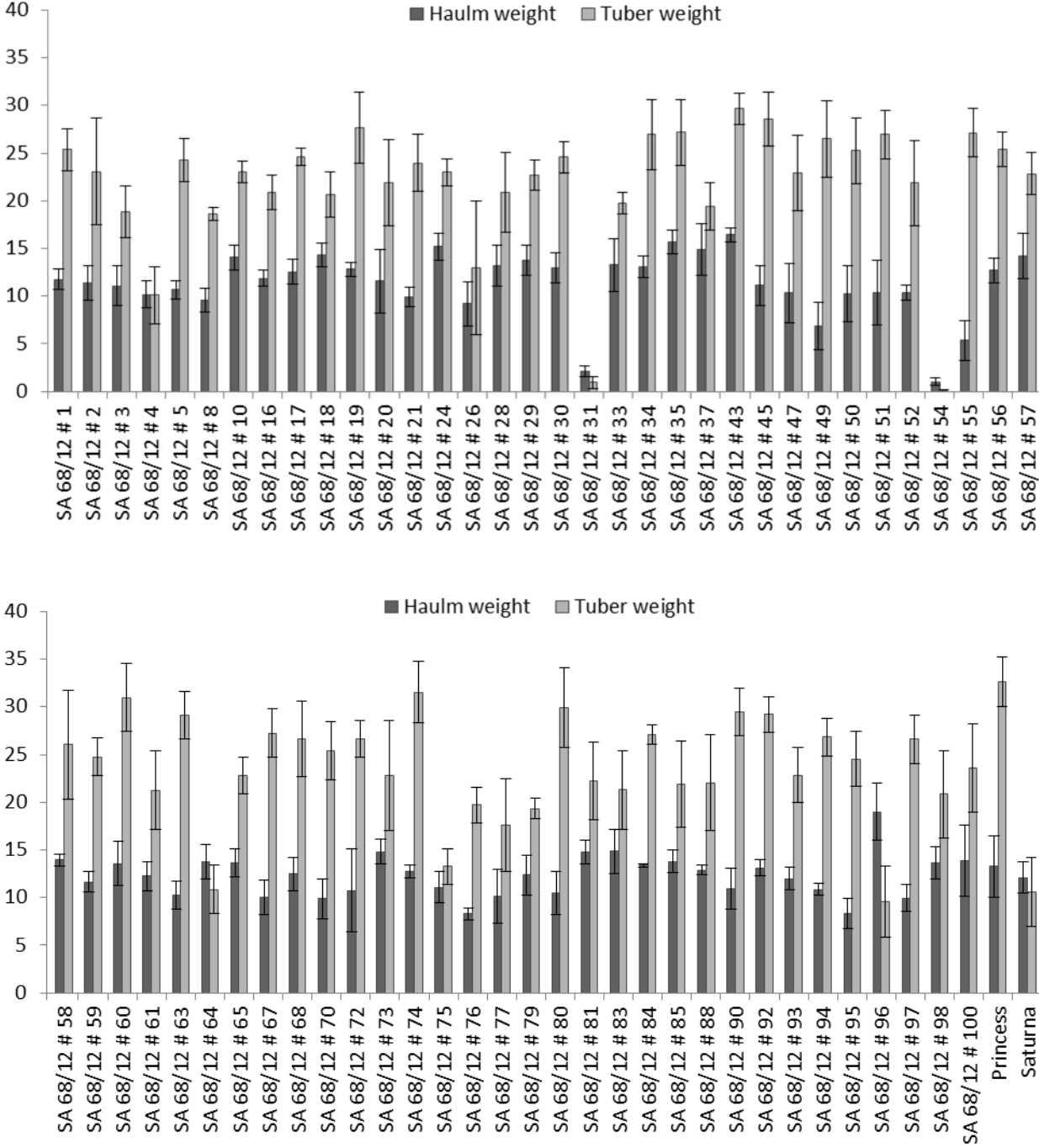
Figure A 2: Bar chart diagram representing average haulm and tuber weights of cross-breeding lines of population SA68/12 – HotPot. Error bars represent standard deviations of four biological replicates.

Table A 4: Second-growth phenotypes in cross-breeding lines of population SA68/12 – HotPot.

Normal growth	Chain tubers	Sprouted tubers	Bottleneck tubers	Elongated tubers	Knobby tubers
3, 4*, 5, 16, 19, 20, 26, 28, 45, 47, 52, 54*, 58, 67, 73, 76*, 77, 81*, 83, 84, 90, 93, 94, 95	24, 35, 55		2, 10, 21*, 49, 51, 57*, 63, 64, 68, 75*, 79, 85, 96*, Princess	17, 29*, 37, 50, 59, 60, 70, 72, 74, 92, 100	1, 8*, 18, 30, 31*, 33, 34, 43, 56, 61, 65, 80, 88, 97, 98, Saturna*

*showed above-ground-tubers with untypical characteristics such as green or purple color, leafy sprouts and green sprouts.
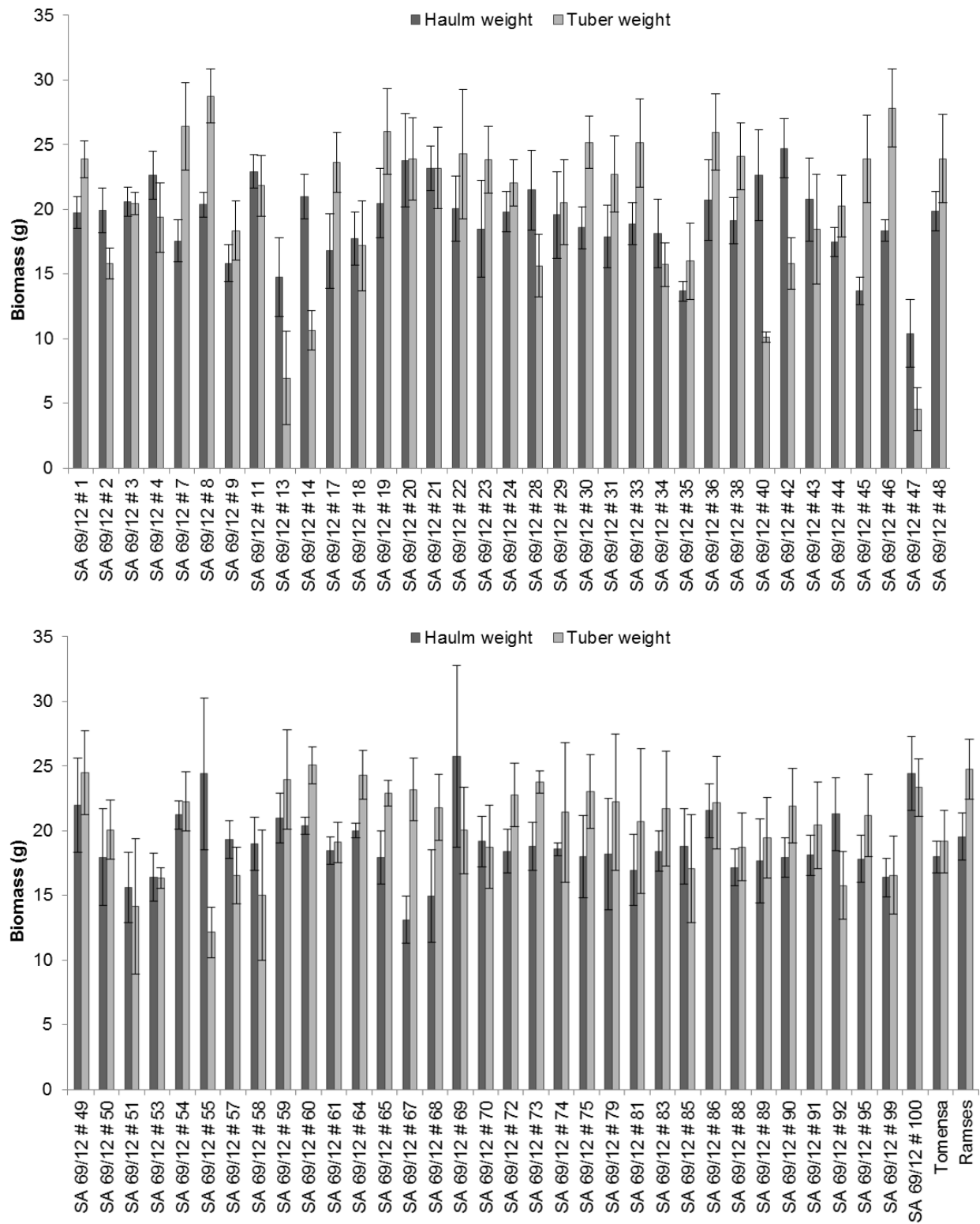
Figure A 3 Bar chart diagram representing average haulm and tuber weights of cross-breeding lines of population SA69/12 – HotPot. Error bars represent standard deviations of four biological replicates.

Table A 5: Second-growth phenotypes in cross-breeding lines of population SA69/12 – HotPot.

Normal growth	Chain tubers	Sprouted tubers	Bottleneck tubers	Elongated tubers	Knobby tubers
2, 3, 4, 9, 11, 13*, 18, 19, 20, 22, 30, 33, 34, 35, 36, 38, 42, 43, 44, 47, 48, 50, 53, 54, 55, 57, 58*, 59, 61, 64, 67*, 68, 69, 70, 73, 74, 75, 79, 81, 83, 85, 86, 88, 89, 91, 92, 95, 99, 100, Ramses			17, 40, 72	23, 29, 46	1, 7, 8, 14, 21, 24, 28*, 31, 45, 49, 51, 60, 65, 90, Tomensa

*showed above-ground-tubers with untypical characteristics such as green or purple color, leafy sprouts and green sprouts.

Appendix

Table A 6: Differentially expressed genes (n = 66) between tubers of selected cross-breeding lines of SA69/12 HotPot grown under heat and control conditions.

| ProbeName	p (Corr)	FC (abs)	Regulation	PrimaryAccession	UniRef based putative functional annotation	category
CUST_17543_PI426222305	0,021	2,005	down	PGSC0003DMT400081211	UPA16	Development
CUST_17319_PI426222305	0,004	2,035	down	PGSC0003DMT400050034	TMS membrane family protein	Development
CUST_31368_PI426222305	0,000	2,109	down	PGSC0003DMT400034864	Auxin-induced protein 5NG4	Development
CUST_17545_PI426222305	0,036	2,510	down	PGSC0003DMT400081210	UPA16	Development
CUST_23736_PI426222305	0,047	3,198	down	PGSC0003DMT400002407	Nodulin family protein	Development
CUST_6850_PI426222305	0,031	2,320	down	PGSC0003DMT400043704	F-box and wd40 domain protein	DNA
CUST_24429_PI426222305	0,000	2,019	down	PGSC0003DMT400074127	Amine oxidase	misc
CUST_43398_PI426222305	0,001	2,111	down	PGSC0003DMT400032990	Cytochrome P450	misc
CUST_51406_PI426222305	0,003	2,148	down	PGSC0003DMT400080529	UDP-glucoronosyl/UDP-glucosyl transferase family protein	misc
CUST_43712_PI426222305	0,003	2,472	down	PGSC0003DMT400004892	Cytochrome P450	misc
CUST_50383_PI426222305	0,047	3,010	down	PGSC0003DMT400072022	Short chain alcohol dehydrogenase	misc
CUST_50386_PI426222305	0,045	3,012	down	PGSC0003DMT400072021	Short chain alcohol dehydrogenase	misc
CUST_50387_PI426222305	0,010	3,268	down	PGSC0003DMT400072020	Short chain alcohol dehydrogenase	misc
CUST_15398_PI426222305	0,008	2,016	down	PGSC0003DMT400092826	Conserved gene of unknown function	Not assigned/Unknown
CUST_20450_PI426222305	0,003	2,046	down	PGSC0003DMT400068342	DNA binding protein	Not assigned/Unknown
CUST_17162_PI426222305	0,000	2,090	down	PGSC0003DMT400057905	Gene of unknown function	Not assigned/Unknown
CUST_48716_PI426222305	0,031	2,558	down	PGSC0003DMT400036281	Transcription factor R2R3-MYB	Not assigned/Unknown
CUST_49778_PI426222305	0,002	2,592	down	PGSC0003DMT400094969	Conserved gene of unknown function	Not assigned/Unknown
CUST_23044_PI426222305	0,011	2,027	down	PGSC0003DMT400021112	Guanylate kinase	nucleotide metabolism
CUST_16102_PI426222305	0,000	2,038	down	PGSC0003DMT400026994	Peptide methionine sulfoxide reductase msrA	Protein
CUST_45931_PI426222305	0,002	2,061	down	PGSC0003DMT400047982	Protein kinase	Protein
CUST_6366_PI426222305	0,000	2,334	down	PGSC0003DMT400036973	Serine carboxypeptidase	Protein
CUST_37325_PI426222305	0,049	2,325	down	PGSC0003DMT400029594	Glutaredoxin	Redox
CUST_49599_PI426222305	0,003	2,364	down	PGSC0003DMT400013649	Glutaredoxin, grx	Redox
CUST_23050_PI426222305	0,001	2,011	down	PGSC0003DMT400076726	Type-a response regulator	RNA
CUST_2338_PI426222305	0,004	2,042	down	PGSC0003DMT400072208	Myb RL3	RNA
CUST_2481_PI426222305	0,003	2,062	down	PGSC0003DMT400072210	DNA binding protein	RNA
CUST_40433_PI426222305	0,002	2,316	down	PGSC0003DMT400050131	Stress-associated protein 7	RNA
CUST_7664_PI426222305	0,004	2,497	down	PGSC0003DMT400009583	Myb family transcription factor	RNA
CUST_45093_PI426222305	0,049	2,184	down	PGSC0003DMT400031366	O-methyltransferase	secondary metabolism
CUST_38376_PI426222305	0,000	2,243	down	PGSC0003DMT400022038	Cryptochrome 1b	signalling
CUST_38379_PI426222305	0,000	2,530	down	PGSC0003DMT400022039	Cryptochrome 1b	signalling
CUST_20381_PI426222305	0,001	2,063	down	PGSC0003DMT400049707	Sulfate/bicarbonate/oxalate exchanger and transporter sat-1	Transport
CUST_4892_PI426222305	0,014	2,533	down	PGSC0003DMT400059645	Equilibrative nucleoside transporter	Transport
CUST_17298_PI426222305	0,000	2,830	up	PGSC0003DMT400057833	VAMP/synaptobrevin-associated protein 27-2	Cell
CUST_33852_PI426222305	0,000	2,036	up	PGSC0003DMT400012517	Nucleosome assembly protein 1 4	DNA
CUST_33912_PI426222305	0,001	2,052	up	PGSC0003DMT400012516	Nucleosome assembly protein 1 4	DNA
CUST_49382_PI426222305	0,000	3,287	up	PGSC0003DMT400016815	Aldo/keto reductase 2	hormone metabolism
CUST_43381_PI426222305	0,000	2,262	up	PGSC0003DMT400032989	Cytochrome P450	misc
CUST_41391_PI426222305	0,000	8,290	up	PGSC0003DMT400079498	Beta-galactosidase	misc
CUST_3289_PI426222305	0,000	10,453	up	PGSC0003DMT400000643	Phragmoplastin	misc
CUST_50389_PI426222305	0,000	20,143	up	PGSC0003DMT400072017	Short chain alcohol dehydrogenase	misc
CUST_5252_PI426222305	0,000	2,063	up	PGSC0003DMT400009069	Abscisic acid and environmental stress-inducible protein TAS14	Not assigned/Unknown
CUST_23033_PI426222305	0,000	2,203	up	PGSC0003DMT400061008	Conserved gene of unknown function	Not assigned/Unknown
CUST_44571_PI426222305	0,046	2,324	up	PGSC0003DMT400041324	Gene of unknown function	Not assigned/Unknown
CUST_482_PI426222305	0,000	2,995	up	PGSC0003DMT400088666	Gene of unknown function	Not assigned/Unknown
CUST_17671_PI426222305	0,000	5,247	up	PGSC0003DMT400067051	Gene of unknown function	Not assigned/Unknown
CUST_28454_PI426222305	0,000	7,020	up	PGSC0003DMT400094383	'chromo' domain containing protein	Not assigned/Unknown
CUST_42253_PI426222305	0,000	7,418	up	PGSC0003DMT400050852	Conserved gene of unknown function	Not assigned/Unknown
CUST_299_PI426222305	0,000	7,691	up	PGSC0003DMT400085779	Gene of unknown function	Not assigned/Unknown
CUST_28212_PI426222305	0,000	8,014	up	PGSC0003DMT400044494	Gene of unknown function	Not assigned/Unknown
CUST_50020_PI426222305	0,000	13,475	up	PGSC0003DMT400011106	Gene of unknown function	Not assigned/Unknown
CUST_11925_PI426222305	0,000	17,341	up	PGSC0003DMT400033456	Cellulose synthase CslG	Not assigned/Unknown
CUST_45076_PI426222305	0,000	18,001	up	PGSC0003DMT400031375	Conserved gene of unknown function	Not assigned/Unknown
CUST_30913_PI426222305	0,000	22,133	up	PGSC0003DMT400017135	Gene of unknown function	Not assigned/Unknown
CUST_15529_PI426222305	0,000	32,534	up	PGSC0003DMT400091715	Integrase core domain containing protein	Not assigned/Unknown
CUST_43572_PI426222305	0,002	3,279	up	PGSC0003DMT400016960	Zinc finger protein	Protein
CUST_8270_PI426222305	0,000	2,257	up	PGSC0003DMT400075427	ARF domain class transcription factor	RNA
CUST_10011_PI426222305	0,000	6,211	up	PGSC0003DMT400028148	Aspartic proteinase nepenthesin-1	RNA
CUST_15581_PI426222305	0,000	8,658	up	PGSC0003DMT400011449	GATA domain class transcription factor	RNA
CUST_31680_PI426222305	0,000	10,357	up	PGSC0003DMT400035119	Leafy cotyledon 1	RNA
CUST_6999_PI426222305	0,004	2,015	up	PGSC0003DMT400031253	Small heat shock protein	stress
CUST_968_PI426222305	0,036	2,898	up	PGSC0003DMT400032851	Heat-shock protein	stress
CUST_36888_PI426222305	0,000	11,628	up	PGSC0003DMT400067509	Bax inhibitor	stress
CUST_33387_PI426222305	0,000	2,295	up	PGSC0003DMT400017754	Mitochondrial outer membrane protein porin of 34 kDa	Transport
CUST_40543_PI426222305	0,000	2,458	up	PGSC0003DMT400074976	Squamosa promoter binding protein-homologue 3	Unclassified

Table A 7: 250 differentially expressed entities of line SA69/12 #57 compared to lines #28, #50, #73 and parental lines Ramses and Tomensa.

ProbeName	Primary accession	UniRef based putative functional annotation	Functional category
CUST_46332_PI426222305	PGSC0003DMT400034146	Tom	Cell
CUST_9181_PI426222305	PGSC0003DMT400006703	AR791 Actin binding protein family	Cell
CUST_11842_PI426222305	PGSC0003DMT400046740	Iron-sulfer cluster scaffold protein ISU1	Co-factor and vitamine metabolism
CUST_43768_PI426222305	PGSC0003DMT400040158	Late embryogenesis abundant protein	Development
CUST_14442_PI426222305	PGSC0003DMT400066731	Pentatricopeptide repeat-containing protein	hormone metabolism
CUST_22740_PI426222305	PGSC0003DMT400078051	20G-Fe(II) oxidoreductase	hormone metabolism
CUST_45317_PI426222305	PGSC0003DMT400001611	Flavonol synthase/flavanone 3-hydroxylase	hormone metabolism
CUST_7878_PI426222305	PGSC0003DMT400086212	Auxin-induced protein 6B (SAUR)	hormone metabolism
CUST_23662_PI426222305	PGSC0003DMT400002337	Long-chain-fatty-acid CoA ligase	Lipid Metabolism
CUST_37041_PI426222305	PGSC0003DMT400061920	Sterol glucosyltransferase	Lipid Metabolism
CUST_47438_PI426222305	PGSC0003DMT400064818	Acyl CoA synthetase	Lipid Metabolism
CUST_47447_PI426222305	PGSC0003DMT400064819	Acyl CoA synthetase	Lipid Metabolism
CUST_47463_PI426222305	PGSC0003DMT400064820	Acyl CoA synthetase	Lipid Metabolism
CUST_47470_PI426222305	PGSC0003DMT400064821	Acyl CoA synthetase	Lipid Metabolism
CUST_45006_PI426222305	PGSC0003DMT400056666	Metal ion binding protein	metal handling
CUST_14037_PI426222305	PGSC0003DMT400060254	Epoxide hydrolase	misc
CUST_14156_PI426222305	PGSC0003DMT400060253	Epoxide hydrolase	misc
CUST_14201_PI426222305	PGSC0003DMT400060250	Epoxide hydrolase	misc
CUST_14338_PI426222305	PGSC0003DMT400060252	Epoxide hydrolase	misc
CUST_19404_PI426222305	PGSC0003DMT400072738	Cytochrome P450	misc
CUST_19421_PI426222305	PGSC0003DMT400072735	Cytochrome P450	misc
CUST_24958_PI426222305	PGSC0003DMT400045138	UDP-glucose:solanidine glucosyltransferase	misc
CUST_25011_PI426222305	PGSC0003DMT400074847	Cytochrome P450	misc
CUST_26951_PI426222305	PGSC0003DMT400052686	Cytochrome P450 71D7	misc
CUST_30284_PI426222305	PGSC0003DMT400069771	UDP-glucosyltransferase family 1 protein	misc
CUST_30372_PI426222305	PGSC0003DMT400069774	UDP-glucosyltransferase family 1 protein	misc
CUST_30404_PI426222305	PGSC0003DMT400069773	UDP-glucosyltransferase family 1 protein	misc
CUST_30406_PI426222305	PGSC0003DMT400069775	UDP-glucosyltransferase family 1 protein	misc
CUST_30431_PI426222305	PGSC0003DMT400069772	UDP-glucosyltransferase family 1 protein	misc
CUST_30855_PI426222305	PGSC0003DMT400037886	Resveratrol/hydroxycinnamic acid O-glucosyltransferase /UDP-glucose:glucosyltransferase	misc
CUST_4205_PI426222305	PGSC0003DMT400007678	Pheophorbide A oxygenase	misc
CUST_4305_PI426222305	PGSC0003DMT400020816	SIT4 phosphatase-associated family protein	misc
CUST_45499_PI426222305	PGSC0003DMT400038055	Dimethylaniline monooxygenase	misc
CUST_46032_PI426222305	PGSC0003DMT400040465	Beta-1,3-glucanase	misc
CUST_46051_PI426222305	PGSC0003DMT400040464	Beta-1,3-glucanase	misc
CUST_47925_PI426222305	PGSC0003DMT400025271	Cytochrome P450	misc
CUST_48349_PI426222305	PGSC0003DMT400043223	Cytochrome P450	misc
CUST_11418_PI426222305	PGSC0003DMT400010676	Internal rotenone-insensitive NADH dehydrogenase	Mitochondrial electron transport
CUST_11459_PI426222305	PGSC0003DMT400010678	Internal rotenone-insensitive NADH dehydrogenase	Mitochondrial electron transport
CUST_11050_PI426222305	PGSC0003DMT400078408	Pentatricopeptide repeat-containing protein, Stigma/style cell cycle inhibitor	Not assigned/Unknown
CUST_11194_PI426222305	PGSC0003DMT400037748	Gene of unknown function	Not assigned/Unknown
CUST_11198_PI426222305	PGSC0003DMT400078461	Gene of unknown function	Not assigned/Unknown
CUST_13262_PI426222305	PGSC0003DMT400053597	Zinc finger, CCHC-type /non-LTR retroelement reverse transcriptase	Not assigned/Unknown
CUST_13400_PI426222305	PGSC0003DMT400087939	Hypothetical Gene of unknown function	Not assigned/Unknown
CUST_1391_PI426222305	PGSC0003DMT400032849	Conserved gene of unknown function /CCT motif family protein	Not assigned/Unknown
CUST_14211_PI426222305	PGSC0003DMT400060082	Conserved gene of unknown function	Not assigned/Unknown
CUST_14757_PI426222305	PGSC0003DMT400066760	Gene of unknown function	Not assigned/Unknown
CUST_15398_PI426222305	PGSC0003DMT400092826	Conserved gene of unknown function / Regulator of Vps4 activity in the MVB pathway protein	Not assigned/Unknown
CUST_19336_PI426222305	PGSC0003DMT400072918	Gene of unknown function	Not assigned/Unknown
CUST_196_PI426222305	PGSC0003DMT400088322	Conserved gene of unknown function	Not assigned/Unknown
CUST_22510_PI426222305	PGSC0003DMT400039369	Transposase	Not assigned/Unknown
CUST_23960_PI426222305	PGSC0003DMT400076522	Gene of unknown function	Not assigned/Unknown
CUST_24447_PI426222305	PGSC0003DMT400074191	Gene of unknown function	Not assigned/Unknown
CUST_26150_PI426222305	PGSC0003DMT400041659	Signal transducer	Not assigned/Unknown
CUST_26225_PI426222305	PGSC0003DMT400041660	Signal transducer	Not assigned/Unknown
CUST_26607_PI426222305	PGSC0003DMT400000866	Ultraviolet-B-repressible protein	Not assigned/Unknown
CUST_27013_PI426222305	PGSC0003DMT400052736	Gene of unknown function /Ubiquitin-like family protein	Not assigned/Unknown
CUST_27954_PI426222305	PGSC0003DMT400081921	Conserved gene of unknown function / Protein PLANT CADMIUM RESISTANCE 2	Not assigned/Unknown
CUST_28359_PI426222305	PGSC0003DMT400044497	Gene of unknown function	Not assigned/Unknown

CUST_28362_PI426222305	PGSC0003DMT400044203	Conserved gene of unknown function / Zinc finger, GRF-type	Not assigned/Unknown
CUST_28682_PI426222305	PGSC0003DMT400083151	Conserved gene of unknown function /DUF674 domain containing protein	Not assigned/Unknown
CUST_28776_PI426222305	PGSC0003DMT400083153	Conserved gene of unknown function /DUF674 domain containing protein	Not assigned/Unknown
CUST_28820_PI426222305	PGSC0003DMT400083044	Hypersensitive-induced reaction protein	Not assigned/Unknown
CUST_29986_PI426222305	PGSC0003DMT400065485	Gene of unknown function	Not assigned/Unknown
CUST_30531_PI426222305	PGSC0003DMT400077388	Conserved gene of unknown function	Not assigned/Unknown
CUST_34318_PI426222305	PGSC0003DMT400056682	Gene of unknown function	Not assigned/Unknown
CUST_34908_PI426222305	PGSC0003DMT400073144	Conserved gene of unknown function / Lipoprotein	Not assigned/Unknown
CUST_34959_PI426222305	PGSC0003DMT400073145	Lipoprotein	Not assigned/Unknown
CUST_35474_PI426222305	PGSC0003DMT400032445	Conserved gene of unknown function	Not assigned/Unknown
CUST_35490_PI426222305	PGSC0003DMT400032471	Conserved gene of unknown function	Not assigned/Unknown
CUST_35542_PI426222305	PGSC0003DMT400032472	Conserved gene of unknown function	Not assigned/Unknown
CUST_35584_PI426222305	PGSC0003DMT400062254	Gene of unknown function	Not assigned/Unknown
CUST_37206_PI426222305	PGSC0003DMT400082498	HJTR2GH1 protein	Not assigned/Unknown
CUST_38945_PI426222305	PGSC0003DMT400070386	Gene of unknown function	Not assigned/Unknown
CUST_40429_PI426222305	PGSC0003DMT400061611	Gene of unknown function	Not assigned/Unknown
CUST_41210_PI426222305	PGSC0003DMT400055840	Gene of unknown function	Not assigned/Unknown
CUST_42074_PI426222305	PGSC0003DMT400050489	Gene of unknown function	Not assigned/Unknown
CUST_42102_PI426222305	PGSC0003DMT400050523	Autophagy protein	Not assigned/Unknown
CUST_42854_PI426222305	PGSC0003DMT400053482	Protein yippee	Not assigned/Unknown
CUST_43830_PI426222305	PGSC0003DMT400040157	Late embryogenesis abundant protein	Not assigned/Unknown
CUST_44286_PI426222305	PGSC0003DMT400010036	Conserved gene of unknown function	Not assigned/Unknown
CUST_44319_PI426222305	PGSC0003DMT400010035	Conserved gene of unknown function	Not assigned/Unknown
CUST_44334_PI426222305	PGSC0003DMT400010034	Conserved gene of unknown function	Not assigned/Unknown
CUST_45445_PI426222305	PGSC0003DMT400074806	Conserved gene of unknown function	Not assigned/Unknown
CUST_46516_PI426222305	PGSC0003DMT400040980	Gene of unknown function	Not assigned/Unknown
CUST_46520_PI426222305	PGSC0003DMT400040979	Gene of unknown function	Not assigned/Unknown
CUST_47345_PI426222305	PGSC0003DMT400021426	Conserved gene of unknown function	Not assigned/Unknown
CUST_49575_PI426222305	PGSC0003DMT400013672	Conserved gene of unknown function	Not assigned/Unknown
CUST_49595_PI426222305	PGSC0003DMT400013673	Conserved gene of unknown function	Not assigned/Unknown
CUST_51427_PI426222305	PGSC0003DMT400034004	Conserved gene of unknown function	Not assigned/Unknown
CUST_52497_PI426222305	PGSC0003DMT400083498	Sn-1 protein	Not assigned/Unknown
CUST_52680_PI426222305	PGSC0003DMT400059919	Conserved gene of unknown function	Not assigned/Unknown
CUST_530_PI426222305	PGSC0003DMT400092522	Chloroplast photosystem II subunit X	Not assigned/Unknown
CUST_7293_PI426222305	PGSC0003DMT400086267	Gene of unknown function	Not assigned/Unknown
CUST_826_PI426222305	PGSC0003DMT400032850	Conserved gene of unknown function	Not assigned/Unknown
CUST_9760_PI426222305	PGSC0003DMT400038502	Gene of unknown function	Not assigned/Unknown
CUST_34856_PI426222305	PGSC0003DMT400073068	Dihydroorotase, mitochondrial	nucleotide metabolism
CUST_15010_PI426222305	PGSC0003DMT400057281	Chloroplast photosystem I reaction center V	Photosynthesis
CUST_20382_PI426222305	PGSC0003DMT400019490	Photosystem II reaction center W protein, chloroplastic	Photosynthesis
CUST_20983_PI426222305	PGSC0003DMT400056635	Photosystem I reaction center subunit IV B isoform 2	Photosynthesis
CUST_24489_PI426222305	PGSC0003DMT400054482	Photosystem I subunit III	Photosynthesis
CUST_24567_PI426222305	PGSC0003DMT400054481	Photosystem I subunit III	Photosynthesis
CUST_32396_PI426222305	PGSC0003DMT400030843	Photosystem I reaction centre PSI-D subunit	Photosynthesis
CUST_37108_PI426222305	PGSC0003DMT400030013	Triosephosphate isomerase, chloroplastic	Photosynthesis
CUST_48299_PI426222305	PGSC0003DMT400002422	Oxygen-evolving enhancer protein 2, chloroplastic	Photosynthesis
CUST_11740_PI426222305	PGSC0003DMT400046760	Conserved gene of unknown function	Protein
CUST_1557_PI426222305	PGSC0003DMT400040451	RING-H2 finger protein ATL2N	Protein
CUST_2167_PI426222305	PGSC0003DMT400028592	Serine/threonine kinase	Protein
CUST_31207_PI426222305	PGSC0003DMT400063879	F-box family protein	Protein
CUST_4384_PI426222305	PGSC0003DMT400020936	Ubiquitin-protein ligase	Protein
CUST_46293_PI426222305	PGSC0003DMT400040763	26S proteasome subunit RPN2a	Protein
CUST_46330_PI426222305	PGSC0003DMT400040764	26S proteasome subunit RPN2a	Protein
CUST_47136_PI426222305	PGSC0003DMT400030420	Alpha-soluble NSF attachment protein	Protein
CUST_49592_PI426222305	PGSC0003DMT400013634	Protein AFR	Protein
CUST_50870_PI426222305	PGSC0003DMT400071583	Ubiquitin carrier protein	Protein
CUST_52701_PI426222305	PGSC0003DMT400083723	Ubiquitin-protein ligase	Protein
CUST_30544_PI426222305	PGSC0003DMT400077393	Glutaredoxin	Redox
CUST_1004_PI426222305	PGSC0003DMT400032848	Conserved gene of unknown function	RNA
CUST_14049_PI426222305	PGSC0003DMT400060403	I-box binding factor	RNA
CUST_14094_PI426222305	PGSC0003DMT400060440	Conserved gene of unknown function	RNA
CUST_14383_PI426222305	PGSC0003DMT400060216	Zinc finger protein	RNA
CUST_15385_PI426222305	PGSC0003DMT400037454	Auxin response factor 2	RNA
CUST_25978_PI426222305	PGSC0003DMT400051682	MYB8	RNA
CUST_27037_PI426222305	PGSC0003DMT400067093	C2H2L domain class transcription factor	RNA
CUST_39020_PI426222305	PGSC0003DMT400070324	Dead box ATP-dependent RNA helicase	RNA
CUST_47618_PI426222305	PGSC0003DMT400005159	Mads box protein	RNA
CUST_14043_PI426222305	PGSC0003DMT400060400	Acyltransferase	secondary metabolism

CUST_48989_PI426222305	PGSC0003DMT400056250	O-methyltransferase 3	secondary metabolism
CUST_52364_PI426222305	PGSC0003DMT400008875	Undecaprenyl pyrophosphate synthetase	secondary metabolism
CUST_11250_PI426222305	PGSC0003DMT400036504	Receptor kinase	signalling
CUST_23419_PI426222305	PGSC0003DMT400064945	Exoenzymes regulatory protein aepA	signalling
CUST_27689_PI426222305	PGSC0003DMT400003166	Leucine-rich repeat protein	signalling
CUST_42186_PI426222305	PGSC0003DMT400038216	Serine/threonine-protein kinase bri1	signalling
CUST_50149_PI426222305	PGSC0003DMT400068848	Twin lov protein	signalling
CUST_50151_PI426222305	PGSC0003DMT400068851	PAS/LOV protein A	signalling
CUST_28858_PI426222305	PGSC0003DMT400033726	Protein CPR-5	stress
CUST_42803_PI426222305	PGSC0003DMT400002131	NBS-coding resistance gene analog	stress
CUST_51975_PI426222305	PGSC0003DMT400006208	Sn-2 protein	stress
CUST_968_PI426222305	PGSC0003DMT400032851	Heat-shock protein	stress
CUST_3575_PI426222305	PGSC0003DMT400064279	Mitochondrial succinate dehydrogenase iron sulfur subunit	TCA
CUST_33392_PI426222305	PGSC0003DMT400017804	Nitrate transporter	Transport
CUST_44191_PI426222305	PGSC0003DMT400038666	Urease accessory protein D	AA metabolism
CUST_41023_PI426222305	PGSC0003DMT400018951	Conserved gene of unknown function	DNA
CUST_23284_PI426222305	PGSC0003DMT400002569	Conserved gene of unknown function	hormone metabolism
CUST_34680_PI426222305	PGSC0003DMT400001851	Peroxidase	misc
CUST_34692_PI426222305	PGSC0003DMT400001848	Peroxidase	misc
CUST_47289_PI426222305	PGSC0003DMT400074044	Salicylic acid-binding protein 2	misc
CUST_52592_PI426222305	PGSC0003DMT400066086	Salicylic acid-binding protein 2	misc
CUST_12509_PI426222305	PGSC0003DMT400063491	Pentatricopeptide repeat-containing protein	Not assigned/Unknown
CUST_15718_PI426222305	PGSC0003DMT400080479	Gene of unknown function	Not assigned/Unknown
CUST_47427_PI426222305	PGSC0003DMT400074746	Gene of unknown function	Not assigned/Unknown
CUST_43342_PI426222305	PGSC0003DMT400064467	Gene of unknown function	Not assigned/Unknown
CUST_50295_PI426222305	PGSC0003DMT400044079	Root phototropism protein	signalling
CUST_18237_PI426222305	PGSC0003DMT400042319	Protein kinase family protein	signalling
CUST_32732_PI426222305	PGSC0003DMT400047312	Root phototropism protein	signalling
CUST_31316_PI426222305	PGSC0003DMT400034952	Conserved gene of unknown function	stress
CUST_8006_PI426222305	PGSC0003DMT400075214	Trans-2-enoyl CoA reductase	Unclassified
CUST_14597_PI426222305	PGSC0003DMT400066657	ATP binding protein	Cell
CUST_939_PI426222305	PGSC0003DMT400026203	Conserved gene of unknown function	Cell
CUST_12397_PI426222305	PGSC0003DMT400063728	Pectinesterase	Cell Wall
CUST_25783_PI426222305	PGSC0003DMT400061821	Pectinesterase	Cell Wall
CUST_40661_PI426222305	PGSC0003DMT400038916	BURP domain-containing protein	Cell Wall
CUST_40669_PI426222305	PGSC0003DMT400038925	Dehydration-responsive protein RD22	Cell Wall
CUST_40671_PI426222305	PGSC0003DMT400038926	BURP domain-containing protein	Cell Wall
CUST_40679_PI426222305	PGSC0003DMT400038919	Dehydration-responsive protein RD22	Cell Wall
CUST_19728_PI426222305	PGSC0003DMT400064050	ATP-dependent RNA helicase	DNA
CUST_28314_PI426222305	PGSC0003DMT400044257	Desacetoxyvindoline 4-hydroxylase	hormone metabolism
CUST_28397_PI426222305	PGSC0003DMT400044442	1-aminocyclopropane-1-carboxylate oxidase homolog	hormone metabolism
CUST_30568_PI426222305	PGSC0003DMT400007963	Leucoanthocyanidin dioxygenase	hormone metabolism
CUST_30600_PI426222305	PGSC0003DMT400018670	Flavonol synthase/flavanone 3-hydroxylase	hormone metabolism
CUST_39045_PI426222305	PGSC0003DMT400003254	E8 protein homolog	hormone metabolism
CUST_45543_PI426222305	PGSC0003DMT400079728	Sucrose synthase 6	major CHO metabolism
CUST_25107_PI426222305	PGSC0003DMT400015046	UDP-glucose:glucosyltransferase	misc
CUST_28582_PI426222305	PGSC0003DMT400009963	UDP-glucoronosyl/UDP-glucosyl transferase family protein	misc
CUST_30245_PI426222305	PGSC0003DMT400012093	Extensin	misc
CUST_34417_PI426222305	PGSC0003DMT400055550	21kD protein	misc
CUST_36423_PI426222305	PGSC0003DMT400079897	Alcohol dehydrogenase	misc
CUST_50391_PI426222305	PGSC0003DMT400072015	Short chain alcohol dehydrogenase	misc
CUST_51406_PI426222305	PGSC0003DMT400080529	UDP-glucoronosyl/UDP-glucosyl transferase family protein	misc
CUST_7798_PI426222305	PGSC0003DMT400009574	Agglutinin isoform	misc
CUST_49900_PI426222305	PGSC0003DMT400019708	Alternative oxidase	Mitochondrial electron transport
CUST_10202_PI426222305	PGSC0003DMT400029034	Conserved gene of unknown function	Not assigned/Unknown
CUST_10463_PI426222305	PGSC0003DMT400029033	Conserved gene of unknown function	Not assigned/Unknown
CUST_13291_PI426222305	PGSC0003DMT400059373	Conserved gene of unknown function	Not assigned/Unknown
CUST_16630_PI426222305	PGSC0003DMT400069577	UPF0497 membrane protein	Not assigned/Unknown
CUST_1799_PI426222305	PGSC0003DMT400093134	Gene of unknown function	Not assigned/Unknown
CUST_21737_PI426222305	PGSC0003DMT400051172	Gene of unknown function	Not assigned/Unknown
CUST_21822_PI426222305	PGSC0003DMT400092438	Gene of unknown function	Not assigned/Unknown
CUST_25170_PI426222305	PGSC0003DMT400014886	Gene of unknown function	Not assigned/Unknown
CUST_34315_PI426222305	PGSC0003DMT400095310	Gene of unknown function	Not assigned/Unknown
CUST_3435_PI426222305	PGSC0003DMT400090079	Transposon MuDR mudrA	Not assigned/Unknown
CUST_34450_PI426222305	PGSC0003DMT400055586	Gene of unknown function	Not assigned/Unknown
CUST_35163_PI426222305	PGSC0003DMT400021464	Conserved gene of unknown function	Not assigned/Unknown

Appendix

CUST_36874_PI426222305	PGSC0003DMT400048224	Tn7 reverse transcriptase	Not assigned/Unknown
CUST_38374_PI426222305	PGSC0003DMT400022017	Miraculin	Not assigned/Unknown
CUST_38378_PI426222305	PGSC0003DMT400022042	Miraculin	Not assigned/Unknown
CUST_38482_PI426222305	PGSC0003DMT400065497	EF hand family protein	Not assigned/Unknown
CUST_39109_PI426222305	PGSC0003DMT400085899	Gene of unknown function	Not assigned/Unknown
CUST_3923_PI426222305	PGSC0003DMT400094431	Gene of unknown function	Not assigned/Unknown
CUST_40185_PI426222305	PGSC0003DMT400005374	Transposon MuDR mudrA	Not assigned/Unknown
CUST_44826_PI426222305	PGSC0003DMT400002273	Quinonprotein alcohol dehydrogenase	Not assigned/Unknown
CUST_44836_PI426222305	PGSC0003DMT400002277	Quinonprotein alcohol dehydrogenase	Not assigned/Unknown
CUST_45117_PI426222305	PGSC0003DMT400092877	Gene of unknown function	Not assigned/Unknown
CUST_46273_PI426222305	PGSC0003DMT400053264	Gene of unknown function	Not assigned/Unknown
CUST_46333_PI426222305	PGSC0003DMT400090371	Gene of unknown function	Not assigned/Unknown
CUST_46934_PI426222305	PGSC0003DMT400048684	Polyphenol oxidase	Not assigned/Unknown
CUST_47512_PI426222305	PGSC0003DMT400059414	Zgc:64189	Not assigned/Unknown
CUST_48222_PI426222305	PGSC0003DMT400055932	Conserved gene of unknown function	Not assigned/Unknown
CUST_50559_PI426222305	PGSC0003DMT400039134	Defensin J1-2	Not assigned/Unknown
CUST_50560_PI426222305	PGSC0003DMT400039133	Defensin J1-2	Not assigned/Unknown
CUST_52842_PI426222305	PGSC0003DMT400082676	Gene of unknown function	Not assigned/Unknown
CUST_7175_PI426222305	PGSC0003DMT400089880	Gene of unknown function	Not assigned/Unknown
CUST_50289_PI426222305	PGSC0003DMT400077788	Nudix hydrolase 1	nucleotide metabolism
CUST_50290_PI426222305	PGSC0003DMT400077787	Nudix hydrolase 1	nucleotide metabolism
CUST_50725_PI426222305	PGSC0003DMT400071737	Adenylate kinase, chloroplastic	nucleotide metabolism
CUST_13305_PI426222305	PGSC0003DMT400001748	Calcineurin-like phosphoesterase family protein	Protein
CUST_13309_PI426222305	PGSC0003DMT400001749	Serine/threonine-protein phosphatase 7 long form homolog	Protein
CUST_13316_PI426222305	PGSC0003DMT400001747	Mutator transposase-like polypeptide	Protein
CUST_2086_PI426222305	PGSC0003DMT400027148	Subtilase	Protein
CUST_2390_PI426222305	PGSC0003DMT400028525	Subtilase	Protein
CUST_23921_PI426222305	PGSC0003DMT400032691	Caspase	Protein
CUST_39949_PI426222305	PGSC0003DMT400076958	Calcineurin-like phosphoesterase family protein	Protein
CUST_48196_PI426222305	PGSC0003DMT400071660	Serine/threonine-protein phosphatase 7 long form homolog	Protein
CUST_52235_PI426222305	PGSC0003DMT400046449	CBL-interacting protein kinase 11	Protein
CUST_52267_PI426222305	PGSC0003DMT400028428	Calcineurin-like phosphoesterase family protein	Protein
CUST_52529_PI426222305	PGSC0003DMT400022705	Protein kinase	Protein
CUST_1227_PI426222305	PGSC0003DMT400003516	Ocs element-binding factor	RNA
CUST_9685_PI426222305	PGSC0003DMT400008752	Transcription factor style2.1	RNA
CUST_30352_PI426222305	PGSC0003DMT400069897	Anthocyanin 5-aromatic acyltransferase	secondary metabolism
CUST_7639_PI426222305	PGSC0003DMT400009457	Oxidoreductase	secondary metabolism
CUST_22497_PI426222305	PGSC0003DMT400039527	Receptor kinase	signalling
CUST_27057_PI426222305	PGSC0003DMT400065856	Leucine rich repeat containing protein	signalling
CUST_27159_PI426222305	PGSC0003DMT400065855	Leucine rich repeat containing protein	signalling
CUST_29674_PI426222305	PGSC0003DMT400047494	Serine-threonine protein kinase, plant-type	signalling
CUST_29811_PI426222305	PGSC0003DMT400002648	Serine-threonine protein kinase, plant-type	signalling
CUST_3165_PI426222305	PGSC0003DMT400000353	Calcium-transporting ATPase, endoplasmic reticulum-type	signalling
CUST_37582_PI426222305	PGSC0003DMT400049533	Conserved gene of unknown function	signalling
CUST_37813_PI426222305	PGSC0003DMT400006173	NPH3 (NON-PHOTOTROPIC HYPOCOTYL 3)	signalling
CUST_42500_PI426222305	PGSC0003DMT400079207	Phi-1 protein	signalling
CUST_42521_PI426222305	PGSC0003DMT400079157	Phi-1 protein	signalling
CUST_31229_PI426222305	PGSC0003DMT400063927	Conserved gene of unknown function	stress
CUST_35489_PI426222305	PGSC0003DMT400005850	Conserved gene of unknown function	stress
CUST_45238_PI426222305	PGSC0003DMT400028000	Heat shock protein	stress
CUST_4959_PI426222305	PGSC0003DMT400009196	Thaumatin protein	stress
CUST_50801_PI426222305	PGSC0003DMT400090746	Endochitinase	stress
CUST_51701_PI426222305	PGSC0003DMT400022685	Endochitinase	stress
CUST_33248_PI426222305	PGSC0003DMT400017915	Carbonic anhydrase	TCA
CUST_33300_PI426222305	PGSC0003DMT400017914	Carbonic anhydrase	TCA
CUST_47536_PI426222305	PGSC0003DMT400030727	Amino acid transporter	Transport
CUST_47546_PI426222305	PGSC0003DMT400030732	Amino acid transporter	Transport

8 List of Abbreviations

°C .... degree Celsius

µg .... microgramm

µl .... microliter

µm .... micrometer

A. thaliana .... *Arabidopsis thaliana*

ABA .... abscisic acid

ADP .... Adenosine-Diphosphate

AG .... Aktiengesellschaft

AMY .... α-amylase

APL .... ADP-glucose pyrophosphorylase Large Subunit

APS .... ADP-glucose pyrophosphorylase Small Subunit

ATP .... Adenosine-Triphosphate

BAM .... β-amylase

BLAST .... Basic local alignment search tool

bp .... base pairs

CDF .... CYCLING DOF FACTOR

cDNA .... complementary DNA

CK .... cytokinin

cm .... centimeter

CO_2 .... carbon dioxide

CT .... computer tomography

cwInv .... cell wall-bound invertase

d .... day(s)

DBE .... Debranching enzyme

DNA .... Deoxyribonucleic acid

DPE .... Disproportionating enzyme

dT .... deoxy thymidine

List of Abbreviations

F6P Fructose-6-Phosphate

FDL .... FLOWERING LOCUS D-Like

Fk .... Fructokinase

Frc .... Fructose

FT .... FLOWERING LOCUS T

G1P Glucose-1-Phosphate

G6P Glucose-6-Phosphate

GBSS .... Granule-bound starch synthase

Glc .... Glucose

GLT .... Glucose Transporter

GmbH .... Gesellschaft mit beschränkter Haftung

GPT .... Glucose-6-phosphate translocator

GWD .... Glucan-water-Dikinase

h .... hour(s)

HEPES .... hydroxyethyl-piperazineethane-sulfonic acid

HPLC .... High-Performance liquid chromatography

HSP .... heat-shock protein

ISA .... Isoamylase

kb .... kilobases

LD .... long day

LDE .... limit dextrinase

LOX .... lipoxygenase

LSF .... Like SEX4

M .... molar

MEX .... maltose transporter

ml .... milliliter

mM .... millimolar

Na .... sodium

NTT .... nucleotide transporter

184

nm .... nanometer

P.. phoshphorus

PCR .... polymerase chain reaction

PGI .... phosphoglucoisomerase

PGM .... phosphoglucomutase

PGSC .... Potato Genome Sequencing Consortium

Pho .... α-glucan/starch phosphorylase

P_i .... inorganic phosphate

PP_i .... inorganic pyrophosphate

PWD .... pyrophosphate-water dikinase

qPCR .... quantitative real-time PCR

rpm .... rounds per minute

RubisCO.. Ribulose-1,5-bisphosphate carboxylase/oxygenase

S. tuberosum...*Solanum tuberosum* (potato)

SD .... short day

SDS .... Sodium Dodecyl Sulfat

SEX .... starch excess

SP3D .... SELF-PRUNING 3D

SP5G ....SELF-PRUNING 5G

SP6A .... SELF-PRUNING 6A

SS .... starch Synthase

SuSy .... sucrose synthase

TP .... triose-phosphate

TPT .... triose-phosphate/phosphate translocator

U .... unit

UDP .... uridine diphosphate

UGPase .... UDP-glucose pyrophosphorylase

UV-light .... ultraviolet light

VGT .... vacuolar glucose transporter

9 Acknowledgements / Danksagung

Hier möchte ich mich bei allen bedanken, die durch ihre Unterstützung, ihren Zuspruch, die vielen Diskussionen und inspirierenden Gespräche sowie ihre Kritik zum Gelingen dieser Arbeit beigetragen haben.

Zunächst gilt mein Dank Prof. Uwe Sonnewald für die Überlassung des Themas sowie die Betreuung und das Interesse am Gelingen dieser Arbeit.

Vielen Dank an Prof. Andreas Burkovski, der das Zweitgutachten dieser Arbeit übernimmt. Außerdem bedanke ich mich bei den Prüfer*innen PD Dr. Ruth Stadler und Prof. Benedikt Kost.

Auch PD Dr. Sophia Sonnewald gilt mein aufrichtiger Dank für die Zusammenarbeit und Unterstützung bei der Erstellung meiner ersten Publikation sowie diversen Microarray-Auswertungen und Diskussionen über Statistik.

Meinen ehemaligen Kolleg*innen am Lehrstuhl gilt besonderer Dank. Ich habe mich bei und mit euch immer sehr wohl gefühlt. Euren Rat und eure Unterstützung weiß ich sehr zu schätzen. Besonders hervorheben möchte ich an dieser Stelle Stephen, Madlen, Pierre, Ingrid, Christian, Marlis, Jörg, David, Alfred, Susanna, Anja. Johannes und Martin. Mein Dank für ihre Hilfe mit den Pflanzen geht an das Team der Gewebekultur Christiane, Anja und Eva sowie Christine aus dem Gewächshaus.

Allen Kolleg*innen des „Neuen Labors" möchte ich für die gute Arbeitsatmosphäre und das freundschaftliche Miteinander danken: Suayib, Matthias, Hildegard, Martina, Haina, Kirsten, Michaela und Anja. Katrin, Mene, Kathrin, Wafaa und Christian danke ich außerdem herzlichst für Ihre anhaltende Freundschaft.

Allen Kooperationspartner*innen der Projekte HotPot und HotSol danke ich für die gute Zusammenarbeit und interessante Gespräche. Den Kooperationspartner*innen am Fraunhofer Institut für Integrierte Schaltungen in Fürth möchte ich für die konstruktive Zusammenarbeit während der Projektphase sowie der Erstellung unserer gemeinsamen Publikation danken. Joelle Claußen und Stefan Gerth möchte ich dabei besonders erwähnen.

Auch möchte ich meinen herzlichen Dank meinen Freund*innen aussprechen. Nine, Lisa, Edda, Basti, Daniel ihr seid mir immer eine Stütze und bringt Freude in mein Leben. Meinen Eltern danke ich für ihren Halt, ihr Vertrauen und ihre Liebe. Meiner Schwester Vanessa und meiner Nichte Leticia für die vielen schönen Momente und Erlebnisse.

Meinem Mann Holger, dessen Geduld, Liebe und Unterstützung niemals aufgewogen werden können, danke ich von ganzem Herzen. Danke, dass Du in meinem Leben bist.